UNIVERSITAT DE BARCELONA

Caracterització de Sistemes de Partició Cromatogràfics per a la Subrogació de Processos de Biopartició

Alejandro Fernández Pumarega

UNIVERSITAT DE BARCELONA

FACULTAT DE QUÍMICA
DEPARTAMENT D'ENGINYERIA QUÍMICA I QUÍMICA ANALÍTICA

Programa de doctorat: Química Analítica i Medi Ambient

Caracterització de Sistemes de Partició Cromatogràfics per a la Subrogació de Processos de Biopartició

Memòria presentada per
Alejandro Fernández Pumarega

per optar al grau de doctor per la Universitat de Barcelona
Sota la direcció de:

Dra. Elisabet Fuguet i Jordà

Professora Agregada Serra Húnter del Departament d'Enginyeria Química i Química Analítica

Dra. Susana Amézqueta Pérez

Professora Agregada del Departament d'Enginyeria Química i Química Analítica

La Dra. Elisabet Fuguet i Jordà i la Dra. Susana Amézqueta Pérez

CERTIFIQUEN

Que la present memòria de tesi doctoral, que porta per títol *"Caracterització de Sistemes de Partició Cromatogràfics per a la Subrogació de Processos de Biopartició"* ha estat realitzada pel Sr. Alejandro Fernández Pumarega sota la seva direcció al Departament d'Enginyeria Química i Química Analítica i que els resultats presentats són fruit de la recerca realitzada per l'esmentat doctorand.

Barcelona, gener de 2020

Dra. Elisabet Fuguet i Jordà

Professora Agregada Serra Húnter del Departament d'Enginyeria Química i Química Analítica

Dra. Susana Amézqueta Pérez

Professora Agregada del Departament d'Enginyeria Química i Química Analítica

AGRAÏMENTS

L’actual tesi ha estat realitzada al grup de recerca Physchem del Departament d’Enginyeria Química i Química Analítica sota la direcció de les doctores Elisabet Fuguet i Jordà i Susana Amézqueta Pérez a les que voldria agrair el suport i la confiança mostrada al llarg d’aquests anys. També voldria ampliar aquest agraïment a la resta de professors del grup (Martí, Clara i Xavi) i als doctorands i estudiants que formen o han format part del grup de recerca, en especial a la Sara i la Lídia. A part, també voldria destacar els bons moments compartits amb altres estudiants del departament, especialment amb l’Ane, en Juanfra i la Clara.

In addition, I would like to acknowledge Sebastiaan Eeltink for giving me the opportunity to join his research group at the *Vrije Universiteit Brussel* (Brussels, Belgium) where I have learned a lot about chromatography, and I have met really nice people, especially José, Thomas and Magali who have become really close friends.

Finalment també voldria estendre aquest agraïment a la meva família i als meus amics; en concret als meus pares els quals m’han donat l’oportunitat, la qual ells no van tenir, de poder realitzar aquests estudis.

ABREVIATURES I ACRÒNIMS

$[S]_o$	Concentració del solut a la fase octanòlica
$[S]_w$	Concentració del solut a la fase aquosa
α	Grau de ionització del compost
$\alpha_{(A-)}$	Fracció molar de l'espècie totalment ionitzada de l'àcid
$\alpha_{(HA)}$	Fracció molar de l'espècie neutra de l'àcid
A	Difusió d'Eddy de l'equació de van Deemter o acidesa per pont d'hidrogen del solut segons el model de paràmetres de solvatació
a	Paràmetre *A* reduït de l'equació de van Deemter o basicitat per pont d'hidrogen del sistema segons el model de paràmetres de solvatació
ACN	Acetonitril
AGESS	Siloxà modificat amb sulfat de dodecà alil glicidil èter o sistema cromatogràfic descrit a la Taula 1
AIBN	Azobisisobutironitril
AP	Permeació en les cèl·lules d'alga
a_u	Coeficient *a* normalitzat del model de paràmetres de solvatació
B	Difusió longitudinal de l'equació de van Deemter o basicitat per pont d'hidrogen del solut segons el model de paràmetres de solvatació
b	Paràmetre *B* reduït de l'equació de van Deemter o acidesa per pont d'hidrogen del sistema segons el model de paràmetres de solvatació
BB	Coeficient de distribució sang-cervell
BBD	Sistema de biopartició: distribució sang-cervell
BBP	Sistema de biopartició: permeació sang-cervell
BG	Sistema de biopartició: toxicitat aquàtica no específica envers Bluegill
Brij	Sistema cromatogràfic descrit a la Taula 1
Brij 35	Èter de dodecilpolioxietilè(23)
BrijSDS	Sistema cromatogràfic descrit a la Taula 1

b_u	Coeficient *b* normalitzat del model de paràmetres de solvatació
C	Resistència a la transferència de massa de l'equació de van Deemter
c	Paràmetre *C* reduït de l'equació de van Deemter
C18	Fase estacionària de cadenes d'octadecilsilà
CD	Sistema de biopartició: toxicitat aquàtica no específica envers *Ceriodaphnia dubia*
CE	Electroforesi capil·lar
CEC	Electrocromatografia capil·lar
Chol	Colesterol
C_m	Resistència a la transferència de massa deguda a la fase mòbil
CMC	Concentració micel·lar crítica
C_{nar}	Concentració de narcosi
CP	Sistema de biopartició: toxicitat aquàtica no específica envers *Chilomonas paramecium*
C_s	Resistència a la transferència de massa deguda a la fase estacionària
ct	Constant del model de paràmetres de solvatació
CZE	Electroforesi capil·lar en zona
Δc	Increment de gradient
d	Distància euclidiana entre dos vectors normalitzats
d_{dom}	Suma de la mida mitjana dels microglòbuls i dels macroporus
DGDC	Sistema cromatogràfic descrit a la Taula 1
DGDCChol	Sistema cromatogràfic descrit a la Taula 1
DHP	Dihexadecilfosfat o sistema cromatogràfic descrit a la Taula 1
DHPChol	Sistema cromatogràfic descrit a la Taula 1
D_M	Coeficient de difusió
DM24	Sistema de biopartició: Toxicitat aquàtica no específica envers *Daphnia magna* (passades 24h)

DM48	Sistema de biopartició: Toxicitat aquàtica no específica envers *Daphnia magna* (passades 48h)
$D_{o/w}$	Coeficient de distribució octanol-aigua
DP	Sistema de biopartició: toxicitat aquàtica no específica enversa *Daphnia pulex*
DPPC	Dipalmitoilfosfatidilcolina
DPPG	Dipalmitoilfosfatidilglicerol
η	Viscositat
E	Refractivitat molar en excés del solut segons el model de paràmetres de solvatació
e	Polaritzabilitat del sistema segons el model de paràmetres de solvatació
EKC	Cromatografia electrocinètica
EOF	Flux electroosmòtic
ES	Sistema de biopartició: toxicitat aquàtica no específica envers *Entosiphon sulcantum*
e_u	Coeficient *e* normalitzat del model de paràmetres de solvatació
ϕ	Fracció de solvent orgànic a la fase mòbil
F	Cabal de la fase mòbil
F	Paràmetre *F* del test de Fisher
FA	Àcid fòrmic
FM	Sistema de biopartició: toxicitat aquàtica no específica envers Fathead minnow
FP	Fase pseudoestacionària
GF	Sistema de biopartició: toxicitat aquàtica no específica envers Goldfish
GO	Sistema de biopartició: toxicitat aquàtica no específica envers Golden orfe
GP	Sistema de biopartició: toxicitat aquàtica no específica envers Guppy
H	Alçada de plat
HIA	Absorció intestinal humana

HPLC	Cromatografia líquida d'alta resolució
IA	Sistema de biopartició: absorció intestinal
IAM	Columna de membrana artificial immobilitzada o sistema cromatogràfic descrit a la Taula 1
IGC	Concentració inhibitòria del creixement
IGC50	Concentració inhibitòria del creixement de la meitat de la població
I_{jap}	Descriptor corresponent a l'espècie *rana japonica*
k	Factor de retenció cromatogràfic
$k_{(A-)}$	Factor de retenció de l'àcid totalment ionitzat
$k_{(AB)}$	Factor de retenció del compost àcid-base neutre
$k_{(AB\pm)}$	Factor de retenció del compost àcid-base ionitzat
$k_{(B)}$	Factor de retenció de la base neutra
$k_{(BH+)}$	Factor de retenció de la base protonada
$k_{(HA)}$	Factor de retenció de l'àcid neutre
k_0	Factor de retenció d'un compost quan la fracció de solvent orgànic a la fase mòbil és 0
K_a'	Constant d'acidesa aparent
k_{cel}	Coeficient de permeació cèl·lula-aigua
K_{oc}	Coeficient de sorció sòl-aigua
k_p	Coeficient de permeació a la pell
K_{sc}	Coeficient de partició en la pell (*stratum corneum*)
l	Longitud del vector format pels coeficients del sistema
L	Longitud de la columna cromatogràfica
LC50	Concentració letal de la meitat de la població
L_D	Longitud efectiva del capil·lar
LEKC	Cromatografia electrocinètica de liposomes
LLEKC	Sistema de cromatografia electrocinètica de liposomes de lecitina

LMEEKC	Sistema de cromatografia electrocinètica de microemulsions de lecitina
LMELC	Sistema de cromatografia líquida de microemulsions de lecitina
log D_{est}	log $D_{o/w}$ estimats en el present treball
log D_{lit}	log $D_{o/w}$ determinats a la literatura a partir dels mètodes tradicionals
L_T	Longitud total del capil·lar
μ	Mobilitat electroforètica del compost
μ_0	Mobilitat del compost en tampó aquós
μ_{fp}	Mobilitat electroforètica del marcador de la fase pseudoestacionària
ME	Microemulsió
MEEKC	Cromatografia electrocinètica de microemulsions
MEKC	Cromatografia electrocinètica micel·lar
MELC	Cromatografia líquida de microemulsions
MIC	Concentració mínima inhibitòria
MK48	Sistema de biopartició: toxicitat aquàtica no específica envers Medaka high-eyes (passades 48h)
MK96	Sistema de biopartició: toxicitat aquàtica no específica envers Medaka high-eyes (passades 96h)
MLC	Cromatografia líquida micel·lar
N	Nombre de plats de la columna cromatogràfica
n	Nombre de punts de la correlació
n_c	Capacitat de pics
n_M	nombre mitjà de mols del solut a la fase mòbil
n_S	nombre mitjà de mols del solut a la fase estacionària
OW	Sistema de partició octanol-aigua
p	Pendent de la correlació
$p_{(AB)}$	Pendent de la correlació entre la propietat de biopartició i la cromatogràfica de compostos àcid-base en la seva forma neutra

$p_{(AB\pm)}$	Pendent de la correlació entre la propietat de biopartició i la cromatogràfica de compostos àcid-base en la seva forma ionitzada
PAAU	Poli(11-acrilamidaundecanoat de sodi) o sistema cromatogràfic descrit a la Taula 1
PC	Component principal
PCA	Anàlisi de components principals
PG	Sistema de biopartició: inhibició del creixement bacterià envers *Porphyromonas gingivalis*
PLM	Columna modificada amb fosfolípids o sistema cromatogràfic descrit a la Taula 1
$P_{o/w}$	Coeficient de partició octanol-aigua
$P_{o/w(A-)}$	Coeficient de partició octanol-aigua de la forma ionitzada de l'àcid
$P_{o/w(AB)}$	Coeficient de partició octanol-aigua de la forma neutra del compost àcid-base
$P_{o/w(AB\pm)}$	Coeficient de partició octanol-aigua de la forma ionitzada del compost àcid-base
$P_{o/w(HA)}$	Coeficient de partició octanol-aigua de la forma neutra de l'àcid
$P_{o/w(ió\ benzoat)}$	Coeficient de partició octanol-aigua de l'ió benzoat
$P_{o/w(ió\ efedrina)}$	Coeficient de partició octanol-aigua de l'efedrina totalment ionitzada
poly-EKC	Cromatografia electrocinètica basada en polímers
POPC	1-palmitoil-2-oleil-*sn*-glicero-3-fosfocolina
POPC/PS	Sistema cromatogràfic descrit a la Taula 1
PP	Sistema de biopartició: toxicitat aquàtica no específica envers *Pseudomonas putida*
PS	Fosfatidil serina
PS	Permeació a través de la barrera sang-cervell
PSUA	Poli(10-undecilenat de sodi) o sistema cromatogràfic descrit a la Taula 1
q	Ordenada a l'origen de la correlació o càrrega de l'ió
$q_{(AB)}$	Ordenada a l'origen de la correlació entre la propietat de biopartició i la cromatogràfica de compostos àcid-base en la seva forma neutra

$q_{(AB\pm)}$	Ordenada a l'origen de la correlació entre la propietat de biopartició i la cromatogràfica de compostos àcid-base en la seva forma ionitzada
Q^2_{LMO}	Coeficient de la validació creuada
QSPR	Relacions quantitatives estructura-propietat
r	Radi de l'ió
R^2	Coeficient de determinació
RP18	Sistema cromatogràfic descrit a la Taula 1
RP-LC	Cromatografia líquida de fase inversa
RT	Sistema de biopartició: narcosi en capgrossos
σ_{bio}^2	Variància de les dades biològiques del sistema de biopartició
σ_{corr}^2	Precisió de la correlació entre el sistema de biopartició i el cromatogràfic
σ_{crom}^2	Variància de les dades cromatogràfiques
σ_d^2	Variància deguda a la dissimilitud dels sistemes correlacionats
S	Dipolaritat/polaritzabilitat del solut segons el model de paràmetres de solvatació o paràmetre de la relació lineal de la força del solvent
s	Dipolaritat del sistema segons el model de paràmetres de solvatació
SA	Sistema de biopartició: toxicitat aquàtica no específica envers *Spirostomum ambiguum*
SAr	Sistema de biopartició: inhibició del creixement bacterià envers *Selenomonas artemidis*
SD	Desviació estàndard
SD_{bio}	Desviació estàndard obtinguda a la caracterització del sistema de biopartició a partir del model de paràmetres de solvatació
SD_{crom}	Desviació estàndard obtinguda a la caracterització del sistema cromatogràfic a partir del model de paràmetres de solvatació
SD_d	Desviació estàndard obtinguda al correlacionar les dades calculades a partir del model de paràmetres de solvatació de dos sistemes de partició
SDS	Dodecilsulfat de sodi o sistema cromatogràfic descrit a la Taula 1
SDS0.8	Sistema cromatogràfic descrit a la Taula 1

SDS1.6	Sistema cromatogràfic descrit a la Taula 1
SDSBrij	Sistema cromatogràfic descrit a la Taula 1
SDSME	Sistema cromatogràfic descrit a la Taula 1
SEM	Microscòpia electrònica de rastreig
SLN	N-lauroilsarcosinat de sodi o sistema cromatogràfic descrit a la Taula 1
SP	Propietat del solut en un sistema de partició
SPA	Sistema de biopartició: partició a la pell
SP_{bio}	Propietat de partició d'un sistema de biopartició
SP_{crom}	Propietat de partició d'un sistema cromatogràfic
SPE	Permeació a la pell
SPM	Model de paràmetres de solvatació
SS	Sistema de biopartició: Inhibició del creixement bacterià envers *Streptococcus sobrinus*
STC	Taurocolat de sodi o sistema cromatogràfic descrit a la Taula 1
s_u	coeficient *s* normalitzat del model de paràmetres de solvatació
SWP	Sistema de biopartició: sorció sòl-aigua
t_0	temps mort
t_{eof}	temps de migració del marcador del flux electroosmòtic
t_{ext}	temps extra-columna
TFA	Àcid trifluoroacètic
t_{fp}	Temps de migració del marcador de la fase pseudoestacionària
t_G	Temps de gradient
t_G/t_0	Pendent del gradient
THF	Tetrahidrofurà
t_m	Temps de migració de l'anàlit
TP	Sistema de biopartició: Toxicitat aquàtica no específica envers *Tetrahymena pyriformis*

t_R	Temps de retenció de l'anàlit
TTAB	Bromur de tetradeciltrimetilamoni o sistema cromatogràfic descrit a la Taula 1
TTABME	Sistema de cromatografia electrocinètica de microemulsions preparat a partir de bromur de tetradeciltrimetilamoni, 1-butanol i heptà
u_0	Velocitat linial de la fase mòbil
u_{opt}	Caudal òptim de la fase mòbil
UP	Sistema de biopartició: Toxicitat aquàtica no específica envers *Uronema parduczi*
V	Voltatge o volum de McGowan del solut segons el model de paràmetres de solvatació
v	Hidrofobicitat del sistema segons el model de paràmetres de solvatació
VEKC	Cromatografia electrocinètica de vesícules
v_u	Coeficient v normalitzat del model de paràmetres de solvatació
w	Amplada de la base del pic cromatogràfic
Y_{exp}	Dades del sistema de biopartició experimentals
Y_{pred}	Dades del sistema de biopartició estimades

ÍNDEX

OBJECTIVES

The aim of this thesis is the development and characterization of new physicochemical systems that could surrogate biopartitioning processes of pharmaceutical and environmental interest using fast-simple-automated chromatographic methods that would reduce experiments *in vivo*.

To this aim, the ability of several chromatographic systems to surrogate toxicity to aquatic species, skin partition and the octanol-water partition system will be tested. Moreover, since this methodology has been mainly applied to neutral compounds in the literature, the feasibility of a method based on microemulsion electrokinetic chromatography to estimate the octanol-water distribution coefficient of ionized acid-base compounds will be studied.

ESTRUCTURA DE LA TESI

La present tesi doctoral es presenta com a compendi d'articles i està dividida principalment en 3 capítols:

Primerament s'inclou una introducció on s'explica en què consisteixen els sistemes de partició i se'n descriuen alguns tant de biològics com fisicoquímics. A continuació, s'exposa el model de paràmetres de solvatació, model que permet caracteritzar sistemes basats en la partició de compostos entre dues fases diferents, i es presenten les eines que s'utilitzen en aquest treball per comparar els diferents sistemes de partició. La comparació permetrà avaluar la similitud entre sistemes i estimar quin sistema fisicoquímic és, *a priori*, el més adient per emular un procés de biopartició concret, el qual, tot seguit, es validarà. Finalment, s'esmenten els nous sistemes cromatogràfics que s'han desenvolupat durant el transcurs de la tesi.

A la segona part de la tesi es mostra una recopilació de les publicacions realitzades fruit de la investigació duta a terme durant aquests anys:

1. Modeling Aquatic Toxicity through Chromatographic Systems.
   Fernández-Pumarega A.; Amézqueta, S.; Farré, S.; Muñoz-Pascual, L.; Abraham, M.H.; Fuguet, E.; Rosés, M.
   Analytical Chemistry (2017), volum: 89, pàgines: 7996-8003.
   DOI: 10.1021/acs.analchem.7b01301.

2. Lecithin Liposomes and Microemulsions as New Chromatographic Phases.
   Amézqueta, S.; Fernández-Pumarega, A.; Farré, S.; Luna, D.; Fuguet, E.; Rosés, M.
   Journal of Chromatography A, en premsa.
   DOI: 10.1016/j.chroma.2019.460596.

3. Determination of the Retention Factor of Ionizable Compounds in Microemulsion Electrokinetic Chromatography.
   Fernández-Pumarega, A.; Amézqueta, S.; Fuguet, E.; Rosés, M.
   Analytica Chimica Acta (2019), volum: 1078, pàgines: 221-230.
   DOI: 10.1016/j.aca.2019.06.007.

4. Comparison of the Retention of Basic Compounds in Anionic and Cationic Microemulsion Electrokinetic Chromatographic Systems.
   Fernández-Pumarega, A.; Olmo, L.; Amézqueta, S.; Fuguet, E.; Rosés, M.
   Manuscrit en preparació.

5. Estimation of the Octanol–Water Distribution Coefficient of Acidic Compounds by Microemulsion Electrokinetic Chromatography.
   Fernández-Pumarega, A.; Amézqueta, S.; Fuguet, E.; Rosés, M.
   Journal of Pharmaceutical and Biomedical Analysis (2020), volum: 179, pàgines: -.
   DOI: 10.1016/j.jpba.2019.112981.

6. Estimation of the Octanol-Water Distribution Coefficient of Basic Compounds by a Cationic Microemulsion Electrokinetic Chromatography System.
   Fernández-Pumarega, A.; Martín-Sanz, B.; Amézqueta, S.; Fuguet, E.; Rosés, M.
   ADMET & DMPK, en revisió.

7. A Comprehensive Investigation of the Peak Capacity for the Reversed-Phase Gradient Liquid-Chromatographic Analysis of Intact Proteins Using a Polymer-Monolithic Capillary Column.
   Fernández-Pumarega, A.; Dores-Sousa, J.L.; Eeltink, S.
   Journal of Chromatography A (2020), volum: 1609, pàgines: -.
   DOI: 10.1016/j.chroma.2019.460462.

La tercera part consisteix en la discussió dels resultats obtinguts en cadascuna de les publicacions i la interconnexió entre totes elles, i consta principalment de 3 apartats. Un primer en el qual es compilen sistemes cromatogràfics ja caracteritzats, es caracteritzen nous sistemes cromatogràfics a partir del model de paràmetres de solvatació i es comparen entre ells. Tot seguit, d'entre tots els sistemes cromatogràfics considerats, s'avaluarà quins serviran per emular propietats de biopartició d'interès farmacèutic (partició a la pell i la partició octanol-aigua) i ambiental (toxicitat aquàtica). El segon apartat es basa en l'estimació de propietats de biopartició per a compostos que es troben parcialment o total ionitzats, en concret

l'estimació del coeficient de distribució octanol-aigua. L'últim apartat consta de la recerca duta a terme a la *Vrije Universiteit Brussel* (Brussel·les, Bèlgica) pel desenvolupament i cerca de nous sistemes cromatogràfics que podrien utilitzar-se addicionalment per subrogar altres propietats de biopartició.

Finalment, a les conclusions s'enumeren les idees més importants extretes d'aquest treball.

ABSTRACT

The title of the present thesis is “Characterization of Chromatographic Systems for the Subrogation of Biopartitioning Processes”.

This study deals with the development, characterization, and evaluation of different chromatographic systems, in order to emulate biopartitioning processes of environmental and pharmaceutical interest. Generally, the determination of biological properties follows expensive and complex procedures which sometimes require the use of living beings, a practice ethically questionable. Thus, the use of physicochemical systems allows the estimation of biological properties in a faster and automated way avoiding *in vivo* testing. Some works about this topic have already been published, although there is a lack of studies regarding ionizable solutes. For this reason, the feasibility of this methodology to estimate biopartitioning properties for ionized compounds will also be evaluated. Particularly, in the present work, the estimation of the octanol-water distribution coefficient of ionized acid-base substances will be studied.

As a result of the research conducted during the last years, 7 scientific papers have been developed based on this topic (5 of them already published in peer-review scientific journals), which represent the bulk of the thesis.

First of all, chromatographic and biopartitioning systems characterized in previous works through the solvation parameter model have been compiled, adding the new developed and characterized systems in the present study. Then, all the systems have been compared using the normalized coefficients resulting from their characterization through the solvation parameter model. Mathematical treatment has allowed selecting those chromatographic systems that could surrogate best the biopartition of solutes in processes of interest such as the toxicity to aquatic species, the skin partition, and the octanol-water partition. Finally, correlations between the biological property of interest and the logarithm of the retention factor determined in the selected chromatographic system have been established. The results have shown that aquatic toxicity for 5 representative aquatic organisms (Rana tadpoles, Fathead minnow, *Daphnia magna (24h)*, *Tetrahymena pyriformis*, and *Pseudomonas putida*) can be estimated employing three systems based on micellar electrokinetic chromatography (using as surfactant sodium taurocholate, tetradecyltrimethylammonium bromide, and a mixture of sodium dodecyl sulfate and polyoxyethylene lauryl ether), and one based on reversed-phase liquid

chromatography (employing a column with an immobilized artificial membrane). Skin partition can be surrogated by a lecithin-based microemulsion electrokinetic chromatography system. The octanol-water partition coefficient can be estimated through two different microemulsion electrokinetic chromatography systems (with a pseudostationary phase composed of either sodium dodecyl sulfate or tetradecyltrimethylammonium bromide, 1-butanol, and heptane).

Regarding the octanol-water partition coefficient, the feasibility of the previous microemulsion electrokinetic chromatography systems to estimate the parameter for ionized compounds has been evaluated. With this aim, retention factor-p*H* profiles have been established for a set of monoprotic acids and bases. In these studies, to avoid ion-pairing, the surfactant used to prepare the microemulsion and the ionized solute have the same charge. In order to calculate the retention factor in this system, the electrophoretic mobility of a compound has to be measured in two different solutions with different viscosities. Since the electrophoretic mobility depends on the viscosity of the medium, a viscosity correction factor needs to be used to obtain accurate retention factors.

In previous studies, a direct log $P_{o/w}$-log k correlation was obtained using a set of representative neutral compounds. In this work, it has been tested the feasibility of this equation to estimate the octanol-water distribution coefficient of ionized compounds. The estimated values of some model compounds have been compared to data from the literature determined by reference methods (mainly by the shake-flask method). Results point out that accurate estimations of the parameter can be achieved up to a 99% of ionization (when the compound is partially ionized), but it is overestimated when the solutes are highly or fully ionized (approximately 100%).

Finally, in order to look for new chromatographic systems presenting different selectivities to those previously used, a stay at Bio-Analytical Separation Science research group of professor Sebastiaan Eeltink at the *Vrije Universiteit Brussel* (VUB) in Brussels (Belgium) has been done. During the stay, an in-house styrene-co-divinylbenzene monolithic capillary column has been developed and characterized for the separation of a mixture of proteins by ion-pairing gradient reversed-phase liquid chromatography. In this work, the influence of the factors affecting the separation performance such as the selection of the ion-pairing agent, the loadability of the column, and the effect of the gradient volume have been evaluated. On one

hand, when trifluoroacetic acid is used as ion-pairing agent, better peak-symmetry, narrower peaks, and a better loadability have been obtained compared to formic acid. On the other hand, when gradient analysis is used the highest efficiencies have been obtained at flow rates 20 times higher than the estimated optimum flow rate by the Van Deemter equation in isocratic mode. This is possible since the efficiency is a compromise between the magnitude of the mass-transfer contribution and the gradient-volume effect.

INTRODUCCIÓ

4.1 Sistemes de partició

La partició es pot definir com la distribució d'un compost entre dues fases immiscibles. Aquesta distribució depèn de l'afinitat de cada compost per cadascuna de les fases. Així, generalment, els sistemes de partició estan formats per dues fases de diferent polaritat: una més polar (en la majoria de casos aquosa) i una de menys polaritat (sovint de caràcter orgànic).

4.1.1 Sistemes de biopartició

En molts sistemes biològics, els soluts experimenten una partició entre una fase fonamentalment aquosa i una membrana biològica (de caràcter apolar), el que conforma un sistema de biopartició. L'estudi d'aquests sistemes esdevé de gran importància en àmbits com el farmacèutic i l'ambiental.

Alguns dels sistemes de partició més importants en l'àmbit farmacèutic són la permeabilitat de la pell [1], l'absorció intestinal [2] i la distribució sang-cervell [3]. La determinació dels paràmetres relacionats amb aquests sistemes permeten determinar quines substàncies poden ser més permeables a les membranes biològiques i ser, per tant, potencials futurs fàrmacs.

Pel que fa a l'àmbit ambiental destaquen la sorció sòl-aigua [4,5] i la toxicitat aquàtica, mesurada a partir de diferents organismes aquàtics incloent-hi peixos [6–8], capgrossos [9–14], protozous [15–17], bacteris [16,18,19] i puces d'aigua [7,16]. A partir d'aquests organismes es pot predir o avaluar els efectes tòxics de compostos generats tant de l'activitat industrial com de la d'origen natural.

En general, l'estudi directe de la partició en medis biològics és complex, ja que els resultats obtinguts en aplicar metodologies experimentals en aquest tipus de medis presenten altes variabilitats i alts errors. A més, aquestes metodologies generalment comporten temps d'anàlisi llargs i, en utilitzar éssers vius, són èticament qüestionables. A causa de tots aquests inconvenients, és necessari desenvolupar mètodes amb sistemes alternatius, com ara la partició en un sistema cromatogràfic o entre dos solvents, que puguin subrogar diferents processos de biopartició.

D'aquesta manera es poden estimar diferents paràmetres de biopartició d'una manera més senzilla, ràpida i automatitzada.

Perquè això sigui possible s'ha d'establir una correlació entre la propietat de biopartició en estudi i una propietat fisicoquímica emprant compostos model tal com es pot apreciar a la Figura 1. D'aquesta manera, si es coneix el valor de la propietat fisicoquímica per a un nou compost, és possible interpolar a l'equació de correlació i estimar la propietat de biopartició.

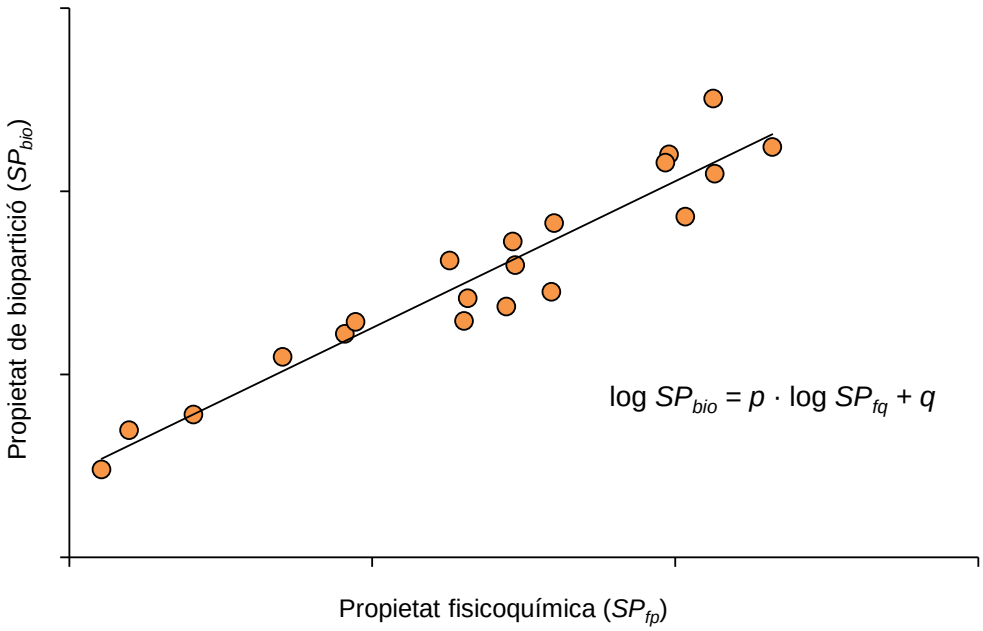

Figura 1. Correlació entre la propietat de biopartició (SP_{bio}) i la fisicoquímica (SP_{fq}).

4.1.2 Sistema de partició octanol-aigua

D'entre els sistemes de partició fisicoquímics, per la seva similitud al sistema medi aquós-membrana biològica, destaca el sistema de partició octanol-aigua [20]. En aquest sistema els diferents compostos experimenten una partició entre una fase octanòlica i una fase aquosa (Figura 2).

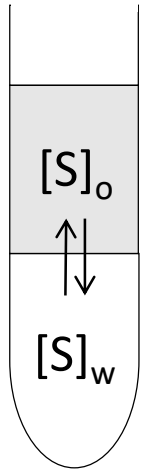

Figura 2. Representació de la partició octanol-aigua (o-w) d'un solut (S).

Com que l'1-octanol presenta una estructura similar als lípids que són part estructural de les membranes biològiques, cap polar i cua hidrofòbica [21], la partició octanol-aigua esdevé directament relacionada amb la lipofilicitat [22]. La lipofilicitat, que es defineix com la facilitat d'un compost a dissoldre's en greixos i solvents no polars [23], és una propietat clau en l'estudi i desenvolupament de nous fàrmacs. Aquesta propietat permet estudiar la facilitat que tenen els compostos per penetrar les diferents membranes biològiques (formades principalment per bicapes lipídiques).

Per avaluar la partició d'un solut en la fase octanòlica s'utilitza com a paràmetre el coeficient de partició octanol-aigua ($P_{o/w}$), que es calcula de la manera següent [20]:

$$P_{o/w} = \frac{[S]_o}{[S]_w} \qquad \text{Eq. 1}$$

On $[S]_o$ i $[S]_w$ són, respectivament, la concentració del solut en la fase octanòlica i aquosa. Com que els valors de $P_{o/w}$ poden ser molt diferents, sovint s'expressa el seu valor com a log $P_{o/w}$. Com més alt sigui el valor del log $P_{o/w}$, més afinitat tindrà el compost per la fase orgànica i més lipòfil serà.

S'ha de tenir en compte que aquest paràmetre és exclusiu per a substàncies neutres o totalment ionitzades. En el cas que la substància es trobi parcialment ionitzada

aquest paràmetre passa a denominar-se coeficient de distribució octanol-aigua ($D_{o/w}$). En substàncies ionitzables el valor de log $D_{o/w}$ disminueix, seguint una funció sigmoide, a mesura que augmenta el grau de ionització del compost, ja que els compostos que estan carregats tenen més afinitat per la fase polar (la fase aquosa) que no pas per la de caràcter orgànic (1-octanol). En el cas dels compostos àcids el valor de log $D_{o/w}$ disminueix a mesura que augmenta el p*H*, a diferència de les bases en el que el seu valor augmenta a p*H*s més elevats [24]. A la Figura 3 es mostra de manera esquemàtica l'evolució del valor de log $D_{o/w}$ al llarg de l'escala de p*H* de l'àcid benzoic [25].

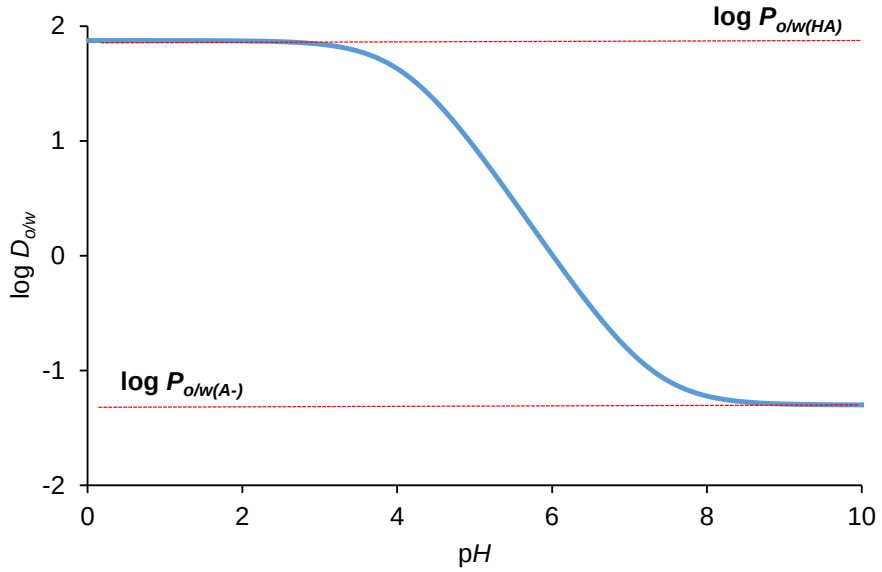

Figura 3. Perfil log $D_{o/w}$-p*H* de l'àcid benzoic [25].

La manera tradicional i de referència per determinar aquest paràmetre és per mitjà del mètode *shake-flask* [26], en el què el compost es dissol en un recipient que conté tant l'octanol (saturat d'aigua) com la fase aquosa (saturada d'octanol) i s'agita. Després d'arribar a l'equilibri, s'analitza la concentració del compost en estudi en cada una de les fases i es calcula el coeficient de partició octanol-aigua a partir de l'Eq. 1. Tot i ser la manera directa d'obtenir el valor de log $P_{o/w}$, aquest mètode

presenta una sèrie d'inconvenients: i) Requereix força temps d'anàlisi, ii) tècnicament és tediós i iii) no està completament automatitzat. A causa d'aquests inconvenients, s'han desenvolupat altres metodologies alternatives a aquest procediment com per exemple els mètodes potenciomètrics, amb molta popularitat entre els compostos àcid-base [27], i l'estimació mitjançant mètodes cromatogràfics [28].

4.1.3 Sistemes de partició cromatogràfics

Un gran grup de sistemes de partició fisicoquímics el componen els sistemes cromatogràfics. En aquests sistemes els compostos particionen entre una fase mòbil i una fase estacionària o pseudoestacionària (si aquesta presenta una mobilitat pròpia dintre del sistema de partició) de diferent polaritat. Generalment, la fase estacionària o pseudoestacionària és més apolar que no pas la mòbil (que sol ser de caràcter aquós). Dintre d'aquest grup es troben, entre d'altres, els sistemes de cromatografia electrocinètica (EKC, en anglès *electrokinetic chromatography*) i de cromatografia líquida d'alta resolució (HPLC, en anglès *high-performance liquid chromatography*).

4.1.3.1 Cromatografia electrocinètica

La cromatografia electrocinètica es basa en l'electroforesi capil·lar [29] (CE, en anglès *capillary electrophoresis*), on s'aplica una diferència de potencial entre els extrems d'un capil·lar de sílice ple d'una solució d'un electròlit. En aplicar aquesta diferència de potencial, els compostos se separen en funció de la seva relació massa/càrrega. Com que els grups silanol de la paret de sílice del capil·lar es troben desprotonats, ja que prèviament es passa per l'interior del capil·lar una solució bàsica diluïda, es genera una capa de cations de l'electròlit al voltant de la paret interna del capil·lar. Quan s'aplica una diferència de potencial positiva, aquests cations són atrets cap al pol negatiu (càtode) i, per tant, es mouen cap aquest pol arrossegant tot el volum de la solució. Aquest flux generat s'anomena flux electroosmòtic (EOF, en anglès *electroosmotic flow*). Tal com es mostra a la Figura 4, primer eluiran els soluts catiònics (ja que a part de la mobilitat deguda al EOF, també tindran una mobilitat pròpia, perquè són atrets pel pol negatiu), després eluirien les substàncies

neutres (a la mateixa velocitat del EOF) i per últim els anions (els quals es trobaran atrets pel pol positiu). A la vegada els anions i cations se separaran entre si en funció de la seva relació massa/càrrega. A igualtat de càrrega, els ions més petits se sentiran més fortament atrets pel corresponent elèctrode. Quan es treballa en CE amb només tampó aquós, el mode d'anàlisis s'anomena electroforesi capil·lar en zona (CZE, en anglès *capillary zone electrophoresis*) [30,31].

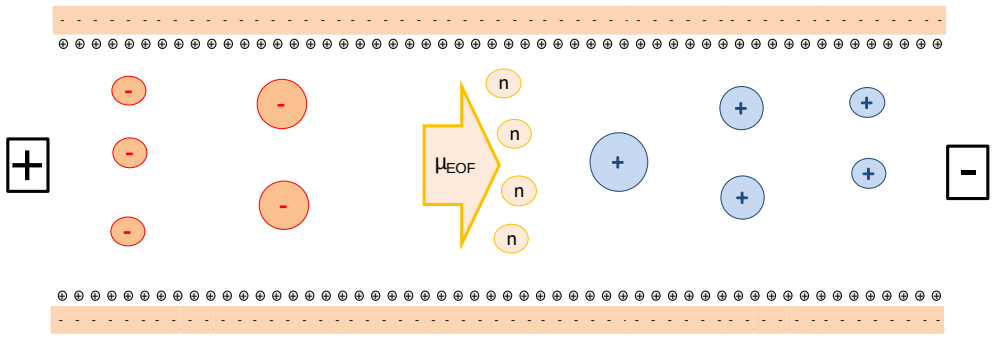

Figura 4. Migració de compostos amb diferents relacions massa/càrrega en CZE.

La mobilitat electroforètica (μ) dels compostos es pot quantificar a partir de la següent equació:

$$\mu = \left[\frac{1}{t_m} - \frac{1}{t_{eof}}\right] \cdot \left[\frac{L_T L_D}{V}\right] \qquad \text{Eq. 2}$$

On L_T i L_D representen, respectivament, la longitud total i efectiva del capil·lar de sílice i V el voltatge aplicat. L_D correspon a la porció del capil·lar que va des de l'inici fins a la finestra de detecció. t_m representa el temps de migració del compost i t_{eof} el temps que triga en eluir el marcador de flux electroosmòtic. Com a marcador de flux electroosmòtic s'utilitzen generalment compostos petits, polars i neutres, com per exemple el dimetil sulfòxid, el metanol, l'acetonitril (ACN) o la formamida [32]. D'acord amb l'Eq. 2, quan s'apliquin diferències de potencial positives, sent el càtode l'elèctrode situat a l'extrem de la finestra del detector, s'obtindran mobilitats positives pels compostos carregats positivament, negatives pels carregats negativament i igual a 0 pels soluts neutres.

La mobilitat electroforètica depèn a la vegada d'altres paràmetres, com per exemple la viscositat (η) de la solució de l'interior del capil·lar. Aquests dos paràmetres estan relacionats segons l'equació següent [31,33]:

$$\mu = \frac{q}{6\pi\eta r} \qquad \text{Eq. 3}$$

On q i r són, respectivament, la càrrega i el radi de l'ió. Per tant, si es realitzen mesures d'un mateix compost en medis que tenen diferent viscositat, μ variarà inversament proporcional a aquesta.

La CZE permet separar compostos que es troben carregats però no compostos neutres, ja que tots ells migraran a la vegada i juntament amb el marcador del flux electroosmòtic. Per aquest motiu, s'han desenvolupat sistemes alternatius basats en la CE anomenats sistemes de cromatogràfica electrocinètica [34]. Aquests sistemes cromatogràfics, a diferència dels d'electroforesi capil·lar en zona, se li afegeix a la fase aquosa una fase pseudoestacionària (FP) que poden ser micel·les, microemulsions (ME), liposomes, etc., fases més hidrofòbiques que l'aquosa. Aquestes s'anomenen fases pseudoestacionàries, ja que es troben carregades i tenen una pròpia mobilitat en el sistema. Aleshores, els compostos no només són separats en funció de la seva relació massa/càrrega, sinó també per la partició que ells experimenten entre la fase pseudoestacionària i la fase aquosa. A la Figura 5 es representa com se separen diferents soluts neutres (S1, S2, S3) en un sistema EKC amb una fase pseudoestacionària aniònica.

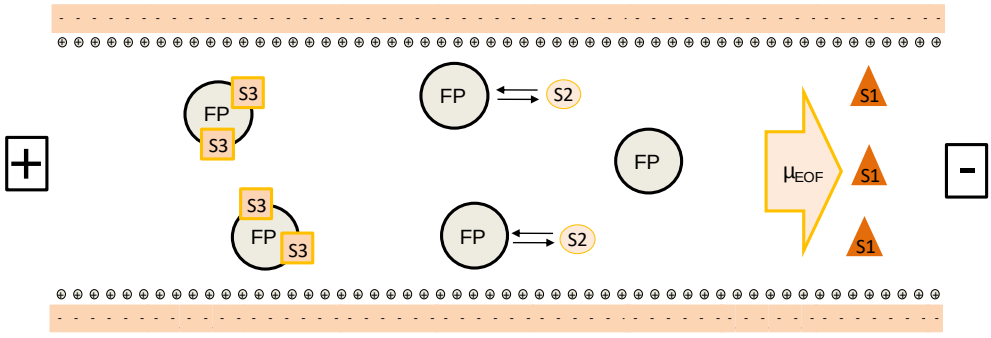

Figura 5. Separació de compostos neutres en un sistema EKC.

A la Figura 5, el solut 1 (S1) no interacciona amb la fase pseudoestacionària i, per tant, eluirà conjuntament amb el flux electroosmòtic, més tard es detectarà el solut 2 (S2) que experimenta una partició entre el tampó aquós i la fase pseudoestacionària. El solut (S3) serà l'últim compost a sortir del capil·lar, ja que interacciona totalment amb la fase pseudoestacionària i migrarà a la mateixa velocitat que aquesta. Així doncs, els compostos neutres no eluiran tots junts, tal com passava en CZE, sinó que ho faran en funció de la seva afinitat per la fase pseudoestacionària.

Per quantificar la partició que experimenten els soluts neutres en la fase pseudoestacionària, tal com passa en cromatografia líquida, s'utilitza com a paràmetre el factor de retenció (*k*) i es calcula utilitzant la següent equació [35]:

$$k = \frac{(t_m - t_{eof})}{\left(1 - \frac{t_m}{t_{fp}}\right) \cdot t_{eof}} \qquad \text{Eq. 4}$$

t_{fp} és el temps que triga a eluir la fase pseudoestacionària, i es determina a través d'un marcador. La dodecanofenona ha estat seleccionada com el millor marcador de la fase pseudoestacionària, ja que és un solut gran i molt hidrofòbic que interacciona totalment amb aquesta [32]. Aquells soluts que interaccionin més amb la fase pseudoestacionària i que, per tant, presentin valors de *k* alts presentaran temps de migració propers al t_{fp}, mentre que les substàncies que pràcticament no interaccionin amb la fase pseudoestacionària presentaran valors de *k* petits i temps de migració iguals al t_{eof}. Per tant, tots els compostos neutres tindran un temps de migració entre el t_{eof} i el t_{fp}, interval de temps anomenat finestra d'elució.

Les substàncies que es troben carregades, a part de l'afinitat per la fase pseudoestacionària, presenten una mobilitat pròpia a causa del camp elèctric aplicat. Per aquest motiu s'ha proposat una altra equació per calcular *k* de compostos àcid-base [36,37].

$$k = \frac{\mu - \mu_0}{\mu_{fp} - \mu} \qquad \text{Eq. 5}$$

On μ i μ_{fp} són, respectivament, la mobilitat electroforètica del compost i la fase pseudoestacionària en el sistema EKC. En canvi, μ_0 és la mobilitat del compost en

la mateixa solució però sense afegir la fase pseudoestacionària, és a dir, en el tampó aquós (mode CZE).

Tal com és conegut [36,38], el valor de *k* varia en funció del grau de ionització d'un compost (*α*). *k* generalment és major, en sistemes EKC, quan el compost es troba en la seva forma neutra que no pas quan es troba ionitzat. Per a un àcid monopròtic, *k* es defineix com la mitjana ponderada del factor de retenció de l'espècie totalment ionitzada ($k_{(A^-)}$) i l'espècie neutra ($k_{(HA)}$) (Eq. 6):

$$k = \alpha_{(\mathrm{HA})} k_{(HA)} + \alpha_{(\mathrm{A}^-)} k_{(A^-)} \qquad \text{Eq. 6}$$

On $\alpha_{(A^-)}$ i $\alpha_{(HA)}$ són, respectivament, les fraccions molars de l'espècie totalment ionitzada i neutra de l'àcid. Les fraccions molars es poden calcular, coneixent la constant d'acidesa aparent (K_a') de l'àcid a qualsevol p*H*, utilitzant les equacions següents:

$$\alpha_{(\mathrm{HA})} = \frac{[\mathrm{H}^+]}{[\mathrm{H}^+]+K_a'} \qquad \text{Eq. 7}$$

$$\alpha_{(\mathrm{A}^-)} = \frac{K_a'}{[\mathrm{H}^+]+K_a'} = 1 - \alpha_{(HA)} \qquad \text{Eq. 8}$$

Finalment si les Eqs. 7-8, se substitueixen a l'Eq. 6, s'obté la següent expressió:

$$k = \frac{k_{(HA)}+k_{(A^-)}\cdot 10^{\mathrm{pH}-\mathrm{p}K_a'}}{1+10^{\mathrm{pH}-\mathrm{p}K_a'}} \qquad \text{Eq. 9}$$

Seguint la mateixa deducció, el factor de retenció per a bases monopròtiques variaria en funció del p*H* en funció de l'equació següent:

$$k = \frac{k_{(BH^+)}+k_{(B)}\cdot 10^{\mathrm{pH}-\mathrm{p}K_a'}}{1+10^{\mathrm{pH}-\mathrm{p}K_a'}} \qquad \text{Eq. 10}$$

On, $k_{(BH+)}$ i $k_{(B)}$ són, respectivament, el factor de retenció de l'espècie totalment protonada i neutra d'un compost bàsic. De manera que, a partir de les Eqs. 9 i 10, podrem calcular el factor de retenció d'un compost àcid-base monopròtic a qualsevol valor de p*H* i, per tant, a qualsevol grau de ionització dels compostos.

- Modalitats de cromatografia electrocinètica

En funció de la fase pseudoestacionària utilitzada es pot parlar principalment de: i) cromatografia electrocinètica micel·lar (MEKC, en anglès *micellar electrokinetic chromatography*) [35,39]; ii) cromatografia electrocinètica de microemulsions (MEEKC, en anglès *microemulsion electrokinetic chromatography*) [40] i iii) cromatografia electrocinètica de liposomes (LEKC, en anglès *liposome electrokinetic chromatography*) [41]. A part d'aquestes modalitats se'n poden trobar d'altres de menys importants com les basades en polímers (poly-EKC, en anglès *polymeric electrokinetic chromatography*) [42] i en vesícules (VEKC, en anglès *vesicular electrokinetic chromatography*) [43].

En MEKC s'utilitzen micel·les com a fase pseudoestacionària [44]. Les micel·les són agregats de tensioactius (que poden ser tant neutres, com aniònics o catiònics) que es formen quan es troben en una concentració superior a la concentració micel·lar crítica (CMC, en anglès *critical micelle concentration*). En general, els caps polars dels tensioactius es troben orientats cap a la fase aquosa, mentre que les cues hidrofòbiques conformen el nucli de la micel·la, tal com es pot veure a la Figura 6.

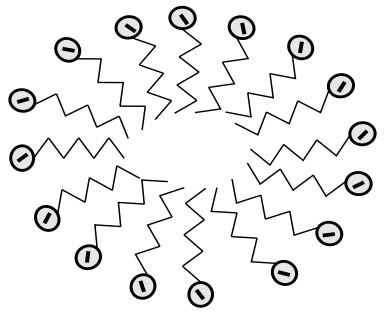

Figura 6. Estructura d'una micel·la.

En MEEKC la microemulsió conforma la fase pseudoestacionària [45]. La microemulsió és un agregat format per un tensioactiu, un cotensioactiu i un oli en solució aquosa. Tal com es mostra a la Figura 7, l'oli i les parts hidrofòbiques dels

tensioactius constitueixen el nucli de la microemulsió, mentre que els caps polars se situen a la seva superfície i són els que estan en contacte amb el medi aquós.

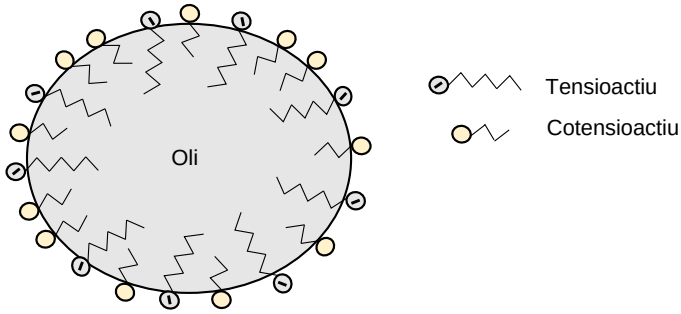

Figura 7. Estructura de la microemulsió.

En LEKC són els liposomes els que constitueixen la fase pseudoestacionària [41]. Els liposomes estan formats per fosfolípids que, en presència d'una fase aquosa, formen una sèrie d'agregats esfèrics consistents en una o més bicapes lipídiques amb una unitat aquosa encapsulada al seu interior [46,47]. Els grups polars dels fosfolípids s'orienten cap a les cares externa o interna de la bicapa, mentre que les cues hidrofòbiques s'orienten cap a l'interior evitant així el contacte amb la fase aquosa. Les propietats dels liposomes, tal com la càrrega superficial neta o la rigidesa d'aquests, varien en funció de la composició lipídica d'aquests. A la Figura 8 es mostra un esquema de l'estructura d'un liposoma.

Com que les membranes cel·lulars també estan constituïdes principalment per una doble capa de fosfolípids, aquests sistemes presenten una gran similitud amb els sistemes biològics.

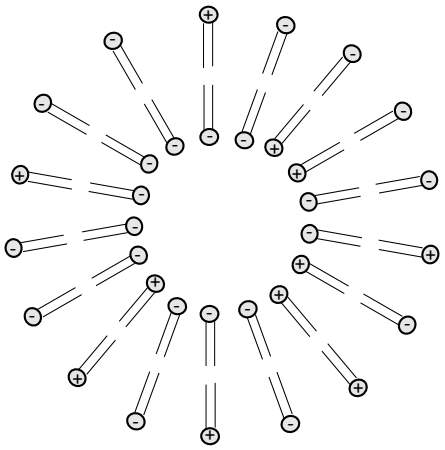

Figura 8. Estructura d'un liposoma.

Els sistemes MEKC, MEEKC i LEKC tenen aplicacions en la separació i identificació de compostos neutres i carregats [48–50], i també s'han utilitzat per a la subrogació de sistemes de biopartició, com la permeabilitat de la pell [51] i la toxicitat aquàtica [52,53], o altres paràmetres de referència com la partició octanol-aigua [54–58].

4.1.3.2 Cromatografia líquida d'alta resolució

En els sistemes de HPLC els compostos experimenten una partició entre la fase estacionària i la fase mòbil. Els compostos analitzats eluiran ràpidament si no interaccionen amb la fase estacionària, o presentaran temps d'elució superiors si experimenten partició amb aquesta. S'ha de tenir en compte que la naturalesa de la fase mòbil també juga un paper important en la partició que experimenten els soluts en el sistema. En funció de la polaritat de la fase estacionària i la fase mòbil els sistemes de cromatografia líquida es divideixen en cromatografia líquida de fase normal, si la fase estacionària és més polar que la fase mòbil, i en cromatografia líquida de fase inversa (RP-LC, en anglès *reversed-phase líquid chromatography*), si és a l'inrevés. Aquest treball se centrarà en sistemes de cromatografia de fase inversa. Altres modalitats de la cromatografia líquida en fase inversa s'obtenen en afegir a la fase mòbil micel·les o microemulsions donant lloc, respectivament, a la

cromatografia líquida micel·lar (MLC, en anglès *micellar liquid chromatography*) [59,60], i la cromatografia líquida de microemulsions (MELC, en anglès *microemulsion líquid chromatography*) [61]. En aquests casos les micel·les i la microemulsió fan la funció del dissolvent orgànic, restant-li polaritat a la fase mòbil.

Els sistemes cromatogràfics tenen un gran ventall d'aplicacions, sent la més habitual la separació de compostos per a la seva identificació o quantificació [62,63]. A més a més, s'han publicat una sèrie de treballs en els quals aquests sistemes han estat usats per estimar paràmetres de biopartició d'interès farmacològic i ambiental. El sistema HPLC amb una columna de membrana artificial immobilitzada (IAM, en anglès *immobilized artificial membrane column*) s'ha usat en l'estimació de la distribució sang-cervell d'alguns fàrmacs [64]. Mentrestant, el sistema de HPLC amb una columna C18 (cadenes d'octadecilsilà unides a la sílice) ha resultat òptim per a l'estimació de la partició octanol-aigua [65] i la permeabilitat de la pell [66,67]. També per un sistema basat en RP-LC utilitzant una columna modificada amb fosfolípids (columna PLM, en anglès *phospholipid modified column*) s'han observat bones correlacions entre el valor de log $P_{o/w}$ i el log *k* mesurat en aquest sistema cromatogràfic [68].

Per poder determinar el grau d'interacció d'un compost amb la fase estacionària s'utilitza com a paràmetre el factor de retenció (*k*), que es calcula a partir de la següent expressió:

$$k = \frac{n_S}{n_M} = \frac{t_R - t_0}{t_0 - t_{ext}} \qquad \text{Eq. 11}$$

On n_S i n_M són el nombre mitjà de mols del solut a la fase estacionària i mòbil, respectivament. t_R és el temps de retenció (temps que triga a eluir el solut i és característic de cada compost), t_0 és el temps mort (temps que triga a eluir un compost que no interacciona gens amb la fase estacionària), i t_{ext} és el temps extra-columna (temps que triga un compost a eluir sense la columna cromatogràfica). De vegades t_{ext} és molt petit i se simplifica l'Eq. 11 considerant-lo igual a 0.

4.2 Model de paràmetres de solvatació.

La partició d'un compost entre dues fases condensades diferents dependrà de l'habilitat que tingui el solut a dissoldre's en cadascuna d'elles. Aquest procés, també anomenat procés de solvatació (Figura 9), consta dels següents passos [69,70]:

i. Formació de la cavitat per acomodar la molècula del solut, que requerirà el trencament de les interaccions solvent-solvent de la fase receptora. Si aquestes interaccions són fortes, el procés de dissolució del solut en aquesta fase estarà desfavorit.
ii. Introducció del solut a la cavitat.
iii. Establiment de les interaccions solut-solvent a la fase receptora.

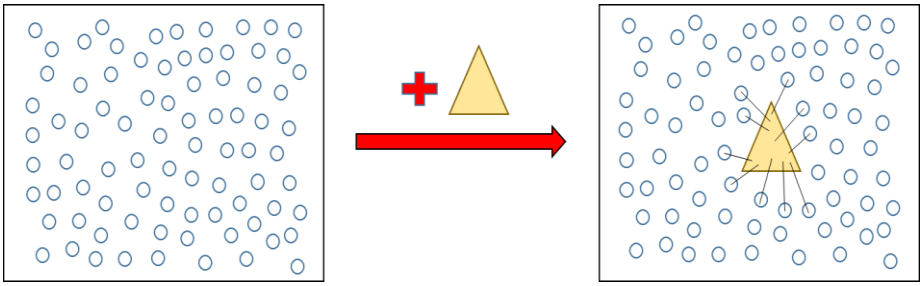

Figura 9. Procés de solvatació

Per avaluar les diferents interaccions existents entre les molècules del solut i del dissolvent, els diferents sistemes de partició es poden caracteritzar a partir del model de paràmetres de solvatació (SPM, en anglès *solvation parameter model*) proposat per Abraham *et al.* [69,71]. En aquest model QSPR (en Anglès, *quantitative structure – property relationships*) a cada tipus d'interacció se li assigna un paràmetre diferent [69,72–76], obtenint per a cada sistema una equació amb l'estructura següent:

$$log\ SP = ct + eE + sS + aA + bB + vV \qquad \text{Eq. 12}$$

On *SP* és la propietat de partició del solut en un sistema determinat. Les lletres majúscules (*E*, *S*, *A*, *B* i *V*) són els descriptors que defineixen les propietats fisicoquímiques dels soluts. *E* representa la refractivitat molar en excés, *S* la

dipolaritat/polaritzabilitat, *A* i *B* representen, respectivament, l'acidesa i la basicitat per pont d'hidrogen, i *V* és el volum de McGowan del solut. Els coeficients (*e*, *s*, *a*, *b* i *v*) són característics del sistema de partició caracteritzat i indiquen les propietats del sistema complementàries al descriptor que acompanyen, i *ct* és una constant que depèn de la relació de fases. Estudiant els valors de cadascun dels coeficients es poden determinar les diferències entre les fases que conformen el sistema de partició. La magnitud i el signe de cadascun dels paràmetres de l'equació indiquen, respectivament, com és d'important el paràmetre en la interacció i quina de les dues fases del sistema de partició presenta una major afinitat per interaccionar amb el solut.

L'Eq. 12 pot fer-se servir per a diferents finalitats [71,77]:

i. Predicció de propietats de partició de nous soluts, un cop establerta per a un sistema de partició concret.
ii. Caracterització de nous sistemes de partició.
iii. Disseny i desenvolupament de compostos biològicament més actius.
iv. Comparació de diferents sistemes i avaluació sobre quins comparteixen característiques similars.

Fuguet *et al.* [78,79] van realitzar un estudi per anàlisi de components principals (PCA, en anglès *principal component analysis*) en el qual a partir d'un conjunt de 2975 compostos diferents, dels quals es coneixien els descriptors, es van seleccionar 71 soluts com a subgrup representatiu. Aquest subconjunt cobria tot l'espai químic del PCA establert pel total de compostos. A part, el conjunt de soluts seleccionats presenta una distribució uniforme per a cadascun dels descriptors.

Per poder caracteritzar un sistema, a part dels descriptors del solut, es necessita el valor de la propietat de partició. Generalment aquesta és el factor de retenció pels sistemes cromatogràfics, però poden ser altres paràmetres relacionats amb una partició en sistemes biològics o ambientals. Per tant, a partir d'una regressió lineal múltiple entre la propietat de partició i els descriptors del grup de soluts representatiu es poden obtenir els coeficients d'un sistema. A la Taula 1 es mostra una recerca bibliogràfica de sistemes cromatogràfics que estiguessin caracteritzats pel SPM i a la Taula 2 es mostren els coeficients i les dades estadístiques resultants de les caracteritzacions dels sistemes de la Taula 1. A continuació, a la Taula 3 es mostren

els coeficients i les dades estadístiques d'un conjunt de sistemes de biopartició, tant d'interès farmacèutic com ambiental, caracteritzats a partir del mateix model.

En el cas dels sistemes cromatogràfics (Taula 2) i per tots els sistemes considerats, els principals descriptors que defineixen la partició dels soluts entre les dues fases dels sistemes són el volum de McGowan (*V*) i la basicitat per pont d'hidrogen (*B*). El primer afavoreix la partició del compost a la fase estacionaria o pseudoestacionària induint a una major retenció del compost (coeficient positiu), mentre que la basicitat per pont d'hidrogen (coeficient negatiu) no afavoreix aquesta partició fent que els compostos amb alts valors de *B* presentin factors de retenció més baixos. Respecte als altres coeficients, destacar les diferències observades entre els diferents sistemes fisicoquímics pel coeficient *a* (presenten valors positius o negatius en funció del sistema estudiat). En canvi, els coeficients *e* i *s* tenen sempre, respectivament, valors positius o negatius. En relació als sistemes de biopartició (Taula 3) els coeficients *b* i *v* segueixen la mateixa tònica que en els sistemes cromatogràfics, sent els que més influeixen en la partició dels compostos entre la fase de caràcter aquós i l'orgànica. També, s'observa una major variabilitat entre sistemes respecte a la magnitud i signe dels altres 3 coeficients (*a*, *s* i *e*).

Taula 1. Selecció d'alguns sistemes cromatogràfics de la bibliografia que han estat caracteritzats a partir del SPM.

Abreviatura	Técnica de separació	Fase mòbil	Fase estacionària o pseudoestacionària	Referències
RP18	LC	CH_3CN:tampó fosfat	C18[1]	[80]
IAM	LC	CH_3CN: tampó fosfat	IAM[2]	[80]
PLM	LC	tampó fosfat:CH_3OH 8:2	PLM[3]	[68]
SDS	MEKC	tampó fosfat	SDS[4]	[78,79]
SLN	MEKC	tampó fosfat	SLN[5]	[81]
STC	MEKC	tampó fosfat	STC[6]	[53]
TTAB	MEKC	tampó fosfat	TTAB[7]	[78,79]
SDSBrij	MEKC	tampó fosfat/borat	SDS:Brij 35[8]	[82]
SDS0.8	MELC	SDS, butanol, 0.80% heptà	C18	[83]
SDS1.6	MELC	SDS C18, butanol, 1.60% heptà	C18	[83]
Brij	MELC	Brij 35, butanol, heptà	C18	[83]
BrijSDS	MELC	Brij 35 SDS, butanol, heptà	C18	[83]
SDSME	MEEKC	tampó fosfat/borat	SDS, butanol, heptà	[54]
DGDCChol	LEKC	Tampó àcid 2-[4-(2-hidroxietil)piperazin-1-il]etasulfònic	DPPG[9]:DPPC[10]:Chol[11]	[84]
DGDC	LEKC	Tampó àcid 2-[4-(2-hidroxietil)piperazin-1-il]etasulfònic	DPPG:DPPC	[84]
PAAU	LEKC	tampó fosfat/borat	PAAU[12]	[85]
PSUA	LEKC	tampó fosfat/borat	PSUA[13]	[85]

Abreviatura	Técnica de separació	Fase mòbil	Fase estacionària o pseudoestacionària	Referències
DHP	VEKC	Tampó tris(hidroxi-metil)aminometà	DHP[14]	[86]
DHPChol	VEKC	Tampó tris(hidroxi-metil)aminometà	DHP:Chol	[86]
POPC/PS	VEKC	Tampó àcid 2-[4-(2-hidroxietil)piperazin-1-il]etasulfònic	POPC[15]/PS[16]	[87]
AGESS	Poly-EKC	tampó fosfat/borat	AGESS[17]	[88]

[1]Cadenes d'octadecilsilà; [2]Membrana artificial immobilitzada; [3]Columna modificada de fosfolípids; [4]Dodecilsulfat de sodi; [5]*N*-lauroilsarcosinat de sodi; [6]Taurocolat de sodi; [7]Bromur de tetradeciltrimetilamoni; [8]Èter de dodecilpolioxietilè(23); [9]Dipalmitoilfosfatidilglicerol; [10]Dipalmitoilfosfatidilcolina; [11]Colesterol; [12]Poli(11-acrilamidaundecanoat de sodi); [13]Poli(10-undecilenat de sodi); [14]Dihexadecilfosfat; [15]1-palmitoil-2-oleil-sn-glicero-3-fosfocolina; [16]Fosfatidil serina; [17]Siloxà modificat amb sulfat de dodecà alil glicidil èter.

Taula 2. Paràmetres i dades estadístiques (número de punts de la correlació, n; coeficient de determinació, R^2; desviació estàndard, SD i paràmetre F de Fisher, F) resultants de caracteritzar diferents sistemes cromatogràfics a partir del SPM.

Sistema fisicoquímic	Paràmetre fisicoquímic	Coeficients						Dades estadístiques				Referència
		c	*e*	*s*	*a*	*b*	*v*	n	R^2	SD	F	
RP18	log *k*	-0,172	0,233	-0,460	-0,260	-1,574	1,582	55	0,992	0,056	1121	[80]
IAM	log *k*	-0,710	0,292	-0,344	0,141	-1,193	1,161	51	0,982	0,047	480	[80]
PLM	log *k*	-0,32	0,56	-0,70	0,34	-3,16	3,17	38	0,97	0,14	230	[68]
SDS	log *k*	-1,680	0,558	-0,596	-0,266	-1,674	2,717	63	0,982	0,120	618	[78,79]
SLN	log *k*	-1,99	0,44	-0,39	0,45	-2,32	2,92	36	0,98	0,06	-	[81]

Sistema fisicoquímic	Paràmetre fisicoquímic	Coeficients						Dades Estadístiques				Referència
		c	*e*	*s*	*a*	*b*	*v*	n	R^2	SD	F	
STC	log *k*	-1,838	0,613	-0,513	0,319	-2,396	2,390	56	0,968	0,112	305	[53]
TTAB	log *k*	-1,851	0,902	-0,617	0,766	-2,410	2,634	53	0,988	0,089	746	[78,79]
SDSBrij	log *k*	-1,412	0,622	-0,516	0,308	-2,699	2,829	27	0,974	0,105	154	[82]
SDS0.8	log *k*	0,665	0,117	-0,454	-0,495	-0,877	0,751	26	0,984	0,050	243	[83]
SDS1.6	log *k*	0,727	0,101	-0,645	-0,922	-0,951	0,901	26	0,980	0,078	205	[83]
Brij C18	log *k*	0,698	-0,003	-0,412	-0,415	-0,912	0,887	26	0,972	0,064	141	[83]
BrijSDS C18	log *k*	0,706	0,027	-0,399	-0,474	-0,842	0,773	26	0,980	0,054	189	[83]
SDSME	log *k*	-1,133	0,279	-0,692	-0,060	-2,805	3,048	53	0,988	0,090	791	[54]
DGDC	log *k*	-2,21	0,45	-0,44	0,71	-3,23	3,13	27	0,990	0,07	-	[84]
DGDCChol	log *k*	-2,30	0,54	-0,55	0,32	-3,12	3,01	27	0,980	0,08	-	[84]
PAAU	log *k*	-1,86	0,26	-0,16	-0,27	-1,05	2,11	18	0,994	0,051	403	[85]
PSUA	log *k*	-2,28	0,18	0,45	-0,15	-1,18	1,64	18	0,986	0,063	174	[85]
DHP	log *k*	-2,68	0,42	-0,65	0,47	-3,27	3,59	41	0,98	-	-	[86]
DHPChol	log *k*	-2,28	0,53	-0,77	0,43	-3,29	3,35	41	0,98	-	-	[86]
POPC/PS	log *k*	-2,04	0,70	-0,54	0,02	-2,90	2,68	26	0,97	-	-	[87]
AGESS	log *k*	-2,40	0,46	-0,43	0,27	-2,46	2,72	38	0,982	-	-	[88]

Taula 3. Paràmetres i dades estadístiques resultants de caracteritzar diferents sistemes de biopartició a partir del SPM.

Abreviatura	Sistema de biopartició	Paràmetre biològic	coeficients						Dades estadístiques				Referència
			c	*e*	*s*	*a*	*b*	*v*	n	R^2	SD	F	
BBD	Distribució sang-cervell	log *BB*[1]	0,044	0,511	-0,886	-0,724	-0,666	0,861	148	0,711	0,367	71	[89]
BBP	Permeació sang-cervell	log *PS*[2]	-0,639	0,312	-1,009	-1,895	-1,636	1,709	30	0,870	0,520	32	[90]
IA	Absorció intestinal	log *HIA*[3]	0,544	-0,025	0,141	-0,409	-0,514	0,204	127	0,799	0,290	94	[2]
SPA	Partició a la pell	log K_{sc}[4]	0,341	0,341	-0,206	-0,024	-2,178	1,850	45	0,925	0,216	97	[91]
SPE	Permeació a la pell	log K_p[5]	-5,426	-0,106	-0,473	-0,473	-3,000	2,296	119	0,832	0,461	112	[91]
RT	Narcosi en capgrossos	-log C_{nar}[6]	0,582	0,770	-0,696	0,243	-2,592	3,343	114	0,910	0,337	217	[92]
AP	Permeació en les cèl·lules d'alga	log K_{cel}[7]	-2,235	0,000	-0,867	-3,143	-1,664	0,731	100	0,885	0,437	183	[93]
SWP	Sorció sòl-aigua	log K_{oc}[8]	0,21	0,74	0,00	-0,31	-2,27	2,09	129	0,955	0,25	655	[94]
OW	$P_{o/w}$	log $P_{o/w}$	0,088	0,562	-1,054	0,034	-3,460	3,814	613	0,994	0,116	23162	[95]
Toxicitat aquàtica no específica envers:													
FM	Fathead minnow (*Pimephales promelas*)	-log *LC50*[9]	0,996	0,418	-0,182	0,417	-3,574	3,377	196	0,953	0,276	780	[6]
GP	Guppy (*Poecilia reticulata*)	-log *LC50*	0,811	0,782	-0,230	0,341	-3,050	3,250	148	0,947	0,280	493	[6]
BG	Bluegill (*Lepomis macrochirus*)	-log *LC50*	0,903	0,583	-0,127	1,238	-3,918	3,306	66	0,964	0,272	360	[6]
GO	Golden orfe (*Leuciscus idus melanotus*)	-log *LC50*	-0,137	0,931	0,379	0,951	-2,392	3,244	49	0,935	0,269	127	[6]
GF	Goldfish (*Carassius auratus*)	-log *LC50*	0,922	-0,653	1,872	-0,329	-4,516	3,078	51	0,966	0,277	254	[6]
MK48	Medaka high-eyes (*Oryzias latipes*)	-log *LC50* (48 h)	0,834	1,047	-0,380	0,806	-2,182	2,667	50	0,939	0,292	133	[6]
MK96	Medaka high-eyes (*Oryzias latipes*)	-log *LC50* (96 h)	-0,176	1,046	0,272	0,931	-2,178	3,155	44	0,960	0,277	182	[6]

Abreviatura	Sistema de biopartició	Paràmetre biològic	coeficients						Dades estadístiques				Referència
			c	*e*	*s*	*a*	*b*	*v*	n	R^2	SD	F	
DM24	*Daphnia magna*	-log *LC50* (24 h)	0,915	0,354	0,173	0,420	-3,935	3,521	107	0,953	0,274	410	[16]
DM48	*Daphnia magna*	-log *LC50* (48 h)	0,841	0,528	-0,025	0,219	-3,703	3,591	97	0,964	0,289	475	[16]
CD	*Ceriodaphnia dubia*	-log *LC50*	2,234	0,373	-0,040	-0,437	-3,276	2,763	44	0,935	0,256	111	[16]
DP	*Daphnia pulex*	-log *LC50*	0,502	0,396	0,309	0,542	-3,457	3,527	45	0,962	0,311	233	[16]
TP	*Tetrahymena pyriformis*	-log *IGC50*[10]	0,616	0,413	-0,048	0,348	-2,707	2,944	192	0,964	0,205	1002	[16]
SA	*Spirostomum ambiguum*	-log *LC50*	0,148	0,111	0,288	0,687	-3,301	3,140	60	0,958	0,246	252	[16]
ES	*Entosiphon sulcantum*	-log *IGC*[11]	0,489	0,894	0,355	1,108	-2,504	2,852	51	0,920	0,333	103	[15]
UP	*Uronema parduczi*	-log *IGC*	2,706	1,426	0,433	0,938	-1,025	2,599	59	0,924	0,326	127	[15]
CP	*Chilomonas paramecium*	-log *IGC*	0,440	1,129	0,160	0,442	-1,826	2,446	55	0,887	0,351	77	[15]
PP	*Pseudomonas putida*	-log *IGC*	0,752	0,955	0,092	-0,081	-2,088	2,947	87	0,927	0,269	209	[16]
Inhibició del creixement bacterià envers:													
PG	*Porphyromonas gingivalis*	-log *MIC*[12]	-3,320	1,111	-0,605	0,727	-1,904	2,423	126	0,906	0,313	232	[18]
SAr	*Selenomonas artemidis*	-log *MIC*	-3,008	0,982	-0,496	0,972	-2,643	2,312	116	0,870	0,268	149	[18]
SS	*Streptococcus sobrinus*	-log *MIC*	-3,465	0,855	-0,465	0,735	-1,671	2,330	112	0,903	0,309	196	[18]

[1]Coeficient de distribució sang-cervell; [2]Permeació a través de la barrera sang-cervell; [3]Absorció intestinal humana; [4]Coeficient de partició en la pell; [5]Coeficient de permeació a la pell; [6]Concentració de narcosi; [7]Coeficient de permeació cèl·lula-aigua; [8]Coeficient de sorció sòl-aigua; [9]Concentració letal de la meitat de la població; [10]Concentració inhibitòria del creixement de la meitat de la població; [11]Concentració inhibitòria del creixement; [12]Concentració mínima inhibitòria;

4.3 Comparació entre sistemes de partició.

Per avaluar la similitud existent entre diferents sistemes de partició, es poden utilitzar tot un seguit d'eines matemàtiques i estadístiques que comparen els coeficients dels sistemes caracteritzats a partir d'un model comú, com ara el SPM. El fet de comparar sistemes i detectar similituds és una tasca útil a l'hora de subrogar sistemes de partició complexos com ara els sistemes biològics.

4.3.1 Paràmetre de distància, *d*.

En treballs anteriors, Lázaro *et al.* [80] van presentar un procediment matemàtic per comparar sistemes que prèviament haguessin estat caracteritzats a partir del model de paràmetres de solvatació. Aquest es basa en el paràmetre distància *d* i representa la distància existent entre els vectors normalitzats de dos sistemes ($\overrightarrow{v_{uI}}$, $\overrightarrow{v_{uJ}}$), considerant-los en un espai de cinc dimensions (cadascuna corresponent a cadascun dels coeficients normalitzats e_u, s_u, a_u, b_u i v_u del SPM). L'ús dels coeficients normalitzats permet distribuir i ordenar els sistemes en funció de les seves selectivitats reduint el pes de la magnitud dels coeficients.

Els 5 components del vector normalitzat d'un sistema (e_u, s_u, a_u, b_u i v_u) es calculen seguint les següents expressions:

$$e_u = \frac{e}{l} \qquad \text{Eq. 13}$$

$$s_u = \frac{s}{l} \qquad \text{Eq. 14}$$

$$a_u = \frac{a}{l} \qquad \text{Eq. 15}$$

$$b_u = \frac{b}{l} \qquad \text{Eq. 16}$$

$$v_u = \frac{v}{l} \qquad \text{Eq. 17}$$

On *l* és la longitud del vector format pels coeficients del sistema:

$$l = \sqrt{e^2 + s^2 + a^2 + b^2 + v^2} \qquad \text{Eq. 18}$$

Per dos sistemes de partició (i, j) caracteritzats a partir del model de paràmetres de solvatació, el paràmetre de distància *d* es calcula segons l'Eq. 19:

$$d = \sqrt{\left(e_{ui} - e_{uj}\right)^2 + \left(s_{ui} - s_{uj}\right)^2 + \left(a_{ui} - a_{uj}\right)^2 + \left(b_{ui} - b_{uj}\right)^2 + \left(v_{ui} - v_{uj}\right)^2} \quad \text{Eq. 19}$$

Es considera que dos sistemes són semblants si el valor d'aquest paràmetre és inferior a 0,25, tot i que com més petit sigui el valor de *d* més semblants seran [80].

La similitud entre sistemes es pot avaluar gràficament a partir de la distribució en forma de dendrograma o a partir de les dades obtingudes mitjançant un PCA. D'aquesta manera és possible avaluar i comparar una gran quantitat de sistemes a la vegada.

4.3.2 Dendrograma

Per una banda, el dendrograma és un diagrama en forma d'arbre que organitza jeràrquicament els diferents sistemes en grups i subgrups en funció de la similitud que presenten aquests. Aquells sistemes que presenten característiques similars formaran part del mateix clúster [96,97]. Les variables que s'analitzen per detectar similituds entre sistemes són els seus coeficients normalitzats i en aquest tipus de representació no es perd informació en cap moment. L'organització dels sistemes en diferents subgrups pot variar en funció dels sistemes escollits i també del mode d'agrupació d'aquests. Generalment es té en compte la distància euclidiana per mesurar la distància existent entre dos sistemes (que representa en l'espai vectorial una línia recta entre aquests) i els modes *single* (distància més curta entre diferents clústers) i *weighted* (distància mitjana entre diferents subgrups) a l'hora de formar els clústers [98]. A la Figura 10 es mostra un exemple per a 6 sistemes diferents (A, B, C, D, E i F).

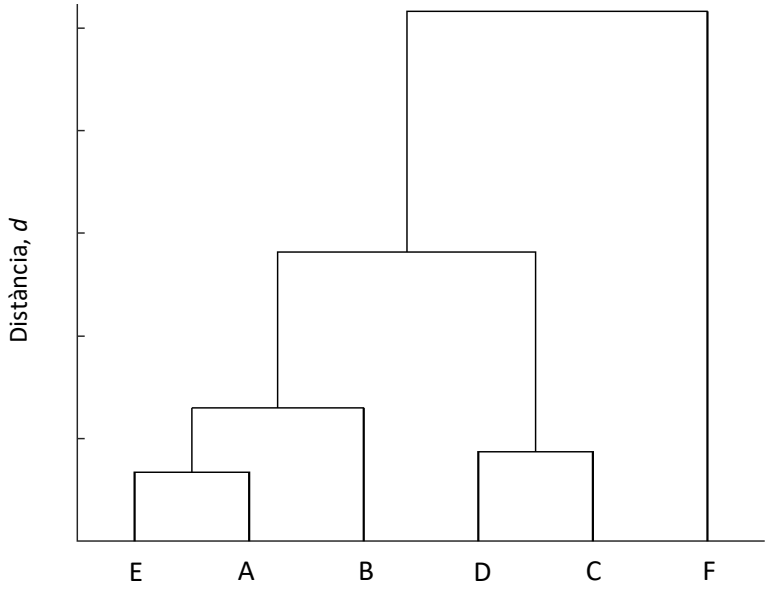

Figura 10. Representació gràfica d'un dendrograma.

Observant la Figura 10 es pot determinar que, per una banda, els sistemes A, B i E són força similars, ja que formen part del mateix subgrup. Tot i que s'ha de tenir en compte que el sistemes E i A seran, *a priori*, més similars entre si que no pas amb el sistema B. Per l'altra, també hi ha un altre subgrup format pels sistemes D i C, els quals serien una mica diferents respecte als anteriors. En canvi, es pot veure que el sistema F seria molt diferent de la resta, ja que no formaria part de cap dels subgrups anteriors.

4.3.3 Anàlisi de components principals

Per l'altra banda, el PCA és un eina quimiomètrica que ens permet reduir la dimensionalitat del conjunt de dades conservant la màxima variabilitat possible. Això s'aconsegueix obtenint un nou conjunt de variables, que es denominen components principals (PC), cadascuna de les quals resulta d'una combinació lineal de les dades originals. Els PCs generats són ortogonals entre si, eliminant la informació

redundant, i es troben ordenats per tal de que els primers retinguin la major part de la variabilitat existent a les variables originals. Com a variables originals s'utilitzen els coeficients normalitzats dels sistemes, a partir dels quals s'obté una matriu d'*scores* (sistemes x PC) i una matriu de *loadings* (PC x coeficients) [99]. Representant el PC2 *vs.* el PC1 dels sistemes de la matriu d'*scores* (els components principals amb més informació) és possible distribuir els sistemes en un espai 2D, en el que estan més a prop aquells amb característiques similars. Ara bé, com només es tenen en compte dos PC, es perd la informació que contenen la resta de components principals. Tot i això, sempre tindran més importància els primers, ja que seran aquells que contenen més informació i que expliquen millor la variabilitat i la similitud existent entre els diferents sistemes. A la Figura 11 es mostra un exemple de com seria un PCA.

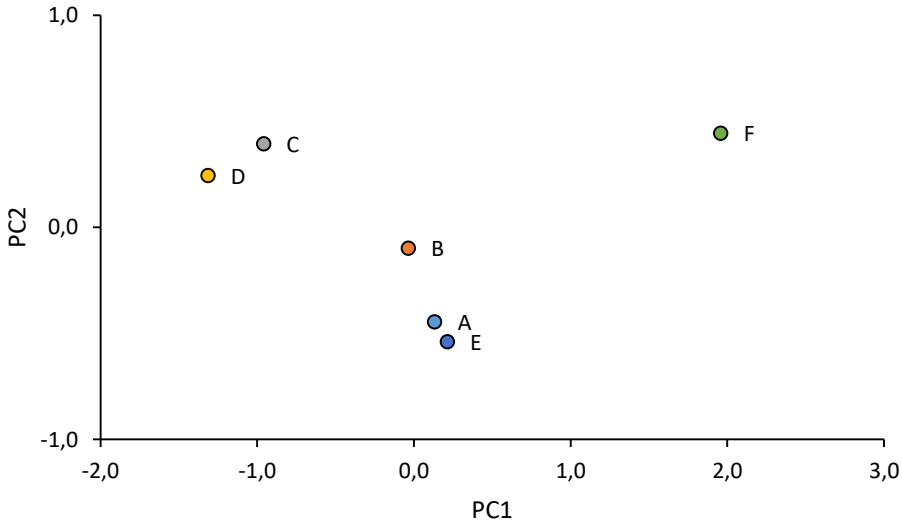

Figura 11. Representació gràfica d'un PCA.

Observant la Figura 11 es pot determinar que, per una banda, els sistemes A, B i E (amb valors de PC1 d'aproximadament 0 i PC2 negatius) són semblants entre si, ja que es troben molt junts al PCA, observant-se una major similitud entre els sistemes A i E. Per l'altra banda, hi ha un segon grup, format pels sistemes C i D (amb valors de PC1 negatius i PC2 positius), els quals, *a priori*, s'assemblarien més als sistemes

A, B i E que no pas al sistema F (amb valors de PC1 i PC2 positius), el qual seria força diferent de la resta. Aquesta interpretació concorda amb el dendrograma obtingut a la Figura 10.

4.3.4 Estimació de la precisió de la correlació entre dos sistemes.

Per comprovar si un sistema de biopartició concret pot ser emulat per un sistema cromatogràfic, es pot calcular la precisió de la correlació entre ambdós sistemes utilitzant un grup de substàncies model [100]. Generalment s'escull aquell grup de soluts que s'ha utilitzat prèviament en la caracterització SPM del sistema biològic. Aquest mètode és més laboriós i per aquest motiu se sol fer amb aquells sistemes que, segons les eines de comparació explicades anteriorment, són, *a priori*, més semblants.

La correlació establerta entre un sistema de biopartició i un sistema fisicoquímic, idealment, respon a una equació del següent tipus:

$$log\ SP_{bio} = q + p\ logSP_{crom} \qquad \text{Eq. 20}$$

On *p* i *q* són, respectivament, el pendent i l'ordenada a l'origen de la regressió. La precisió obtinguda en correlacionar ambdós sistemes té tres contribucions diferents:

$$\sigma^2_{corr} = \sigma^2_{bio} + \sigma^2_{crom} + \sigma^2_d \qquad \text{Eq. 21}$$

On σ^2_{corr} és la precisió de la correlació entre el sistema de biopartició i el cromatogràfic, σ^2_{bio} i σ^2_{crom} són, respectivament, la variància de les dades biològiques (del sistema de biopartició) i cromatogràfiques, i, finalment, σ^2_d correspon a la variància deguda a la dissimilitud dels sistemes correlacionats. Per calcular cadascuna de les contribucions:

- $\sigma^2_{bio} \approx SD^2_{bio}$; Correspon a la precisió resultant de la caracterització del sistema de biopartició a partir del model de paràmetres de solvatació (SD_{bio}).
- $\sigma^2_{crom} \approx (p \cdot SD_{crom})^2$; Correspon a la desviació estàndard obtinguda en la caracterització del sistema cromatogràfic a partir del model de paràmetres de solvatació (SD_{crom}) multiplicada pel factor *p* i elevada al quadrat. *p* és el pendent obtingut a l'Eq. 20 quan es correlacionen la propietat calculada a

través del model SPM del sistema de biopartició amb la propietat calculada a través del model SPM del sistema cromatogràfic.

- $\sigma_d^2 \approx SD_d^2$; SD_d correspon a la variància obtinguda al correlacionar les dades calculades d'ambdós sistemes.

Per poder concloure que dos sistemes són semblants, σ_{corr}^2 ha de ser baixa, per tant σ_d^2 ha de ser també baixa, ja que σ_{crom}^2 i σ_{bio}^2 venen fixades per la precisió de les dades cromatogràfiques i biològiques.

4.4 Establiment i validació dels models QSPR

Entre una propietat de biopartició i una propietat fisicoquímica s'estableixen en molts casos correlacions unilineals, tal com mostra l'Eq. 20. De vegades aquestes correlacions no són del tot satisfactòries i és necessari introduir, a part de la propietat fisicoquímica, altres descriptors addicionals (correlació multilineal) que poden millorar les correlacions obtingudes. Aquests descriptors addicionals poden ser altres propietats fisicoquímiques, un dels descriptors del SPM (com podria ser el volum de McGowan [66,67,82,92,101]), o també els anomenats *flag descriptors* [102]. Aquests últims consisteixen en un codi en el qual s'atribueix valors d'1 ó 0 a cada una de les dades amb les quals s'estableix el model depenent de, respectivament, si aquestes formen part o no d'un subgrup de dades en concret (sigui bé perquè pertanyin a la mateixa família de compostos, o perquè corresponguin a una espècie determinada).

A l'hora d'establir una relació lineal fiable entre una propietat de biopartició i una fisicoquímica s'han de tenir en compte una sèrie d'aspectes [70,103–105]:

- És important que el conjunt de dades utilitzat en l'establiment del model presenti una distribució uniforme i homogènia.
- El conjunt de substàncies escollit ha de ser representatiu. Amb aquesta fi, els compostos escollits han de ser químicament i estructuralment diversos.
- Els valors dels descriptors utilitzats han d'estar normalitzats. D'aquesta manera es poden comparar o relacionar dades amb diferents ordres de magnitud.
- Es necessiten un mínim de 20-30 substàncies diferents per establir el model.

- S'han d'eliminar els possibles *outliers*. Per exemple, un dels criteris que se segueix és eliminar els soluts que presentin residus estàndards superiors a 2,5. Tot i això, en alguns casos si el residu estàndard d'un compost és lleugerament superior a 2,5 i no implica un canvi important sobre la regressió pot no descartar-se, ja que dóna lloc a un model amb més significat químic.

A continuació, després de seleccionar el conjunt de dades òptim, es procedeix a l'establiment del model i a la seva avaluació. Aquest és acceptable si:

- El coeficient de determinació (R^2) és superior a 0,6-0,7.
- La desviació estàndard (SD) és de l'ordre de les dades biològiques (generalment al voltant de 0,3).
- El paràmetre calculat F, del test de Fisher, és superior al tabulat per un interval de confiança del 95% pels mateixos graus de confiança.
- Tots els coeficients de la regressió tenen significat estadístic al 95% de confiança.

Si es compleixen aquests requisits, s'accepta el model establert i es procedeix a la seva validació [70,103–105]. Amb aquesta fi es distribueixen els soluts utilitzats per establir el model en dos subgrups: *training set* i *test set*. Aproximadament 2/3 dels soluts conformarien el *training set* i s'utilitzarien en la validació interna, mentre que la resta formarien l'anomenat *test set* i s'usarien en la validació externa. A l'hora d'establir el model és important que tant el *training set* com el *test set* estiguin formats per un grup de substàncies homogeni i representatiu.

Primer amb el *training set* es duu a terme la validació interna. L'objectiu d'aquesta validació és la d'avaluar la robustesa del model. Amb aquesta fi, s'estableix la mateixa regressió tal com s'ha fet en l'establiment del model però ara només amb les substàncies que formen part del *training set* i eliminant els possibles *outliers*. Per determinar que un model és robust, la nova regressió ha de complir els següents criteris:

- R^2, SD i F han de complir els mateixos criteris que els de l'establiment del model.
- Els coeficients del sistema no han de ser significativament diferents dels del model global (establert amb totes les substàncies).

- El coeficient de la validació creuada (Q^2_{LMO}) ha de ser superior a 0,6. Aquest paràmetre és una eina estadística que permet determinar si els resultats obtinguts són independents de les substàncies escollides en el *training set*.

Finalment es duu a terme la validació externa amb el *test set*. En aquest cas s'avalua la capacitat predictiva del model. Per cada un dels compostos que formen part del *test set* s'estima la propietat biològica a partir de l'equació obtinguda amb els compostos que constitueixen el *training set*. A continuació, s'estableix una regressió lineal entre les dades predites (Y_{pred}) i les experimentals (Y_{exp}). El model s'acceptarà si es compleixen els següents requisits:

- R^2, SD i F han de complir els mateixos criteris que en els casos anteriors.
- El pendent i la intercepció de l'equació resultant no han de ser significativament diferents de, respectivament, 1 i 0 (per un interval de confiança del 95%).
- Q^2_{LMO} ha de ser superior a 0,5.

4.5 Desenvolupament de nous sistemes cromatogràfics

Apart dels sistemes ja caracteritzats anteriorment pel model SPM (secció 4.2), és interessant buscar i desenvolupar nous sistemes de partició amb diferents propietats i selectivitats i que, per tant, puguin tenir interès per a la subrogació i estimació de propietats de biopartició. Alguns d'aquests sistemes podrien ser fases pseudoestacionàries basades en preparats de lecitina de soja i fases estacionàries basades en columnes capil·lars monolítiques.

4.5.1 Sistemes cromatogràfics basats en preparats de lecitina de soja

La lecitina de soja està composta per una sèrie de fosfolípids com són la fosfatidilcolina, la fosfatidiletanolamina i el fosfatidilinositol i també per altres glicolípids. A la lecitina de soja, en percentatge pes/pes, la fosfatidilcolina representa el 10-15% del total, la fosfatidiletanolamina el 9-12% i el fosfatidilinositol el 8-10%

[106]. Cal tenir en compte que, per exemple en les cèl·lules de la pell dels humans aquests fosfolípids també són els majoritaris representant la fosfatidilcolina en percentatge pes/pes el 38,5%, la fosfatidiletanolamina el 19,1% i el fosfatidilinositol el 9,5% [107]. Per aquest motiu, com les membranes cel·lulars de molts organismes estan formades principalment per aquests fosfolípids, l'ús de liposomes basats en lecitina de soja en les fases pseudoestacionàries (EKC) o mòbils (HPLC) pot ser de gran interès per desenvolupar sistemes fisicoquímics capaços d'estimar propietats de caràcter biològic. S'ha de tenir en compte que altres sistemes cromatogràfics basats en lecitina han demostrat ser òptims per a l'estimació de propietats biològiques com l'absorció intestinal [108]. A la Figura 12 es mostra l'estructura molecular del fosfolípid majoritari de la lecitina: la fosfatidilcolina.

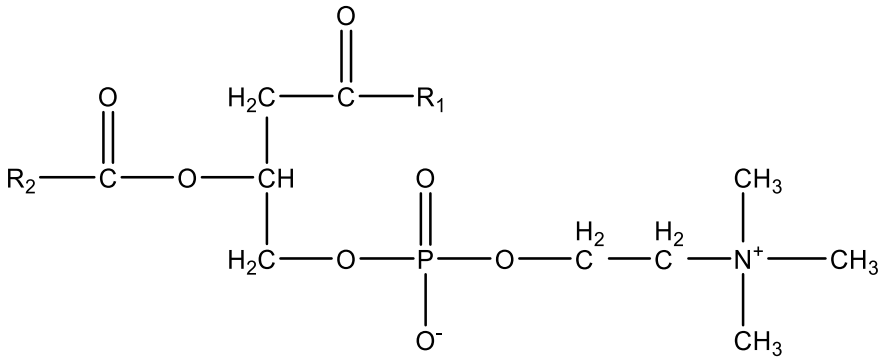

Figura 12. Estructura molecular de la fosfatidilcolina

Generalment, per a la preparació de liposomes se segueix un procediment laboriós [109] i de vegades no s'obtenen preparats liposòmics reproduïbles. Actualment, es disposa d'uns productes comercials que podrien fer-se servir per generar liposomes d'una manera més senzilla, ràpida i de baix cost, bàsicament mitjançant la dilució directa de preparats de lecitina de soja en aigua. Aquests productes es comercialitzen actualment per a la fabricació de productes cosmètics i farmacèutics (Lucas Meyer Cosmetics).

4.5.2 Sistemes cromatogràfics basats en columnes monolítiques

Durant els primers anys de la dècada dels 90 es va desenvolupar un nou format de columna cromatogràfica alternatiu: fases estacionàries de polímer-monòlit [110]. Aquest nou format consisteix en una estructura continua d'un material macroporós que s'expandeix per tota la columna cromatogràfica, a diferència de les columnes empaquetades on un gran nombre de partícules es troben compactades conjuntament. Les columnes monolítiques polimèriques poden preparar-se *in situ*, amb un gran ventall de selectivitats diferents, ja que hi ha una gran varietat de monòmers que es poden utilitzar per a la seva preparació, i, a més, pot modificar-se la seva morfologia per obtenir una estructura amb un compromís entre permeabilitat i eficàcia. Tot i que la seva aplicació més important és en la separació de compostos (especialment de biomolècules) per electrocromatografia capil·lar [111] (CEC, en anglès *capillary electrochromatography*) i per RP-LC [112], la síntesi de noves columnes amb característiques diferents pot proporcionar nous sistemes fisicoquímics que podrien ser utilitzats per emular sistemes de biopartició.

4.5.2.1 Síntesi de columnes monolítiques polimèriques

Les columnes monolítiques polimèriques es preparen *in situ* dintre de capil·lars de sílice seguint el procediment descrit a continuació. Aquest consta de dues etapes principals, una primera on es modifica la superfície interna del capil·lar, perquè el polímer pugui establir enllaços covalents amb les parets internes d'aquest, i una segona etapa on es genera el polímer a partir d'una polimerització per radicals lliures (Figura 13).

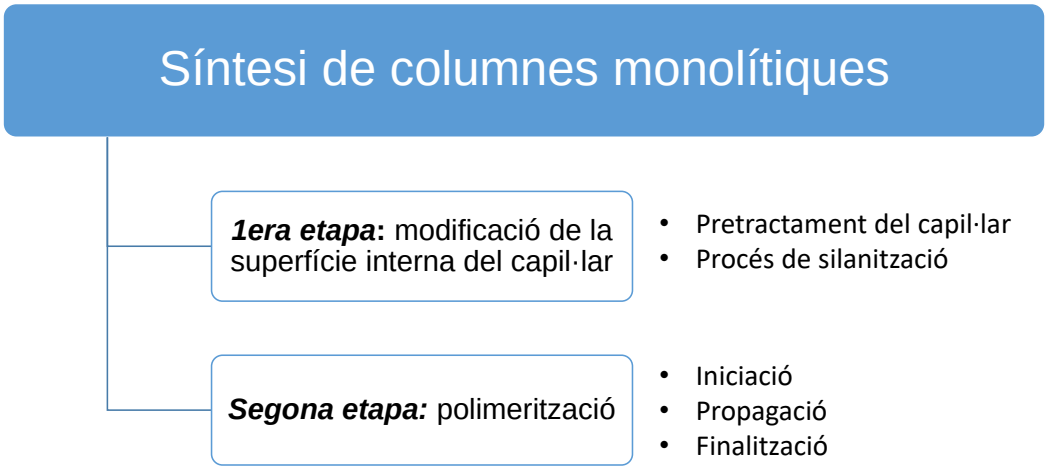

Figura 13. Esquema del procés de síntesi de columnes monolítiques.

Primera etapa: modificació de la superfície interna del capil·lar

Primerament s'ha de modificar la superfície interna del capil·lar per poder unir covalentment el polímer al capil·lar [113]. Amb aquesta fi, s'ha de realitzar un pretractament previ del capil·lar per tot seguit continuar amb el procés de silanització.

i) Pretractament del capil·lar. Es procedeix primer injectant una solució d'hidròxid de sodi, seguit d'aigua i una solució d'àcid clorhídric. Finalment el capil·lar s'asseca a partir d'aire a pressió.

ii) Procés de silanització. S'aconsegueix injectant pel capil·lar un agent d'acoblament, com seria per exemple el 3-(trimetoxisilil)propil metacrilat. Aquest compost permetrà unir el polímer format en les posteriors etapes amb la superfície interna del capil·lar.

Segona etapa: polimerització

Les mescles de polimerització estan formades, generalment, per un iniciador, dos monòmers (un de funcional i un altre d'entrecreuament) que donaran lloc al polímer i un porogen (generalment, una mescla de dos solvents diferents) que influirà en la

porositat final del monòlit [114]. Els dissolvents escollits per formar part del porogen no han de reaccionar químicament i han de tenir punts d'ebullició alts. Aquest procés consta de tres etapes [115]:

i) Iniciació. L'iniciador, com per exemple l'AIBN (Azobisisobutironitril), per efecte de la calor o de la radiació ultraviolada es degrada en un radical que inicia el procés de polimerització.

ii) Propagació. Els dos monòmers comencen a reaccionar amb els radicals formats donant lloc a cadenes polimèriques de mida creixent. Durant aquest procés, gràcies al monòmer d'entrecreuament, les diferents cadenes s'entrecreuen entre si donant lloc a la formació d'agregats anomenats microglòbuls.

iii) Finalització. El procés de polimerització finalitza quan els radicals formats reaccionen entre si i es neutralitzen.

4.5.2.2 Optimització del disseny

Quan es desenvolupen noves columnes monolítiques s'ha de tenir cura del seu disseny, és important que aquest sigui l'adient per obtenir la màxima eficàcia possible i que els pics cromatogràfics corresponents a cadascun dels compostos analitzats siguin els més estrets i gaussians possibles. Per millorar l'eficàcia d'una columna monolítica es poden modificar diferents paràmetres com són, per una banda, l'optimització de la mida dels microglòbuls i dels macroporus, i, per l'altra, el percentatge de porositat total de la columna.

La mida dels microglòbuls i dels macroporus pot modificar-se en funció de quins dissolvents conformen el porogen i quines són les seves concentracions [116,117]. El porogen, generalment, és una mescla binaria de dos dissolvents diferents, un que dissol molt bé el polímer format, que s'anomena "bon" dissolvent, i un altre que no el dissol tan bé, anomenat "mal" dissolvent. Si s'augmenta la proporció del primer, el polímer es dissoldrà millor al porogen produint-se la separació de fases més tard, d'aquesta manera s'allarga el procés de polimerització en el temps i es produeix la formació de microglòbuls i macroporus més petits [116]. A la Figura 14 s'observa aquest fenomen, on a mesura que s'augmenta la proporció de tetrahidrofurà (THF)

al porogen, que actua com a "bon" dissolvent, s'obtenen unes columnes polimèriques amb macroporus i microglòbuls més petits.

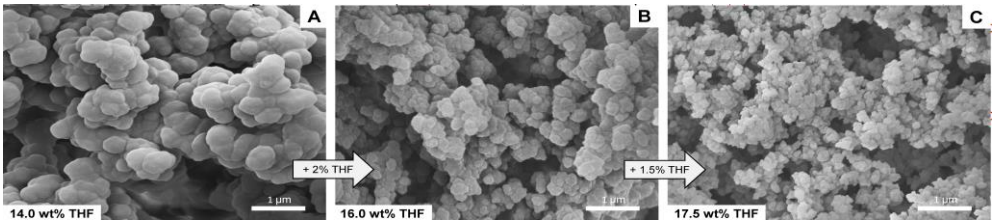

Figura 14. Imatges de microscòpia electrònica de rastreig (SEM) de tres columnes monolítiques polimèriques preparades amb diferents proporcions de THF al porogen [116,117].

Altres paràmetres que també poden alterar la mida dels microglòbuls i dels macroporus serien el percentatge en pes/pes d'iniciador i del monòmer d'entrecreuament present a la mescla de polimerització. A més, la porositat total de la columna monolítica pot variar depenent de la relació monòmer/porogen que hi ha a la mescla de polimerització. L'augment de la proporció de porogen respecte al total de la mescla de polimerització contribueix a l'obtenció de columnes monolítiques més poroses [117].

4.5.2.3 Eficàcia de la separació cromatogràfica

A l'hora d'avaluar la capacitat separativa d'una columna cromatogràfica, sovint s'estudia aquesta a partir de l'equació de Van Deemter que relaciona l'alçada de plat (*H*) amb els diferents paràmetres que influeixen en l'eixamplament dels pics cromatogràfics (Eq. 22) [118]:

$$H = A + B/u_0 + C \cdot u_0 \qquad \text{Eq. 22}$$

On *A* és la difusió d'Eddy (terme relacionat amb la multiplicitat de camins), *B* és la difusió longitudinal (relacionat amb la tendència dels anàlits a expandir-se en la

direcció de la fase mòbil), *C* és la resistència a la transferència de massa (que presenta dues contribucions una deguda a la fase estacionària, C_s, i una altra deguda a la fase mòbil, C_m) i per últim u_0 és la velocitat lineal de la fase mòbil. Com més petita sigui l'alçada de plat, *a priori*, s'obtindran pics més estrets i separats amb una millor resolució. El terme *B* de l'equació de Van Deemter és específic de cada compost, ja que depèn del seu coeficient de difusió, mentre que els termes *A* i *C* varien en relació amb el disseny de la fase estacionària com seria, en el cas d'una columna monolítica, la mida dels microglòbuls i dels macroporus [116].

A la Figura 15 es mostra com varia *H* en funció de u_0 segons l'Eq. 22. En general, tal com es mostra a la figura, si el cabal augmenta respecte de l'òptim (u_{opt}, cabal on s'obté la millor eficàcia) *H* augmentarà disminuint l'eficàcia de la columna.

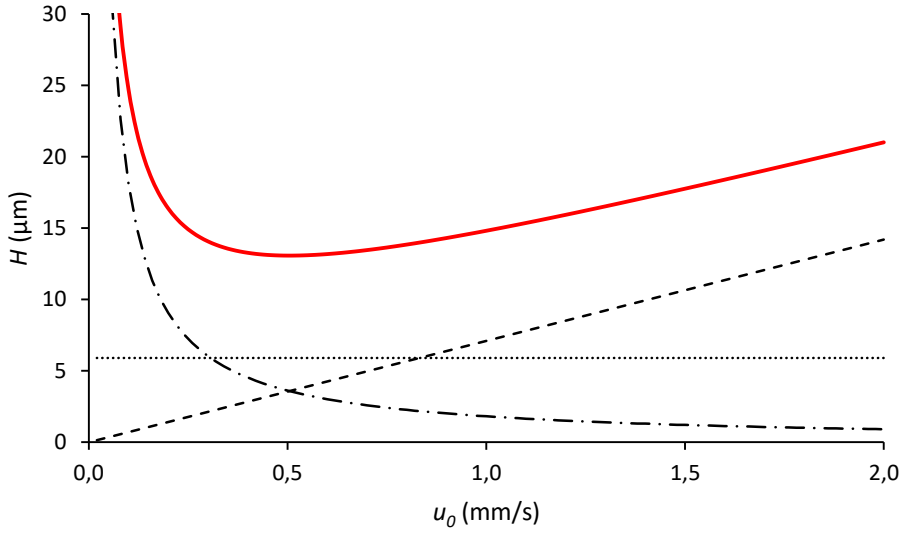

Figura 15. Representació gràfica de l'equació de van Deemter, on es representa *H* (—), el terme *A* (⋯), el terme B/u_0 (—·) i el terme $C \cdot u_0$ (---) en funció de u_0 per uns valors model *A*: 6 µm, *B*: 0.0018 $mm^2 \cdot s^{-1}$, *C*: 7 ms.

En canvi, per avaluar la capacitat separativa en mode gradient s'ha introduït un nou paràmetre anomenat capacitat de pics (n_c). Aquest paràmetre es defineix com el

màxim nombre de components que es poden separar de manera òptima, per una columna cromatogràfica i unes condicions d'anàlisi determinades, amb una resolució igual a 1 [119]. Per calcular aquest paràmetre es fa servir l'equació següent:

$$n_c = \frac{t_G}{W} + 1 \qquad \text{Eq. 23}$$

On t_G és el temps de gradient i w l'amplada de la base del pic cromatogràfic. A més, Neue *et al.* [120] van desenvolupar un nou model per pèptids on es podia aproximar el valor de n_c a partir de l'equació següent:

$$n_c = 1 + \frac{\sqrt{N}}{4} \cdot \frac{S \cdot \Delta c}{S \cdot \Delta c \cdot \frac{t_0}{t_g} + 1} \qquad \text{Eq. 24}$$

On N és el nombre de plats, relacionat amb H i la longitud de la columna cromatogràfica (L) segons l'Eq. 25:

$$H = \frac{L}{N} \qquad \text{Eq. 25}$$

t_G/t_0 és el pendent del gradient, definit com la relació entre el temps de gradient i el temps mort de la columna; Δc correspon a l'increment de gradient, definit com la diferència entre la composició final de la fase mòbil i la inicial (en referència al dissolvent orgànic) i S el paràmetre de la relació lineal de la força del solvent que es calcula a partir de l'equació següent [121]:

$$\ln k = \ln k_0 - S \cdot \phi \qquad \text{Eq. 26}$$

On ϕ representa la fracció de solvent orgànic a la fase mòbil i k_0 és el factor de retenció del compost quan ϕ és igual a 0.

Tot i que el disseny de la columna monolítica intervé en l'eficàcia de la separació, altres paràmetres com la capacitat de càrrega, l'agent formador de parell iònic o el temps de gradient utilitzat també tenen una gran influència.

PUBLICACIONS

ARTICLE I

Modeling Aquatic Toxicity through Chromatographic Systems

Alejandro Fernández-Pumarega, Susana Amézqueta, Sandra Farré, Laura Muñoz-Pascual, Michael H. Abraham, Elisabet Fuguet, and Martí Rosés

Analytical Chemistry (2017), volum: 89, pàgines: 7996-8003

DOI: 10.1021/acs.analchem.7b01301

analytical chemistry

Article

pubs.acs.org/ac

Modeling Aquatic Toxicity through Chromatographic Systems

Alejandro Fernández-Pumarega,[†] Susana Amézqueta,[†] Sandra Farré,[†] Laura Muñoz-Pascual,[†] Michael H. Abraham,[‡] Elisabet Fuguet,[†,§] and Martí Rosés*[,†]

[†]Departament de Química Analítica and Institut de Biomedicina (IBUB), Facultat de Química, Universitat de Barcelona, Martí i Franquès 1-11, 08028, Barcelona, Spain

[‡]Department of Chemistry, University College London, 20 Gordon Steet, London WC1H 0AJ, U.K.

[§]Serra Húnter Programme, Generalitat de Catalunya, 08002 Barcelona, Spain

Supporting Information

ABSTRACT: Environmental risk assessment requires information about the toxicity of the growing number of chemical products coming from different origins that can contaminate water and become toxicants to aquatic species or other living beings via the trophic chain. Direct toxicity measurements using sensitive aquatic species can be carried out but they may become expensive and ethically questionable. Literature refers to the use of chromatographic measurements that correlate to the toxic effect of a compound over a specific aquatic species as an alternative to get toxicity information. In this work, we have studied the similarity in the response of the toxicity to different species and we have selected eight representative aquatic species (including tadpoles, fish, water fleas, protozoan, and bacteria) with known nonspecific toxicity to chemical substances. Next, we have selected four chromatographic systems offering good perspectives for surrogation of the eight selected aquatic systems, and thus prediction of toxicity from the chromatographic measurement. Then toxicity has been correlated to the chromatographic retention factor. Satisfactory correlation results have been obtained to emulate toxicity in five of the selected aquatic species through some of the chromatographic systems. Other aquatic species with similar characteristics to these five representative ones could also be emulated by using the same chromatographic systems. The final aim of this study is to model chemical products toxicity to aquatic species by means of chromatographic systems to reduce in vivo testing.

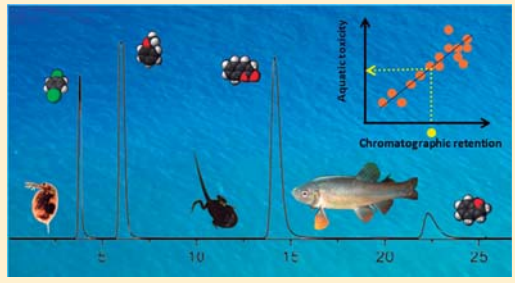

Aquatic environments receive directly and indirectly chemical substances that may result in toxicity to their inhabitants. There are several protocols and analytical methods to determine the toxicity of these chemicals to aquatic species.[1] While in vivo experiments provide reliable measurements, they often require expensive, long, and complex procedures. The US Environmental Protection Agency and the European Chemicals Agency promote the use of alternative methods to avoid unnecessary animal testing.[2,3] Models based on in silico methods or other predictive models based on physicochemical properties measurements can be used as alternatives.[4]

A popular quantitative structure−property relationships (QSPR) model to estimate aquatic toxicity and other biochemical properties is the solvation parameter model (SPM) proposed by Abraham.[5] The following equation that includes five different molecular descriptors is used to model the solvation that a neutral solute undergoes in a biphasic system.

$$\log \mathrm{SP} = c + eE + sS + aA + bB + vV \quad (1)$$

Here, SP is the dependent solute property in a given partitioning system, that is, equilibrium constant or some other free energy related property such as a lethal dose. The E, S, A, B, and V independent variables are the solute descriptors proposed by Abraham. E represents the excess molar refraction, S is the solute dipolarity/polarizability, A and B are the solute's effective hydrogen-bond acidity and hydrogen-bond basicity, respectively, and V is McGowan's solute volume. The coefficients of the equation are characteristic of the biphasic system and reflect the difference of the two phases in properties complementary to the corresponding solute property. For any system, the coefficients of this equation can be obtained by multiple linear regression analysis between the log SP values acquired for an appropriate group of solutes and their descriptor values. Equations based on the SPM have been used to characterize many biological systems that depend on the solutes partition into two phases, that is, an aqueous solution and a biological membrane. Literature proposes equations based on this model to estimate the toxicity of chemical substances to tadpoles, fish, water fleas, protozoa, and

Received: April 7, 2017
Accepted: June 22, 2017
Published: June 22, 2017

DOI: 10.1021/acs.analchem.7b01301
Anal. Chem. 2017, 89, 7996−8003

bacteria.[6−11] Furthermore, more than one hundred physicochemical systems, mainly based on liquid−liquid partition and chromatographic and electrophoretic partition systems, have been characterized using this model.[12−18]

Characterizing biological and physicochemical systems using the same model (the SPM in this work) makes them comparable, since similar partitioning systems will have similar coefficients. To compare similarity between toxicity systems and physicochemical systems (mainly chromatographic and electrophoretic) the d distance parameter on the SPM coefficients can be calculated. Dendrogram and principal components analysis (PCA) plots lead to a visual representation of the systems closeness. In addition, the precision of the correlation between the toxicity parameter and the physicochemical parameter can also be estimated. This precision depends on the errors of the biological and physicochemical models and the systems dissimilarity.[16,19−21] Those physicochemical systems closer to the biological one (with smallest d or closest in the dendrogram and principal components space plots) and with highest estimated correlation precision will probably best emulate the toxicity parameter. To this end, the physicochemical property (mainly the retention factor in chromatographic and electrophoretic systems) is determined and a correlation with the biological property is carried out for a series of representative compounds. If a good correlation is established between the properties of these two different systems, the biological property of a new chemical compound can be predicted by measuring the corresponding physicochemical property. The main advantage of this approach over QSPR studies is that it is not necessary to know the molecular descriptor values of the new compound such as in the SPM model. Furthermore, the use of chromatographic and electrophoretic measurements for prediction of biological properties is of main interest because of the high level of automatization, speed of analysis, low cost, and high reproducibility of these techniques.

Previous works on aquatic toxicology have shown that a micellar electrokinetic chromatography (MEKC) system based on sodium taurocholate (STC) micelles and chromatographic measurements using an immobilized artificial membrane (IAM) column are able to predict the neutral organic substances toxicity to Fathead minnow (FM) fish[22] and *Rana* tadpoles (RT).[23] The aim of this work is to check if one of these chromatographic systems or others based on HPLC (high performance liquid chromatography) or MEKC could be used to model in a more general way the toxicity to aquatic species. In this sense, some representative biological systems have been selected and the ability of some representative and promising physicochemical systems to emulate the toxicity of chemical compounds to these aquatic species have been evaluated. Those biological systems ruled by similar toxicity mechanisms could be putatively emulated using the same physicochemical system.

EXPERIMENTAL SECTION

Equipment. HPLC measurements were done using a 10A series chromatograph from Shimadzu (Kyoto, Japan) equipped with a quaternary pump and a diode array detector and fitted with either a Symmetry C18 column (15 cm × 4.6 mm i.d., 5 μm particle size) (Waters, Milford, MA, US) preceded by the corresponding guard cartridge (1 cm), or an IAM.DD 2 immobilized artificial membrane column (10 cm × 4.6 mm i.d., 12 μm particle size) (Regis Technologies, Morton Grove, IL, US).

MEKC measurements were done using the CE capillary electrophoresis system from Agilent Technologies (Santa Clara, CA, US) equipped with a diode array detector. The fused-silica capillary (40 cm effective length, 50 μm i.d.) was obtained from Composite Metal Services, Ltd. (Shipley, UK).

Reagents. Methanol (HPLC-grade), hydrochloric acid (25% in water), sodium hydroxide (>99%), sodium dihydrogen phosphate monohydrate (>99%), disodium hydrogen phosphate (>99%), and sodium dodecyl sulfate (SDS, >99%) were from Merck (Darmstadt, Germany). Acetonitrile (HPLC grade) was from VWR International (West Chester, Pennsylvania, US). Taurocholic acid sodium salt monohydrate (STC, 98%) was from Acros Organics (Geel, Belgium) and Brij 35 was from Scharlab (Sentmenat, Spain). Tetradecyltrimethylammonium bromide (TTAB, >98%) and dodecanophenone (98%) were from Sigma-Aldrich (St. Louis, MO, US). Water was purified by a Milli-Q plus system from Millipore (Bedford, MA, US), with a resistivity of 18.2 MΩ cm.

Tested substances were reagent grade or better and obtained from several manufacturers (Merck, Sigma-Aldrich, Carlo Erba (Milano, Italy), Baker (Center Valley, PA, US), Panreac (Castellar del Vallès, Spain), Thermo Fisher Scientific (Waltham, MA, US), and Scharlab).

Analysis by HPLC. Tested substances were solved and analyzed as described elsewhere.[23] The detection wavelength was 214 nm.

The HPLC retention factor (k), was calculated according to eq 2.

$$k = \frac{t_R - t_0}{t_0} \tag{2}$$

where t_R corresponds to the solute retention time and t_0 is the column hold-up time determined by an aqueous potassium bromide solution.

Analysis by MEKC. The target compounds were analyzed using three different pseudostationary phases: a 50 mM solution of taurocholic acid sodium salt monohydrate in 20 mM phosphate aqueous buffer adjusted to pH 7.0; a 20 mM solution of TTAB in 20 mM phosphate aqueous buffer adjusted to pH 7.0; and a mixture of surfactants that consists of 50 mM SDS and 10 mM Brij 35 in 20 mM phosphate aqueous buffer adjusted to pH 7.0.

Tested substances were solved and analyzed as described elsewhere.[23] In the case of TTAB, solutes and dodecanophenone (micellar marker) were prepared at 200 mg L^{-1}.

The MEKC retention factor (k), was calculated according to eq 3.

$$k = \frac{t_m - t_{eof}}{\left(1 - \frac{t_m}{t_{mc}}\right) t_{eof}} \tag{3}$$

where t_m is the solute migration time, t_{eof} corresponds to the migration time of methanol or acetonitrile (electroosmotic flow markers), and t_{mc} is the migration time of dodecanophenone (micelle marker).

Comparison of Biological and Physicochemical Systems. The SPM normalized coefficients[22] of both kind of systems have been used as input data to calculate the d distance and plot of the corresponding PCA and dendrogram. These approaches are based on simple and fast calculations and allow handling with a high number of data at once. They provide information about the systems similarity and are very adequate

DOI: 10.1021/acs.analchem.7b01301
Anal. Chem. 2017, 89, 7996−8003

to choose representative biological systems and to do a first selection of the physicochemical systems that can better emulate the toxicity ones.[16,20] Another strategy to select the more promising physicochemical systems is to estimate the precision of the correlation between the toxicity parameter and the physicochemical parameter.[21] This kind of estimation is more laborious, so it has been performed only for those systems preselected with the previous approaches. Finally, after a general evaluation of all comparison approaches and other technical considerations, those physicochemical systems with similar characteristics to the representative biological ones have been selected for ongoing experimental tests.

d Distance Parameter. The similarity between two systems both characterized by means of the SPM can be measured through the *d* distance parameter.[16] Considering the coefficients of any system as a vector in a five-dimensional space, the *d* parameter measures the distance between the normalized unitary vectors of a pair of systems. Thus, the *d* distance provides a measure of the similarity between the two considered systems: the smaller *d* is, the closer the two systems are. In previous works, we assumed that distances below 0.25 indicate that the two compared systems are quite similar.[22,23]

Dendrogram Plot. The dendrogram is a diagram plotted using a hierarchical clustering algorithm that shows the distances between pairs of sequentially merged classes. In this work, the distances between each pair of classes (toxicity and physicochemical systems) have been calculated through the normalized coefficients of the SPM equations. Clustering has been performed using the *d* distance parameter (straight-line distance) and the weighted-linkage method (the distance between two groups is defined as the weighted average distance). Those systems located nearer in the dendrogram plot will have more similar chemical characteristics.

Principal Components Analysis. PCA is a chemometric tool used to transform the input data in a multivariate space (normalized SPM equation coefficients) to a new multivariate space (principal components (PCs) space) whose axes are uncorrelated and rotated with respect to the original space. The number of PCs is equal to the number of original variables and the first PCs are those that more explain the system variance. The main PCs plot (PC2 vs PC1 scores centered plot) using the normalized coefficients of the SPM equations of the different toxicity and physicochemical systems as the input data distributes the different systems in the new chemical space, so that systems with similar characteristics are close in the scores plot. In this work, the PCA analysis helps to visualize the physicochemical space. However, in some cases, the simplification leads to a loss of information.

Estimation of the Precision of the Correlation between a Biological and a Physicochemical System. In this work, the physicochemical systems used are based on chromatography, so to estimate the precision of biological−chromatographic correlations (eq 4), the approach described elsewhere[22] has been used.

$$\log SP_{bio} = q + p \log SP_{chrom} \quad (4)$$

Here, SP_{bio} is the solute biological property, SP_{chrom} is the solute chromatographic property (in this case, the chromatographic or electrophoretic retention factor), and *q* and *p* are the ordinate and slope of the correlation, respectively.

In short, the correlation precision (SD_{corr}^2) can be considered as the sum of three different contributions to the variance of the correlation: the biological data precision ($\sigma_{bio}^2 \approx SD_{bio}^2$), the chromatographic data precision ($\sigma_{chrom}^2 \approx (p \times SD_{chrom})^2$ and the error due to the dissimilarity between the correlated systems (SD_d^2). SD_{bio} and SD_{chrom} values are obtained from the respective standard deviations of the SPM characterizations. To know *p* and also SD_d^2 the biological property and the chromatographic property are calculated through their SPM equations and solutes' descriptors. In this way, SD_{bio} and SD_{chrom} are zero. The slope of the correlation of these calculated values provides *p*, and the SD of the correlation can be entirely attributed to the dissimilarity between both systems.

Data Analysis. PCA and dendrogram plots were performed with Matlab package from MathWorks (Natick, MA, USA). Excel 2010 from Microsoft (Redmond, WA, US) was used for data calculations and multiple linear regression analyses.

Substances' pK_a values and Abraham descriptors were obtained from Percepta software version 2014 from ACD/Laboratories (Toronto, Canada).

RESULTS AND DISCUSSION

Similarity of Biological Systems. Twenty-one biological systems related to toxicity to different aquatic species have been considered in the present study. They are tadpoles (RT, *Rana* tadpoles), fish (fathead minnow (FM, *Pimephales promelas*); guppy (GP, *Poecilia reticulata*); bluegill (BG, *Lepomis macrochirus*); golden orfe (GO, *Leuciscus idus melanotus*); goldfish (GF, *Carassius auratus*); medaka high-eyes 48 and 96 h (MK48 and MK96, respectively, *Oryzias latipes*)), water fleas (DM24, *Daphnia magna* 24 h; DM48, *Daphnia magna* 48 h; CD, *Ceriodaphnia dubia*; DP, *Daphnia pulex*), protozoa (TP, *Tetrahymena pyriformis*; SA, *Spirostomum ambiguum*; ES, *Entosiphon sulcantum*; UP, *Uronema parduczi*; CP, *Chilomonas paramecium*), and bacteria (PP, *Pseudomonas putida*; PG, *Porphyromonas gingivalis*; SR, *Selenomonas artemidis*; SS, *Streptococcus sobrinus*). All of them have been characterized through the SPM and results are presented in Table S-1.

In general, hydrogen-bond basicity and solute volume are the major factors that influence the compounds toxic action. Solutes with high hydrogen-bond basicity and low volume will result less toxic to aquatic species.

To show the similarity of these toxicity systems, the normalized SPM coefficients of the systems have been analyzed according to a dendrogram of *d* distances and a PCA of the normalized coefficients. These plots are represented in Figure 1 and they lead to the same conclusions about similarity. The dendrogram shows that at the *d*-levels of 0.35−0.5, all systems are clustered together except UP and GF. These two systems are radically different from the other ones (also shown in the PCA plot) probably because of the big differences on e and b coefficients from the ones of the other systems, and also on s coefficient for GF. Therefore, they will not be further considered for similarity. At the 0.3 *d*-level, the cluster divides in two different clusters of 10 and 9 systems. The PCA plot shows that the two clusters are differentiated by the PC1 value. The first cluster contains systems with negative PC1 value and includes all bacteria and tadpole, and several fish and protozoan systems. The second cluster is composed of all water fleas and several fish and protozoan systems, which have positive PC1 values.

At the 0.25 *d*-level, CD separates from the cluster of positive PC1, whereas the cluster of negative PC1 divides into three different clusters. One cluster is formed by GO, ES, MK96, and CP which have negative PC2 values. SR, MK48, SS, and PG

DOI: 10.1021/acs.analchem.7b01301
Anal. Chem. 2017, 89, 7996−8003

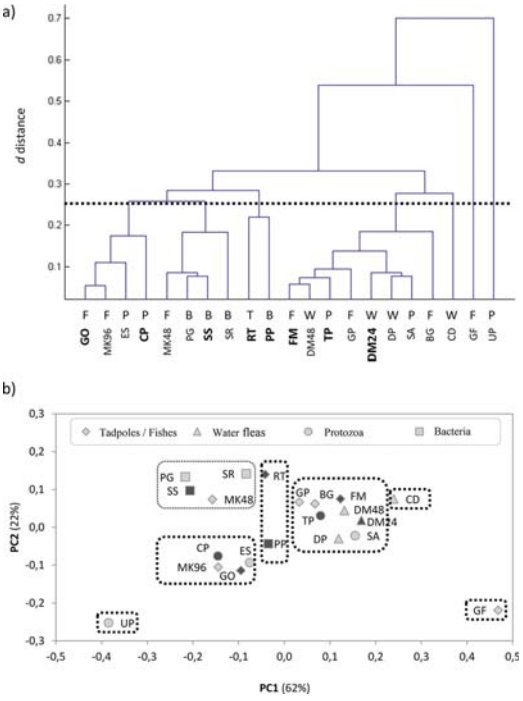

Figure 1. (a) Dendrogram plot of the biological systems included in Table S-1: tadpoles (T), fish (F), water fleas (W), protozoan (P), and bacteria (B). Selected systems are shown in boldface. (b) PCA scores plot of the biological systems included in Table 1. Selected systems are shown in dark gray.

form another cluster with positive PC2. The third cluster is formed with RT and PP, which have positive and negative PC2, respectively, but very similar and close to 0 negative PC1. However, RT and PP separates according to PC2 at *d*-level of 0.23. Notice that the main clustering factor is PC1 which explains 62% of the variance, whereas PC2, explaining only 22% of variance, has a minor effect on clustering.

In previous works,[22,23] a *d* distance of 0.25 or less was considered as adequate for surrogating biological systems by chromatographic ones. Following this criteria, we can consider similar all systems in the same cluster at 0.25 *d*-level and select one or several representative systems of each cluster, in general the ones that have larger number of chemical compounds with known toxicity data. Thus, GO fish and CP protozoa have been selected as representatives of the cluster including GO and MK96 fish and CP and ES protozoa. SS bacteria is representative of MK48 fish, and SR, SS, and PG bacteria cluster. RT tadpole and PP bacteria have been taken both as representatives of their cluster. FM fish, TP protozoa, and DM24 water flea are representative of last cluster composed of FM, GP, and BG fish, TP and SA protozoa, and DP, DM48, and DM24 water fleas. In all, we have selected systems belonging to the five different species (tadpoles, fish, water fleas, protozoa, and bacteria), in each of the four main clusters.

Selection of Physicochemical Systems to Emulate Toxicity of Neutral Organic Compounds. The SPM has been applied to nearly one hundred physicochemical systems including solvent partition, HPLC (high-performance liquid chromatography), MLC (micellar liquid chromatography), MELC (microemulsion liquid chromatography), MEKC (micellar electrokinetic chromatography), MEEKC (microemulsion electrokinetic chromatography), LEKC (liposome electrokinetic chromatography), and poly-EKC (polymeric electrokinetic chromatography) systems.[12−17] Similar to the case of the biological systems, the main factors that drive solute partition are the magnitude of the coefficients *v* and *b*.

Among these physicochemical systems, 11 (coefficients detailed in Table S-2) commonly used to surrogate biological systems and that showed *d* values below 0.25 to at least one of the selected toxicity biological systems were selected (Table 1). The selection comprises the octanol−water partition system (O/W), two liquid chromatography systems, five MEKC systems, one microemulsion electrokinetic chromatography MEEKC system, one LEKC system, and one EKC system based on a polymeric surfactant.

In addition, the variance of the final correlation ($SD_{corrcal}^2$) between aquatic toxicity data and the physicochemical property data (either the partition coefficient or the retention factor) of the selected systems was estimated. The detailed calculations are given in Table S-3 and final results are shown in Table 2.

According to the results of Tables 1 and 2, the cluster of GO and CP (also including MK96 and ES) is best surrogated by TTAB, followed by SLN (sodium *N*-lauroylsarcosinate), STC, and SDS-Brij 35 systems, which show the shortest predicted *d* distances and correlation variances to them. The TTAB is also clearly the system showing best *d* distance and variance to SS, and thus expected to emulate well MK48, PG, and SR of the same cluster. This is not surprising because these two clusters are very close on the dendrogram of Figure 1. The toxicity cluster of RT and PP is well surrogated by STC, SDS-Brij 35, and SLN. Finally, SLN, SDS-Brij 35, and DPPG-DPPC (dipalmitoylphosphatidyl glycerol−dipalmitoylphosphatidyl choline) are the best systems to surrogate the cluster with

Table 1. *d* Distance Values in the Correlations between Aquatic Species Toxicity Data and Chromatographic or Partitioning Data of the Considered Physicochemical and Biological Systems

system		O/W	RP18	IAM	SDS MEKC	SLN	STC	TTAB	SDS-Brij 35	SDS MEEKC	DPPG-DPPC	AGESS
tadpoles	RT	0.121	0.223	0.143	0.173	0.105	0.09	0.178	0.109	0.155	0.198	0.103
fish	FM	0.198	0.259	0.186	0.347	0.162	0.183	0.246	0.128	0.176	0.095	0.118
	GO	0.391	0.480	0.360	0.417	0.246	0.306	0.271	0.298	0.395	0.282	0.290
water fleas	DM24	0.267	0.310	0.258	0.402	0.224	0.240	0.307	0.201	0.238	0.158	0.190
protozoan	TP	0.205	0.277	0.208	0.310	0.121	0.156	0.238	0.131	0.186	0.123	0.107
	CP	0.380	0.448	0.343	0.371	0.280	0.270	0.262	0.293	0.396	0.327	0.300
bacteria	PP	0.295	0.329	0.315	0.238	0.242	0.172	0.316	0.252	0.295	0.320	0.244
	SS	0.313	0.424	0.258	0.344	0.217	0.274	0.123	0.246	0.352	0.270	0.257

DOI: 10.1021/acs.analchem.7b01301
Anal. Chem. 2017, 89, 7996−8003

Table 2. Calculated Precision ($SD_{correal}^2$) Values in the Correlations between Aquatic Species Toxicity Data and Chromatographic or Partitioning Data of the Considered Physicochemical and Biological Systems

system		O/W	RP18	IAM	SDS MEKC	SLN	STC	TTAB	SDS-Brij 35	SDS MEEKC	DPPG-DPPC	AGESS
tadpoles	RT	0.206	0.317	0.201	0.167	0.177	0.168	0.172	0.095	0.224	0.162	
fish	FM	0.183	0.250	0.145	0.251	0.123	0.140	0.188	0.114	0.183	0.094	
	GO	0.351	0.408	0.318	0.288	0.245	0.204	0.205	0.241	0.356	0.246	
water fleas	DM24	0.248	0.342	0.181	0.244	0.125	0.135	0.144	0.127	0.252	0.117	
protozoan	TP	0.125	0.180	0.087	0.168	0.069	0.074	0.112	0.066	0.132	0.057	
	CP	0.509	0.617	0.383	0.500	0.297	0.303	0.227	0.307	0.529	0.279	
bacteria	PP	0.292	0.353	0.242	0.239	0.157	0.144	0.169	0.176	0.297	0.182	
	SS	0.150	0.174	0.137	0.138	0.112	0.114	0.107	0.120	0.154	0.125	

FM, DM24, and TP (in addition to DM48, GP, DP, SA, and BG).

From the above reasoning, it can be deduced that among the electrophoretic systems, TTAB, on one hand, and STC, SLN, SDS-Brij 35, and DDPG-DPPC, on the other hand, are the best ones to emulate aquatic toxicity, whereas SDS MECK and SDS MEECK do not perform as well. It is noteworthy that the classical and widely used O/W partition and C18 and IAM HPLC systems are not expected to provide the best correlations for any of the aquatic toxicity systems. In fact, only IAM seems to be suitable for aquatic systems of the cluster of SS and the cluster of FM, DM24 and TP. These conclusions can be graphically observed in Figure 2, which presents the dendrogram and PCA plots of the joint aquatic toxicity and physicochemical systems. At 0.25 *d*-level, there are four clusters. One cluster is only formed by physicochemical systems (O/W, RP18 (C_{18} reverse phase HPLC column), SDS MEECK, and SDS MEKC), without any toxicity system, and placed in the upper left side corner of PCA plot. Another cluster in the central part of the PCA plot includes the toxicity systems of RT, FM, TP, and DM24, and the physicochemical systems of STC, SLN, SDS-Brij 35, AGESS (dodecane allyl glycidyl ether sulfite-modified siloxane), DPPG-DPPC, and even IAM. IAM is placed in one side of the cluster, close to the O/W cluster. TTAB and SS are in another cluster. Finally, there is one cluster with only toxicity systems (PP, GO, and CP), but TTAB is the physicochemical system closest to this cluster. In fact, the central position of TTAB among all the selected toxicity systems suggests that it can surrogate well all the aquatic toxicity systems, confirmed by the good *d* distances and predicted variances for TTAB presented in Tables 1 and 2. Also SLN, STC, and SDS-Brij 35 are also close to TTAB, in the central part of PC plot, and may surrogate well many aquatic toxicity systems. According to the results obtained through the different comparison tools and our previous experience on aquatic toxicity modeling,[22,23] three MEKC systems (STC, TTAB, and SDS-Brij 35) and one HPLC system (IAM) have been selected to correlate their experimental values against the ones of the biological systems. STC and SDS-Brij 35 micelles are anionic surfactants whereas TTAB belongs to cationic surfactants class. SLN has been discarded because it has a high UV−vis absorbance and may interfere with the tested substances detection. The other SDS-based systems are not expected to model toxicity as well as the ones selected. DPPG-DPPC system, which uses liposomes as pseudostationary phase, has not been selected because liposomes are not as easy to prepare and manageable as the other systems present in the same cluster. As regard HPLC systems, the one based on an IAM column is the one that can better model the aquatic toxicity; thus, it has been included in the experimental study.

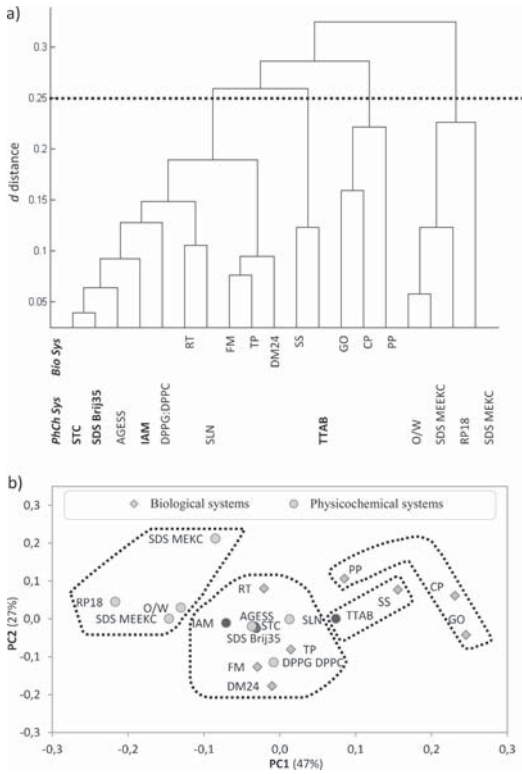

Figure 2. (a) Dendrogram plot of the biological and physicochemical systems included in Table 1. Selected systems are shown in boldface. (b) PCA scores plot of the eight biological systems (diamond) and the 11 physicochemical systems (circle) evaluated in this work. The four final selected physicochemical systems are shown in dark gray.

Selection of the Solutes to Be Tested. Nearly 500 substances with known toxicity values to at least one of the eight selected aquatic species have been considered in this work.[7,9−11,24−33] A PCA analysis of the available solutes has been done according to their SPM molecular descriptors.[14] In this way, compounds are distributed in the scores plot according to their physicochemical properties. Four criteria have been followed to select the compounds that will further be analyzed in the chosen chromatographic systems: first, substances must cover all the PCA chemical space to ensure a set of compounds that are chemically diverse (this is, their

DOI: 10.1021/acs.analchem.7b01301
Anal. Chem. 2017, 89, 7996−8003

Table 3. Experimental Evaluation of the Performance of the Studied Chromatographic Systems to Emulate Toxicity of Organic Compounds to Eight Aquatic Species (Standard Deviations in Brackets)[a]

		q (SD_q)	p (SD_p)	i(SD_i)	$SD_{correxp}^2$	n	R^2	F	$n_{outliers}$
R. tadpoles	IAM	3.10 (0.06)	2.67 (0.13)	0.21 (0.08)	0.080	60	0.900	255	5
	STC	3.21 (0.05)	1.24 (0.06)	0.08 (0.07)	0.065	56	0.897	231	4
	SDS-Brij 35	2.40 (0.05)	1.00 (0.05)	0.10 (0.08)	0.067	57	0.896	232	3
	TTAB	2.66 (0.08)	0.86 (0.09)	0.19 (0.12)	0.162	54	0.691	57	1
F. minnow	IAM	3.55 (0.05)	2.26 (0.14)		0.152	63	0.815	268	3
	STC	3.77 (0.04)	0.93 (0.06)		0.072	54	0.840	273	5
	SDS-Brij 35	2.71 (0.11)	1.18 (0.10)		0.296	41	0.763	126	1
	TTAB	3.24 (0.06)	0.97 (0.07)		0.155	58	0.784	203	1
D. magna (24 h)	IAM	3.58 (0.07)	2.74 (0.16)		0.197	47	0.865	289	1
	STC	4.02 (0.07)	0.86 (0.10)		0.129	40	0.679	80	1
	SDS-Brij 35	2.61 (0.12)	1.42 (0.12)		0.237	32	0.819	135	1
	TTAB	3.24 (0.10)	1.16 (0.11)		0.216	37	0.774	120	1
T. pyriformis	IAM	0.02 (0.05)	2.08 (0.12)		0.129	61	0.825	277	3
	STC	0.28 (0.04)	0.85 (0.06)		0.099	53	0.784	185	1
	SDS-Brij 35	−0.71 (0.04)	1.09 (0.05)		0.054	45	0.930	571	5
	TTAB	−0.28 (0.04)	0.92 (0.05)		0.071	55	0.862	331	4
S. sobrinus	IAM	−0.93 (0.07)	1.75 (0.17)		0.113	28	0.811	112	0
	STC	−0.84 (0.06)	1.11 (0.08)		0.096	30	0.875	195	0
	SDS-Brij 35	−1.50 (0.08)	0.77 (0.06)		0.055	24	0.879	160	2
	TTAB	−1.57 (0.08)	0.82 (0.07)		0.055	23	0.871	142	2
G. orfe	IAM	3.29 (0.15)	2.30 (0.42)		0.364	19	0.641	30	0
	STC	3.49 (0.11)	0.38 (0.20)		0.153	13	0.247	4	1
	SDS-Brij 35	2.51 (0.15)	1.20 (0.20)		0.402	23	0.638	37	0
	TTAB	2.93 (0.11)	1.20 (0.16)		0.194	18	0.782	57	1
C. paramecium	IAM	3.46 (0.18)	1.62 (0.58)		0.401	17	0.342	8	0
	STC	3.89 (0.21)	1.22 (0.34)		0.277	15	0.501	13	0
	SDS-Brij 35	2.93 (0.15)	1.01 (0.26)		0.379	19	0.474	15	0
	TTAB	3.16 (0.14)	1.10 (0.27)		0.323	17	0.518	16	0
P. putida	IAM	3.56 (0.11)	2.14 (0.32)		0.315	33	0.594	45	0
	STC	3.81 (0.12)	0.67 (0.19)		0.259	25	0.357	13	0
	SDS-Brij 35	2.98 (0.10)	0.96 (0.13)		0.309	34	0.617	52	0
	TTAB	3.41 (0.09)	1.02 (0.15)		0.209	26	0.666	48	1

[a]The biological systems have been grouped according to the clustering in the dendrogram (Figure 2a).

descriptors must be representative of the chemical space[14]); second, they must be neutral at the working pH, since all the SPM equations compared stand only for neutral compounds; third, selected compounds must have chromophore groups due to detection requirements; and finally, a minimum of 10 solutes for each species must be selected. According to these criteria, a selection of 152 compounds of known toxicity data was made (Table S-4). Figure S-1 shows the final distribution of the selected compounds; all of the graphic area is covered with the selected solutes.

Evaluation of the Performance of Chromatographic Systems to Estimate Nonspecific Toxicity to Aquatic Species. After selection of the compounds, their retention factors were determined in the physicochemical systems (Table S-5). Then, a regression analysis of experimental toxicity property logarithm values vs retention factor logarithm value was done, according to (eq 4). In case of RT, literature reports narcosis data of different RT species, most of them belonging to *R. temporaria* and *R. japonica* ones. Similarly to previous studies,[9] a flag descriptor (I_{jap}) was introduced into the global equation to obtain more accurate predictions. Therefore, toxicity to RT was correlated through the following equation:

$$\log C_{nar} = q + p \log k + iI_{jap} \quad (5)$$

The indicator variable I_{jap} is set to 1 when the toxicological property has been evaluated on *R. japonica* species and to 0 otherwise (*R. temporaria*).

Table 3 includes the regression parameters of all of the systems evaluated. As already shown on a previous research work, toxicity to RT can be modeled using any of the three systems in its cluster (STC, SDS-Brij 35, and IAM). TTAB prediction is not so good. In the case of FM, the system that best can surrogate the toxicity is STC, followed by IAM. SDS-Brij 35 and TTAB can also be used, but they show weaker prediction abilities. Toxicity to DM24 and TP, in the same cluster as RT and FM, can be modeled well using either IAM or SDS-Brij 35; STC is not a so precise system. TTAB shows good prediction ability for TP but not so good for DM24.

Initial predictions pointed out that TTAB would be the best system to emulate SS. We also found that SDS-Brij 35 and STC could be alternatives. These results agree quite well with the predictions based on Tables 1 and 2 and Figure 2. SDS-Brij 35 and STC were in the neighbor cluster to that of SS, the d distance was close to 0.25 and the $SD_{corrcal}^2$ value was similar to that of TTAB.

TTAB was not clustered to GO, CP, and PP systems but was in the neighborhood and would be the best of the tested systems to emulate the toxicity to these aquatic species. In fact, this system has moderate ability to emulate GO, CP, and PP

DOI: 10.1021/acs.analchem.7b01301
Anal. Chem. 2017, 89, 7996−8003

Table 4. Correlation Parameters and Statistics of the Internal Validation

biological system	physicochemical system	q (SD_q)	p (SD_p)	i_{jap} ($SD_{i,jap}$)	SD_{corr}^2	nR^2	F	Q_{LMO}^2	toxicity range evaluated	
RT	STC	3.23 (0.07)	1.29 (0.09)	0.07 (0.11)	0.075	31	0.893	117	0.90	1.6−5.3[a]
	SDS-Brij 35	2.44 (0.07)	1.05 (0.07)	−0.05 (0.12)	0.083	32	0.904	137	0.90	0.8−4.4[a]
FM	STC	3.81 (0.05)	0.99 (0.08)		0.071	31	0.849	163	0.85	2.4−5.3[b]
DM24	IAM	3.53 (0.08)	2.94 (0.18)		0.175	32	0.900	269	0.90	1.1−6.7[b]
	SDS-Brij 35	2.57 (0.15)	1.43 (0.16)		0.250	21	0.812	82	0.85	1.1−4.8[b]
TP	SDS-Brij 35	−0.73 (0.05)	1.08 (0.06)		0.047	27	0.929	328	0.93	−1.8−1.6[c]
SS	TTAB	−1.61 (0.07)	0.85 (0.06)		0.026	16	0.943	233	0.94	−1.6−0.5[d]

[a]−log C_{nar} (C_{nar} = narcosis concentration). [b]−log LC_{50} (LC_{50} = median lethal concentration, 50%). [c]−log IGC_{50} (IGC_{50} = median inhibitory growth concentration, 50%). [d]−log MIC (MIC = minimum inhibitory concentration toward bacterial growth).

Table 5. Correlation Parameters and Statistics of the External Validation

biological system	physicochemical system	q (SD_q)	p (SD_p)	SD_{corr}^2	n	R^2	R_{adj}^2	F	Q_{LMO}^2
RT	STC	0.05 (0.20)	0.99 (0.07)	0.06	25	0.90	0.90	213	0.92
	SDS-Brij 35	0.30 (0.23)	0.91 (0.07)	0.05	25	0.86	0.86	147	0.92
FM	STC	0.24 (0.34)	0.96 (0.09)	0.08	23	0.85	0.84	116	0.86
DM24	IAM	−0.21 (0.61)	1.03 (0.15)	0.30	15	0.79	0.78	49	0.81
	SDS-Brij 35	0.43 (0.46)	0.85 (0.13)	0.22	11	0.83	0.82	46	0.83
TP	SDS-Brij 35	−0.08 (0.06)	0.92 (0.06)	0.07	17	0.93	0.93	201	0.94
SS	TTAB	−0.19 (0.22)	0.80 (0.24)	0.14	7	0.70	0.64	12	0.77

toxicity. As expected, R^2 and F are not as high as in the case of SS because these three systems do not have the same level of similarity as SS to TTAB. Further efforts have to be done to find suitable chromatographic systems to model the toxicity to PP. In the case of GO and CP, the TTAB system seems promising but the number of tested solutes should be increased to confirm its ability to model toxicity.

Validation of the Best Chromatographic Models. Those systems showing the best correlation parameters have been validated to prove their robustness and prediction ability. The selected models have been internally and externally validated to check their robustness and predictive ability, respectively. To perform the model's validation, the set of solutes was divided into a training set (around 2/3 of the compounds) and a test set (around 1/3 of the compounds). To ensure all type of compounds were included in both the training and test sets, this selection was done on the basis of a PCA with solute SPM descriptors that represents the chemical space (see Figure S-1). For the internal validation, the models were established again, but only with the solutes of the training set. Table 4 shows the correlation parameters obtained and also the toxicity range evaluated for each of the systems. Equations' coefficients are similar to those of the models with all solutes (Table 3), which is indicative of the robustness of the models. Adequate determination coefficients, standard deviations and F values were obtained. Furthermore, an additional parameter, the leave-multiple-out cross-validation coefficient was calculated. This coefficient was higher than 0.6 in all cases, which also points out the robustness of the selected systems.[34]

Finally, the external validation was performed. A regression was done between the experimental toxicity and the one predicted through the training set equations for the compounds of the test set. Table 5 shows the correlation parameters and statistics, including the leave-multiple-out cross-validation coefficient. According to statistics, all models considered show good prediction ability: the slopes of the trend lines are not significantly different from unity and the intercepts from zero at 95% confidence level by students t test; the variances (SD^2) are of the same order of that of the biological data, the determination coefficients (R^2) are above 0.6 and similar to $R_{adjusted}^2$; the correlation cross-validation coefficients ($QLMO^2$) are above 0.5; and Fisher's F parameter is significant.

CONCLUSION

The similarity analysis from d distances between different biological systems used to predict aquatic toxicity shows that most systems provide similar toxicity information. The same methodology together with estimation of the variance of the toxicity-chromatographic retention prediction show that some chromatographic systems can surrogate aquatic toxicity measurement systems. Thus, the toxicity of chemicals to a particular aquatic species can be easily estimated from the chromatographic retention of the chemicals in the surrogating chromatographic systems. The similarity analysis shows that the chromatographic systems that are able to best emulate the aquatic toxicology to eight representative species (*Rana* tadpoles, Fathead minnow, Golden orfe, *Dapnia magna 24h*, *Tetrahymena pyriformis*, *Chilomonas paramecium*, *Pseudomonas putida*, and *Streptococus sobrinus*) are the micellar electrokinetic chromatographic systems with micellar pseudoestationary phases of STC, a mixture of SDS and Brij 35, or TTAB. The similarity analysis also shows that other biological systems ruled by similar toxicity mechanisms (such as Guppy, Bluegill, Medaka high-eyes, *Daphnia magna* 48 h, *Ceriodaphnia dubia*, *Daphnia pulex*, *Spirostomum ambiguum*, *Porphyromonas gingivalis*, or *Selenomonas artemidis*) can be surrogated using the same chromatographic systems.

ASSOCIATED CONTENT

Supporting Information

The Supporting Information is available free of charge on the ACS Publications website at DOI: 10.1021/acs.analchem.7b01301.

Coefficients, statistics, and normalized coefficients of the SPM characterization of systems related to toxicity to aquatic species and physicochemical systems characterized through the SPM, contributions that determine the

DOI: 10.1021/acs.analchem.7b01301
Anal. Chem. 2017, 89, 7996−8003

overall variance ($SD_{corrcal}^2$) in the correlations between aquatic species toxicity data and chromatographic or partitioning data of the considered physicochemical systems, experimental toxicity data for the selected solutes, solute retention factor logarithm under the different chromatographic conditions, PCA scores plot of solutes with known toxicity data and the projection of the solute selection made in this work and plots of biological property logarithm versus experimental retention factor logarithm of the physicochemical systems with the best regressions (PDF)

AUTHOR INFORMATION

Corresponding Author

*E-mail: marti.roses@ub.edu. Phone: (+34) 93 403 92 75. Fax: (+34) 93 402 12 33.

ORCID

Susana Amézqueta: 0000-0001-8976-467X

Martí Rosés: 0000-0001-5303-3242

Notes

The authors declare no competing financial interest.

ACKNOWLEDGMENTS

Financial support from the Ministerio de Economía y Competitividad from the Spanish Government (CTQ2014-56253-P) and the Catalan Government (2014SGR277) is acknowledged. AFP wishes to thank the University of Barcelona for his APIF PhD fellowship.

REFERENCES

(1) Ankley, G. T.; Villeneuve, D. L. *Aquat. Toxicol.* **2006**, *78*, 91−102.

(2) ECHA (European Chemicals Agency). What about animal testing? http://echa.europa.eu/chemicals-in-our-life/animal-testing-under-reach (accessed Apr 11, 2016).

(3) U.S. EPA. Process for evaluating & implementing alternative approaches to traditional in vivo acute toxicity studies for FIFRA regulatory use. https://www.epa.gov/pesticide-science-and-assessing-pesticide-risks/process-establishing-implementing-alternative (accessed Jan 31, 2017).

(4) Poole, C. F.; Ariyasena, T. C.; Lenca, N. *J. Chromatogr. A* **2013**, *1317*, 85−104.

(5) Abraham, M. H. *Chem. Soc. Rev.* **1993**, *22*, 73.

(6) Abraham, M. H.; Rafols, C. *J. Chem. Soc., Perkin Trans. 2* **1995**, No. 10, 1843.

(7) Hoover, K. R.; Acree, W. E.; Abraham, M. H. *Chem. Res. Toxicol.* **2005**, *18*, 1497−1505.

(8) Bowen, K. R.; Flanagan, K. B.; Acree, W. E.; Abraham, M. H. *Sci. Total Environ.* **2006**, *369*, 109−118.

(9) Bowen, K. R.; Flanagan, K. B.; Acree, W. E.; Abraham, M. H.; Rafols, C. *Sci. Total Environ.* **2006**, *371*, 99−109.

(10) Mintz, C.; Acree, W. E.; Abraham, M. H. *QSAR Comb. Sci.* **2006**, *25*, 912−920.

(11) Hoover, K. R.; Flanagan, K. B.; Acree, W. E., Jr.; Abraham, M. H. *J. Environ. Eng. Sci.* **2007**, *6*, 165−174.

(12) Abraham, M. H.; Chadha, H. S.; Whiting, G. S.; Mitchell, R. C. *J. Pharm. Sci.* **1994**, *83*, 1085−1100.

(13) Trone, M. D.; Khaledi, M. G. *Electrophoresis* **2000**, *21*, 2390−2396.

(14) Fuguet, E.; Ràfols, C.; Bosch, E.; Abraham, M. H.; Rosés, M. *J. Chromatogr. A* **2002**, *942*, 237−248.

(15) Schulte, S.; Palmer, C. P. *Electrophoresis* **2003**, *24*, 978−983.

(16) Lázaro, E.; Ràfols, C.; Abraham, M. H.; Rosés, M. *J. Med. Chem.* **2006**, *49*, 4861−4870.

(17) Liu, J.; Sun, J.; Wang, Y.; Liu, X.; Sun, Y.; Xu, H.; He, Z. *J. Chromatogr. A* **2007**, *1164*, 129−138.

(18) Kipka, U.; Di Toro, D. M. *Environ. Toxicol. Chem.* **2009**, *28*, 1429−1438.

(19) Fuguet, E.; Ràfols, C.; Bosch, E.; Abraham, M. H.; Rosés, M. *Electrophoresis* **2006**, *27*, 1900−1914.

(20) Castillo-Garit, J. a.; Marrero-Ponce, Y.; Escobar, J.; Torrens, F.; Rotondo, R. *Chemosphere* **2008**, *73*, 415−427.

(21) Hidalgo-Rodríguez, M.; Fuguet, E.; Ràfols, C.; Rosés, M. *Anal. Chem.* **2010**, *82*, 10236−10245.

(22) Hidalgo-Rodríguez, M.; Fuguet, E.; Ràfols, C.; Rosés, M. *Anal. Chem.* **2012**, *84*, 3446−3452.

(23) Fernández-Pumarega, A.; Amézqueta, S.; Fuguet, E.; Rosés, M. *J. Chromatogr. A* **2015**, *1418*, 167−176.

(24) Overton, E. *Studien über die Narkose, zurgleich eing Bertrag zur allgemeinen Pharmakologie*; Gustav Fischer: Jena, 1901.

(25) Huang, H.; Wang, X.; Ou, W.; Zhao, J.; Shao, Y.; Wang, L. *Chemosphere* **2003**, *53*, 963−970.

(26) Wang, X.; Dong, Y.; Xu, S.; Wang, L.; Han, S. *Bull. Environ. Contam. Toxicol.* **2000**, *64*, 859−865.

(27) Overton, E. *Studies on Narcosis*; Lipnick, R. L., Ed.; Chapman and Hall: London, 1991.

(28) Meyer, K.; Hemmi, H. *Biochem. Z.* **1935**, *277*, 39−71.

(29) Kita, Y.; Bennett, L. J.; Miller, K. W. *Biochim. Biophys. Acta, Biomembr.* **1981**, *647*, 130−139.

(30) Juhnke, I.; Luedemann, D. *Z. Wasser Abwasser Forsch* **1978**, *11*, 161−164.

(31) Bringmann, G.; Kühn, R. *Water Res.* **1980**, *14*, 231−241.

(32) *Aquatic Toxicology and Environmental Fate*; Suter, G., Lewis, M., Eds.; ASTM: Philadelphia, 2007.

(33) Dobbins, L. L.; Usenko, S.; Brain, R. A.; Brooks, B. W. *Environ. Toxicol. Chem.* **2009**, *28*, 2744−2753.

(34) Roy, K. *Expert Opin. Drug Discovery* **2007**, *2*, 1567−1577.

DOI: 10.1021/acs.analchem.7b01301
Anal. Chem. 2017, 89, 7996−8003

SUPPLEMENTARY INFORMATION

MODELING AQUATIC TOXICITY THROUGH CHROMATOGRAPHIC SYSTEMS

Alejandro Fernández-Pumarega[1], Susana Amézqueta[1], Sandra Farré[1], Laura Muñoz-Pascual[1], Michael H. Abraham[2], Elisabet Fuguet[1,3], Martí Rosés[1*]

[1] Departament de Química Analítica and Institut de Biomedicina (IBUB), Facultat de Química, Universitat de Barcelona, Martí i Franquès 1-11, 08028, Barcelona, Spain.

[2] Department of Chemistry, University College London, 20 Gordon Steet, London WC1H 0AJ, UK.

[3] Serra Húnter Programme. Generalitat de Catalunya. Spain

* Correspondence:

Prof. Martí Rosés. E-mail: marti.roses@ub.edu

Departament de Química Analítica, Facultat de Química, Universitat de Barcelona

c/ Martí i Franquès 1-11, 08028, Barcelona, Spain

Phone: (+34) 93 403 92 75

Fax: (+34) 93 402 12 33

Running title. Modeling aquatic toxicity through chromatographic systems.

This supplementary information file contains data about:

Table S-1

Coefficients, statistics and normalized coefficients of the SPM characterization of systems related to toxicity to aquatic species.

	System	-log TP[1]	Coefficients						Statistics				Normalized coefficients					References
			c	*e*	*s*	*a*	*b*	*v*	n	r	SD	F	e_u	s_u	a_u	b_u	v_u	
Tadpoles	*Rana* tadpoles	-log C_{nar}[2]	0.582	0.770	-0.696	0.243	-2.592	3.343	114	0.954	0.337	217	0.177	-0.160	0.056	-0.594	0.766	[1]
Fish	Fathead minnow (*Pimephales promelas*)	-log LC50[3]	0.996	0.418	-0.182	0.417	-3.574	3.377	198	0.976	0.276	779.5	0.084	-0.037	0.084	-0.721	0.681	[2]
	Guppy (*Poecilia reticulata*)	-log LC50	0.811	0.782	-0.230	0.341	-3.050	3.250	148	0.973	0.280	493	0.172	-0.051	0.075	-0.671	0.715	[2]
	Bluegill (*Lepomis macrochirus*)	-log LC50	0.903	0.583	-0.127	1.238	-3.918	3.306	66	0.984	0.272	360	0.110	-0.024	0.233	-0.738	0.623	[2]
	Golden orfe (*Leuciscus idus melanotus*)	-log LC50	-0.137	0.931	0.379	0.951	-2.392	3.244	49	0.967	0.269	127	0.218	0.089	0.223	-0.561	0.761	[2]
	Goldfish (*Carassius auratus*)	-log LC50	0.922	-0.653	1.872	-0.329	-4.516	3.078	51	0.983	0.277	254	-0.112	0.321	-0.057	-0.776	0.529	[2]
	Medaka high-eyes (*Oryzias latipes*)	-log LC50 (48 h)	0.834	1.047	-0.380	0.806	-2.182	2.667	50	0.969	0.292	133	0.282	-0.102	0.217	-0.588	0.719	[2]
	Medaka high-eyes (*Oryzias latipes*)	-log LC50 (96 h)	-0.176	1.046	0.272	0.931	-2.178	3.155	44	0.980	0.277	182	0.256	0.066	0.228	-0.532	0.771	[2]
Water fleas	*Daphnia magna*	-log LC50 (24 h)	0.915	0.354	0.173	0.420	-3.935	3.521	107	0.976	0.274	410	0.067	0.033	0.079	-0.741	0.663	[3]
	Daphnia magna	-log LC50 (48 h)	0.841	0.528	-0.025	0.219	-3.703	3.591	96	0.982	0.289	475	0.102	-0.005	0.042	-0.714	0.692	[3]
	Ceriodaphnia dubia	-log LC50	2.234	0.373	-0.040	-0.437	-3.276	2.763	44	0.967	0.256	111	0.086	-0.009	-0.101	-0.758	0.639	[3]
	Daphnia pulex	-log LC50	0.502	0.396	0.309	0.542	-3.457	3.527	45	0.981	0.311	233	0.079	0.062	0.109	-0.692	0.706	[3]

Protozoan	*Tetrahymena pyriformis*	-log IGC50[4]	0.616	0.413	-0.048	0.348	-2.707	2.944	192	0.982	0.205	1002	0.102	-0.012	0.086	-0.671	0.729	[3]
	Spirostomum ambiguum	-log LC50	0.148	0.111	0.288	0.687	-3.301	3.140	60	0.979	0.246	252	0.024	0.062	0.149	-0.715	0.680	[3]
	Entosiphon sulcantum	-log IGC[5]	0.489	0.894	0.355	1.108	-2.504	2.852	51	0.959	0.333	103	0.220	0.087	0.272	-0.615	0.701	[4]
	Uronema parduczi	-log IGC	2.706	1.426	0.433	0.938	-1.025	2.599	59	0.961	0.326	127	0.432	0.131	0.284	-0.310	0.787	[4]
	Chilomonas paramecium	-log IGC	0.440	1.129	0.160	0.442	-1.826	2.446	56	0.942	0.351	77	0.343	0.049	0.134	-0.555	0.744	[4]
Bacteria	*Pseudomonas putida*	-log IGC	0.752	0.955	0.092	-0.081	-2.088	2.947	87	0.963	0.269	209	0.255	0.025	-0.022	-0.559	0.788	[3]
	Porphyromonas gingivalis	-log MIC[6]	-3.320	1.111	-0.605	0.727	-1.904	2.423	126	0.952	0.313	232	0.326	-0.177	0.213	-0.558	0.711	[5]
	Selenomonas artemidis	-log MIC	-3.008	0.982	-0.496	0.972	-2.643	2.312	116	0.933	0.268	149	0.258	-0.130	0.255	-0.694	0.607	[5]
	Streptococcus sobrinus	-log MIC	-3.465	0.855	-0.465	0.735	-1.671	2.330	112	0.950	0.309	196	0.274	-0.149	0.236	-0.536	0.748	[5]

[1]TP: toxicity parameter; [2]C_{nar}: narcosis concentration; [3]LC50: median lethal concentration, 50 %; [4]IGC50: median inhibitory growth concentration, 50 %;

[5]IGC: inhibitory growth concentration; [6]MIC: minimum inhibitory concentration towards bacterial growth.

Table S-2

Coefficients, statistics and normalized coefficients for physicochemical systems characterized through the SPM.

System[1]	-log PP[2]	Coefficients						Statistics				Normalized coefficients					References
		c	*e*	*s*	*a*	*b*	*v*	n	r	SD	F	e_u	s_u	a_u	b_u	v_u	
O/W	$\log P_{o/w}$	0.088	0.562	-1.054	0.034	-3.460	3.814	613	0.997	0.116	23162	0.106	-0.199	0.006	-0.655	0.721	6
RP18 (40 % CH_3CN)	$\log k_{HPLC}$	-0.172	0.233	-0.460	-0.260	-1.574	1.582	55	0.996	0.056	1121	0.101	-0.200	-0.113	-0.683	0.686	7
IAM (40 % CH3CN)	$\log k_{HPLC}$	-0.710	0.292	-0.344	0.141	-1.193	1.161	51	0.991	0.047	480	0.169	-0.199	0.081	-0.689	0.671	7
SDS MEKC	$\log k_{MEKC}$	-1.680	0.558	-0.596	-0.266	-1.674	2.717	63	0.991	0.120	618	0.169	-0.180	-0.080	-0.507	0.822	8
SLN	$\log k_{MEKC}$	-1.99	0.44	-0.39	0.45	-2.32	2.92	36	0.99	0.06	-	0.116	-0.103	0.118	-0.610	0.768	9
STC	$\log k_{MEKC}$	-1.838	0.613	-0.513	0.319	-2.396	2.390	56	0.984	0.112	305	0.175	-0.147	0.091	-0.686	0.684	10
TTAB	$\log k_{MEKC}$	-1.851	0.902	-0.617	0.766	-2.410	2.634	53	0.994	0.089	746	0.237	-0.162	0.201	-0.632	0.691	8
SDS-Brij 35	$\log k_{MEKC}$	-1.412	0.622	-0.516	0.308	-2.699	2.829	27	0.987	0.105	154	0.155	-0.129	0.077	-0.674	0.706	11
SDS MEEKC	$\log k_{MEEKC}$	-1.133	0.279	-0.692	-0.060	-2.805	3.048	53	0.994	0.090	791	0.066	-0.164	-0.014	-0.667	0.724	12
DPPG-DPPC	$\log k_{LEKC}$	-2.21	0.45	-0.44	0.71	-3.23	3.13	27	0.995	0.07	-	0.098	-0.096	0.154	-0.703	0.681	13
AGESS	$\log k_{poly\text{-}EKC}$	-2.40	0.46	-0.43	0.27	-2.46	2.72	38	0.991	-	-	0.123	-0.115	0.072	-0.659	0.729	14

[1]RP: C_{18} reverse phase HPLC column; IAM: immobilized artificial membrane HPLC column; SDS: sodium dodecyl sulfate; SLN: sodium *N*-lauroylsarcosinate; STC: sodium taurocholate; TTAB: tetradecyltrimethylammonium bromide; Brij 35: polyoxyethylene(23)dodecyl ether; DPPG: dipalmitoylphosphatidyl glycerol; DPPC: dipalmitoylphosphatidyl choline; AGESS: dodecane allyl glycidyl ether sulfite-modified siloxane

[2]PP: physicochemical parameter

Table S-3

Contributions that determine the overall variance ($SD_{corr\ cal}^2$) in the correlations between aquatic species toxicity data and chromatographic or partitioning data of the considered physicochemical systems.

Systems	Nonspecific toxicity to *R.* tadpoles (SD_{bio}^2= 0.114, n_{bio}=114)					
	q_{cal}	p_{cal}	$(p_{cal}SD_{chrom})^2$	n_{chrom}	SD_d^2	$SD_{corr\ cal}^2$
O/W	1.201	0.820	0.009	613	0.083	0.206
RP18	1.998	1.765	0.010	55	0.194	0.317
IAM	3.151	2.564	0.015	51	0.073	0.201
SDS MEKC	2.584	1.250	0.022	63	0.031	0.167
SLN	2.766	1.159	0.005	36	0.010	0.128
STC	3.439	1.349	0.015	40	0.013	0.141
TTAB	2.834	1.129	0.010	53	0.049	0.172
SDS-Brij 35	2.490	1.135	0.009	27	0.019	0.141
SDS MEEKC	2.448	1.030	0.009	53	0.102	0.224
DPPG-DPPC	3.197	1.010	0.005	27	0.043	0.162
AGESS	3.700	1.219	-	40	0.012	-

Systems	Nonspecific toxicity to F. minnow (SD_{bio}^2= 0.076, n_{bio}=198)					
	q_{cal}	p_{cal}	$(p_{cal}SD_{chrom})^2$	n_{chrom}	SD_d^2	$SD_{corr\ cal}^2$
O/W	1.312	0.921	0.011	613	0.095	0.183
RP18	2.158	2.048	0.013	55	0.161	0.250
IAM	3.405	2.945	0.019	51	0.049	0.145
SDS MEKC	2.999	1.378	0.027	63	0.148	0.251
SLN	3.124	1.275	0.006	36	0.041	0.123
STC	3.747	1.451	0.017	40	0.047	0.140
TTAB	3.112	1.310	0.014	53	0.098	0.188
SDS-Brij 35	2.686	1.239	0.017	27	0.021	0.114
SDS MEEKC	2.731	1.143	0.011	53	0.096	0.183
DPPG-DPPC	3.475	1.108	0.006	27	0.012	0.094
AGESS	4.043	1.318	-	40	0.020	-

Systems	Nonspecific toxicity to G. orfe (SD_{bio}^2=0.072, n_{bio}=49)					
	q_{cal}	p_{cal}	$(p_{cal}SD_{chrom})^2$	n_{chrom}	SD_d^2	$SD_{corr\ cal}^2$
O/W	1.285	0.734	0.007	613	0.271	0.351
RP18	1.913	1.599	0.008	55	0.327	0.408
IAM	3.036	2.323	0.012	51	0.234	0.318
SDS MEKC	2.672	1.163	0.019	63	0.196	0.288
SLN	2.877	1.119	0.005	36	0.132	0.209
STC	3.443	1.271	0.013	40	0.119	0.204
TTAB	2.932	1.123	0.010	53	0.123	0.205
SDS-Brij 35	2.505	1.048	0.012	27	0.157	0.241
SDS MEEKC	2.396	0.924	0.007	53	0.277	0.356
DPPG-DPPC	3.169	0.945	0.004	27	0.169	0.246
AGESS	3.646	1.129	-	40	0.157	-

Systems	Nonspecific toxicity to *D. magna* (SD_{bio}^2=0.075, n_{bio}=107)					
	q_{cal}	p_{cal}	$(p_{cal}SD_{chrom})^2$	n_{chrom}	SD_d^2	$SD_{corr\ cal}^2$
O/W	1.503	0.931	0.012	613	0.161	0.248
RP18	2.450	1.967	0.012	55	0.254	0.342
IAM	3.559	2.915	0.019	51	0.087	0.181
SDS MEKC	3.245	1.362	0.027	63	0.142	0.244
SLN	3.297	1.352	0.007	36	0.043	0.125
STC	3.936	1.436	0.017	40	0.043	0.135
TTAB	3.222	1.287	0.013	53	0.055	0.144
SDS-Brij 35	3.006	1.250	0.010	27	0.032	0.117
SDS MEEKC	2.944	1.180	0.005	53	0.172	0.252
DPPG-DPPC	3.637	1.182	0.007	27	0.035	0.117
AGESS	4.256	1.371	-	40	0.038	-

Systems	Nonspecific toxicity to *T. pyriformis* (SD_{bio}^2=0.042, n_{bio}=192)					
	q_{cal}	p_{cal}	$(p_{cal}SD_{chrom})^2$	n_{chrom}	SD_d^2	$SD_{corr\ cal}^2$
O/W	1.193	0.779	0.008	613	0.075	0.125
RP18	1.928	1.729	0.009	55	0.128	0.180
IAM	2.988	2.489	0.014	51	0.031	0.087
SDS MEKC	2.624	1.164	0.019	63	0.106	0.168
SLN	2.709	1.074	0.004	36	0.022	0.069
STC	3.283	1.229	0.012	40	0.019	0.074
TTAB	2.734	1.090	0.009	53	0.061	0.112
SDS-Brij 35	2.378	1.042	0.012	27	0.012	0.066
SDS MEEKC	2.388	0.963	0.008	53	0.082	0.132
DPPG-DPPC	3.105	0.927	0.004	27	0.011	0.057
AGESS	3.505	1.109	-	40	0.014	-

Systems	Nonspecific toxicity to *C. paramecium* (SD_{bio}^2=0.123, n_{bio}=56)					
	q_{cal}	p_{cal}	$(p_{cal}SD_{chrom})^2$	n_{chrom}	SD_d^2	$SD_{corr\ cal}^2$
O/W	1.675	0.664	0.006	613	0.380	0.509
RP18	2.306	1.328	0.006	55	0.488	0.617
IAM	3.301	2.284	0.012	51	0.248	0.383
SDS MEKC	2.833	0.950	0.013	63	0.364	0.500
SLN	3.006	1.042	0.004	36	0.170	0.297
STC	3.535	1.164	0.011	40	0.169	0.303
TTAB	3.087	1.058	0.009	53	0.095	0.227
SDS-Brij 35	2.714	1.005	0.011	27	0.172	0.307
SDS MEEKC	2.669	0.821	0.005	53	0.401	0.529
DPPG-DPPC	3.359	0.930	0.004	27	0.152	0.279
AGESS	3.783	1.069	-	40	0.193	-

Systems	Nonspecific toxicity to *P. putida* (SD_{bio}^2=0.072, n_{bio}=87)					
	q_{cal}	p_{cal}	$(p_{cal}SD_{chrom})^2$	n_{chrom}	SD_d^2	$SD_{corr\ cal}^2$
O/W	1.898	0.723	0.007	613	0.213	0.292
RP18	2.543	1.501	0.007	55	0.273	0.353
IAM	3.600	2.298	0.012	51	0.158	0.242
SDS MEKC	3.246	1.155	0.019	63	0.148	0.239
SLN	3.414	1.122	0.005	36	0.080	0.157
STC	3.946	1.225	0.012	40	0.060	0.144
TTAB	3.423	1.082	0.009	53	0.087	0.169
SDS-Brij 35	3.051	1.025	0.012	27	0.092	0.176
SDS MEEKC	2.988	0.907	0.007	53	0.218	0.297
DPPG-DPPC	3.693	0.931	0.004	27	0.106	0.182
AGESS	4.180	1.113	-	40	0.095	-

Systems	Nonspecific toxicity to *S. sobrinus* (SD_{bio}^2=0.095, n_{bio}=112)					
	q_{cal}	p_{cal}	$(p_{cal}SD_{chrom})^2$	n_{chrom}	SD_d^2	$SD_{corr\ cal}^2$
O/W	-2.233	0.606	0.005	613	0.050	0.150
RP18	-1.552	1.417	0.006	55	0.072	0.174
IAM	-0.986	2.019	0.009	51	0.033	0.137
SDS MEKC	-1.160	0.831	0.010	63	0.033	0.138
SLN	-1.285	0.815	0.002	36	0.014	0.112
STC	-0.800	0.958	0.007	40	0.011	0.114
TTAB	-1.475	0.897	0.006	53	0.005	0.107
SDS-Brij 35	-1.532	0.837	0.008	27	0.017	0.120
SDS MEEKC	-1.267	0.760	0.005	53	0.054	0.154
DPPG-DPPC	-1.049	0.767	0.003	27	0.026	0.125
AGESS	-0.605	0.872	-	40	0.019	-

Table S-4

Experimental toxicity data for the selected solutes. Mean value has been used when several experimental values are available.

Solute	*R.* tadpoles	F. Minnow	G. Orfe	*D. Magna*	*T. Pyriformis*	*C. Paramecium*	*P. Putida*	*S. sorbrinus*
	15–20	2,21	2,22	3,21	3,23	4	3,24	5
	-log C_{nar} (M)	-log LC_{50} (M)	-log LC_{50} (M)	-log LC_{50} (M)	-log IGC_{50} (mM)	-log IGC (M)	-log IGC (M)	-log MIC (mM)
1,2,4-trimethylbenzene	-	4.19	-	4.53	-	-	-	-
(1*R*,2*S*,5*R*)-(-)-menthol	3.97[1]	-	-	-	-	-	-	-1.505
1,2-dichlorobenzene	3.79[2]	4.19	3.70	4.77	0.53	-	3.99	-
1,2-dinitrobenzene	4.050[2]	-	-	-	-	-	-	-
1,3-dimethylbenzene	3.42[1]	3.82	-	4.02	-	-	-	-
1,3-dinitrobenzene	-	4.12	4.38	4.20	0.76	-	4.08	-
1,3-propanediol	-	-	-	0.96	-	-	-	-
1,4-butanediol	-	-	-	-	-2.24	-	-	-
1,4-dichlorobenzene	3.85[2]	4.27	-	4.54	0.53	-	-	-
1,4-dimethylbenzene	-	4.08	-	-	0.19	-	-	-
1,5-pentanediol	-	-	-	-	-1.93	-	-	-
1-butanol	-	1.63	1.75	1.52	-1.43	-	2.06	-
1-chloro-4-nitrobenzene	3.93[2]	-	-	4.01	-	-	-	-
1-hexanol	-	2.96	2.90	2.71	-0.38	-	3.22	-
1-nitronaphthalene	-	4.46	-	-	-	-	-	-
1-octanol	3.40[1]	3.99	3.84	3.76	0.58	-	3.42	-
1-pentanol	-	2.27	2.26	2.09	-1.03	2.76	2.60	-
1-propanol	-	1.12	1.12	1.15	-1.75	2.53	1.35	-
2-(1-adamantyl)-4-methylphenol	-	-	-	-	-	-	-	1.854
2,3-benzofuran	-	3.93	-	-	-0.11	-	-	-
2,4-diclhoroaniline	3.73[2]	-	-	-	-	-	-	-
2,4-dichlorophenol	3.87[2]	4.32	4.51	4.64	1.04	4.45	4.43	-
2,4-dimethylphenol	-	3.87	-	4.14	0.14	-	-	-0.913
2,4-dinitrotoluene	4.06[2]	-	-	-	-	-	3.5	-
2,4-di-*tert*-butylphenol	-	-	-	-	-	-	-	0.398
2,6-diisopropylphenol	-	-	-	-	-	-	-	-0.688
2,6-dimethylphenol	3.32[2]	3.75	-	3.93	-0.08	-	-	-1.281
2-benzyloxyphenol	-	-	-	-	-	-	-	-0.220
2-bromophenol	-	-	-	4.58	-	-	-	-1.063
2-butanol	-	1.31	1.33	1.22	-1.54	1.99	2.17	-
2-butoxyethanol	-	-	-	-	-1.37	-	2.2	-
2-chloro-5-nitroaniline	3.47[2]	-	-	-	-	-	-	-
2-chloroaniline	-	4.35	-	-	-0.17	-	-	-
2-chlorophenol	3.01[2]	4.05	-	4.05	0.18	-	-	-
2-chlorotoluene	-	-	-	3.80	-	-	3.93	-
2-fluorophenol	-	-	-	-	-	-	-	-1.552
2-hydroxyacetanilide	-	-	-	-	-	-	-	-0.900
2-methoxyphenol	2.57[1]/2.65[2]	-	-	-	-	-	-	-1.633
2-methyl-1-butanol	-	-	-	-	-0.95	-	-	-
2-methyl-1-propanol	1.35[1]	1.71	1.69	1.74	-1.37	-	2.42	-
2-methyl-2-butanol	1.24[1]	-	1.56	-	-1.17	1.50	2.33	-
2-methyl-2-propanol	0.89[1]	1.06	-	1.13	-1.79	-	-	-

2-methylaniline	-	-	2.96	-	-0.16	2.66	3.83	-
2-methylfuran	-	-	-	-	-	2.87	2.96	-
2-naphthol	3.89[2]	4.62	-	-	-	-	-	-
2-nitroaniline	2.60[1]	-	-	-	0.08	-	-	-
2-nitroanisole	-	-	-	3.37	-	-	-	-
2-pentanol	-	-	-	-	-1.16	-	-	-
2-phenylphenol	-	4.44	-	4.81	1.09	-	-	-0.137
2-propanol	-	0.81	0.83	0.87	-1.88	2.76	1.76	-
2-*tert*-butyl-4-methylphenol	-	-	-	-	-	-	-	-0.079
3,5-dichlorophenol	-	-	-	-	1.57	-	-	-
3-aminophenol	2.064[2]	-	-	-	-	-	-	-
3-bromophenol	-	-	-	-	-	-	-	-0.517
3-cyanophenol	-	-	-	-	-	-	-	-1.225
3-methyl-1-butanol	1.64[1]	-	-	-	-1.04	-	-	-
3-methyl-2-butanol	-	-	-	-	-1.00	-	-	-
3-methylphenol	2.75[1]	3.29	3.75	3.77	-0.08	2.98	3.31	-1.170
3-nitroaniline	-	-	-	-	0.03	-	-	-
3-nitrophenol	3.51[2]	-	-	-	-	4.03	4.30	-
3-pentanol	-	-	-	-	-1.24	-	-	-
4-acetylphenol	-	-	-	-	-	-	-	-1.434
4-benzoylphenol	-	-	-	-	-	-	-	-0.305
4-benzyloxyphenol	-	-	-	-	-	-	-	0.000
4-bromophenol	3.66[2]	-	-	-	0.68	-	-	-0.517
4-chloroaniline	-	3.61	-	-	0.05	-	-	-
4-chlorophenol	3.42[2]	4.32	-	4.21	0.54	-	-	-
4-fluorophenol	2.69[2]	-	-	-	0.017	-	-	-1.251
4-heptyloxyphenol	-	-	-	-	-	-	-	0.854
4-hexyloxyphenol	-	-	-	-	-	-	-	0.538
4-hydroxy-4-methyl-2-pentanone	-	-	1.041	-	-	-	2.15	-
4-hydroxyacetanilide	-	2.27	-	-	-0.82	-	-	-
4-hydroxyacetophenone	2.50[2]	-	-	-	-	-	-	-
4-iodophenol	-	-	-	-	0.85	-	-	-
4-methylaniline	-	2.83	-	-	-0.05	-	-	-
4-methylphenol	2.75[1]/3.06[2]	3.58	-	3.99	-0.16	-	-	-1.333
4-methylpyridine	-	-	-	-	-0.4548	-	-	-
4-nitro-naphthalen-1-ylamine	4.236[2]							
4-nitroaniline	-	3.08	-	-	-	4.44	4.54	-
4-nitrotoluene	3.62[2]	3.76	3.76	4.26	0.65	3.93	3.72	-
4-octylphenol	-	-	-	-	-	-	-	1.000
4-pentylphenol	-	-	-	4.91	-	-	-	0.523
4-*tert*-butylphenol	4.03[2]	4.46	-	-	0.91	-	-	-0.601
4-*tert*-butylpyridine	-	-	-	-	0.164	-	-	-
acetamide	0.77[1]	-	-	-	-	-	-	-
acetanilide	2.31[1]	-	-	-	-	-	-	-
acetophenone	3.04[1]	-	-	-	-	-	-	-
adalin	2.70[1]	-	-	-	-	-	-	-
aniline	1.96[1]	2.95	-	-	-0.23	2.57	2.85	-
anisole	2.82[1]	-	2.95	-	-0.10	-	-	-
anthracene	-	-	-	5.93	-	-	-	-
antipyrine	1.89[1]	-	-	-	-	-	-	-
benzaldehyde	-	-	-	-	-0.20	-	2.90	-
benzamide	2.52[1]	2.26	-	-	-0.91	-	-	-
benzene	2.68[1]	3.50	3.37	3.48	-0.12	2.25	2.93	-

benzonitrile	-	2.98	3.02	-	-0.52	2.89	3.97	-
benzophenone	-	4.09	-	-	0.87	-	-	-
benzyl alcohol	2.70[3]	2.37	-	-	-0.83	-	-	-
benzylparaben	-	4.84	-	4.76	-	-	-	-
Biphenyl	-	4.80	-	5.15	1.05	-	-	-
bromobenzene	-	4.45	-	4.40	0.75	-	-	-
butylbenzene	-	-	-	5.34	1.25	-	-	-
butylparaben	-	4.67	-	4.56	-	-	-	-
caffeine	1.92[1]	3.11	-	-	-	-	-	-
carbazole	-	5.33	-	-	-	-	-	-
catechol	2.12[1]	4.08	-	-	-	-	-	-
chlorobenzene	3.20[2]	3.70	-	4.01	-0.13	-	3.83	-
coumarin	3.24[1]	-	-	-	-	-	-	-
cyclohexanol	-	2.15	-	-	-0.77	-	-	-
dibutylphthalate	-	5.33	-	4.44	-	-	-	-
diethylphthalate	-	3.84	-	3.45	-	3.62	-	-
diethyleneglycol	-	-	-	-	-	-	1.1	-
dimethylphthalate	-	3.70	-	2.76	-	-	-	-
diphenylamine	4.43[1]	4.65	-	-	-	-	-	-
diphenylolethane	3.91[2]	-	-	-	-	-	-	-
diphenylolpropane	4.20[2]	-	-	-	-	-	-	-
diuron	-	4.13	-	-	-	-	-	-
ethanol	-	0.50	0.753	0.65	-1.99	0.66	0.85	-
ethyl 4-aminobenzoate	-	3.67	-	-	0.70	-	-	-
ethylbenzene	-	4.00	3.38	4.69	-	-	3.95	-
ethyleneglycol	0.19[1]	0.04	-	0.01	-	-	0.79	-
ethylparaben	-	3.69	-	3.95	-	-	-	-
furan	-	3.05	-	-	-	-	-	-
heptanophenone	-	-	-	-	1.56	-	-	-
hydroquinone	2.12[1]	-	-	-	-	3.70	3.28	-
isopropylbenzene	-	4.28	3.40	4.93	0.69	-	-	-
methanol	-	0.05	-	0.38	-2.67	1.86	0.69	-
methyl 2-hydroxybenzoate	3.32[2]	-	-	-	-	-	-	-
methylparaben	3.16[2]	-	-	-	-	-	-	-
naphthalene	4.19[1]	4.32	-	4.75	-	-	-	-
nitrobenzene	3.29[2]	3.01	3.31	3.52	0.14	3.86	4.25	-
n-methylaniline	-	3.03	-	-	0.06	-	-	-
n,n-dimethylaniline	2.85[1]	-	-	-	-	-	-	-
pentylbenzene	-	4.94	-	-	1.79	-	-	-
phenanthrene	5.25[1]	-	-	5.32	-	-	-	-
phenol	2.28[1]/2.77[2]	3.46	3.64	3.42	-0.35	3.16	3.17	-1.549
phenylacetate	-	-	-	-	-	2.53	3.07	-
phenylthiourea	2.18[1]	-	-	-	-	-	-	-
phenylurea	2.34[1]	-	-	-	-	-	-	-
phthalide	2.37[1]	-	-	-	-	-	-	-
piperonal	2.78[1]	-	-	-	-	-	-	-
propiophenone	-	-	-	-	0.05	-	-	-
propylparaben	-	4.27	-	4.17	-	-	-	-
pyrene	-	-	-	6.65	-	-	-	-
pyridine	1.60[1]	2.90	-	-	-1.32	-	2.37	-
pyrrole	-	2.50	-	-	-1.09	-	-	-
quinoline	2.72[1]	3.22	-	-	0.09	-	-	-0.942
resorcinol	1.64[1]/2.07[2]	3.34	-	-	-0.65	-	-	-
salicylaldehyde	-	-	-	-	-	-	4.09	-

thymol	4.26[1]	4.67	-	-	-	-	-	-0.425
toluene	-	3.42	3.11	3.83	0.25	-	3.50	-
triethyleneglycol	-	-	-	-	-	-	2.7	-

Toxicity data for: [1]*R. temporaria*, [2]*R. japonica*, [3]*R. pipiens*.

Table S-5

Solutes retention factor logarithm under the different chromatographic conditions.

Solute (log k)	HPLC systems	MEKC systems		
	IAM	STC	TTAB	SDS-Brij 35
1,2,4-trimethylbenzene	0.413	0.879	1.055	1.588
(1*R*,2*S*,5*R*)-(-)-menthol	e	e	e	-0.637
1,2-dichlorobenzene	0.349	0.747	0.992	1.541
1,2-dinitrobenzene	-0.076	-0.224	0.273	0.612
1,3-dimethylbenzene	0.236	0.465	0.698	1.034
1,3-dinitrobenzene	0.080	-0.779	0.014	0.287
1,3-propanediol	-0.697	e	e	e
1,4-butanediol	e	e	e	e
1,4-dichlorobenzene	0.340	0.619	0.875	1.359
1,4-dimethylbenzene	-	0.478	0.696	1.184
1,5-pentanediol	-0.703	e	e	e
1-butanol	-0.697	e	-0.937	-0.341
1-chloro-4-nitrobenzene	0.053	-0.182	0.262	0.641
1-hexanol	e	e	e	0.410
1-nitronaphthalene	0.343	0.641	1.330	1.634
1-octanol	e	e	e	1.160
1-pentanol	-0.697	e	-0.294	-0.051
1-propanol	e	e	e	-0.864
2-(1-adamantyl)-4-methylphenol	e	1.631	m	m
2,3-benzofuran	0.329	0.079	0.509	0.917
2,4-dichloroaniline	0.227	0.450	1.105	1.440
2,4-dichlorophenol	0.316	0.583	m	1.574
2,4-dimethylphenol	0.249	0.042	0.843	0.876
2,4-dinitrotoluene	-0.032	-0.238	0.337	0.635
2,4-di-tert-butylphenol	0.875	1.578	m	m
2,6-diisopropylphenol	0.448	0.563	1.499	1.700
2,6-dimethylphenol	-0.030	-0.128	0.566	0.714
2-benzyloxyphenol	0.180	0.231	1.497	1.342
2-bromophenol	0.084	0.042	1.030	0.901
2-butanol	-0.701	e	-1.267	-0.566
2-butoxyethanol	-0.319	e	-0.979	-0.281
2-chloro-5-nitroaniline	0.065	-0.030	0.690	0.886
2-chloroaniline	0.121	-0.318	0.307	0.540

2-chlorophenol	-0.008	-0.141	0.811	0.694
2-chlorotoluene	0.346	0.744	0.938	1.419
2-fluorophenol	-0.038	-0.530	0.193	0.199
2-hydroxyacetanilide	-0.374	-0.675	-0.309	-0.228
2-methoxyphenol	-0.268	-0.576	0.040	0.125
2-methyl-1-butanol	e	e	-0.466	-0.133
2-methyl-1-propanol	-0.474	e	-0.990	-0.402
2-methyl-2-butanol	0.028	e	-1.092	-0.428
2-methyl-2-propanol	-0.521	e	e	-0.863
2-methylaniline	-0.092	-0.806	-0.079	0.135
2-methylfuran	-0.017	-0.866	0.135	0.082
2-naphthol	0.181	0.434	1.631	1.295
2-nitroaniline	-0.082	-0.235	0.362	0.568
2-nitroanisole	0.044	-0.292	0.107	0.447
2-pentanol	0.430	e	-0.693	-0.177
2-phenylphenol	0.320	0.450	m	1.578
2-propanol	e	e	e	e
2-*tert*-butyl-4-methylphenol	0.547	0.816	2.146	1.986
3,5-dichlorophenol	0.778	0.785	0.640	1.830
3-aminophenol	-0.460	-0.891	-0.386	-0.455
3-bromophenol	0.407	0.261	1.174	1.168
3-cyanophenol	-0.153	-0.419	0.254	0.253
3-methyl-1-butanol	-0.483	e	e	-0.127
3-methyl-2-butanol	0.127	e	-0.750	-0.230
3-methylphenol	-0.109	-0.350	0.467	0.382
3-nitroaniline	0.023	-0.443	0.143	0.409
3-nitrophenol	-0.025	-0.138	0.625	0.558
3-pentanol	0.122	e	-0.814	-0.308
4-acetylphenol	-0.337	-0.352	0.096	0.114
4-benzoylphenol	0.173	0.532	m	1.323
4-benzyloxyphenol	0.225	0.596	1.807	1.583
4-bromophenol	0.149	0.257	1.122	1.115
4-chloroaniline	0.128	-0.203	0.408	0.727
4-chlorophenol	0.076	0.102	0.914	0.968
4-fluorophenol	-0.175	-0.443	0.281	0.345
4-heptyloxyphenol	0.782	1.401	m	1.380
4-hexyloxyphenol	0.610	1.244	2.042	2.401
4-hydroxy-4-methyl-2-pentanone	-0.394	e	-0.781	-0.316
4-hydroxyacetanilide	-0.440	-0.682	-0.662	-0.399

4-hydroxyacetophenone	-0.338	-0.352	0.096	0.114
4-iodophenol	0.302	0.561	1.424	1.403
4-methylaniline	-0.072	-0.769	-0.058	0.258
4-methylphenol	-0.105	-0.352	0.491	0.449
4-methylpyridine	-0.180	-1.729	-0.268	-0.368
4-nitro-naphthalen-1-ylamino	0.259	0.713	m	1.765
4-nitroaniline	0.042	-0.319	0.231	0.452
4-nitrotoluene	0.023	-0.081	0.330	0.697
4-octylphenol	1.219	1.571	1.513	m
4-pentylphenol	0.609	1.263	2.146	2.416
4-*tert*-butylphenol	0.258	0.723	1.461	1.451
4-*tert*-butylpyridine	0.226	-0.292	0.264	0.718
acetamide	-0.704	e	e	-1.042
acetanilide	-0.339	-0.710	-0.281	-0.012
acetophenone	-0.238	-0.534	-0.251	0.122
adalin	-0.211	-0.377	0.096	0.440
aniline	-0.322	-0.988	-0.443	-0.175
anisole	-0.087	-0.355	0.003	0.396
anthracene	0.843	1.395	m	m
antipyrine	-0.446	-0.820	-1.059	-0.423
benzaldehyde	-0.108	-0.749	-0.078	0.255
benzamide	-0.460	-0.736	-0.558	-0.314
benzene	-0.062	-0.395	-0.076	0.286
benzonitrile	-0.044	-0.766	-0.340	0.060
benzophenone	0.256	0.438	1.043	1.361
benzyl alcohol	-0.350	-0.919	-0.492	-0.224
benzylparaben	0.370	0.924	m	m
biphenyl	0.856	1.026	1.671	m
bromobenzene	0.256	0.348	0.594	1.130
butylbenzene	0.600	1.332	1.469	2.096
butylparaben	0.317	0.784	m	1.756
caffeine	-0.609	-0.671	-1.045	-0.592
carbazole	0.558	m	1.368	1.712
catechol	-0.276	-0.688	0.196	-0.093
chlorobenzene	0.145	0.138	0.451	0.923
coumarin	0.240	-0.391	-0.140	0.218
cyclohexanol	-0.701	e	e	-0.124
dibutyl phthalate	0.548	1.105	m	0.440
diethyl phthalate	0.183	-0.075	0.562	0.884
diethyleneglycol	e	e	e	-1.161

dimethyl phthalate	-0.085	-0.437	0.020	0.347
diphenylamine	0.408	0.636	1.797	1.881
diphenylol ethane	0.172	0.706	m	1.827
diphenylol propane	0.262	0.865	m	2.023
diuron	0.450	0.618	0.957	1.418
ethanol	e	e	e	e
ethyl 4-aminobenzoate	0.039	-0.115	0.507	0.632
ethylbenzene	0.235	0.367	0.595	1.090
ethyleneglycol	-0.686	e	-0.942	e
ethylparaben	0.178	0.081	0.967	0.868
furan	-0.178	-0.432	-0.895	1.378
heptanophenone	0.589	1.057	m	2.322
hydroquinone	-0.457	-0.715	-0.391	-0.485
isopropylbenzene	0.358	0.767	0.892	1.432
methanol	e	e	e	e
methyl 2-hydroxybenzoate	-0.034	0.026	0.281	0.695
methylparaben	-0.180	-0.185	0.542	0.479
naphthalene	0.329	0.704	1.221	1.527
nitrobenzene	-0.102	-0.435	-0.080	0.279
n-methylaniline	0.022	-0.826	-0.078	1.186
n,n-dimethylaniline	0.026	-0.199	0.138	0.487
pentylbenzene	0.787	1.771	m	1.340
phenanthrene	0.800	1.474	m	m
phenol	-0.221	-0.753	0.059	0.057
phenyl acetate	-0.213	-0.800	-0.201	0.072
phenylthiourea	-0.376	-0.784	-0.104	-0.136
phenylurea	-0.363	-0.625	-0.008	0.019
phthalide	-0.366	-0.666	-0.549	-0.183
piperonal	-0.254	-0.459	-0.248	0.132
propiophenone	0.110	-0.296	0.072	0.468
propylparaben	0.392	0.424	1.581	1.268
pyrene	1.072	1.563	m	1.419
pyridine	-0.412	-1.287	-0.992	-0.675
pyrrole	-0.257	-1.166	-0.628	-0.412
quinoline	-0.142	-0.236	0.091	0.437
resorcinol	-0.363	-0.639	0.146	-0.171
salicylaldehyde	-0.052	-0.474	0.062	0.192
thymol	0.303	0.529	1.453	1.546
toluene	0.083	0.020	0.283	0.732
triethyleneglycol	-0.706	e	e	-1.142

Compound not detected, or that coelutes with the EOF or with the chromatographic front (e); compound that coelutes with the micelle marker (m)

Figure S-1

PCA scores plot of solutes with known toxicity data (O) and the projection of the solute selection made in this work (+) according to their SPM molecular descriptors.

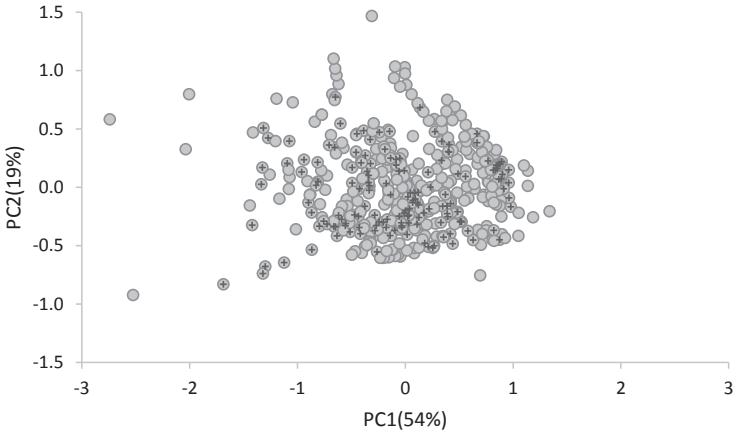

Figure S-2

Plots of biological property logarithm vs. experimental retention factor logarithm of the physicochemical systems with the best regressions. Solid lines are the plot of the regression equation.

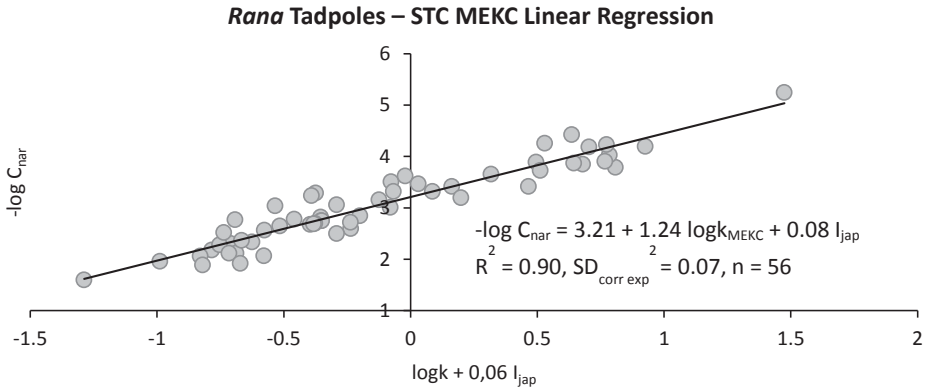

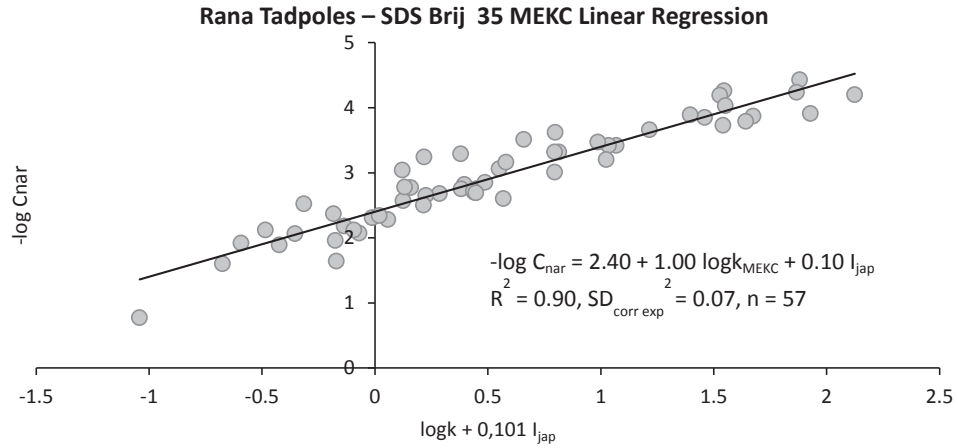

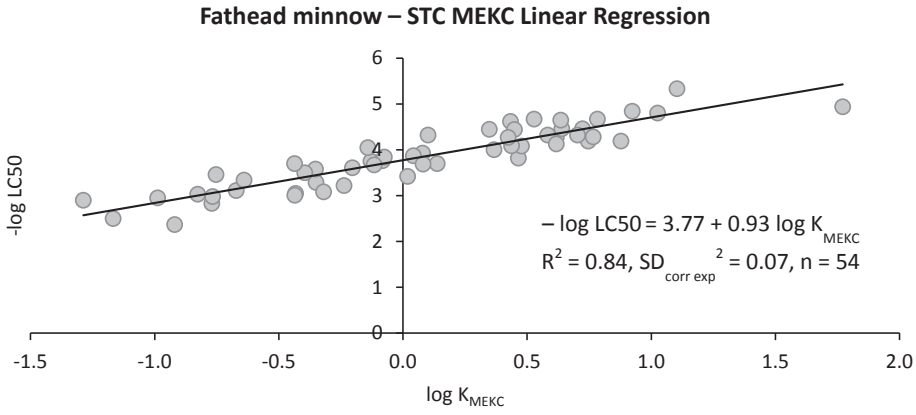
Fathead minnow – STC MEKC Linear Regression
-log LC50
log K_MEKC
– log LC50 = 3.77 + 0.93 log K_MEKC
R² = 0.84, SD_corr exp² = 0.07, n = 54

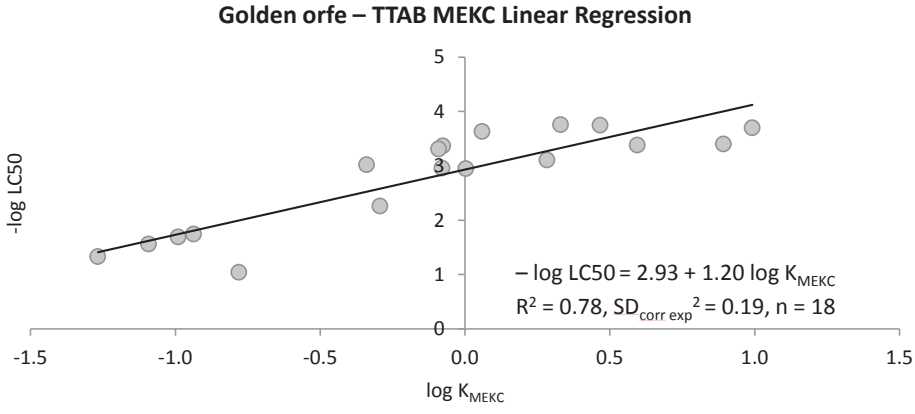
Golden orfe – TTAB MEKC Linear Regression
-log LC50
log K_MEKC
– log LC50 = 2.93 + 1.20 log K_MEKC
R² = 0.78, SD_corr exp² = 0.19, n = 18

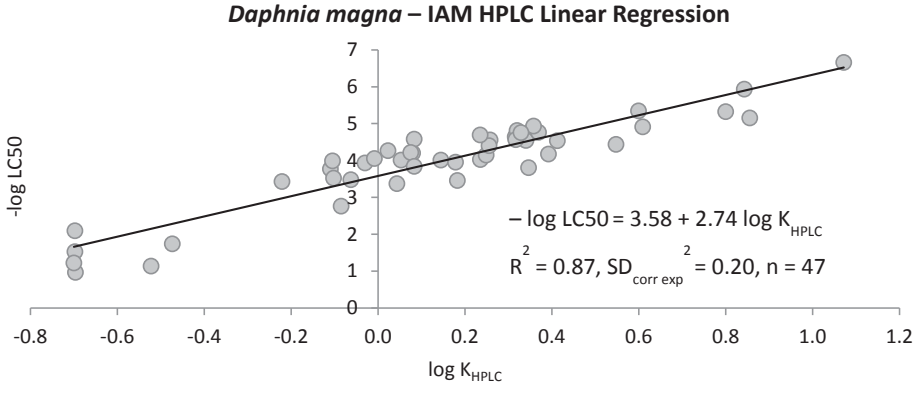
Daphnia magna – IAM HPLC Linear Regression
-log LC50
log K_HPLC
– log LC50 = 3.58 + 2.74 log K_HPLC
R² = 0.87, SD_corr exp² = 0.20, n = 47

***Daphnia magna* – SDS Brij35 MEKC Linear Regression**

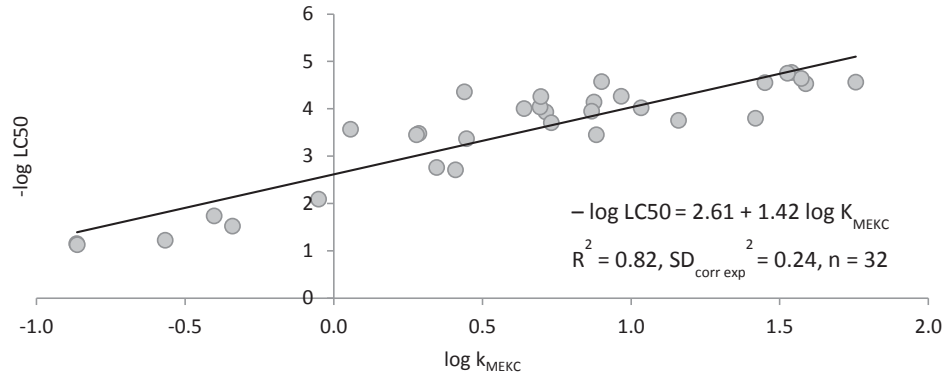

***Tetrahymena pyriformis* – SDS Brij 35 MEKC Linear Regression**

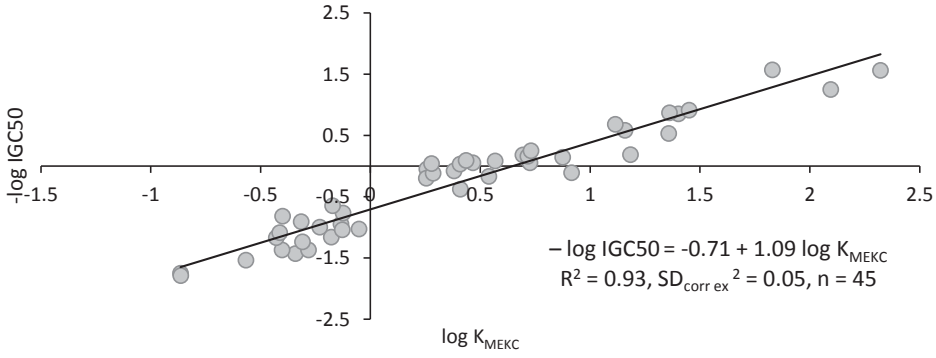

***Chilomonas paramecium* – TTAB MEKC Linear Regression**

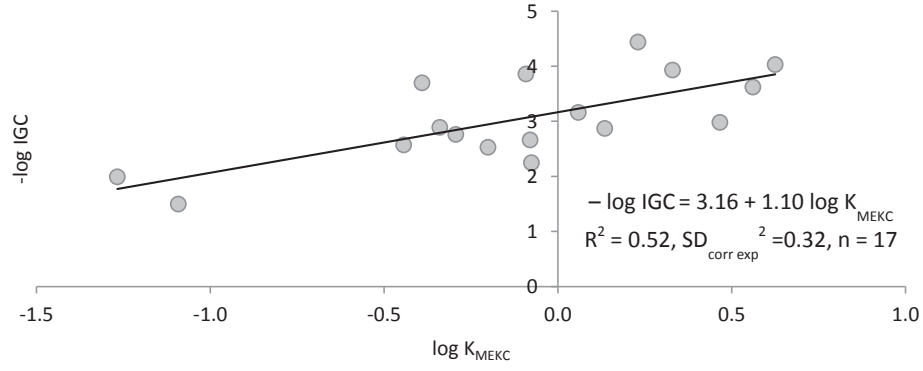

***Pseudomonas putida* – TTAB MEKC Linear Regression**

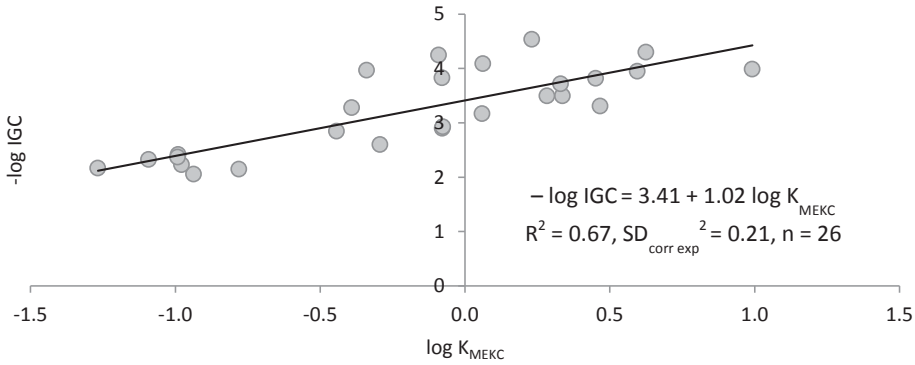

***Streptococcus sobrinus* – SDS Brij 35 MEKC Linear Regression**

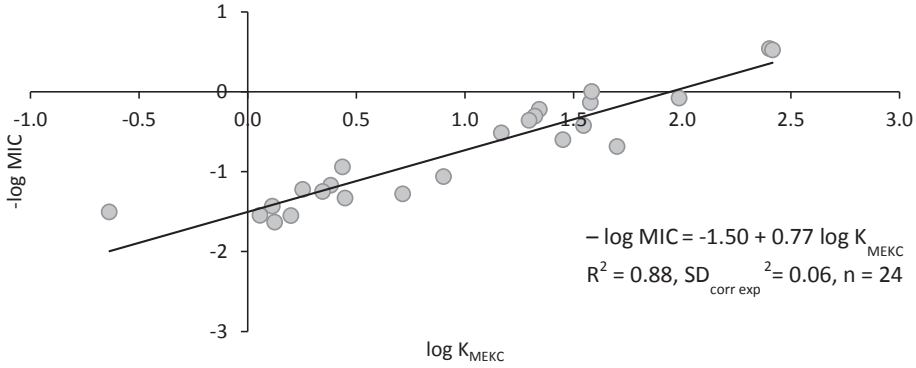

***Streptococcus sobrinus* – TTAB MEKC Linear Regression**

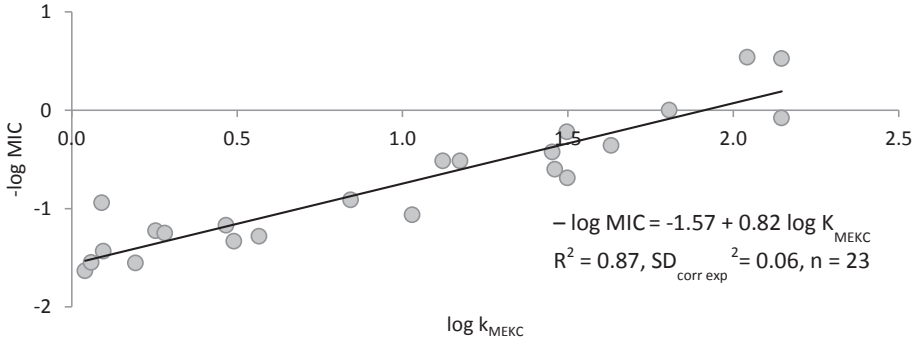

REFERENCES

(1) Abraham, M. H.; Rafols, C. *J. Chem. Soc. Perkin Trans. 2* **1995**, No. 10, 1843.

(2) Hoover, K. R.; Acree, W. E.; Abraham, M. H. *Chem. Res. Toxicol.* **2005**, *18* (9), 1497–1505.

(3) Hoover, K. R.; Flanagan, K. B.; Acree Jr., W. E.; Abraham, M. H. *Sect. Title Toxicol.* **2007**, *6* (2), 165–174.

(4) Bowen, K. R.; Flanagan, K. B.; Acree, W. E.; Abraham, M. H. *Sci. Total Environ.* **2006**, *369* (1–3), 109–118.

(5) Mintz, C.; Acree, W. E.; Abraham, M. H. *QSAR Comb. Sci.* **2006**, *25* (10), 912–920.

(6) Abraham, M. H.; Chadha, H. S.; Whiting, G. S.; Mitchell, R. C. *J. Pharm. Sci.* **1994**, *83* (8), 1085–1100.

(7) Lázaro, E.; Ràfols, C.; Abraham, M. H.; Rosés, M. *J. Med. Chem.* **2006**, *49* (16), 4861–4870.

(8) Fuguet, E.; Ràfols, C.; Bosch, E.; Abraham, M. H.; Rosés, M. *J. Chromatogr. A* **2002**, *942* (1–2), 237–248.

(9) Trone, M. D.; Khaledi, M. G. *Electrophoresis* **2000**, *21* (12), 2390–2396.

(10) Hidalgo-Rodríguez, M.; Fuguet, E.; Ràfols, C.; Rosés, M. *Anal. Chem.* **2012**, *84* (7), 3446–3452.

(11) Rosés, M.; Ràfols, C.; Bosch, E.; Martínez, A. M.; Abraham, M. H.; Martınez, A. M. *J. Chromatogr. A* **1999**, *845*, 217–226.

(12) Abraham, M. H.; Treiner, C.; Roses, M.; Rafols, C.; Ishihama, Y. *J. Chromatogr. A* **1996**, *752* (1–2), 243–249.

(13) Burns, S. T.; Agbodjan, A. A.; Khaledi, M. G. *J. Chromatogr. A* **2002**, *973* (1–2), 167–176.

(14) Schulte, S.; Palmer, C. P. *Electrophoresis* **2003**, *24* (6), 978–983.

(15) Overton, E. *Studien über die Narkose, zurgleich eing Bertrag zur allgemeinen*

Pharmakologie.; Jena, Gustav Fischer, 1901.

(16) Huang, H.; Wang, X.; Ou, W.; Zhao, J.; Shao, Y.; Wang, L. *Chemosphere* **2003**, *53* (8), 963–970.

(17) Wang, X.; Dong, Y.; Xu, S.; Wang, L.; Han, S. *Bull. Environ. Contam. Toxicol.* **2000**, *64* (6), 859–865.

(18) Overton, E. *Studies on Narcosis*; Lipnick, R. L., Ed.; Chapman and Hall: London, 1991.

(19) Meyer, K.; Hemmi, H. *Biochem. Z.* **1935**, *277*, 39–71.

(20) Kita, Y.; Bennett, L. J.; Miller, K. W. *Biochim. Biophys. Acta - Biomembr.* **1981**, *647* (1), 130–139.

(21) Dobbins, L. L.; Usenko, S.; Brain, R. A.; Brooks, B. W. *Environ. Toxicol. Chem.* **2009**, *28* (12), 2744–2753.

(22) Juhnke, I.; Luedemann, D. *Z. Wasser Abwasser Forsch* **1978**, *11* (5), 161–164.

(23) *Aquatic toxicology and environmental fate*; Suter, G., Lewis, M., Eds.; ASTM: Philadelphia, 2007.

(24) Bringmann, G.; Kühn, R. *Water Res.* **1980**, *14* (3), 231–241.

(25) Fernández-Pumarega, A.; Amézqueta, S.; Fuguet, E.; Rosés, M. *J. Chromatogr. A* **2015**, *1418*, 167–176.

ARTICLE II

Lecithin Liposomes and Microemulsions as New Chromatographic Phases

Susana Amézqueta Alejandro Fernández-Pumarega, Sandra Farré, Daniel Luna, Elisabet Fuguet, and Martí Rosés

Journal of Chromatography A, en premsa

DOI: 10.1016/j.chroma.2019.460596

Journal of Chromatography A xxx (xxxx) xxx

Contents lists available at ScienceDirect

Journal of Chromatography A

journal homepage: www.elsevier.com/locate/chroma

Lecithin liposomes and microemulsions as new chromatographic phases

Susana Amézqueta[a,*], Alejandro Fernández-Pumarega[a], Sandra Farré[a], Daniel Luna[a], Elisabet Fuguet[a,b], Martí Rosés[a]

[a] Departament de Química Analítica and Institut de Biomedicina (IBUB), Facultat de Química, Universitat de Barcelona, Martí i Franquès 1-11, 08028, Barcelona, Spain
[b] Serra Húnter Programme. Generalitat de Catalunya. Spain

ARTICLE INFO

Article history:
Received 25 July 2019
Revised 25 September 2019
Accepted 1 October 2019
Available online xxx

Keywords:
Solvation parameter model
Physicochemical characterization
Lecithin
Surrogation
Skin partition
Chromatography

ABSTRACT

Lecithins are phospholipidic mixtures that can be part of microemulsions and liposomes. In this work, ready-to-use preparations of lecithin have been tested as pseudostationary and mobile phases in EKC and LC, respectively. The selectivity of two EKC systems, one based on lecithin microemulsions (LMEEKC) and another on liposomes (LLEKC), and of a LC system based on lecithin microemulsions (MELC) has been evaluated through the solvation parameter model. In all cases, solute volume and hydrogen-bond basicity are the main descriptors that drive the partition process. While solute volume favors the retention of solutes, hydrogen-bond basicity has the contrary effect. In lecithin-based EKC systems the hydrogen-bond acidity of the solute leads to a higher retention while in the lecithin-based LC system a minor retention is produced. The three lecithin systems have been compared through the solvation parameter model to other chromatographic systems, most of them containing phospholipids. Principal component analysis reveals that lecithin systems cluster together with the other EKC systems based on phospholipids, with an immobilized artificial membrane (IAM) LC system, with the octanol/water reference partition system, and with a SDS-based microemulsion. Thus, they all show similar selectivity. However, the great advantage of using the ready-to use lecithin systems is that the laborious liposome preparation is avoided, and that their commercial availability makes them more affordable than IAM LC columns. Finally, taking into account that lecithin has a high semblance to the mammalian cell membranes composition, the ability of the three lecithin systems to mimic the pass of the solutes through the membranes has been evaluated. Experimental determinations have demonstrated that the skin partition of neutral solutes can be easily emulated, especially using the lecithin-microemulsion EKC method. The model is robust and shows good prediction ability.

1. Introduction

Capillary electrophoresis (CE) is a separation technique used in a wide number of applications that include either the determination of small compounds (pollutants, nutrients, drugs, biomarkers, etc.) and of large ones (enzymes, proteins, DNA, etc.). CE is also used for the physicochemical characterization of chemical substances (pK_a and log $P_{o/w}$ determination); the evaluation of the interaction with other molecules such as the drug-protein binding; or the subrogation of biological properties of environmental or biomedical interest [1–3].

Microemulsion electrokinetic chromatography (MEEKC) and liposome electrokinetic chromatography (LEKC) are CE modalities that use a mobile phase containing a microemulsion or liposomes, respectively. Microemulsions are formed by surfactant-coated oil droplets, and usually a cosurfactant that acts as a stabilizer. Liposomes consist of a phospholipid bilayer with an encapsulated inner aqueous cavity. The surfactants or phospholipids used are charged and thus the microemulsion or the liposomes have their own electrophoretic mobility. In both cases, the solutes under analysis will migrate depending not only on their charge-to-size ratio (as in capillary zone electrophoresis (CZE)) but also on the partition with the corresponding pseudostationary phase (microemulsion or liposome) [4]. The partition is analogous to that in reversed-phase liquid chromatography (RPLC) and thus both techniques are considered CE-LC hybrids. Microemulsions can also be part of the mobile phase in reversed-phase chromatography and they give place to microemulsion liquid chromatography (MELC) [5]. As far as we are concerned, liposomes are not usually used as the mobile phase

* Corresponding author.
E-mail address: samezqueta@ub.edu (S. Amézqueta).

https://doi.org/10.1016/j.chroma.2019.460596
0021-9673/

Please cite this article as: S. Amézqueta, A. Fernández-Pumarega and S. Farré et al., Lecithin liposomes and microemulsions as new chromatographic phases, Journal of Chromatography A, https://doi.org/10.1016/j.chroma.2019.460596

in LC. However, liposomes can be trapped in the pores of gel beads to generate immobilized liposome chromatography (ILC) or immobilized on the stationary phase to form an immobilized artificial membrane (IAM) [6,7].

Lecithins are mixtures of phospholipids (phosphatidylcholine, phosphatidylethanolamine, phosphatidylinositol, phosphatidylserine, etc.) that are extracted from different natural sources such as soy or egg. Commercial preparations based on lecithins are available to prepare emulsions and liposomes with cosmetic and pharmaceutical uses (Emulmetik™, Pro-Lipo™, Lipoid™). However, they have not been used yet to prepare chromatographic mobile phases. In the search of new chromatographic systems with different selectivity and taking into account the complexity when preparing a microemulsion or a liposome, it would be of great interest to investigate the viability of the ready-to-use commercial products as chromatographic phases and characterize their selectivity. In the present work we will evaluate the selectivity of a lecithin-based microemulsion in MEEKC (LMEEKC) and MELC (LMELC), and lecithin liposomes in LEKC (LLEKC). In LMEEKC and LLEKC lecithin acts as pseudostationary phase, and buffer as aqueous phase; inversely, in LMELC, C18 acts as stationary phase and lecithin as mobile phase.

The solvation parameter model (SPM) proposed by Abraham [8] is a popular quantitative structure-property relationship (QSPR) model to characterize the selectivity of chromatographic systems [9,10]. The following equation is used to model the solvation that a neutral solute undergoes in a biphasic system and includes five different molecular descriptors.

$$\log \mathrm{SP} = c + eE + sS + aA + bB + vV \quad (1)$$

Here, SP is the dependent solute property in a given partitioning system, *i.e.* equilibrium constant or some other free energy related property such as the chromatographic retention factor or a membrane partition. The *E, S, A, B* and *V* independent variables are the solute descriptors proposed by Abraham. *E* represents the excess molar refraction, *S* is the solute dipolarity/polarizability, *A* and *B* are the solute's effective hydrogen-bond acidity and hydrogen-bond basicity, respectively, and *V* is McGowan's solute volume. The coefficients of the equation are characteristic of the biphasic system and reflect the difference of the two phases in properties complementary to the ones of solute descriptors. For any system, the coefficients of this equation can be obtained by multiple linear regression analysis between the log SP values acquired for an appropriate group of solutes and their descriptor values. Equations based on the SPM have been reported (some of them are shown in Table SI-1 of the Supplementary Material) to characterize several chromatographic systems. Similarly to the physicochemical systems ruled by partition, the literature proposes equations based on the SPM for different biological processes (Tables SI-2 and SI-3 of the Supplementary Material).

Characterizing two systems using the same model (the SPM in this work) makes them comparable, since similar partitioning systems will have similar coefficients [11]. Thus, after characterizing the three new systems with the SPM they will be compared with other physicochemical and biological systems. One parameter to compare their similarity we have proposed is the *d* distance of the SPM coefficients [12]. The *d* distance is calculated from the normalized coefficients of the two correlations to be compared. To do so, each system is considered as a five-dimensional vector of system coefficients (*e, s, a, b*, and *v*), with a vector's length (*l*) mathematically defined as:

$$l = \sqrt{e^2 + s^2 + a^2 + b^2 + v^2} \quad (2)$$

and each system coefficient is divided by *l* in order to obtain the normalized coefficients (e_u, s_u, a_u, b_u, and v_u).

The *d* parameter is the distance between the two normalized vectors, *i.e.*

$$d = \sqrt{\left(e_{u1}^2 - e_{u2}^2\right) + \left(s_{u1}^2 - s_{u2}^2\right) + \left(a_{u1}^2 - a_{u2}^2\right) + \left(b_{u1}^2 - b_{u2}^2\right) + \left(v_{u1}^2 - v_{u2}^2\right)} \quad (3)$$

where the two subscripts 1 and 2 refer to the two systems to be compared. In previous works [13,14], a *d* distance of 0.25 or less was stablished as adequate for surrogation. When many systems want to be compared, dendrograms of the *d* distance and Principal Components Analysis (PCA) of the normalized coefficients can be used to identify the most similar systems. These approaches are based on simple and fast calculations and allow handling with a high number of data at once. They provide information about the similarity of the systems and are very adequate to compare the selectivity of two different physicochemical systems and to do a first selection of the physicochemical systems that can better emulate a biological property. Detailed information on these comparison tools is described elsewhere [19].

Once the most similar coefficients have been identified, the precision of the correlation between two of the systems (*i.e.* estimation of a biological parameter from a physicochemical one) can also be estimated from the errors of the biological and physicochemical system models and the systems dissimilarity [12,15–17]. Estimation from chromatographic measurements is usually performed through a linear equation of the type of Eq. (4).

$$\log \mathrm{SP_{bio}} = q + p\ log \mathrm{SP_{chrom}} \quad (4)$$

Here, SP_{bio} is the solute biological property, SP_{chrom} is the solute chromatographic property (in this case, the chromatographic or electrophoretic retention factor), and *q* and *p* are the ordinate and slope of the correlation, respectively.

In short, the expected precision of the correlation (SD_{corr}^2) can be considered as the sum of three different contributions to the variance of the correlation: the biological data precision (SD_{bio}^2), the chromatographic data precision $(p \times SD_{chrom})^2$ and the error due to the dissimilarity between the correlated systems (SD_d^2). SD_{bio} and SD_{chrom} values are estimated from the respective standard deviations of the SPM characterizations. In order to know *p* and also SD_d^2 the biological property and the chromatographic property are calculated through their SPM equations and solutes' descriptors. In this way, SD_{bio} and SD_{chrom} are zero. The slope of the correlation of these calculated values provides *p*, and the SD of the correlation can be entirely attributed to the dissimilarity between both systems.

This kind of estimation is more laborious, so it is usually performed only for those pairs of systems that show the highest similarity according to *d* distances.

Those systems closer (with smallest *d* or closest in the dendrogram and principal components space plots) and with a good estimated correlation precision are identified as good candidates to surrogate each one the other system. In the case of physicochemical-biological pairs, the closest physicochemical system will probably be good surrogates for the biological system. To prove this, the physicochemical property (the retention factor in the chromatographic or the electrophoretic system) is measured and a correlation with the biological property is carried out for a series of representative compounds (Eq. (4)). If a good correlation is established between the properties of these two different systems, the biological property of a new chemical compound can be predicted by measuring the corresponding retention factor in the chromatographic system. The main advantage of this approach over QSPR studies is that it is not necessary to know the molecular descriptor values of the new compound such as in the SPM model. Furthermore, the use of chromatographic and electrophoretic mea-

Please cite this article as: S. Amézqueta, A. Fernández-Pumarega and S. Farré et al., Lecithin liposomes and microemulsions as new chromatographic phases, Journal of Chromatography A, https://doi.org/10.1016/j.chroma.2019.460596

surements for prediction of biological properties is of main interest due the high level of automatization, speed of analysis, low cost, and high reproducibility of these techniques that lead to the *ex vivo* and *in vivo* tests avoidance. Due to the high structural and compositional similarity between mammalian cell membranes and lecithin-based microemulsions and liposomes it would be very interesting to test the possibility to mimic properties of environmental or biomedical concern using chromatographic measurements. In fact, lecithin-based chromatographic systems have already been used to mimic the intestinal absorption [18].

2. Material and methods

2.1. Equipment

MELC measurements were done using a 10A series chromatograph from Shimadzu (Kyoto, Japan) equipped with a quaternary pump and a diode array detector and fitted with a Gemini C18 column (15 cm × 4.6 mm i.d., 5 µm particle size) (Phenomenex, Torrance, CA, US) preceded by the corresponding guard cartridge (1 cm).

MEEKC and LEKC measurements were done using the G1600A CE capillary electrophoresis system from Agilent Technologies (Santa Clara, CA, US) equipped with a diode array detector. The fused-silica capillary (30 cm effective length for MEEKC and 40 cm for LEKC, 38.5 cm total length for MEEKC and 48.5 cm for LEKC, 50 µm i.d.) was obtained from Composite Metal Services Ltd (Shipley, UK).

2.2. Reagents

Methanol (HPLC-grade), hydrochloric acid (25% in water), sodium hydroxide (>99%), sodium dihydrogenphosphate monohydrate (>99%), disodium hydrogenphosphate (>99%), and phenanthrene (>97%) were from Merck (Darmstadt, Germany). Potassium bromide (≥99.5%), 1-butanol (≥99.7%), heptane (99%), and dodecanophenone (98%) were from Sigma-Aldrich (St. Louis, MO, US). Water was purified by a Milli-Q plus system from Millipore (Bedford, MA, US), with a resistivity of 18.2 MΩ cm. The lecithin products to prepare the microemulsions and the liposomes were Emulmetik™ 300 and Pro-Lipo™ Neo, respectively, from Lucas Meyer Cosmetics (Champlan, France). They were kindly supplied by Comercial Química Jover (Terrassa, Spain).

Tested substances were reagent grade or better and obtained from several manufacturers (Merck, Sigma-Aldrich, Carlo Erba (Milano, Italy), Baker (Center Valley, PA, US), Panreac (Castellar del Vallès, Spain), Thermo Fisher Scientific (Waltham, MA, US), and Scharlab).

2.3. Microemulsion and liposomes preparation

Lecithin microemulsions contained 0.5% (w/v) of lecithin and were prepared using Emulmetik™ 300 as starting material, product that contains 97% of phospholipids. In the case of MEEKC, lecithin (0.25 g) was mixed with 35 mL of phosphate buffer (20 mM, pH 7.0) in a magnetic stirrer at low speed (200 rpm). Next, 1-butanol (8.15% (v/v)) was added drop by drop and the solution was stirred for 30 min. Then, heptane (1.15% (v/v)) was added and the suspension stirred for 30 min more. This suspension was transferred to a 50 mL volumetric flask and diluted with buffer. Finally, it was stirred for 1–2 h at low speed (200 rpm) until the mixture turned semitransparent. In the case of MELC, a higher volume (0.5 L) was prepared using the proportional amounts of the reagents and stirring at higher speed (650 rpm).

Lecithin liposomes contained 0.5% (w/v) of lecithin and were prepared using the preliposome Pro-Lipo™ Neo as starting material, product that contains around 20% of phospholipids. Preliposome (0.5 g) was mixed with 20 mL of buffer in a magnetic stirrer at high speed (1000 rpm) for 45 min at 25–30 °C. The use of other brands of ready-to-use lecithin products to form microemulsions or liposomes should not provide very different results from those obtained in the present work. Notwithstanding, note that a new calibration curve has to be done for every batch-to-batch or brand-to-brand analysis.

2.4. Preparation of the test compounds solutions

For MELC, stock solutions (2000 mg/L) of the solutes and the hold-up time marker (potassium bromide) were prepared in methanol. Working solutions were prepared from stock solutions at a concentration of 50 mg/L, solving the corresponding amount of stock solution in the microemulsion.

In the case of MEEKC, stock solutions of the solutes and the microemulsion marker (phenanthrene) (2000 mg/L) were prepared in methanol. Working solutions were prepared from the stock solutions and contained 400 mg/L of the solutes and 200 mg/L of the microemulstion marker. They were diluted to obtain a final methanol:buffer relation of 1:1. Methanol was used as the electroosmotic flow marker.

For LEKC, a stock solution containing the solutes (1000 mg/L) and the liposome marker (dodecanophenone) was prepared in methanol. Work solutions were prepared by direct dilution of the stock solution with buffer, and contained 200 mg/L of the solutes or the liposome marker. The final methanol:buffer relation was 1:4. Again methanol was used as the electroosmotic flow marker.

Finally, all solutions were passed through a 0.45 µm nylon syringe filter obtained from Filter-Lab (Sant Pere de Riudebitlles, Spain).

2.5. Analysis by LC

Target compounds were analyzed using the microemulsion as mobile phase at 1 mL/min. The injection volume was 50 µL and the column temperature 25 °C. After a preliminary scan, detection wavelengths were set at 200 and 254 nm depending on the compound absorption profile. All measurements were taken in triplicate. After analyses, the system was cleaned by passing through water for 60 min, acetonitrile:water for 60 min and acetonitrile for 30 min.

The LC retention factor (k), was calculated according to Eq. (5),

$$k = \frac{t_R - t_0}{t_0 - t_e} \quad (5)$$

where t_R corresponds to the solute retention time, t_0 is the column hold-up time, and t_e is the extra column time determined by an analysis that excludes the chromatographic column. To measure t_e a chromatographic correction with negligible hold-up volume has been used. t_0 and t_e have been determined using an aqueous potassium bromide solution.

2.6. Analysis by EKC

Target compounds were analyzed using the microemulsion or the liposomes as pseudostationary phase. Before the first use, the capillary was activated by the following washing sequence: water (5 min), 1 M NaOH (20 min), water (2 min), 0.1 M NaOH (10 min), water (2 min) and microemulsion or liposome suspension (20 min). As daily conditioning, the capillary was flushed with water for 6 min, followed by methanol (3 min), water (3 min), 1 M NaOH (5 min), water (3 min), 0.1 M NaOH (3 min), water (1 min) and microemulsion or liposome suspension (5 min). Before each separation, the capillary was flushed with water (2 min), methanol

Please cite this article as: S. Amézqueta, A. Fernández-Pumarega and S. Farré et al., Lecithin liposomes and microemulsions as new chromatographic phases, Journal of Chromatography A, https://doi.org/10.1016/j.chroma.2019.460596

(2 min), water (1 min), 0.1 M NaOH (2 min), water (1 min), and microemulsion or liposome suspension (4 min).

The injection was done during 3 s at 50 mbar, the capillary temperature was 25 °C, and the voltage was +15 kV. After a preliminary scan, wavelengths were set at 200, 214, and 254 nm depending on the compound absorption profile. All measurements were done in triplicate. In terms of practicality, LMEEKC and LLEKC analytical procedures were similar, and both systems were robust in batch-to-batch analyses. Also, we did not detect run-to-run differences after applying the cleaning protocols described.

The retention factor (k), was calculated according to Eq. (6),

$$k = \frac{t_m - t_{eof}}{\left(1 - \frac{t_m}{t_{ps}}\right) t_{eof}} \quad (6)$$

where t_m is the solute migration time, t_{eof} corresponds to the migration time of methanol, and t_{ps} is the migration time of the pseudostationary phase marker.

2.7. Data analysis

PCA and dendrogram plots were performed with Matlab package from MathWorks (Natick, MA, USA). Excel from Microsoft (Redmond, WA, US) was used for data calculations and multiple linear regression analyses. The Abraham descriptors of the substances were the same used in a previous study [19]. The biological data have been extracted from literature [20,21].

3. Results and discussion

3.1. Characterization of the lecithin-based systems through the SPM model

The retention factor of 59 solutes has been determined. These solutes were selected from a total of 71 set in a previous work [19] due to their variety of descriptors magnitude, their representability of the physicochemical space, and their compatibility with the lecithin systems. These solutes are neutral in the pH of work. Table 1 shows the set of compounds together with the retention factors obtained in the three chromatographic systems (an example of the chromatograms and electropherograms obtained is included in Figs. 1-3 of the Supplementary Information). The results are an average of a minimum of 3 determinations and the RSD is under 5%. Next, the logarithm of the retention factor determined in the corresponding chromatographic system has been correlated to the descriptors *A, B, S, E* and *V* of the solutes also presented in Table 1. Multiple linear regression between log k and the descriptors provide the coefficients and statistics for the physicochemical systems considered in the present work, which are shown in Table 2.

The systems are properly characterized by the SPM model: the determination coefficient (R^2) is higher than 0.90 in all cases, the standard error is low and in the order of that of other physicochemical systems characterized through this same model [19], F_{cal} value is much higher than F_{tab} at a 95% confidence level, and all the SPM coefficients present statistical significance. Outliers, those compounds that present a residual value over |2.5|, non-detectable substances, and compounds that coeluted with the markers were not considered to set the model.

The direct comparison between the normalized coefficients of the SPM of each system (a graphical representation is shown in Fig. 1) and the evaluation of the distance between these coefficients (Table 3) shows that the three lecithin based systems are very similar. The two electrophoretic systems (LMEEKC and LLEKC) are the most similar ($d_{LMEEKC/LLEKC} = 0.15$), whereas the chromatographic LMELC is slightly less similar ($d_{LMELC/LMEEKC} = 0.18$, $d_{LMELC/LLEKC} = 0.20$). The big similarity of LMELC to the two electrophoretic systems is somewhat surprising because in LMEEKC and LLEKC lecithin acts as pseudostationary phase and the aqueous buffer as mobile phase, but in LMELC C18 acts as stationary

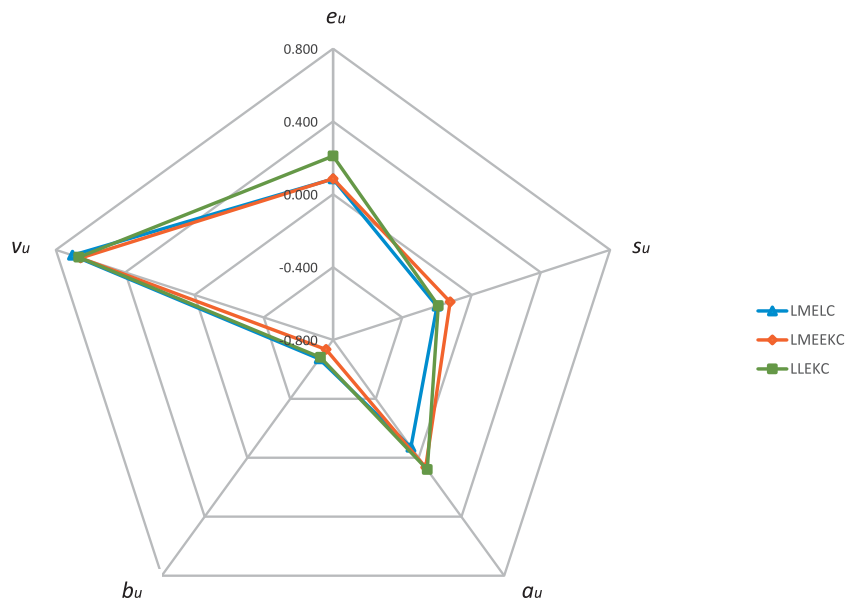

Fig. 1. Comparison of the normalized SPM properties of the three lecithin-based systems (LMELC: ▲; LMEEKC: ♦; LLEKC: ■).

Please cite this article as: S. Amézqueta, A. Fernández-Pumarega and S. Farré et al., Lecithin liposomes and microemulsions as new chromatographic phases, Journal of Chromatography A, https://doi.org/10.1016/j.chroma.2019.460596

Table 1
SPM descriptors and logarithm of the retention factor of the solutes used to characterize the LMELC, LMEEKC and LLEKC systems based on lecithin.

	E	*S*	*A*	*B*	*V*	log k_{LMELC}	log k_{LMEEKC}	log k_{LLEKC}
1,2,3-Trihydroxybenzene	1.165	1.350	1.350	0.620	0.8925	−0.37	−1.16	−0.68
2,3-Benzofuran	0.888	0.830	0.000	0.150	0.9053	1.89	0.14	0.44
2,3-Dimethylphenol	0.850	0.850	0.520	0.360	1.0569	–	−0.20	0.29
2,4-Dimethylphenol	0.843	0.800	0.530	0.390	1.0569	–	−0.23	0.31
2-Naphthol	1.520	1.080	0.610	0.400	1.1441	1.67	0.30	0.73
2-Nitroaniline	1.180	1.370	0.300	0.360	0.9904	1.20	−0.58	−0.08
2-Nitroanisole	0.968	1.340	0.000	0.450	1.0902	1.20	−0.72	−0.25
3-Chloroaniline	1.053	1.100	0.300	0.300	0.9386	1.35	−0.37	0.00
3-Methylphenol	0.822	0.880	0.570	0.340	0.9160	1.28	−0.56	−0.20
3-Nitroaniline	1.200	1.710	0.400	0.350	0.9904	1.00	−0.73	−0.27
4-Aminobenzamide	1.340	1.940	0.800	0.940	1.0726	0.02	−1.30	−1.18
4-Chloroacetanilide	0.980	1.470	0.640	0.510	1.2361	1.33	−0.45	−0.06
4-Chloroaniline	1.060	1.130	0.300	0.310	0.9386	1.32	−0.38	−0.06
4-Chlorophenol	0.915	1.080	0.670	0.200	0.8975	1.56	−0.04	0.10
4-Nitroaniline	1.220	1.930	0.460	0.350	0.9904	0.95	−0.75	−0.23
Acetanilide	0.900	1.390	0.480	0.670	1.1137	0.65	−1.25	−0.93
Acetophenone	0.818	1.010	0.000	0.480	1.0139	1.16	−0.94	−0.73
Aniline	0.955	0.960	0.260	0.410	0.8162	0.66	−1.22	−0.92
Anisole	0.708	0.750	0.000	0.290	0.9160	1.61	−0.41	−0.15
Antipyrine	1.320	1.500	0.000	1.480	1.4846	0.17	–	−1.61
α-Pinene	0.446	0.140	0.000	0.120	1.2574	1.23	–	0.44
Benzaldehyde	0.820	1.000	0.000	0.390	0.8730	1.08	0.76	−0.76
Benzamide	0.990	1.500	0.490	0.670	0.9728	0.42	–	−1.10
Benzene	0.610	0.520	0.000	0.140	0.7164	1.19	−0.41	−0.10
Benzyl benzoate	1.264	1.420	0.000	0.510	1.6804	–	1.17	–
Methyl benzoate	0.733	0.850	0.000	0.460	1.0726	1.56	−0.46	−0.20
Benzophenone	1.447	1.500	0.000	0.500	1.4808	2.00	0.40	0.83
Benzonitrile	0.742	1.110	0.000	0.330	0.8711	1.13	−0.94	−0.66
Bromobenzene	0.882	0.730	0.000	0.090	0.8914	1.86	0.43	0.58
Butyrophenone	0.797	0.950	0.000	0.510	1.2957	–	−0.08	0.23
Caffeine	1.500	1.720	0.050	1.280	1.3632	0.04	–	–
Catechol	0.970	1.100	0.880	0.470	0.8338	0.65	−1.04	−0.56
Chlorobenzene	0.718	0.650	0.000	0.070	0.8388	–	0.26	0.46
Corticosterone	1.860	3.430	0.400	1.630	2.7389	1.21	−0.61	0.10
Cortisone	1.960	3.500	0.360	1.870	2.7546	0.84	−1.02	−0.38
Estradiol	1.800	1.770	0.860	1.100	2.1988	1.17	0.37	–
Estratriol	1.970	1.740	1.060	1.630	2.2575	–	−0.74	–
Ethylbenzene	0.613	0.510	0.000	0.150	0.9982	–	0.53	0.83
Phenol	0.805	0.890	0.600	0.300	0.7751	0.95	−0.92	−0.51
Furan	0.369	0.510	0.000	0.130	0.5363	−0.47	–	–
Geraniol	0.513	0.630	0.390	0.660	1.4903	–	0.19	0.36
Heptanophenone	0.720	0.950	0.000	0.500	1.7184	–	1.56	1.64
Hydrocortisone	2.030	3.490	0.710	1.900	2.7976	0.91	−0.90	−0.31
Hydroquinone	1.063	1.270	1.060	0.570	0.8338	0.31	–	–
Monuron	1.140	1.500	0.470	0.780	1.4768	1.20	−0.78	−0.46
Naphthalene	1.340	0.920	0.000	0.200	1.0854	2.05	0.82	1.09
Nitrobenzene	0.871	1.110	0.000	0.280	0.8906	1.37	−0.61	−0.27
o-Toluidine	0.966	0.920	0.230	0.450	0.9571	0.94	−0.98	−0.75
Pyrimidine	0.606	0.930	0.000	0.670	0.6342	0.03	–	–
Pyrrole	0.613	0.910	0.220	0.250	0.5774	−0.03	–	−1.09
Propylbenzene	0.604	0.500	0.000	0.150	1.1391	1.24	1.07	−0.14
Propiophenone	0.804	0.950	0.000	0.510	1.1548	1.56	−0.51	−0.22
p-Xylene	0.613	0.520	0.000	0.160	0.9982	–	0.57	0.74
Quinoline	1.268	0.970	0.000	0.540	1.0443	1.37	−0.81	−0.55
Resorcinol	0.980	1.110	1.090	0.520	0.8338	0.52	−1.11	−0.56
Thymol	0.822	0.790	0.520	0.440	1.3387	1.92	0.44	0.91
Thiourea	0.840	0.820	0.770	0.870	0.5696	−0.03	–	–
Toluene	0.601	0.520	0.000	0.140	0.8573	–	0.08	0.36
Valerophenone	0.795	0.950	0.000	0.500	1.4366	2.07	0.42	0.55

-: Compounds not detected in the chromatographic system.

phase and lecithin as mobile phase. We speculate that due to its structure, lecithin probably has intermediate properties between the aqueous buffer and C18 and thus the partition C18/lecithin (LMELC) is similar in properties to the partition lecithin/water, being in any case C18 and water saturated with lecithin.

Solute volume (V) and hydrogen-bond basicity (B) present high coefficients for the three systems. The cavity contribution is more favorable to partition to the stationary or pseudostationary phase than to the mobile phase or to the buffer ($v > 0$), and the hydrogen-bond acidity of the stationary (C18) or pseudostationary phase (lecithin microemulsion and liposomes) is much lower, especially for the lecithin microemulsion, than that of the aqueous phase. All systems show a moderate negative polarizability value (s), so the lecithin mobile phase is more polar than C18 stationary phase in LMELC, whereas lecithin pseudostationary phases are less polar than water in LMEEKC and LLECK especially in the latter system.

The liposomes system shows the highest e value, which means that the liposomes are highly polarizable. The two electrophoretic systems show positive hydrogen-bond basicity value (a), so they are more hydrogen-bond basic than the aqueous buffer, while the LMELC system presents a negative value, which means that lecithin

Please cite this article as: S. Amézqueta, A. Fernández-Pumarega and S. Farré et al., Lecithin liposomes and microemulsions as new chromatographic phases, Journal of Chromatography A, https://doi.org/10.1016/j.chroma.2019.460596

Table 2
Coefficients and statistics of the SPM model for the systems based on lecithin.

	LSER coefficients					Normalized LSER coefficients				Statistics				
	c (SD_c)	e (SD_e)	s (SD_s)	a (SD_a)	b (SD_b)	v (SD_v)	e_u	s_u	a_u	b_u	v_u	n	R^2	SD	F	$n_{outliers}$
LMELC	0.525 (0.046)	0.250 (0.067)	−0.591 (0.039)	−0.212 (0.039)	−1.984 (0.059)	2.084 (0.059)	0.085	−0.200	−0.072	−0.671	0.705	39	0.984	0.078	410	9[a]
LMEEKC	−2.217 (0.098)	0.431 (0.104)	−0.624 (0.067)	0.330 (0.074)	−3.709 (0.161)	3.317 (0.115)	0.085	−0.124	0.065	−0.735	0.658	47	0.937	0.131	246	3[b]
LLEKC	−1.869 (0.083)	0.885 (0.118)	−0.809 (0.078)	0.339 (0.065)	−2.865 (0.112)	2.809 (0.092)	0.211	−0.193	0.081	−0.682	0.669	46	0.968	0.125	241	5[c]

[a] Furan, α-pinene, pyrogallol (1,2,3-trihydroxybenzene), pyrrole, propylbenzene, thiourea, aniline, benzene, *o*-toluidine.
[b] Benzaldehyde, 4-aminobenzamide, β-estradiol.
[c] Propylbenzene, α-pinene, monuron, quinolone, 4-aminobenzamide.

Table 3
d distance values between lecithin-based and other physicochemical systems, according to the SPM coefficients comparison. Values under 0.25 are in bold format.

System	LMELC	LMEEKC	LLEKC
LMELC	–	**0.18**	**0.20**
LMEEKC	**0.18**	–	**0.15**
LLEKC	**0.20**	**0.15**	–
OW	**0.08**	**0.14**	**0.14**
IAM	**0.18**	**0.12**	**0.04**
PLM	**0.16**	**0.07**	**0.10**
SDS0.8	0.36	0.50	0.50
SDS1.6	0.54	0.69	0.69
Brij	0.27	0.42	0.45
BrijSDS	0.34	0.48	0.50
SDSME	**0.07**	**0.13**	**0.18**
DGDCChol	**0.17**	**0.05**	**0.12**
DGDC	**0.25**	**0.10**	**0.17**
PAAU	**0.18**	**0.11**	**0.15**
PSUA	**0.17**	**0.08**	**0.11**
DHP	0.32	0.42	0.41
DHPChol	0.44	0.42	0.48
POPCPS	**0.15**	**0.11**	**0.11**

microemulsion is more basic than the C18 stationary phase. Among other factors, the constant (c) of the correlations is related to the phase ratio for the separation system, and this one depends on the microemulsion/liposome concentration and the molar volume of these suspensions [19].

3.2. Comparison of the lecithin-based systems with other chromatographic systems

The three lecithin-based systems (LMELC, LMEEKC, LLEKC) have been compared to other chromatographic systems included in Table 4. The selected systems use any of the three techniques of separation – MELC, MEEKC, LEKC – (SDS0.8, SDS1.6, Brij, and BrijSDS for MELC; SDSME for MEEKC; DGDCChol, DGDC, PAAU, and PSUA for LEKC), or contain phospholipids in the stationary phase (IAM, PLM) or in the pseudostationary phase (DHP, DHPChol and POPCPS), In addition, the octanol/water partition (OW) has been included as reference system in the evaluation of partition processes [22].

The similarity of these systems with the lecithin-based ones has been evaluated from the distance between the corresponding normalized SPM coefficients (Table 3). The systems that are more similar to the lecithin-based ones show a distance value under 0.25 units and are OW, SDSME, DHP, DHPChol, and all the systems formed by phospholipids (IAM, PLM, DGDC, DGDCChol, and POPCPS) independently of the technique used. The MELC systems that contain SDS in the mobile phase (SDS0.8, SDS1.6 and BrijSDS) show the biggest differences (in general, $d > 0.45$).

Fig. 2 presents the dendrogram of d distances, and the PCA of the normalized coefficients for all the selected chromatographic systems. Plots show three different clusters at $d = 0.25$ level; the first one includes the lecithin-based systems (OW, SDSME, DHP, DHPChol, IAM, PLM, DGDC, DGDCChol, and POPCPS). The others include PSUA and PAAU (second cluster, polymeric-based LEKC systems); and SDS0.8, SDS1.6, Brij, BrijSDS (third cluster, surfactant-based MELC systems). Systems of the first cluster show negative PC1 and negative PC2. They differ from the third cluster mainly in the first principal component (PC1) and from the second cluster in the second principal component (PC2). The descriptors that have the main impact on PC1 are the solute's effective hydrogen-bond basicity (B) and the McGowan's solute volume (V). In PC2, all of the descriptors have some influence except for the McGowan's solute volume.

Please cite this article as: S. Amézqueta, A. Fernández-Pumarega and S. Farré et al., Lecithin liposomes and microemulsions as new chromatographic phases, Journal of Chromatography A, https://doi.org/10.1016/j.chroma.2019.460596

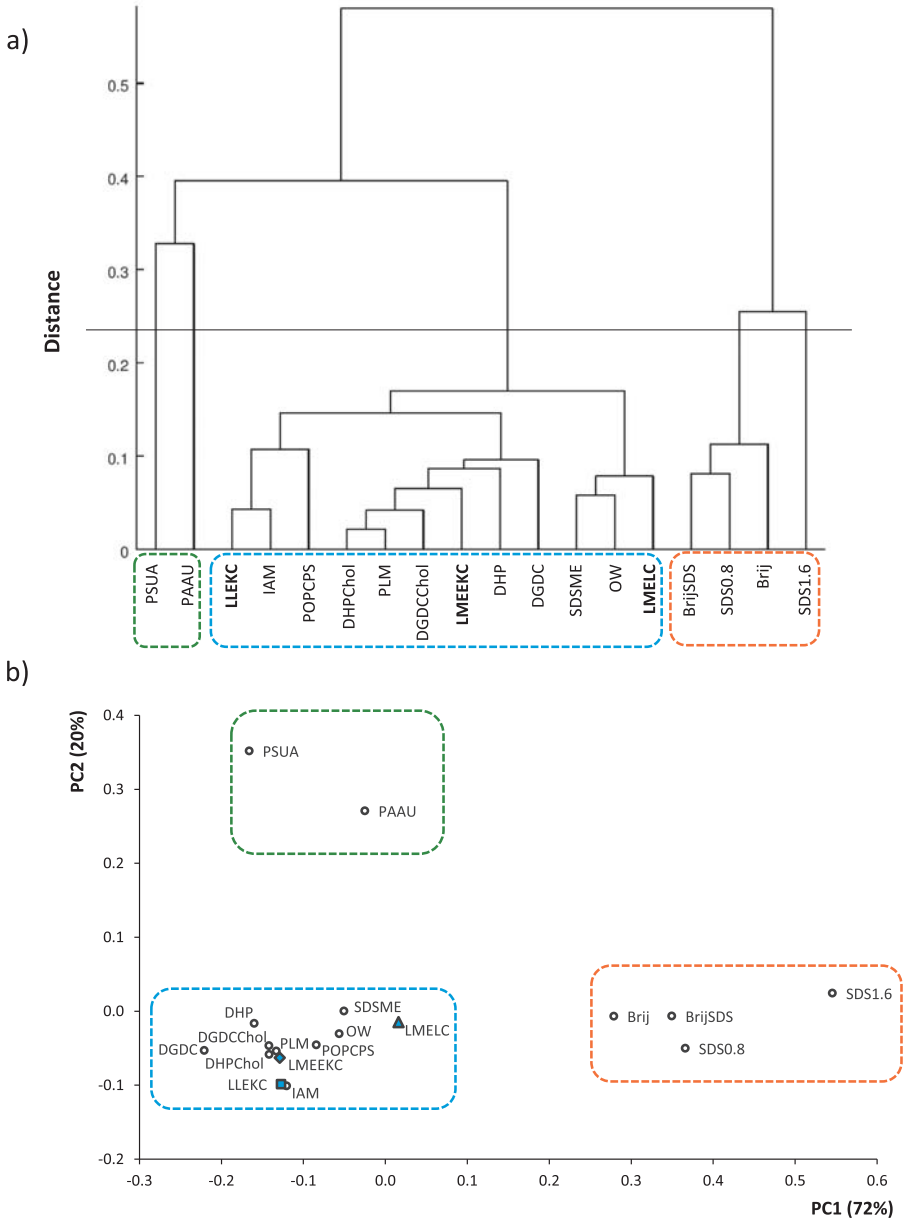

Fig. 2. Comparison of the similarity between the three lecithin-based systems and other physicochemical systems. (a) Dendrogram plot of the selected physicochemical systems, together with the lecithin-based ones. (b) PCA scores plot of the physicochemical systems (o) and the lecithin systems evaluated in this work (symbols as in Fig. 1).

Please cite this article as: S. Amézqueta, A. Fernández-Pumarega and S. Farré et al., Lecithin liposomes and microemulsions as new chromatographic phases, Journal of Chromatography A, https://doi.org/10.1016/j.chroma.2019.460596

Table 4
Composition of the physicochemical systems evaluated in the present work.

Acronym	Technique of separation	Mobile phase	Stationary or Pseudostationary phase	Reference
OW	Liquid/liquid partition	Octanol/Water		[26]
IAM	LC	CH_3CN:phosphate buffer, gradient	IAM	[12]
PLM	LC	Phosphate buffer:CH_3OH 8:2	PLM	[27]
LMELC	MELC	Lecithin-based microemulsion	C18	Present work
SDS0.8	MELC	SDS, butanol, 0.80% heptane	C18	[28]
SDS1.6	MELC	SDS C18, butanol, 1.60% heptane	C18	[28]
Brij	MELC	Brij 35, butanol, heptane	C18	[28]
BrijSDS	MELC	Brij 35 SDS, butanol, heptane	C18	[28]
LMEEKC	MEEKC	Phosphate buffer	Lecithin-based microemulsion	Present work
SDSME	MEEKC	Phosphate/Borate buffer	SDS, butanol, heptane	[29]
LLEKC	LEKC	Phosphate buffer	Lecithin-based liposomes	Present work
DGDCChol	LEKC	2-[4-(2-*hydroxyethyl*)*piperazin*-1-*yl*]ethanesulfonic acid buffer	DPPG:DPPC:Chol	[30]
DGDC	LEKC	2-[4-(2-*hydroxyethyl*)*piperazin*-1-*yl*]ethanesulfonic acid buffer	DPPG:DPPC	[30]
PAAU	LEKC	Phosphate/Borate buffer	PAAU	[31]
PSUA	LEKC	Phosphate/Borate buffer	PSUA	[31]
DHP	VEKC	Tris(hydroxy– methyl)aminomethane buffer	DHP	[32]
DHPChol	VEKC	Tris(hydroxy– methyl)aminomethane buffer	DHP:Chol	[32]
POPC/PS	VEKC	2-[4-(2-*hydroxyethyl*)*piperazin*-1-*yl*]ethanesulfonic acid buffer	POPC/PS	[33]

Brij 35, polyoxyethylene(23) dodecyl ether; Chol, cholesterol; DGDC, dipalmitoylphosphatidyl glycerol + dipalmitoylphosphatidyl choline; DGDCChol, dipalmitoylphosphatidyl glycerol + dipalmitoylphosphatidyl choline + cholesterol; DHP, dihexadecylphosphate; DHPC, 1-palmitoyl-2-oleyl-sn–glycero–3-phosphocholine + cholesterol; DPPC: dipalmitoylphosphatidyl choline; DPPG, dipalmitoylphosphatidyl glycerol; IAM, immobilized artificial membrane; LEKC, liposome electrokinetic chromatography; LLEKC, lecithin liposome electrokinetic chromatography; LMEEKC, lecithin microemulsion electrokinetic chromatography; LMELC, lecithin microemulsion liquid chromatography; MEEKC, microemulsion electrokinetic chromatography; MEKC, micellar electrokinetic chromatography; OW, octanol/water; PAAU: poly(sodium 11-acrylamidoundecanoate); PLM, phospholipid modified; POPC, 1-palmitoyl-2-oleyl-sn–glycero–3-phosphocholine; PS, phosphatidyl serine; PSUA, poly(sodium 10-undecylenate); SDS, sodium dodecyl sulfate; VEKC, vesicle electrokinetic chromatography.

A relevant outcome is that all the systems containing phospholipids cluster together and are very similar to the reference OW, with independence of the chromatographic approach used. The lecithin-based LEKC system (LLEKC) behaves like the other LEKC systems based on phospholipids (DGDC, DHP, DHPChol and DGDCChol). It shows also high semblance to IAM, an immobilized artificial membrane of phospholipids used as stationary phase in RPLC. On the contrary, it shows different selectivity than the polymeric-based LEKC systems (PAAU and PSUA), probably due to the chemical difference between natural phospholipids and synthetic polymers. Generally, liposome preparation is laborious, time-consuming and it requires the characterization of the liposomes formed. The main advantage of using LLEKC over the other liposome systems is that the former is prepared by direct dilution of a ready-to-use commercial product and does not imply a mandatory liposome characterization due to the simplicity of the preparation process. It is also more affordable than IAM columns.

In the case of MEEKC, the two systems evaluated (LMEEKC and SDSME) cluster together ($d < 0.25$) and are different from the pure surfactant MELC systems (SDS0.8, SDS1.6, Brij, BrijSDS) that use C18 as stationary phase and form the second cluster. Probably, the contribution of the type of surfactant in the ME properties is negligible in favor of the presence of other components such as 1-butanol or heptane. Therefore, the partition is mainly influenced by the presence or absence of the C18 column. Despite the clustering of the two microemulsion EKC systems, LMEEKC and SDSME, they show some slight differences in selectivity. LMEEKC is more similar to LECK systems based on phospholipids, and to the phospholipid membrane LPS used as stationary phase in RPLC. Whereas, SDSME is more similar to LMELC. Surprisingly, LMELC system does not cluster with the surfactant-based MELC systems in the second cluster. A reason could be that lecithin in MELC is probably mostly adsorbed to the surface of the stationary phase and thus it is more similar to IAM (immobilized artificial membrane formed of phospholipids), PLM (phospholipid membrane) and SDSME (SDS microemulsion used as pseudostationary phase in EKC), also in the same cluster, than to surfactant-based MELC systems.

3.3. Similarity of the lecithin-based systems and the biological systems

Forty-two biological systems characterized through the SPM model have been considered in the present study (their SPM characterization is described in the Tables SI-2 and SI-3 of the Supplementary Material). They evaluate different properties of pharmaceutical interest related with the blood-tissue partition, permeation or absorption and others of environmental interest related to aquatic toxicity, cell permeation and soil absorption.

As before, the similarity of these systems with the lecithin-based ones has been evaluated through the d distance parameter (Table 5). According to this criterion, the nineteen systems with the lowest d distances have been selected. They include five and fourteen systems of pharmaceutical and environmental interest, respectively. A previous study used a lecithin-based system to predict intestinal absorption [18], however our predictions do not consider any of the three lecithin systems as candidates to model this parameter ($d \sim 0.85$).

Next, the dendrogram of d distances, and the PCA of the normalized coefficients of these nineteen systems have been plotted (Fig. 3). These plots show that the biological systems that are closer, and hence show similar characteristics to the lecithin ones, are toxicity to rana tadpoles and blood brain barrier permeability estimated by the parallel artificial membrane permeability assay (PAMPA) in the case of LLEKC and LMELC, and skin partition, blood-lung partition, and toxicity to several aquatic species in the case of LMEEKC. In concrete and according to both the distance and the clustering criteria, the biological systems that probably will be best emulated by the lecithin systems are toxicity to tadpoles and skin partition. Our group of research has recently reported a method using MEKC to surrogate the toxicity to tadpoles [13] and other species [23] and a method using RPLC to surrogate skin partition [24]. The RPLC method uses a C18 stationary phase and 10 mM phosphate buffer (pH 7) : acetonitrile 60:40 as mobile phase and requires two descriptors to model the property, the retention factor in the chromatographic system and the McGowan volume of the solute. Thus now we will test the possibility to emulate the skin partition (log K_{SC}) using a direct method that only requires

Please cite this article as: S. Amézqueta, A. Fernández-Pumarega and S. Farré et al., Lecithin liposomes and microemulsions as new chromatographic phases, Journal of Chromatography A, https://doi.org/10.1016/j.chroma.2019.460596

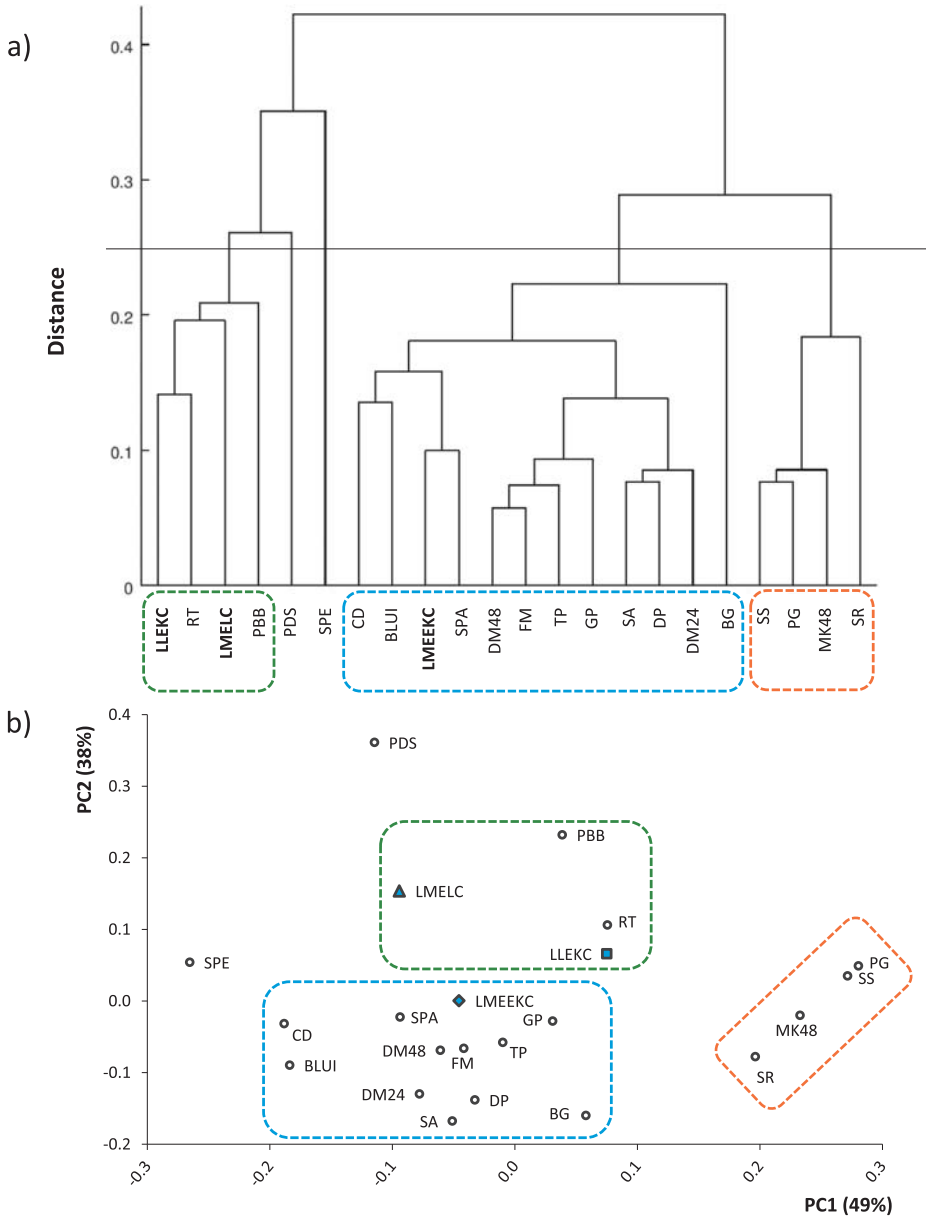

Fig. 3. Comparison of the similarity between the three lecithin-based systems and biological systems. (a) Dendrogram plot of the selected biological systems, together with the lecithin-based ones. (b) PCA scores plot of the biological systems (o) and the lecithin systems evaluated in this work (symbols as in Fig. 1).

Please cite this article as: S. Amézqueta, A. Fernández-Pumarega and S. Farré et al., Lecithin liposomes and microemulsions as new chromatographic phases, Journal of Chromatography A, https://doi.org/10.1016/j.chroma.2019.460596

Table 5
d distance values between biological and chromatographic systems, according to the SPM coefficients comparison. Values under 0.25 are in bold format.

	System[a]	LMELC	LMEEKC	LLEKC		System[i]	LMELC	LMEEKC	LLEKC
BBD	Blood-brain distribution	0.63	0.77	0.70	*RT*	*Rana* tadpoles	**0.19**	**0.20**	**0.14**
BBP	Blood-brain permeation	0.58	0.73	0.73	*FM*	Fathead minnow (*Pimephalespromelas*)	**0.23**	**0.09**	**0.20**
IA	Intestinal absorption	0.78	0.82	0.89	*GP*	Guppy (*Poeciliareticulata*)	**0.23**	**0.14**	**0.15**
SPA	Skin partition	**0.18**	**0.10**	**0.19**	*BG*	Bluegill (*Lepomismacrochirus*)	0.37	**0.20**	0.26
SPE	Skin permeation	**0.21**	**0.23**	0.34	GO	Golden orfe (*Leuciscusidusmelanotus*)	0.45	0.36	0.35
BBI	Blood–brain partition /in vitro	0.55	0.70	0.67	GF	Goldfish (*Carassiusauratus*)	0.59	0.52	0.64
BMI	Blood–muscle partition/in vitro	0.71	0.81	0.80	MK48	Medaka high-eyes (*Oryziaslatipes*)	0.37	0.30	**0.21**
BLII	Blood–liver partition /in vitro	0.62	0.78	0.75	MK96	Medaka high-eyes (*Oryziaslatipes*)	0.46	0.38	0.35
BLUI	Blood–lung partition /in vitro	0.26	**0.17**	0.31	*DM24*	*Daphnia magna*	0.29	**0.16**	0.27
BKI	Blood–kidney partition /in vitro	1.08	1.22	1.18	*DM48*	*Daphnia magna*	**0.23**	**0.13**	**0.22**
BHI	Blood–heart partition /in vitro	0.56	0.60	0.59	*CD*	*Ceriodaphniadubia*	**0.22**	**0.20**	0.30
BFI	Blood–fat partition /in vitro	0.52	0.61	0.67	*DP*	*Daphnia pulex*	0.32	**0.20**	0.29
PBB	PAMPA-BBB[b] permeability	**0.20**	0.26	**0.23**	*TP*	*Tetrahymena pyriformis*	0.25	**0.15**	**0.22**
PPO	PAMPA-Po[c] permeability	0.34	0.50	0.49	*SA*	*Spirostomumambiguum*	0.35	**0.21**	0.32
PDS	PAMPA-DS[d] permeability	**0.23**	0.39	0.39	ES	*Entosiphonsulcantum*	0.47	0.35	0.35
pH	PAMPA-HDM[e] permeability	0.42	0.56	0.59	UP	*Uronemaparduczi*	0.70	0.66	0.59
PDO	PAMPA-DOPC[f] permeability	0.35	0.48	0.51	CP	*Chilomonas paramecium*	0.43	0.38	0.32
PC	PAMPA-COS[g] permeability	0.62	0.76	0.78	PP	*Pseudomonas putida*	0.32	0.33	0.30
PP16	PAMPA-P16[h] permeability	0.49	0.54	0.59	PG	*Porphyromonasgingivalis*	0.39	0.34	**0.22**
					SR	*Selenomonasartemidis*	0.39	0.26	**0.20**
					SS	*Streptococcus sobrinus*	0.39	0.34	**0.24**
					AP	Alga cell permeation	0.95	1.07	1.08
					SWP	Soil-water sorption	0.26	0.25	0.26

[a] Systems of pharmaceutical interest.
[b] PAMPA: parallel artificial membrane permeability assays / BBB: blood brain barrier.
[c] Po: intrinsic permeability.
[d] DS: double-sink permeability measurement.
[e] HDM: n-hexadecane PAMPA model.
[f] DOPC: dioleyoylphosphatidylcholine in n-dodecane PAMPA model.
[g] COS: cosolvent PAMPA method.
[h] P16: hexadecane membrane system.
[i] Systems of environmental interest (the toxicity to several aquatic species, the alga-cell permeation and the soil-water sorption).

Table 6
Contributions that determine the overall variance ($SD_{corr\ cal}{}^2$) in the correlations between skin partition data and chromatographic data of the lecithin-based systems.

	q_{cal}	p_{cal}	$(p_{cal}SD_{chrom})^2$	n_{chrom}	$SD_d{}^2$	$SD_{corr\ cal}{}^2$
	Skin partition ($SD_{bio}{}^2 = 0.047$, $n_{bio} = 45$)					
LMELC	0.261	0.850	0.004	40	0.028	0.079
LMEEKC	1.747	0.563	0.005	47	0.009	0.062
LLEKC	1.505	0.687	0.007	46	0.013	0.067

the retention factor determination, and more ecofriendly analyses that do not use high volume of organic solvents.

To this end, the variance of the final correlation ($SD_{corr\ cal}{}^2$) between skin partition and the physicochemical property data (the retention factor) of the selected systems has been estimated. Results are shown in Table 6. The $SD_{corr\ cal}{}^2$ value is very low and little variance is added due to the dissimilarity between compared systems ($SD_d{}^2$). Thus, skin partition is a promising system to be surrogated by the three lecithin-based systems, probably best by LMEEKC and LLEKC, which show low dissimilarity with the biological system and the lowest $SD_d{}^2$ and $SD_{corr\ cal}{}^2$ values. This fact, together with the higher complexity in the preparation of high volumes of microemulsion, and the intensive cleaning protocols needed when working with microemulsions in LC systems have led to the suppression of the LMELC system as candidate for the surrogation. As indicated in Section 2.6, LMEEKC and LLEKC did not show big differences in terms of practicality. Therefore, the ability of the LMEEKC and LLEKC systems to surrogate the skin partition of neutral solutes has been evaluated.

3.4. Evaluation of the performance of lecithin systems to estimate skin partition

To evaluate the skin partition the retention factor of the solutes included in Table 1 with known skin partition values (K_{SC}) [21] has been determined (Eq. (3)) by LLEKC and LMEEKC. Also other compounds with known K_{SC} values have been incorporated into the analysis to get more statistical significance in the further skin partition estimation study (Table 7). They present different K_{SC} values [21], physicochemical representability and detectability in the UV–

Table 7
Experimental log K_{SC} values from the literature [22] and experimental log *k* values measured in this work by LLEKC and LMEEKC for different solutes.

Solute	log K_{SC}	log k_{LLEKC}	log k_{LMEEKC}
2-Nitro-*p*-phenylenediamine	0.57	−0.89	−1.25
Cortexolone	0.86	0.13	−0.54
Cortisone acetate	0.80	0.29	−0.72
Diazepam	1.25	0.64	0.07
Estrone	1.13	1.05	0.42
Hydroxyprogesterone	1.08	0.86	−0.10
m-Cresol	1.06	−0.20	−0.61
Nicotinamide	0.07	–	−1.32
o-Phenylenediamine	0.37	−1.18	−1.26
p-Bromophenol	1.46	0.10	0.11
Testosterone	1.40	0.45	−0.11
Progesterone	1.75	1.40	0.57
p-Chlorophenol	1.34	0.10	−0.04
2-Naphthol	1.55	0.73	0.30
Benzene	1.48	−0.10	−0.41
Corticosterone	0.74	0.10	−0.61
Cortisone	0.50	−0.38	−1.03
Estradiol	1.13	1.15	0.37
Estriol	0.86	–	−0.74
Hydrocortisone	0.44	−0.31	−0.90
p-Cresol	1.06	0.78	−0.56
Phenol	0.76	−0.51	−0.92
Pregnenolone	1.70	−1.09	–
Resorcinol	0.29	−0.56	−1.11
Thymol	1.89	0.99	0.44

–: Compounds not detected in the chromatographic system.

Please cite this article as: S. Amézqueta, A. Fernández-Pumarega and S. Farré et al., Lecithin liposomes and microemulsions as new chromatographic phases, Journal of Chromatography A, https://doi.org/10.1016/j.chroma.2019.460596

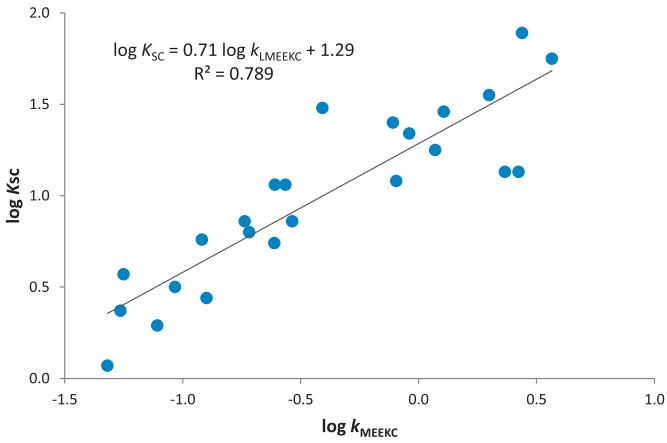

Fig. 4. Correlation between skin partition and retention in the LMEEKC system. The solid line is the plot of the regression equation.

Vis, and are neutral at the working pH. Then, a regression analysis between the biological property logarithm values and the retention factor logarithm values (k_{LLEKC} and k_{LMEEKC} for LLEKC and LMEEKC systems, respectively) has been done according to Eq. (4). Eqs. (7) and (8) include the regression parameters and the statistics for LEKC and MEEKC, respectively. SD^2_{correl} stands for the variance of the correlation log K_{SC} *vs* log *k*.

$$\log K_{SC} = 1.24(0.08) + 0.59(0.05)\ \log k_{LLEKC}\ \left(SD^2_{correl} = 0.089;\ n = 21\ (2\ outliers);\ R^2 = 0.671;\ F = 39\right) \quad (7)$$

$$\log K_{SC} = 1.29(0.06) + 0.71(0.08)\ \log\ k_{LMEEKC}\ \left(SD^2_{correl} = 0.050;\ n = 24;\ R^2 = 0.789;\ F = 82\right) \quad (8)$$

As expected considering the initial predictions, it has been possible to surrogate skin partition directly from the retention of the solute in the chromatographic system. Significant coefficients and good statistical parameters (determination coefficient over 0.60, standard deviation in the order of the biological data, significant F value) have also been obtained. In accordance with the clustering in Fig. 3, all statistics are slightly better for the LMEEKC system. Furthermore, the number of solutes considered is higher and it does not contain outliers. Therefore, we have selected the LMEEKC system as best candidate to model the skin partition of the solutes. Fig. 4 shows the graphical representation of the regression of log K_{SC} *vs* log k_{LMEEKC}.

The LMEEKC system has been validated to prove its robustness and ability to predict skin partition following the method proposed previously [25]. To perform the model's validation, the set of solutes (24 compounds) has been divided into a training set (15 compounds, around 2/3 of the compounds) and a test set (9 compounds, around 1/3 of the compounds). This selection has been done considering the solutes distribution in a PCA plotted using the SPM descriptors that represents the chemical space. In this way, compounds are distributed in the scores plot according to their physicochemical properties, and a representative selection of compounds of different nature has been done for both, the training set and the test set. For the internal validation, the model is established again, but only with the solutes of the training set.

$$\log K_{SC} = 1.33(0.08) + 0.77(0.10)\ \log\ k_{LMEEKC}\ \left(SD^2_{correl} = 0.052;\ n = 15;\ R^2 = 0.828;\ F = 63;\ Q^2_{LMO} = 0.98\right) \quad (9)$$

Eq. (9) shows the correlation parameters obtained. Equations' coefficients are similar to those of the model with all solutes (Eq. (8)), which is indicative of the robustness of the model. Adequate determination coefficient, standard deviation, F value, and leave-multiple-out cross-validation coefficient (over 0.90) have also been obtained.

Finally, the external validation has been carried out. A regression between the experimental skin partition parameter and the one predicted through the training set equation has been done for the compounds of the test set (Eq. (10)). According to statistics, the model considered shows good prediction ability: the slope of the trend line is not significantly different from unity and the intercept from zero at 95% confidence level by the Students *t*-test; the variance (SD^2) is of the same order of that of the biological data (SD^2 = 0.047), the determination coefficient (R^2) is above 0.70; the correlation cross-validation coefficient ($QLMO^2$) is above 0.6; and the Fisher's *F* parameter is significant.

$$\log K_{SC,\ predicted} = 0.12(0.25) + 0.93(0.23)\ \log\ K_{SC,\ experimental}\ \left(SD^2_{correl} = 0.063;\ n = 9;\ R^2 = 0.711;\ F = 17;\ Q^2_{LMO} = 0.66\right) \quad (10)$$

4. Conclusion

Three different chromatographic systems based on lecithin have been characterized through the SPM model. They are quite similar regarding the interaction with neutral compounds, and the main driving forces implied are hydrophobicity and the hydrogen-bond acidity of the systems. The main differences between them lie in the hydrogen-bond basicity and polarizability. They also show very similar partition physicochemical characteristics to other phospholipid-based chromatographic systems, while they offer more easy preparation and availability because they are based on ready-to-use commercial products. Chemometric evaluation has shown that all three are good candidates to model skin partition of compounds, especially that of LMEEKC. Moreover, EKC systems are more practical in terms of technical issues compared to the LC one. Experimental evaluation has confirmed that the electrokinetic system based on lecithin microemulsions (LMEEKC) is able to model skin partition through a direct correlation between the logarithms of the chromatographic retention factor and the skin partition parameter. Therefore, it offers an alternative to skin *in vivo* or tissue *in vitro* testing.

Please cite this article as: S. Amézqueta, A. Fernández-Pumarega and S. Farré et al., Lecithin liposomes and microemulsions as new chromatographic phases, Journal of Chromatography A, https://doi.org/10.1016/j.chroma.2019.460596

Declaration of Competing Interest

The authors declare no competing financial interest.

Acknowledgements

This article is dedicated to Professor Colin F. Poole to commemorate his 70th birthday. We acknowledge his guidance in chromatography during all these years.

Financial support from the Ministerio de Economía y Competitividad from the Spanish Government (CTQ2017-88179-P) and the Catalan Government (2017SGR1074) is acknowledged. AFP wishes to thank the University of Barcelona for his APIF PhD fellowship. Thanks are given to Comercial Química Jover (Terrassa, Spain) for providing the lecithin Emulmetik™ 300 and Pro-Lipo™ Neo products.

Supplementary materials

Supplementary material associated with this article can be found, in the online version, at doi:10.1016/j.chroma.2019.460596.

References

[1] S. El Deeb, H. Wätzig, D. Abd El-Hady, C. Sänger-van de Griend, G.K.E. Scriba, Recent advances in capillary electrophoretic migration techniques for pharmaceutical analysis (2013–2015), Electrophoresis 37 (2016) 1591–1608, doi:10.1002/elps.201600058.
[2] C.F. Poole, A.D. Gunatilleka, S.K. Poole, In search of a chromatographic model for biopartitioning, Adv. Chromatogr. 40 (1999) 159–229.
[3] D.M. Cimpean, C.F. Poole, Systematic search for surrogate chromatographic models of biopartitioning processes, Analyst 127 (2002) 724–729.
[4] S.K. Wiedmer, J. Lokajová, M.L. Riekkola, Marker compounds for the determination of retention factors in EKC, J. Sep. Sci. 33 (2010) 394–409, doi:10.1002/jssc.200900625.
[5] A. Marsh, B.J. Clark, K.D. Altria, A review of the background, operating parameters and applications of microemulsion liquid chromatography (MELC), J. Sep. Sci. 28 (2005) 2023–2032, doi:10.1002/jssc.200500129.
[6] F. Tsopelas, T. Vallianatou, A. Tsantili-Kakoulidou, Advances in immobilized artificial membrane (IAM) chromatography for novel drug discovery, Expert Opin. Drug Discov. 11 (2016) 473–488, doi:10.1517/17460441.2016.1160886.
[7] C. Lepont, C.F. Poole, Retention characteristics of an immobilized artificial membrane column in reversed-phase liquid chromatography, J. Chromatogr. A 946 (2002) 107–124, doi:10.1016/S0021-9673(01)01579-5.
[8] M.H. Abraham, Scales of solute hydrogen-bonding: their construction and application to physicochemical and biochemical processes, Chem. Soc. Rev. 22 (1993) 73, doi:10.1039/cs9932200073.
[9] C.F. Poole, Selectivity characterization of pseudostationary phases using the solvation parameter model, in: U. Pyell (Ed.), Electrokinet. Chromatogr. Theory, Instrum. Appl., First, Chichester, Wiley, 2007, pp. 55–78.
[10] C.F. Poole, S.K. Poole, Column selectivity from the perspective of the solvation parameter model, J. Chromatogr. A 965 (2002) 263–299, doi:10.1016/S0021-9673(01)01361-9.
[11] C.F. Poole, T.C. Ariyasena, N. Lenca, Estimation of the environmental properties of compounds from chromatographic measurements and the solvation parameter model, J. Chromatogr. A. 1317 (2013) 85–104, doi:10.1016/j.chroma.2013.05.045.
[12] E. Lázaro, C. Ràfols, M.H. Abraham, M. Rosés, Chromatographic estimation of drug disposition properties by means of immobilized artificial membranes (IAM) and C18 columns, J. Med. Chem. 49 (2006) 4861–4870, doi:10.1021/jm0602108.
[13] A. Fernández-Pumarega, S. Amézqueta, E. Fuguet, M. Rosés, Tadpole toxicity prediction using chromatographic systems, J. Chromatogr. A. (2015) 1418, doi:10.1016/j.chroma.2015.09.056.
[14] M. Hidalgo-Rodríguez, E. Fuguet, C. Ràfols, M. Rosés, Modeling nonspecific toxicity of organic compounds to the fathead minnow fish by means of chromatographic systems, Anal. Chem. 84 (2012) 3446–3452, doi:10.1021/ac2034453.
[15] E. Fuguet, C. Ràfols, E. Bosch, M.H. Abraham, M. Rosés, Selectivity of single, mixed, and modified pseudostationary phases in electrokinetic chromatography, Electrophoresis 27 (2006) 1900–1914, doi:10.1002/elps.200500464.
[16] J.A. Castillo-Garit, Y. Marrero-Ponce, J. Escobar, F. Torrens, R. Rotondo, A novel approach to predict aquatic toxicity from molecular structure, Chemosphere 73 (2008) 415–427, doi:10.1016/j.chemosphere.2008.05.024.
[17] M. Hidalgo-Rodríguez, E. Fuguet, C. Ràfols, M. Rosés, Estimation of biological properties by means of chromatographic systems: evaluation of the factors that contribute to the variance of biological-chromatographic correlations, Anal. Chem. 82 (2010) 10236–10245, doi:10.1021/ac102626u.
[18] X.Y. Liu, C. Nakamura, Q. Yang, N. Kamo, J. Miyake, Immobilized liposome chromatography to study drug-membrane interactions: correlation with drug absorption in humans, J. Chromatogr. A. 961 (2002) 113–118, doi:10.1016/S0021-9673(02)00505-8.
[19] E. Fuguet, C. Ràfols, E. Bosch, M.H. Abraham, M. Rosés, Solute-solvent interactions in micellar electrokinetic chromatography: III. characterization of the selectivity of micellar electrokinetic chromatography systems, J. Chromatogr. A. 942 (2002) 237–248, doi:10.1016/S0021-9673(01)01383-8.
[20] M.H. Abraham, F. Martins, Human skin permeation and partition: general linear free-enegy relationship analyses, J. Pharm. Sci. 93 (2004) 1508–1523.
[21] L. Wang, L. Chen, G. Lian, L. Han, Determination of partition and binding properties of solutes to stratum corneum, Int. J. Pharm. 398 (2010) 114–122, doi:10.1016/j.ijpharm.2010.07.035.
[22] C.F. Poole, N. Lenca, Applications of the solvation parameter model in reversed-phase liquid chromatography, J. Chromatogr. A. 1486 (2017) 2–19, doi:10.1016/j.chroma.2016.05.099.
[23] A. Fernández-Pumarega, S. Amézqueta, S. Farré, L. Muñoz-Pascual, M.H. Abraham, E. Fuguet, et al., Modeling aquatic toxicity through chromatographic systems, Anal. Chem. 89 (2017) 7996–8003, doi:10.1021/acs.analchem.7b01301.
[24] M. Hidalgo-Rodríguez, S. Soriano-Meseguer, E. Fuguet, C. Ràfols, M. Rosés, Evaluation of the suitability of chromatographic systems to predict human skin permeation of neutral compounds, Eur. J. Pharm. Sci. 50 (2013) 557–568, doi:10.1016/j.ejps.2013.04.005.
[25] K. Roy, On some aspects of validation of predictive quantitative structure–activity relationship models, Expert Opin. Drug Discov. 2 (2007) 1567–1577, doi:10.1517/17460441.2.12.1567.
[26] M.H. Abraham, H.S. Chadha, G.S. Whiting, R.C. Mitchell, Hydrogen bonding. 32. An analysis of water-octanol and water-alkane partitioning and the Δlogp parameter of seiler, J. Pharm. Sci. 83 (1994) 1085–1100, doi:10.1002/jps.2600830806.
[27] T. Godard, E. Grushka, The use of phospholipid modified column for the determination of lipophilic properties in high performance liquid chromatography, J. Chromatogr. A. 1218 (2011) 1211–1218, doi:10.1016/j.chroma.2010.12.105.
[28] J. Liu, J. Sun, Y. Wang, X. Liu, Y. Sun, H. Xu, Z. He, Characterization of microemulsion liquid chromatography systems by solvation parameter model and comparison with other physicochemical and biological processes, J. Chromatogr. A. 1164 (2007) 129–138, doi:10.1016/j.chroma.2007.06.066.
[29] M.H. Abraham, C. Treiner, M. Roses, C. Rafols, Y. Ishihama, Linear free energy relationship analysis of microemulsion electrokinetic chromatographic determination of lipophilicity, J. Chromatogr. A. 752 (1996) 243–249 http://www.sciencedirect.com/science/article/pii/S0021967396005183. (accessed June 16, 2015).
[30] S.T. Burns, A.A. Agbodjan, M.G. Khaledi, Characterization of solvation properties of lipid bilayer membranes in liposome electrokinetic chromatography, J. Chromatogr. A. 973 (2002) 167–176 www.elsevier.com.
[31] C. Fujimoto, Application of linear solvation energy relationships to polymeric pseudostationary phases in micellar electrokinetic chromatography, Electrophoresis 22 (2001) 1322–1329, doi:10.1002/1522-2683(200105)22:7<1322::AID-ELPS1322>3.0.CO;2-3.
[32] A.A. Agbodjan, H. Bui, M.G. Khaledi, Study of solute partitioning in biomembrane-mimetic pseudophases by electrokinetic chromatography: Dihexadecyl phosphate small unilamellar vesicles, Langmuir 17 (2001) 2893–2899, doi:10.1021/la001120n.
[33] R.J. Pascoe, J.P. Foley, Characterization of surfactant and phospholipid vesicles for use as pseudostationary phases in electrokinetic chromatography, Electrophoresis 24 (2003) 4227–4240, doi:10.1002/elps.200305655.

Please cite this article as: S. Amézqueta, A. Fernández-Pumarega and S. Farré et al., Lecithin liposomes and microemulsions as new chromatographic phases, Journal of Chromatography A, https://doi.org/10.1016/j.chroma.2019.460596

LECITHIN LIPOSOMES AND MICROEMULSIONS AS NEW CHROMATOGRAPHIC PHASES

Susana Amézqueta[1,*], Alejandro Fernández-Pumarega[1], Sandra Farré[1], Daniel Luna[1], Elisabet Fuguet[1,2], Martí Rosés[1]

[1] Departament de Química Analítica and Institut de Biomedicina (IBUB), Facultat de Química, Universitat de Barcelona, Martí i Franquès 1-11, 08028, Barcelona, Spain.

[2] Serra Húnter Programme. Generalitat de Catalunya. Spain

* Correspondence:

Susana Amézqueta Pérez

Departament de Química Analítica, Facultat de Química, Universitat de Barcelona

c/ Martí i Franquès 1-11, 08028, Barcelona, Spain

e-mail: samezqueta@ub.edu

Phone: (+34) 93 402 12 77

Fax: (+34) 93 402 12 33

Running title

Lecithin liposomes and microemulsions as new chromatographic phases

SUPPLEMENTARY MATERIAL

Table SI-1

Coefficients, statistics and normalized coefficients of the SPM characterization of physicochemical systems.

	Physicochemical system	Physicochemical parameter	Coefficients						Statistics				Normalized coefficients					Reference
			c	*e*	*s*	*a*	*b*	*v*	n	R^2	SD	F	e_u	s_u	a_u	b_u	v_u	
OW	Octanol/water partition	log *P*	0.088	0.562	-1.054	0.034	-3.460	3.814	613	0.994	0.116	23162	0.106	-0.199	0.006	-0.655	0.721	[1]
IAM	IAM (HPLC) [1,13]	log *k*	-0.710	0.292	-0.344	0.141	-1.193	1.161	51	0.982	0.047	480	0.169	-0.199	0.081	-0.689	0.671	[2]
PLM	PLM, 20% methanol (HPLC) [2]	log *k*	-0.32	0.56	-0.70	0.34	-3.16	3.17	38	0.970	0.140	230	0.122	-0.153	0.074	-0.690	0.693	[3]
SDS0.8	SDS C18, 0.80% heptane (MELC) [3]	log *k*	0.665	0.117	-0.454	-0.495	-0.877	0.751	26	0.984	0.050	243	0.087	-0.339	-0.369	-0.654	0.560	[4]
SDS1.6	SDS C18, 1.60% heptane (MELC)	log *k*	0.727	0.101	-0.645	-0.922	-0.951	0.901	26	0.980	0.078	205	0.058	-0.373	-0.533	-0.550	0.521	[4]
Brij	Brij 35 C18 (MELC) [4]	log *k*	0.698	-0.003	-0.412	-0.415	-0.912	0.887	26	0.972	0.064	141	-0.002	-0.294	-0.296	-0.651	0.633	[4]
BrijSDS	Brij 35 SDS C18 (MELC)	log *k*	0.706	0.027	-0.399	-0.474	-0.842	0.773	26	0.980	0.054	189	0.021	-0.307	-0.364	-0.647	0.594	[4]
SDSME	SDS (MEEKC)	log *k*	-1.133	0.279	-0.692	-0.060	-2.805	3.048	53	0.988	0.09	791	0.066	-0.164	-0.014	-0.667	0.724	[5]
DGDCChol	DPPG:DPPC:Chol (LEKC) [5,6,7]	log *k*	-2.30	0.54	-0.55	0.32	-3.12	3.01	27	0.980	0.08	NA [15]	0.122	-0.125	0.072	-0.707	0.682	[6]
DGDC	DPPG:DPPC (LEKC)	log *k*	-2.21	0.45	-0.44	0.71	-3.23	3.13	27	0.990	0.07	NA	0.098	-0.096	0.154	-0.703	0.681	[6]
PAAU	PAAU (LEKC) [8]	log *k*	-1.86	0.26	-0.16	-0.27	-1.05	2.11	18	0.994	0.051	403	0.109	-0.067	-0.113	-0.439	0.882	[7]
PSUA	PSUA (LEKC) [9]	log *k*	-2.28	0.18	0.45	-0.15	-1.18	1.64	18	0.986	0.063	174	0.086	0.216	-0.072	-0.566	0.787	[7]
DHP	DHP (VEKC) [10,14]	log *k*	-2.68	0.42	-0.65	0.47	-3.27	3.59	41	0.980	NA	NA	0.085	-0.132	0.095	-0.662	0.727	[8]
DHPChol	DHP+Chol (VEKC)	log *k*	-2.28	0.53	-0.77	0.43	-3.29	3.35	41	0.980	NA	NA	0.110	-0.160	0.089	-0.684	0.697	[8]
POPC/PS	POPC/PS (VEKC) [11,12]	log *k*	-2.04	0.70	-0.54	0.02	-2.90	2.68	26	0.97	NA	NA	0.173	-0.133	0.005	-0.717	0.662	[9]

[1] IAM: immobilized artificial membrane column; [2] PLM: phospholipid modified column; [3] SDS: sodium dodecyl sulfate; [4] Brij 35: polyoxyethylene(23) dodecyl ether; [5] DPPG: dipalmitoylphosphatidyl glycerol; [6] DPPC: dipalmitoylphosphatidyl choline; [7] Chol: cholesterol; [8] PAAU: poly(sodium 11-acrylamidoundecanoate); [9] PSUA: poly(sodium 10-undecylenate); [10] DHP: dihexadecylphosphate; [11] POPC: 1-palmitoyl-2-oleyl-sn-glycero-3-

phosphocholine; [12] PS: phosphatidyl serine; [13] HPLC: high-performance liquid chromatography; [14] VEKC: vesicular electrokinetic chromatography; [15] NA: data not available

Table SI-2

Coefficients, statistics and normalized coefficients of the SPM characterization of systems related to biological properties of pharmaceutical interest.

	Biopartitioning system	Biological parameter	Coefficients						Statistics				Normalized coefficients					Reference
			c	*e*	*s*	*a*	*b*	*v*	n	R^2	SD	F	e_u	s_u	a_u	b_u	v_u	
BBD	Blood-brain distribution	log BB	0.044	0.511	-0.886	-0.724	-0.666	0.861	148	0.711	0.367	71	0.308	-0.534	-0.436	-0.401	0.519	[10]
BBP	Blood-brain permeation	log PS	-0.639	0.312	-1.009	-1.895	-1.636	1.709	30	0.870	0.520	32	0.097	-0.314	-0.590	-0.510	0.532	[11]
IA	Intestinal absorption	log HIA	0.544	-0.025	0.141	-0.409	-0.514	0.204	127	0.799	0.290	94	-0.036	0.201	-0.582	-0.732	0.290	[12]
SPA	Skin partition	log K_{sc}	0.341	0.341	-0.206	-0.024	-2.178	1.850	45	0.925	0.216	97	0.118	-0.071	-0.008	-0.755	0.641	[13]
SPE	Skin permeation	log K_p	-5.426	-0.106	-0.473	-0.473	-3.000	2.296	119	0.832	0.461	112	-0.028	-0.123	-0.123	-0.782	0.598	[13]
BBI	Blood–brain partition /*in vitro*	log P	-0.057	0.017	-0.563	-0.323	-0.335	0.731	78	0.725	0.203	37.9	0.016	-0.545	-0.313	-0.324	0.707	[14]
BMI	Blood–muscle partition/*in vitro*	log P	-0.185	-0.209	-0.593	-0.081	-0.168	0.741	110	0.537	0.207	24.1	-0.211	-0.599	-0.082	-0.170	0.749	[15]
BLII	Blood–liver partition /*in vitro*	log P	-0.095	0.000	-0.366	-0.357	-0.180	0.730	125	0.583	0.228	41.9	0.000	-0.403	-0.393	-0.198	0.803	[16]
BLUI	Blood–lung partition /*in vitro*	log P	-0.143	0.000	0.000	0.000	-0.383	0.308	43	0.264	0.190	7.2	0.000	0.000	0.000	-0.779	0.627	[17]
BKI	Blood–kidney partition /*in vitro*	log P	-0.155	0.193	-0.462	-0.922	0.232	0.750	70	0.593	0.218	18.6	0.147	-0.353	-0.704	0.177	0.572	[18]
BHI	Blood–heart partition /*in vitro*	log P	0.047	0.041	-0.045	0.083	-0.224	0.948	31	0.719	0.194	12.8	0.042	-0.046	0.085	-0.229	0.968	[18]
BFI	Blood–fat partition /*in vitro*	log P	0.474	0.016	-0.005	-1.577	-2.246	1.560	126	0.847	0.304	132.7	0.005	-0.002	-0.500	-0.711	0.494	[19]
PBB	PAMPA[1]-BBB[2] permeability	logPo	-4.860	0.250	-1.290	0.250	-2.370	3.030	66	0.737	0.760	33.7	0.061	-0.317	0.061	-0.582	0.744	[20]
PPO	PAMPA-Po[3] permeability	logPo	-4.120	0.250	-1.840	-1.480	-2.460	4.020	147	0.798	1.200	111.5	0.047	-0.349	-0.280	-0.466	0.762	[20]
PDS	PAMPA-DS[4] permeability	logPo	-3.970	-0.026	-2.170	-0.951	-3.450	5.010	28	0.885	0.900	33.5	-0.004	-0.332	-0.146	-0.528	0.767	[20]
PH	PAMPA-HDM[5] permeability	logPo	-3.350	0.106	-1.440	-3.180	-4.240	4.090	20	0.789	0.760	11.2	0.015	-0.210	-0.464	-0.619	0.597	[20]
PDO	PAMPA-DOPC[6] permeability	logPo	-4.640	0.510	-0.860	-2.570	-4.070	3.990	31	0.796	1.010	21.1	0.081	-0.136	-0.406	-0.643	0.630	[20]
PC	PAMPA-COS[7] permeability	logPo	-1.500	-0.130	-1.170	-3.650	-2.760	3.330	24	0.817	0.890	16.9	-0.022	-0.202	-0.631	-0.477	0.576	[20]
PP16	PAMPA-*P16*[8] permeability	logPe	-3.384	0.000	-0.121	-0.188	-0.479	0.194	36	0.558	0.325	NA	0.000	-0.215	-0.334	-0.851	0.345	[21]

[1]PAMPA: parallel artificial membrane permeability assays; [2]BBB: blood brain barrier; [3]Po: intrinsic permeability; [4]DS: double-sink permeability measurement; [5]HDM: n-hexadecane PAMPA model; [6]DOPC: dioleyoylphosphatidylcholine in n-dodecane PAMPA model; [7]COS: cosolvent PAMPA method; [8]P16: hexadecane membrane system

Table SI-3

Coefficients, statistics and normalized coefficients of the SPM characterization of systems related to biological properties of environmental interest.

	Biopartitioning system	Biological parameter	Coefficients						Statistics				Normalized coefficients					Reference
			c	*e*	*s*	*a*	*b*	*v*	n	R^2	SD	F	e_u	s_u	a_u	b_u	v_u	
RT	*Rana* tadpoles	-log C_{nar}[1]	0.582	0.770	-0.696	0.243	-2.592	3.343	114	0.954	0.337	217	0.177	-0.160	0.056	-0.594	0.766	[22]
FM	Fathead minnow (*Pimephales promelas*)	-log LC50[2]	0.996	0.418	-0.182	0.417	-3.574	3.377	196	0.976	0.276	780	0.084	-0.037	0.084	-0.721	0.681	[23]
GP	Guppy (*Poecilia reticulata*)	-log LC50	0.811	0.782	-0.230	0.341	-3.050	3.250	148	0.973	0.280	493	0.172	-0.051	0.075	-0.671	0.715	[23]
BG	Bluegill (*Lepomis macrochirus*)	-log LC50	0.903	0.583	-0.127	1.238	-3.918	3.306	66	0.984	0.272	360	0.110	-0.024	0.233	-0.738	0.623	[23]
GO	Golden orfe (*Leuciscus idus melanotus*)	-log LC50	-0.137	0.931	0.379	0.951	-2.392	3.244	49	0.967	0.269	127	0.218	0.089	0.223	-0.561	0.761	[23]
GF	Goldfish (*Carassius auratus*)	-log LC50	0.922	-0.653	1.872	-0.329	-4.516	3.078	51	0.983	0.277	254	-0.112	0.321	-0.057	-0.776	0.529	[23]
MK48	Medaka high-eyes (*Oryzias latipes*)	-log LC50 (48 h)	0.834	1.047	-0.380	0.806	-2.182	2.667	50	0.969	0.292	133	0.282	-0.102	0.217	-0.588	0.719	[23]
MK96	Medaka high-eyes (*Oryzias latipes*)	-log LC50 (96 h)	-0.176	1.046	0.272	0.931	-2.178	3.155	44	0.980	0.277	182	0.256	0.066	0.228	-0.532	0.771	[23]
DM24	*Daphnia magna*	-log LC50 (24 h)	0.915	0.354	0.173	0.420	-3.935	3.521	107	0.976	0.274	410	0.067	0.033	0.079	-0.741	0.663	[24]
DM48	*Daphnia magna*	-log LC50 (48 h)	0.841	0.528	-0.025	0.219	-3.703	3.591	97	0.982	0.289	475	0.102	-0.005	0.042	-0.714	0.692	[24]
CD	*Ceriodaphnia dubia*	-log LC50	2.234	0.373	-0.040	-0.437	-3.276	2.763	44	0.967	0.256	111	0.086	-0.009	-0.101	-0.758	0.639	[24]
DP	*Daphnia pulex*	-log LC50	0.502	0.396	0.309	0.542	-3.457	3.527	45	0.981	0.311	233	0.079	0.062	0.109	-0.692	0.706	[24]
TP	*Tetrahymena pyriformis*	-log IGC50[3]	0.616	0.413	-0.048	0.348	-2.707	2.944	192	0.982	0.205	1002	0.102	-0.012	0.086	-0.671	0.729	[24]
SA	*Spirostomum ambiguum*	-log LC50	0.148	0.111	0.288	0.687	-3.301	3.140	60	0.979	0.246	252	0.024	0.062	0.149	-0.715	0.680	[24]
ES	*Entosiphon sulcantum*	-log IGC[4]	0.489	0.894	0.355	1.108	-2.504	2.852	51	0.959	0.333	103	0.220	0.087	0.272	-0.615	0.701	[25]
UP	*Uronema parduczi*	-log IGC	2.706	1.426	0.433	0.938	-1.025	2.599	59	0.961	0.326	127	0.432	0.131	0.284	-0.310	0.787	[25]
CP	*Chilomonas paramecium*	-log IGC	0.440	1.129	0.160	0.442	-1.826	2.446	55	0.942	0.351	77	0.343	0.049	0.134	-0.555	0.744	[25]
PP	*Pseudomonas putida*	-log IGC	0.752	0.955	0.092	-0.081	-2.088	2.947	87	0.963	0.269	209	0.255	0.025	-0.022	-0.559	0.788	[24]
PG	*Porphyromonas gingivalis*	-log MIC[5]	-3.320	1.111	-0.605	0.727	-1.904	2.423	126	0.952	0.313	232	0.326	-0.177	0.213	-0.558	0.711	[26]

SR	*Selenomonas artemidis*	-log MIC	-3.008	0.982	-0.496	0.972	-2.643	2.312	116	0.933	0.268	149	0.258	-0.130	0.255	-0.694	0.607	[26]
SS	*Streptococcus sobrinus*	-log MIC	-3.465	0.855	-0.465	0.735	-1.671	2.330	112	0.950	0.309	196	0.274	-0.149	0.236	-0.536	0.748	[26]
AP	Alga cell permeation	log K_{cel}[6]	-2.235	0.000	-0.867	-3.143	-1.664	0.731	100	0.941	0.437	183	0.000	-0.232	-0.842	-0.446	0.196	[27]
SWP	Soil-water sorption	log K_{oc}[7]	0.210	0.740	0.000	-0.310	-2.270	2.090	129	0.977	0.250	655	0.232	0.000	-0.097	-0.712	0.656	[28]

[1]C_{nar}: narcosis concentration; [2]LC50: median lethal concentration, 50 %; [3]IGC50: median inhibitory growth concentration, 50 %; [4]IGC: inhibitory growth concentration; [5]MIC: minimum inhibitory concentration towards bacterial growth; [6]K_{cel}: cell-water permeability coefficient; [7]K_{oc}: soil organic carbon-water partitioning coefficient.

Figure SI-1. Chromatogram of acetanilide obtained by LMELC at λ=254 nm. [(1) Acetanilide]

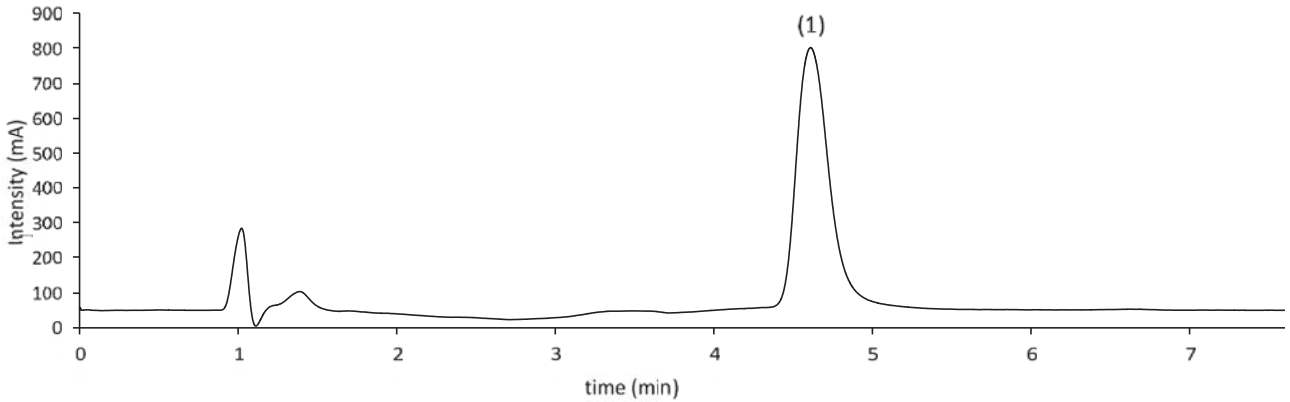

114

Figure SI-2. Electropherogram of *m*-cresol obtained by LMEEKC at λ=254 nm. [(1) EOF marker, (2) *m*-Cresol, (3) Microemulsion marker]

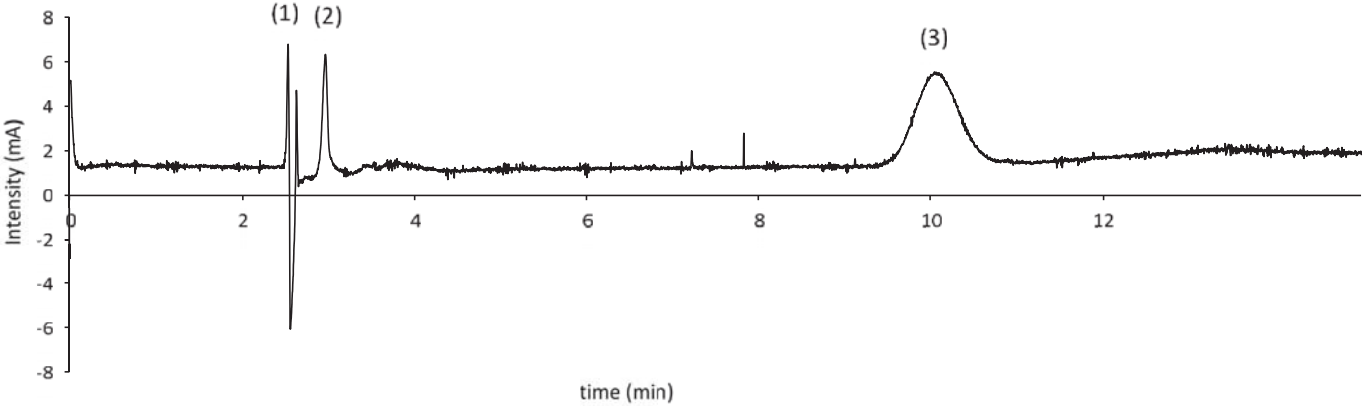

115

Figure SI-3. Electropherogram *o*-toluidine obtained by LLEKC at λ=254 nm. [(1) EOF marker, (2) *o*-Toluidine, (3) Liposome marker]

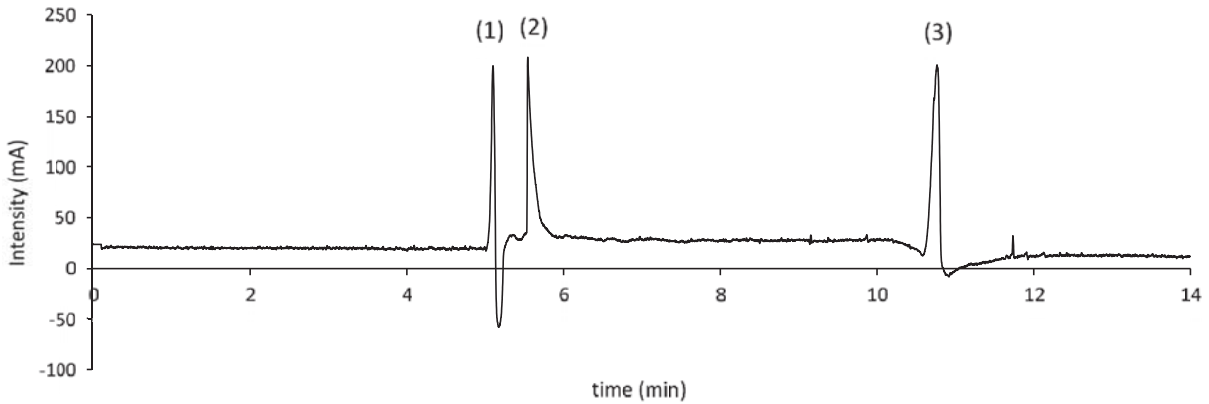

REFERENCES

[1] M.H. Abraham, H.S. Chadha, G.S. Whiting, R.C. Mitchell, Hydrogen bonding. 32. An analysis of water-octanol and water-alkane partitioning and the Δlogp parameter of seiler, J. Pharm. Sci. 83 (1994) 1085–1100. doi:10.1002/jps.2600830806.

[2] E. Lázaro, C. Ràfols, M.H. Abraham, M. Rosés, Chromatographic estimation of drug disposition properties by means of immobilized artificial membranes (IAM) and C18 columns, J. Med. Chem. 49 (2006) 4861–4870. doi:10.1021/jm0602108.

[3] T. Godard, E. Grushka, The use of phospholipid modified column for the determination of lipophilic properties in high performance liquid chromatography, J. Chromatogr. A. 1218 (2011) 1211–1218. doi:10.1016/j.chroma.2010.12.105.

[4] J. Liu, J. Sun, Y. Wang, X. Liu, Y. Sun, H. Xu, Z. He, Characterization of microemulsion liquid chromatography systems by solvation parameter model and comparison with other physicochemical and biological processes, J. Chromatogr. A. 1164 (2007) 129–138. doi:10.1016/j.chroma.2007.06.066.

[5] M.H. Abraham, C. Treiner, M. Roses, C. Rafols, Y. Ishihama, Linear free energy relationship analysis of microemulsion electrokinetic chromatographic determination of lipophilicity, J. Chromatogr. A. 752 (1996) 243–249. http://www.sciencedirect.com/science/article/pii/S0021967396005183 (accessed June 16, 2015).

[6] S.T. Burns, A.A. Agbodjan, M.G. Khaledi, Characterization of solvation properties of lipid bilayer membranes in liposome electrokinetic chromatography, J. Chromatogr. A. 973 (2002) 167–176. www.elsevier.com.

[7] C. Fujimoto, Application of linear solvation energy relationships to polymeric pseudostationary phases in micellar electrokinetic chromatography, Electrophoresis. 22 (2001) 1322–1329. doi:10.1002/1522-2683(200105)22:7<1322::AID-ELPS1322>3.0.CO;2-3.

[8] A.A. Agbodjan, H. Bui, M.G. Khaledi, Study of solute partitioning in biomembrane-mimetic pseudophases by electrokinetic chromatography: Dihexadecyl phosphate small unilamellar vesicles, Langmuir. 17 (2001) 2893–

2899. doi:10.1021/la001120n.

[9] R.J. Pascoe, J.P. Foley, Characterization of surfactant and phospholipid vesicles for use as pseudostationary phases in electrokinetic chromatography, Electrophoresis. 24 (2003) 4227–4240. doi:10.1002/elps.200305655.

[10] J.A. Platts, M.H. Abraham, Y.H. Zhao, A. Hersey, L. Ijaz, D. Butina, Correlation and prediction of a large blood-brain distribution data set - An LFER study, Eur. J. Med. Chem. 36 (2001) 719–730. doi:10.1016/S0223-5234(01)01269-7.

[11] M.H. Abraham, The factors that influence permeation across the blood-brain barrier, Eur. J. Med. Chem. 39 (2004) 235–240. doi:10.1016/j.ejmech.2003.12.004.

[12] M.H. Abraham, Y.H. Zhao, J. Le, A. Hersey, C.N. Luscombe, D.P. Reynolds, G. Beck, B. Sherborne, I. Cooper, On the mechanism of human intestinal absorption, Eur. J. Med. Chem. 37 (2002) 595–605. http://www.sciencedirect.com/science/article/pii/S0223523402013843 (accessed June 14, 2015).

[13] M.H. Abraham, F. Martins, Human skin permeation and partition: General linear free-enegy relationship analyses, J. Pharm. Sci. 93 (2004) 1508–1523.

[14] M.H. Abraham, A. Ibrahim, W.E. Acree, Air to brain, blood to brain and plasma to brain distribution of volatile organic compounds: linear free energy analyses, Eur. J. Med. Chem. 41 (2006) 494–502. doi:10.1016/j.ejmech.2006.01.004.

[15] M.H. Abraham, A. Ibrahim, W.E. Acree, Air to muscle and blood/plasma to muscle distribution of volatile organic compounds and drugs: Linear free energy analyses, Chem. Res. Toxicol. 19 (2006) 801–808. doi:10.1021/tx050337k.

[16] M.H. Abraham, A. Ibrahim, W.E. Acree, Air to liver partition coefficients for volatile organic compounds and blood to liver partition coefficients for volatile organic compounds and drugs, Eur. J. Med. Chem. 42 (2007) 743–751. doi:10.1016/j.ejmech.2006.12.011.

[17] M.H. Abraham, A. Ibrahim, W.E. Acree, Air to lung partition coefficients for volatile organic compounds and blood to lung partition coefficients for volatile organic compounds and drugs, Eur. J. Med. Chem. 43 (2008) 478–485. doi:10.1016/j.ejmech.2007.04.002.

[18] M.H. Abraham, J.M.R. Gola, A. Ibrahim, W.E. Acree, X. Liu, The prediction of blood-tissue partitions, water-skin partitions and skin permeation for agrochemicals, Pest Manag. Sci. 70 (2014) 1130–1137. doi:10.1002/ps.3658.

[19] M.H. Abraham, A. Ibrahim, Air to fat and blood to fat distribution of volatile organic compounds and drugs: Linear free energy analyses, Eur. J. Med. Chem. 41 (2006) 1430–1438. doi:10.1016/j.ejmech.2006.07.012.

[20] J. He, M.H. Abraham, W.E. Jr, Y.H. Zhao, A Linear Free Energy Analysis of PAMPA models for Biological Systems., Int. J. Pharm. 496 (2015) 717–722. doi:10.1016/j.ijpharm.2015.10.064.

[21] M.H. Abraham, Human intestinal absorption - Neutral molecules and ionic species, J. Pharm. Sci. 103 (2014) 1956–1966. doi:10.1002/jps.24024.

[22] M.H. Abraham, C. Rafols, Factors that influence tadpole narcosis. An LFER analysis, J. Chem. Soc. Perkin Trans. 2. (1995) 1843. doi:10.1039/p29950001843.

[23] K.R. Hoover, W.E. Acree, M.H. Abraham, Chemical toxicity correlations for several fish species based on the Abraham solvation parameter model, Chem. Res. Toxicol. 18 (2005) 1497–1505. doi:10.1021/tx050164z.

[24] K.R. Hoover, K.B. Flanagan, W.E. Acree Jr., M.H. Abraham, Chemical toxicity correlations for several protozoas, bacteria, and water fleas based on the Abraham solvation parameter model., Sect. Title Toxicol. 6 (2007) 165–174. doi:10.1139/S06-041.

[25] K.R. Bowen, K.B. Flanagan, W.E. Acree, M.H. Abraham, Correlating toxicities of organic compounds to select protozoa using the Abraham model, Sci. Total Environ. 369 (2006) 109–118. doi:10.1016/j.scitotenv.2006.05.008.

[26] C. Mintz, W.E. Acree, M.H. Abraham, Correlation of minimum inhibitory concentrations toward oral bacterial growth based on the Abraham model, QSAR Comb. Sci. 25 (2006) 912–920. doi:10.1002/qsar.200630011.

[27] J.A. Platts, M.H. Abraham, A. Hersey, D. Butina, Estimation of molecular linear free energy relationship descriptors. 4. Correlation and prediction of cell permeation, Pharm. Res. 17 (2000) 1013–1018. doi:10.1023/A:1007543708522.

[28] S.K. Poole, C.F. Poole, Chromatographic models for the sorption of neutral

organic compounds by soil from water and air, J. Chromatogr. A. 845 (1999) 381–400. doi:10.1016/S0021-9673(98)01085-1.

ARTICLE III

Determination of the Retention Factor of Ionizable Compounds in Microemulsion Electrokinetic Chromatography

Alejandro Fernández-Pumarega, Susana Amézqueta, Elisabet Fuguet, and Martí Rosés

Analytica Chimica Acta (2019), volum: 1078, pàgines: 221-230

DOI: 10.1016/j.aca.2019.06.007

Analytica Chimica Acta 1078 (2019) 221–230

Contents lists available at ScienceDirect

Analytica Chimica Acta

journal homepage: www.elsevier.com/locate/aca

Determination of the retention factor of ionizable compounds in microemulsion electrokinetic chromatography

Alejandro Fernández-Pumarega [a], Susana Amézqueta [a], Elisabet Fuguet [a, b, *], Martí Rosés [a]

[a] Departament d'Enginyeria Química i Química Analítica and Institut de Biomedicina (IBUB), Facultat de Química, Universitat de Barcelona, Martí i Franquès 1-11, 08028, Barcelona, Spain
[b] Serra Húnter Programme, Generalitat de Catalunya, Spain

HIGHLIGHTS

- Viscosity affects retention factor determination of ionizable compounds in MEEKC.
- Microemulsion buffer medium has different viscosity than CZE buffer medium.
- Microemulsion buffer medium cannot be externally reproduced for the CZE measurements.
- Viscosity change can be corrected by mobility measurements of an unretained compound.

GRAPHICAL ABSTRACT

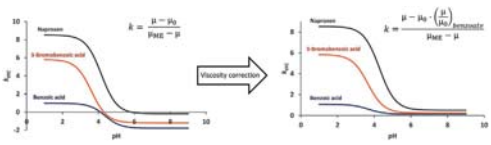

ARTICLE INFO

Article history:
Received 8 March 2019
Received in revised form
30 May 2019
Accepted 2 June 2019
Available online 5 June 2019

Keywords:
Retention factor
Ionizable compounds
Microemulsion
Microemulsion Electrokinetic Chromatography
Viscosity

ABSTRACT

Determination of the retention factor of ionized compounds in microemulsion electrokinetic chromatography requires two mobility measurements at the same pH: one in the presence of the microemulsion and another in plain buffer. However, it has been observed that in some cases subtracting one mobility from another determined in a different medium leads to negative retention factors, which makes no sense from a chemical point of view. This indicates that there is some error in the process which has a direct impact when retention factors are used for further applications.

Here, we evaluate how the components of the microemulsion confer different properties to the buffer medium, particularly varying the viscosity parameter (which is inversely related to mobility). Whereas sodium dodecyl sulfate, the surfactant used in the microemulsion, has little effect on the medium viscosity (only an increase of 5%–6%), the presence of 1-butanol, used as a stabilizer, increases it by around 30%. Meanwhile, heptane, which is used as an oil, provokes a slight decrease. Consequently, the mobilities obtained in the microemulsion system are shifted to higher values (less negative mobilities) compared to mobilities obtained in the aqueous buffer, and so one cannot be directly subtracted from the other. Since the microemulsion-buffer medium cannot be directly reproduced, we propose a correction that takes into account the variation of viscosities. This is determined from the electrophoretic mobility of the benzoate ion. As this ion does not interact with the microemulsion, the ratio of its mobilities (measured in plain buffer and microemulsion) is equivalent to the ratio of viscosities, and can be used as the correction factor for other measurements. Thus, mobilities in buffer and microemulsion media are placed on the same scale, overcoming the errors in retention factor determination.

* Corresponding author. Departament d'Enginyeria Química i Química Analítica and Institut de Biomedicina, Facultat de Química, Universitat de Barcelona, c/ Martí i Franquès 1-11, 08028, Barcelona, Spain.
E-mail address: elifuguetj@ub.edu (E. Fuguet).

https://doi.org/10.1016/j.aca.2019.06.007
0003-2670/

Abbreviations

CMC	critical micelle concentration
CZE	capillary zone electrophoresis
DMSO	dimethyl sulfoxide
EOF	electroosmotic flow
F	Fisher's F parameter
I	ionic strength
k	retention factor
λ	wavelength
ME	microemulsion
MEKC	micellar electrokinetic chromatography
MEEKC	microemulsion electrokinetic chromatography
R^2	determination coefficient
SD	standard deviation
SDS	sodium dodecyl sulfate
UV–vis	ultraviolet–visible

1. Introduction

Capillary electrophoresis is a widely used technique that separates different solutes depending on their charge/size ratio. Although this technique cannot separate non-charged compounds, over the last few decades other modalities of the technique that can separate neutral compounds, such as micellar electrokinetic chromatography (MEKC) [1,2] and microemulsion electrokinetic chromatography (MEEKC) [3], have been developed. In these latter techniques, the solutes become distributed between an aqueous buffer and a pseudo-stationary phase. In MEEKC, the pseudo-stationary phase is a microemulsion (ME) formed by an ionic surfactant, a cosurfactant, and an oil that are mixed together in an aqueous solution at specific concentrations. The surfactant and the cosurfactant act as stabilizers, reducing the surface tension that exists between the oil droplets and water, and allowing the creation of the ME [4]. MEEKC has been used in different applications over recent years, as a separation technique for highly hydrophobic compounds [5–7], or as a method to predict biopartitioning properties, such as lipophilicity, which can be estimated from the retention factor of compounds in the ME media [8–11], among others.

The determination of the retention factor (k) of neutral substances is not a complex issue in MEEKC, as the migration of the compound is affected only by its partition between the buffer and the charged ME. For neutral solutes, k can be calculated from the mobilities of the compounds and the ME. However, the mobility of partly ionized compounds depends on the partition of the neutral form that is within the ME and also on the electrophoretic mobility of the charged forms [12,13].

In order to evaluate how ionized compounds are partitioned between the aqueous buffer and ME phase, the contribution of the electrophoretic mobility of the compound (i.e. the ionic mobility of the compound caused by the application of an electric field) must be subtracted from the observed mobility. Therefore, two different analyses of the compounds are required: one under MEEKC conditions, in which observed mobility is measured; the other only in the plain buffer (capillary zone electrophoresis (CZE) mode), in which the electrophoretic mobility of the compound is measured [12]. In addition, the acid-base compound has to be equally ionized in both media, i.e. both solutions must be at the same pH.

The use of two different media can sometimes be an important handicap in the accurate determination of k values. For instance, some works report negative MEKC retention factors for ionizable compounds, especially for quite polar ones [14,15]. In a strict sense, the two media in which we determine the values that are subtracted one from the other should be the same, except for the presence of the ME. Therefore, some attempts have been made to emulate the aqueous composition of the solutions that contain micelles (MEKC) or microemulsions (MEEKC). Muijselaar et al. [16] pointed out an increase in the absolute mobility value of ionized acids when surfactant monomers below the critical micelle concentration (CMC) were present in the CZE buffer, compared to the value obtained just in plain buffer. This difference was greater for the most hydrophobic compounds. Other authors have proposed other approximations, such as adding sodium chloride to the CZE buffer in order to compensate for the difference in ion composition between solutions [17], or adding the cosurfactant (1-butanol) to the buffer used in CZE measurements [18,19]. The addition of the cosurfactant produced important differences between the mobility values obtained with or without it, although the reason for these differences has not been systematically studied. Taking into account that the retention factor of a substance in a given system is often used to estimate other of its properties, such as $\log P_{o/w}$ [8–11] or biopartitioning parameters [20–24], it is very important to ensure it is determined correctly.

In the present work we evaluate the effect of the medium on the electrophoretic mobility of ionizable compounds, which in turn is directly related to the retention factors obtained. To this end, we determine the retention factor vs. pH profiles of six monoprotic acids selected as test compounds. Then, the influence of the different components of the ME on the electrophoretic mobilities used to calculate the retention factors is evaluated, and finally we propose a correction of the medium effect.

2. Theory

Due to the similarity between the retention mechanisms involved, we indistinctly apply equations developed for MEKC [12] to MEEKC in the present study. The retention factor of an acid is defined as the weighted average of the retention factor of the ionized (A^-) and the neutral (HA) species (Eq. (1)):

$$k = \alpha_{(HA)} k_{(HA)} + \alpha_{(A-)} k_{(A-)} \quad (1)$$

where $k_{(HA)}$ and $k_{(A-)}$ are the retention factor of the fully protonated and the totally ionized forms of the acid, respectively, and $\alpha_{(HA)}$ and $\alpha_{(A-)}$ are their mole fractions. If the acidity constant of the compound is known, the mole fractions of both species can be calculated for any pH value using the following equations:

$$\alpha_{(HA)} = \frac{[H^+]}{[H^+] + K_a'} \quad (2)$$

$$\alpha_{(A-)} = \frac{K_a'}{[H^+] + K_a'} = 1 - \alpha_{(HA)} \quad (3)$$

where K_a' is the apparent acidity constant of the acid. Substituting Eqs. (2) and (3) into Eq. (1), and reorganizing terms, we obtain:

$$k = \frac{k_{(HA)} + k_{(A-)} \cdot 10^{pH - pK_a'}}{1 + 10^{pH - pK_a'}} \quad (4)$$

Eq. (4) relates the retention factor of a monoprotic acid with the pH of the media. This expression has been used by several authors [12,15,16] to model the retention behavior of ionizable acids in micellar systems. Nevertheless, there is a lack of studies based on the retention of ionizable compounds in ME-based systems.

As mentioned in the introduction, to calculate the retention factor of an acid, its electrophoretic mobility has to be subtracted from the overall observed mobility. Khaledi et al. [12] proposed an equation for MEKC in which the overall observed mobility of acidic compounds is expressed as a weighted average of their mobilities in the aqueous phase in absence of micelles and in the micellar phase. This equation can be adapted to MEEKC:

$$\mu = \left[\frac{k}{k+1}\right]\mu_{ME} + \left[\frac{1}{k+1}\right]\mu_0 \quad (5)$$

where μ is the overall observed mobility, μ_{ME} the mobility of the ME phase, and μ_0 the mobility of the compound in an aqueous buffer without ME. Rearranging Eq. (5), the following expression is obtained:

$$k = \frac{\mu - \mu_0}{\mu_{ME} - \mu} \quad (6)$$

The mobility of a compound can be calculated from its retention time as follows:

$$\mu = \left[\frac{1}{t_r} - \frac{1}{t_0}\right] \cdot \left[\frac{L_T L_D}{V}\right] \quad (7)$$

In this expression, t_r is the retention time of the compound of interest, t_0 the retention time of the electroosmotic flow (EOF) marker, L_T the total length of the capillary, L_D the effective length of the capillary, that is, the portion from the inlet to the detector, and V the voltage applied.

3. Experimental

3.1. Apparatus and conditions

A capillary electrophoresis system equipped with a diode array from Agilent Technologies (Santa Clara, CA, USA) was used to obtain the MEEKC measurements. The effective length of the capillary was 25 cm or 30 cm, depending on pH.

A GLP 22 pH-meter from Crison (Barcelona, Spain) was used to measure the pH of the buffer solutions.

For the analysis, fused-silica capillaries from Polymicro Technologies (Lisle, IL, USA) were used. The effective length of the capillaries was 25 cm (pH 2.0 and pH 3.0) or 30 cm (other pH values studied), with the total length of the capillaries being, respectively, 33.5 and 38.5 cm. Different conditions (pressure and voltage) were used at each pH in order to obtain the best possible electrophoretic window. The applied voltage ranged between 8 and 15 kV, and the pressure applied during separation between 0 and 50 mbar. In all cases, the temperature was set at 25 °C. The solutes were injected applying a pressure of 50 mbar for 5s, and detected at $\lambda = 200$, 214 or 254 nm (depending on the solute). A minimum of 3 replicate measurements were performed for each determination.

3.2. Reagents and materials

Sodium dihydrogen phosphate monohydrate (≥99%), dimethyl sulfoxide (DMSO, ≥99.9%), hydrochloric acid (1 N Titrisol™), and sodium hydroxide (0.5 N Titrisol™) were from Merck (Darmstadt, Germany). Methanol (HPLC grade) was obtained from Thermo Fisher Scientific (Waltham, MA, USA). Sodium dodecyl sulfate (SDS, ≥99%), 1-butanol (≥99.7%), heptane (99%), sodium phosphate dodecahydrate (>98%), and dodecanophenone (98%) were from Sigma-Aldrich (St. Louis, MO, USA). Disodium hydrogen phosphate (99.5%) and sodium acetate anhydrous (99.6%) were from Baker (Center Valley, PA, USA). Water was purified using a Milli-Q plus system from Millipore (Bedford, MA, USA), with a resistivity of 18.2 MΩ cm.

The test compounds were ibuprofen (≥98%), 2,4,6-trichlorophenol (98%), ketoprofen (≥98%), and naproxen (≥98%) from Sigma-Aldrich; benzoic acid (99.99%) from Baker; and 3-bromobenzoic acid (98%) from Merck.

3.3. Preparation of solutions

3.3.1. Buffer preparation

Different buffer solutions in the pH range between 2.0 and 8.0 were prepared. Aliquots of a 0.2 M sodium dihydrogen phosphate stock solution were adjusted with 1 M hydrochloric acid to prepare the buffer solutions at pH 2.0 and pH 3.0. The pH 4.0 and pH 5.0 buffers were prepared also by addition of 1 M hydrochloric acid to aliquots of a 0.2 M anhydrous sodium acetate stock solution. Finally, the other buffer solutions used (pH 6.0, 7.0, and 8.0) were prepared by mixing different amounts of 0.2 M sodium dihydrogen phosphate and 0.2 M disodium hydrogen phosphate stock solutions. A buffer solution at pH 11.0 was prepared by mixing different amounts of 0.2 M disodium hydrogen phosphate and 0.2 M sodium phosphate dodecahydrate. All the buffer solutions were prepared maintaining the ionic strength (I) at 0.05 M. Table 1 shows the final concentration of individual buffer components.

Additionally, another full set of buffer solutions in which SDS was added at a concentration of 2 mM (just below the CMC) was prepared.

3.3.2. Microemulsion preparation

In the present work, the ME was composed of SDS (surfactant), 1-butanol (cosurfactant), and heptane (oil). The ME was prepared by first dissolving 1.30 g of SDS in 70 mL of the aqueous buffer. Then 8.15 mL of 1-butanol and 1.15 mL of heptane were added. The additions were performed at room temperature, employing a burette and under continuous magnetic stirring. If after stirring the ME remained turbid, it was sonicated until it clarified [8]. Finally, more buffer solution was added up to 100 mL (total final volume). The final concentrations of each component with respect to the total volume of the ME were: 1.30% w/v of SDS, 8.15% v/v of 1-butanol, and 1.15% v/v of heptane.

3.3.3. Sample preparation

For the MEEKC analysis, the test compounds were dissolved at a concentration of 200 mg L^{-1} in a microemulsion:methanol mixture (9:1, v:v). Similarly, in the CZE analysis, they were dissolved at 200 mg L^{-1} in a water:methanol mixture, also at a 9:1 (v:v) ratio. The ME marker was dodecanophenone (200 mg L^{-1}), and the EOF marker was DMSO (0.2% v/v) [25].

3.4. Data analysis

Retention profiles were adjusted with TableCurve 2D v5.01 from

Table 1
Final concentration of individual buffer components expressed in molarity (M).

pH	$[Na^+]$	$[Cl^-]$	$[H_3PO_4]$	$[H_2PO_4^-]$	$[HPO_4^{2-}]$	$[PO_4^{3-}]$	[HAc]	$[Ac^-]$
2.0	0.040	0.033	0.023	0.017	–	–	–	–
3.0	0.049	0.007	0.006	0.043	–	–	–	–
4.0	0.050	0.042	–	–	–	–	0.042	0.008
5.0	0.050	0.018	–	–	–	–	0.018	0.032
6.0	0.047	–	–	0.042	0.003	–	–	–
7.0	0.039	–	–	0.018	0.011	–	–	–
8.0	0.034	–	–	0.003	0.016	–	–	–
11.0	0.033	–	–	–	0.015	0.001	–	–

Systat Software Inc. (San Jose, CA, USA). Data calculations were performed using Excel 2010 from Microsoft (Redmond, WA, USA).

The pK_a and the logarithm of the octanol-water partition coefficient ($logP_{o/w}$) of the test compounds were obtained from Bio-Loom database v1.7 from BioByte Corporation (Claremont, CA, USA).

4. Results and discussion

We selected 6 compounds with different acidity and lipophilicity values to study their behavior in MEEKC. They all have pK_a values in the electrophoretic working pH range (2.0–12.0), and contain chromophore groups in their structure (in order to be detected by UV–vis). Moreover, their different lipophilicity values allowed us to test their different degrees of partition with the ME. The six compounds selected were: naproxen, ketoprofen, and ibuprofen (non-steroidal anti-inflammatory drugs); 2,4,6-trichlorophenol (a potentially polluting substance used as a fungicide, insecticide and preservative); benzoic acid (an important chemical precursor); and 3-bromobenzoic acid (a derivate of benzoic acid). Their physicochemical properties (pK_a and $logP_{o/w}$) are presented in Table 2 [26–38]. The most acidic of the compounds studied was 3-bromobenzoic acid, and benzoic acid was the least lipophilic. Meanwhile, 2,4,6-trichlorophenol and ibuprofen were the solutes with the highest $logP_{o/w}$ value, so they are supposed to be those that interact most with the inner hydrophobic core of the ME.

4.1. Determination of the retention factor vs. pH profiles

The retention factor of the selected compounds was calculated at each pH value between 2.0 and 8.0. To this end, mobility was measured under MEEKC conditions, and also in CZE using the 50 mM constant-ionic-strength buffers. Eq. (7) was used to obtain the mobility values from the migration time, and then the retention factor was calculated from these mobilities according to Eq. (6). Fig. 1 shows the experimental k vs. pH profiles (circles), and also the fitting profile (dashed line). Table 3 shows the results of the fitting together with statistics (determination coefficient, R^2; Fisher's F parameter, F; and standard deviation, SD) of the fit. The k and pH values were the input data and pK_a', $k_{(A^-)}$, and $k_{(HA)}$ were obtained from the fit.

The profile was similar in all cases and, as expected, the neutral form of the compounds had a stronger interaction with the ME than the ionic form. The point of inflection of the curve corresponds to the pK_a' value. If the pK_a' values obtained (Table 3) are compared to those in Table 2, quite good agreement is observed. This indicates that the presence of the ME seems to have only a minor effect on the acidity of the compounds. As regards the interaction with the ME, the neutral form of ibuprofen and 2,4,6-trichlorophenol are those that show the greatest retention factors, whereas benzoic acid is the compound that shows a weakest interaction with the ME. This behavior is in agreement with the log $P_{o/w}$ values shown in Table 2, which indicates the correlation between retention in the ME system studied and the hydrophobicity of the compounds. Anyway, the results obtained for ibuprofen must be treated with caution, as this compound demonstrated a very strong interaction with the ME at pH values below 4.0, always co-eluting with the ME marker. As a consequence, k could not be determined experimentally at low pH values, and considerable extrapolation was necessary in the fit. Therefore, it is quite likely that the ibuprofen pK_a' and $k_{(HA)}$ values are not properly estimated and therefore present a high uncertainty.

The most notable fact derived from Fig. 1 and Table 3 are the negative values obtained for some of the retention factors of the ionic form of the compounds; this cannot be realistic but is also seen in other studies [14,15]. As explained in the introduction, subtracting mobilities obtained in two different media to calculate k can influence the value obtained if the two systems (one with and one without ME) are not really equivalent.

Table 2
Physicochemical properties (pK_a and log $P_{o/w}$) of the compounds tested.

Compound	pK_a (SD)[a]	pK_a' (SD)[b]	log $P_{o/w}$[c]	Ref.[d]
benzoic acid	4.19 (0.02)	4.11 (0.02)	1.87	[26–31]
3-bromobenzoic acid	3.81	3.72	2.75	[32]
naproxen	4.24 (0.10)	4.16 (0.10)	3.18	[33–36]
ketoprofen	4.13 (0.12)	4.04 (0.12)	3.12	[31,34,35,37]
ibuprofen	4.36 (0.08)	4.28 (0.08)	3.50	[35–37]
2,4,6-trichlorophenol	6.17 (0.04)	6.08 (0.04)	3.69	[38]

[a] Average of the thermodynamic pK_a values reported in the literature.
[b] pK_a' at 0.05 M ionic strength.
[c] From Bio-Loom database v1.7.
[d] References for pK_a values.

4.2. Effect of SDS monomers on electrophoretic mobility

In MEEKC and MEKC the aqueous phase is saturated with SDS monomers, whereas the CZE buffer solution is not. Some authors [16] point out that determination of the k value in MEKC should take into account the presence of SDS monomers in the aqueous phase in order to make them fully comparable. That is, the buffer for CZE analysis should also contain the surfactant monomers at a concentration corresponding to that of the CMC.

Fuguet et al. [39] observed that the CMC of a surfactant is related to the concentration of counter-ions (C) in the electrolyte used to prepare the electrophoretic buffer. The equation obtained for SDS, with the sodium ion as counter-ion was:

$$\log CMC = -3.230 - 0.486 \log C \quad (8)$$

The concentration of sodium present in the buffers in this study was never above 50 mM, so the CMC, according to Eq. (8), cannot be lower than 2.5 mM. Thus, in order to test the effect of the free monomers on the k values obtained, μ-pH profiles were performed with plain buffer and using buffers with a concentration of SDS just below the CMC (2 mM) to avoid the formation of micelles.

Similarly to Eq. (4) for k, μ–pH profiles can be fitted to Eq. (9):

$$\mu = \frac{\mu_{(HA)} + \mu_{(A-)} \cdot 10^{pH-pK_a'}}{1 + 10^{pH-pK_a'}} \quad (9)$$

where, μ is the mobility of the acid at a specific pH value, and $\mu_{(HA)}$ and $\mu_{(A^-)}$ are, respectively, the electrophoretic mobility of the neutral and the fully ionized acid. As $\mu_{(HA)}$ is referred to a neutral compound, its value is equal to 0, simplifying the equation to:

$$\mu = \frac{\mu_{(A-)} \cdot 10^{pH-pK_a'}}{1 + 10^{pH-pK_a'}} \quad (10)$$

Fig. 2 shows the results for comparison. No differences are apparent between the experimental conditions since the mobilities are practically the same in both media, for all the compounds. Thus, the presence of monomers of SDS in the CZE buffer does not have a direct effect on k calculation, at least not for compounds such as those used in this study. Nonetheless, it becomes evident that some other phenomenon, mostly related with the different nature of the solutions used in MEEKC and CZE analysis, is present.

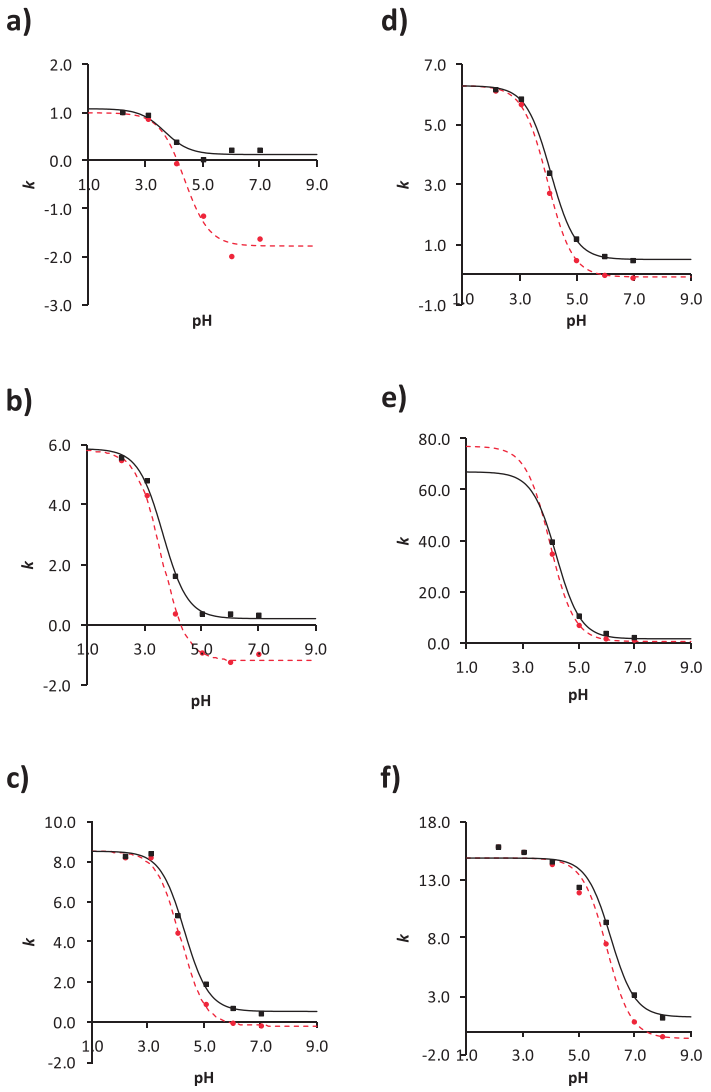

Fig. 1. Retention factor vs. pH profiles of the six test compounds in MEEKC, before (•) and after (■) viscosity correction. The dashed and solid lines show the result of the fit of Eq. (4) to the experimental points, respectively, before and after viscosity correction. a) benzoic acid, b) 3-bromobenzoic acid, c) naproxen, d) ketoprofen, e) ibuprofen, and f) 2,4,6-trichlorophenol.

Table 3
Parameters and statistics for fitting the retention factor to pH (Eq. (4)). Standard deviations are shown in brackets.

Compound	pK_a'	$k_{(A^-)}$	$k_{(HA)}$	R^2	F	SD
benzoic acid	4.37 (0.16)	−1.79 (0.14)	0.98 (0.16)	0.985	99	0.20
3-bromobenzoic acid	3.61 (0.07)	−1.19 (0.13)	5.81 (0.23)	0.997	478	0.21
naproxen	4.16 (0.07)	−0.18 (0.19)	8.52 (0.24)	0.997	479	0.28
ketoprofen	3.99 (0.04)	−0.08 (0.07)	6.29 (0.09)	0.999	1810	0.11
ibuprofen	3.99 (0.04)	0.54 (0.11)	76.79 (3.60)	1.000	17178	0.15
2,4,6-trichlorophenol	6.01 (0.12)	−0.58 (0.78)	14.88 (0.51)	0.988	160	0.94

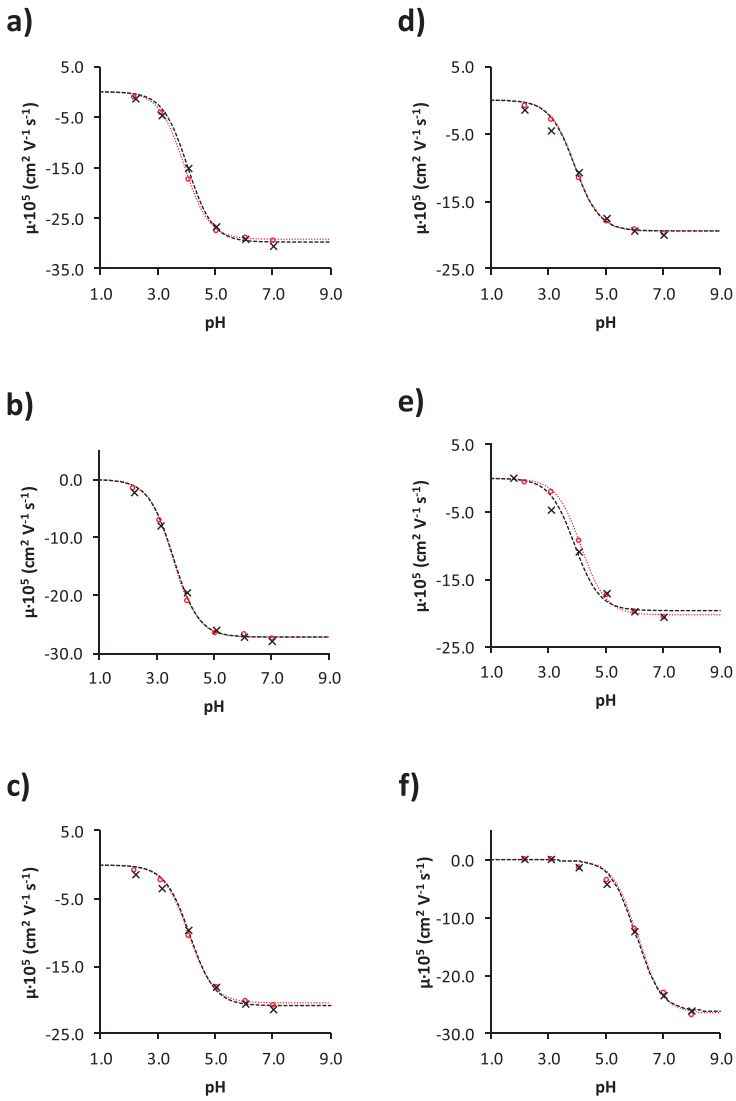

Fig. 2. Mobility profiles of the six test compounds in CZE, in plain buffers (○), and in buffers containing 2 mM SDS (x). The lines are the fit of Eq. (10) to the experimental points in plain buffers (dotted red line), and in the buffers containing 2 mM SDS (dashed black line). a) benzoic acid, b) 3-bromobenzoic acid, c) naproxen, d) ketoprofen, e) ibuprofen, and f) 2,4,6-trichlorophenol. (For interpretation of the references to colour in this figure legend, the reader is referred to the Web version of this article.)

4.3. Evaluation of the different mobility contributions in retention factor determination

In order to understand the reason behind the negative retention factors obtained, we analyzed the different mobility values involved in the calculation of the parameter (Eq. (6)). Fig. 3 shows the variation of the mobilities for benzoic acid (the compound with the largest negative k values) with pH. Thus, three profiles are presented: benzoic acid in CZE (circles); benzoic acid in MEEKC (squares); and dodecanophenone in MEEKC, which acts as the ME marker (triangles). All the mobilities are negative as they correspond to anionic compounds. Moreover, in MEEKC a compound not interacting with the ME would have $\mu = 0$. As can be observed, the mobility of the ME is not pH dependent. In MEEKC, benzoic acid elutes between the EOF ($\mu = 0$) and the ME marker ($\mu = \mu_{ME}$). Thus, the denominator of Eq. (6) is always negative (μ_{ME}-$\mu < 0$), and the numerator has to be negative to obtain $k > 0$, *i.e.* $\mu_0 > \mu$. The mobility plot for benzoic acid in CZE (μ_0) always has to be between 0 (for neutral benzoic acid) and μ (for benzoate), and this is not the case for pH > 4.0. The reason for this disagreement must lie in the

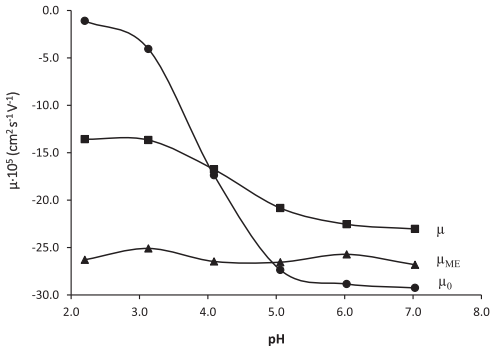

Fig. 3. Effect of pH on the mobility of benzoic acid in CZE (●), and in MEEKC (■). Effect of pH on the mobility of the ME (▲).

different natures of the running buffers in CZE and MEEKC.

4.4. Effect of the microemulsion components on medium viscosity and electrophoretic mobility

To test how different the mobilities of the same compound are in the two media, the mobility of benzoic acid was determined at pH 11.0 in solutions with different concentration of SDS. At this pH value, benzoic acid is totally ionized, so it is expected to have the same mobility in the different media (Fig. 4, squares). In the plot, 0% corresponds to measurements in plain buffer solution, 100% to measurements in a solution with 1.30% w/v of SDS (the amount of SDS equivalent to that in the ME), and the other percentages are measurements in electrophoretic buffers which are mixtures (v/v) of these two solutions. The mobility of the benzoate ion in CZE is $-29.9 \cdot 10^{-5}$ $cm^2 s^{-1} V^{-1}$, meanwhile a solution of SDS at 1.30% w/v shows a mobility of $-28.1 \cdot 10^{-5}$ $cm^2 s^{-1} V^{-1}$. This indicates that SDS decreases the mobility of benzoate by around 6% in absolute value.

The reason for the change of ionic mobilities when the SDS at 1.30% w/v is added to the buffer is presumably the change in viscosity caused by the SDS. According to Eq. (11) [40], the viscosity (η) of the electrophoretic solution is inversely related to the mobility of the compounds. Provided that at a given pH the charge (q) of a compound is the same in MEEKC, MEKC, and CZE, and assuming that the hydrated radius (r) does not change, differences of mobility for a given compound in two different solutions could be attributed to the differences in viscosity between the solutions.

$$\mu = \frac{q}{6\pi\eta r} \tag{11}$$

Some works [41–43] show that the addition of a surfactant to an aqueous solution causes an increase in the viscosity of the solution. Kushner et al. [41] measured the viscosity of aqueous solutions containing different SDS concentrations at 25 °C. Their results show an increase in the viscosity of the solution of more than 3% from 0% to 0.8% (w/v) of SDS content (Fig. 5a). In the present work, the SDS content in the ME is 1.3% (w/v) which, if we assume linear behavior, would imply around a 5% difference in viscosity between the aqueous buffer and the SDS solution. This percentage matches the

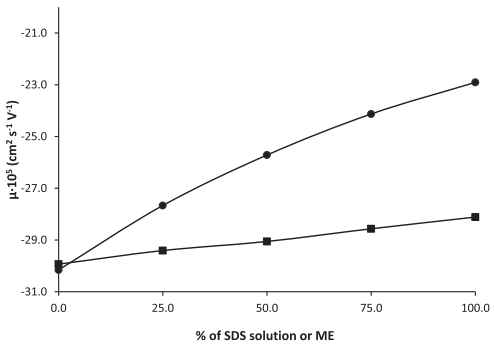

Fig. 4. Effect of amount of SDS (■), and ME (●) on the mobility of benzoate ion. The analysis was performed applying a voltage of 12 kV and with no additional pressure, in a buffer at pH 11.

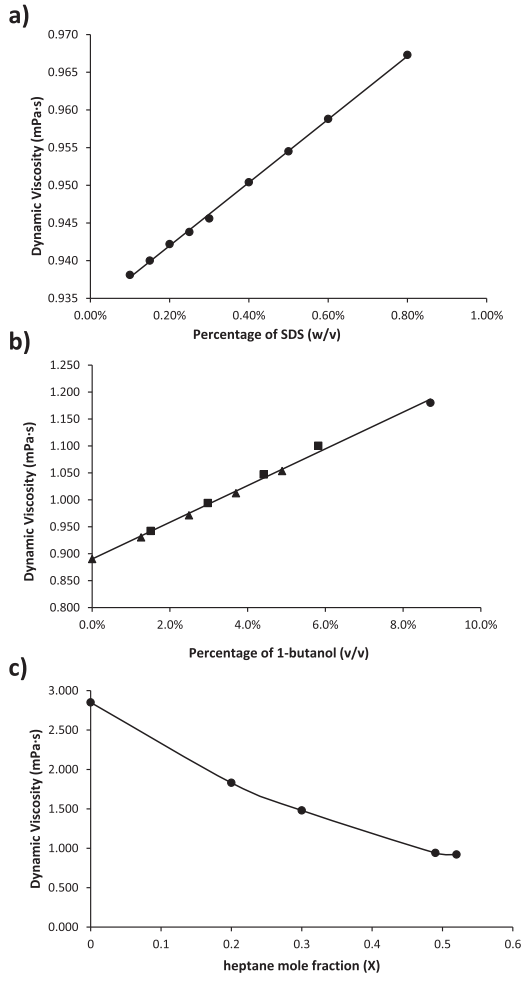

Fig. 5. Effect of individual ME components on dynamic viscosity. a) Mixtures of SDS:water, according to the percentage (w/v) of SDS [41]. b) Mixtures of 1-butanol:water, according to the percentage (v/v) of 1-butanol: (●) from Ref. [44], (▲) from Ref. [45], and (■) from Ref. [46]. c) Mixtures of 1-butanol:heptane, according to the mole fraction (X) of heptane [47].

difference in mobility between CZE and MEKC shown in Fig. 4. Muijselaar et al. [16] already pointed out that the differences in viscosity may have an effect on the calculation of retention factors from MEKC measurements; although they concluded that this difference was small enough to be considered negligible. Note that typical SDS concentrations in MEKC are around 50 mM, which corresponds to 1.44% (w/v); so viscosity differences should be close to 5%–6%. This variation agrees with that expected from Fig. 4, but it is not enough to explain the variation in the mobility plots in Fig. 3, which is about 20%–30%. Thus, we also investigated the effect of the other ME components.

The literature indicates that the viscosity of 1-butanol and heptane, the cosurfactant and oil used in the ME respectively, are quite different from that of water [44–47]. Thus, the overall viscosity of the ME-buffer medium may be significantly altered. As the proportion of 1-butanol in the ME is much greater than that of heptane, the differences in mobilities due to the change in medium should mostly be attributed to the former. In fact, 8.15% (v/v) of 1-butanol increases the viscosity of an aqueous solution by more than 30%, according to Fig. 5b [44–46]. Fig. 5c is a plot of the dynamic viscosity of 1-butanol/heptane mixtures at different mole fractions. As can be seen in the figure, an increase of heptane in the mixture leads to a reduction of the overall dynamic viscosity [47]. A heptane mole fraction of 0.08 (that in the ME, taking into account only 1-butanol and heptane as components), implies a decrease of dynamic viscosity of around 15%, compared with pure 1-butanol. This suggests that the heptane present in the ME will slightly diminish (by around 15%) the increment of the viscosity due to the 1-butanol also present. Unfortunately, it is not possible to evaluate the individual effect of 1-butanol in the CZE buffer directly because, although it is miscible with water, it is not miscible with the buffer due to the presence of salts that increase the polarity of the aqueous phase. Furthermore, heptane is not miscible with water and so could not be tested either.

As it was not possible to evaluate the effect of each compound independently, we studied the effect of the overall ME on mobilities. Fig. 4 shows the electrophoretic mobility of the benzoate ion at different proportions of aqueous buffer and ME (circles). As before, the point at 0% shows the mobility of the benzoate ion in CZE ($\mu_0 = -30.2 \cdot 10^{-5}$ $cm^2 s^{-1} V^{-1}$), with no ME; and the point at 100% shows its mobility in the MEEKC conditions used in this work ($\mu = -22.9 \cdot 10^{-5}$ $cm^2 s^{-1} V^{-1}$). There is an important difference in mobilities when comparing the CZE and MEEKC values (around a 24% decrease in absolute value).

Taking into account all contributions, and being aware that the viscosities of the different components of a mixture are not additive at all, the ME is expected to have a viscosity some 20%–30% higher than that of the buffer solution (according to Fig. 5). This matches the shifted mobilities obtained from Figs. 3 and 4. Therefore, we can conclude that differences in mobility due to the different solutions can mostly be attributed to differences in viscosity between the media involved.

As can be observed in the profiles in Fig. 1, this situation has an important impact on calculation of k, since mobilities in MEEKC and CZE will be different, not only due to the retention of the compound in the ME, but also due to the considerable difference in viscosity between the solutions. As a consequence, mobility in CZE becomes more negative than mobility in MEEKC, especially for those compounds that show a weak interaction with the ME, leading to negative retention factors when direct subtraction of mobilities in MEEKC and CZE is performed for the numerator of Eq. (6). This error may be negligible in MEKC because the increase of viscosity caused by the addition of surfactant is not very high, but it becomes much more important in MEEKC.

4.5. Determination of corrected retention factors

Since it is not possible to measure the mobility in the exact ME-buffer medium, we propose a mobility correction based on the difference of viscosity of the 2 solutions (that with ME and the plain buffer), which can be calculated very easily. We selected benzoic acid to do the correction, because it is a relatively small compound, quite polar, with absorbance in the UV range, and it is not supposed to interact with ME when it is fully ionized ($\log P_{o/w(benzoate)} \approx -1.3$ [48]).

Eq. (11) gives the relation between μ of a compound and the viscosity of the electrophoretic solution. If constant terms are grouped together (c), we obtain:

$$\mu = \frac{C}{\eta} \tag{12}$$

In this way, the difference in viscosities and mobilities between the ME and CZE conditions can be related thus:

$$\frac{\mu}{\mu_0} = \frac{\eta_0}{\eta} \tag{13}$$

So, the calculation of the retention factor for any compound can be corrected by the difference of viscosity according to the expression:

$$k = \frac{\mu - \left(\frac{\eta_0}{\eta}\right) \cdot \mu_0}{\mu_{ME} - \mu} \tag{14}$$

Viscosities are not directly measured, but since the ratio of viscosities is the inverse of the ratio of mobilities of the benzoate ion (Eq. (13)), for any compound the correction is given by:

$$k = \frac{\mu - \left(\frac{\mu}{\mu_0}\right)_{benzoate} \cdot \mu_0}{\mu_{ME} - \mu} \tag{15}$$

We then recalculated retention factors of the test compounds in accordance with this correction (the viscosity correction $\left(\frac{\mu}{\mu_0}\right)_{benzoate}$ has a value of 0.76). The profiles obtained (squares) and results of the fit (solid line) are shown in Fig. 1 and Table 4, respectively. No significant differences are observed for pK_a' and $k_{(HA)}$ values compared to those in Table 3. Notwithstanding, values of $k_{(A^-)}$ are now all positive, being zero or close to zero for benzoate and 3-bromobenzoic acid, a bit higher for naproxen and ketoprofen (which indicates a slight interaction of their anionic form with the ME), and relatively high for ibuprofen and 2,4,6-trichlorophenol (the two most hydrophobic compounds). In the last two cases, there is a clear interaction between the anionic forms of the compounds and the ME. The plots in Fig. 1 demonstrate that differences in the nature of the solutions needed for the calculation of k can be compensated by a correction using a compound that does not interact with the ME.

5. Conclusions

This work demonstrates that the nature of the solutions used for the calculation of retention factors of ionizable compounds in MEKC and MEEKC can have a considerable effect on the values obtained. This is especially so when the viscosities of the aqueous buffer and the micellar or ME solutions are very different. This effect is not so important in MEKC measurements, since the presence of surfactant micelles does not increase the viscosity of the aqueous buffer to a great extent. However, it can make an important

Table 4
Parameters and statistics for fitting the retention factor to pH (Eq. (4)) after viscosity correction. Standard deviations are shown in brackets.

Compound	pK_a'	$k_{(A-)}$	$k_{(HA)}$	R^2	F	SD
benzoic acid	3.68 (0.30)	0.13 (0.07)	1.07 (0.13)	0.948	28	0.12
3-bromobenzoic acid	3.66 (0.08)	0.23 (0.11)	5.84 (0.19)	0.996	415	0.19
naproxen	4.29 (0.08)	0.50 (0.21)	8.54 (0.25)	0.996	360	0.30
ketoprofen	4.10 (0.04)	0.52 (0.07)	6.30 (0.09)	0.999	1424	0.11
ibuprofen	4.21 (0.05)	1.79 (0.28)	67.04 (3.55)	1.000	3448	0.36
2,4,6-trichlorophenol	6.15 (0.14)	1.24 (0.82)	14.87 (0.51)	0.983	119	0.94

contribution to MEEKC retention factors, as the viscosity of some of the components of microemulsions can be very different from that of water (mainly that of 1-butanol in this case). As the viscosity of different microemulsions can change to a greater or lesser extent depending on the proportion and viscosity of the components used in their formation, a viscosity correction has to be introduced. In the present work, we propose a calculation of this viscosity correction using the ratio of mobilities (in MEEKC and CZE) of a compound that does not interact with the pseudo-stationary phase, such as the benzoate ion.

With the proposed correction, the error introduced into the determination of the retention factor in MEKC and MEEKC due to the different viscosities of the media is removed. It has been demonstrated that such an error is especially important for quite polar ionizable compounds, and the correction should always be performed when the retention factor is used for further applications, such as the optimization of analytical separations or the estimation of biological or physicochemical parameters of compounds through quantitative structure-activity relationships.

Conflict of interest

The authors declare no competing financial interests.

Acknowledgements

Financial support from the Spanish Ministerio de Economía y Competitividad (award: CTQ2017-88179-P) and the Catalan Government (award: 2017SGR1074) is acknowledged. AFP wishes to thank the University of Barcelona for his APIF PhD fellowship.

References

[1] S. Terabe, K. Otsuka, T. Ando, Electrokinetic chromatography with micellar solution and open-tubular capillary, Anal. Chem. 57 (1985) 834–841.
[2] S. Terabe, K. Otsuka, K. Ichikawa, A. Tsuchiya, T. Ando, Electrokinetic separations with micellar solutions and open-tubular capillaries, Anal. Chem. 56 (1984) 111–113.
[3] H. Watarai, Microemulsion capillary electrophoresis, Chem. Lett. 231 (1991) 391–394.
[4] R. Ryan, K. Altria, E. McEvoy, S. Donegan, J. Power, A review of developments in the methodology and application of microemulsion electrokinetic chromatography, Electrophoresis 34 (2013) 159–177.
[5] C.W. Chang, Y.C. Chen, C.Y. Liu, Separation and on-line preconcentration of nonsteroidal anti-inflammatory drugs by microemulsion electrokinetic chromatography, Electrophoresis 36 (2015) 2745–2753.
[6] W. Xiao, Q. Zhang, C. Chen, Q.H. Zhang, Y.J. Hu, Z.N. Xia, F.Q. Yang, Analysis of eight isoflavones in Radix Puerariae by MEEKC: comparison on three different oil phases, J. Chromatogr. Sci. 54 (2016) 1678–1686.
[7] Q. Zhou, J. Mao, G. Xie, J. Xiao, Separation and sensitive analysis of chlorophenols by MEEKC, Chromatographia 71 (2010) 875–880.
[8] X. Subirats, H.P. Yuan, V. Chaves, N. Marzal, M. Rosés, Microemulsion electrokinetic chromatography as a suitable tool for lipophilicity determination of acidic, neutral, and basic compounds, Electrophoresis 37 (2016) 2010–2016.
[9] M.H. Abraham, C. Treiner, M. Rosés, C. Ràfols, Y. Ishihama, Linear free energy relationship analysis of microemulsion electrokinetic chromatographic determination of lipophilicity, J. Chromatogr. A. 752 (1996) 243–249.
[10] S.K. Poole, D. Durham, C. Kibbey, Rapid method for estimating the octanol – water partition coefficient (log Pow) by microemulsion electrokinetic chromatography, J. Chromatogr. B Biomed. Sci. Appl. 745 (2000) 117–126.
[11] A. Fernández, S. Amézqueta, E. Fuguet, M. Rosés, Feasibility of the estimation of octanol-water distribution coefficients of acidic drugs by microemulsion electrokinetic chromatography, ADMET DMPK 6 (2018) 55–60.
[12] M.G. Khaledi, S.C. Smith, J.K. Strasters, Micellar electrokinetic capillary chromatography of acidic solutes: migration behavior and optimization strategies, Anal. Chem. 63 (1991) 1820–1830.
[13] J.K. Strasters, M.G. Khaledi, Migration behavior of cationic solutes in micellar electrokinetic capillary chromatography, Anal. Chem. 63 (1991) 2503–2508.
[14] C.E. Lin, W.C. Lin, W.C. Chiou, Migration behaviour and selectivity of dichlorophenols in micellar electrokinetic capillary chromatography influence of micelle concentration and buffer pH, J. Chromatogr. A. 722 (1996) 333–343.
[15] A. Téllez, E. Fuguet, M. Rosés, Comparison of migration models for acidic solutes in micellar electrokinetic chromatography, J. Chromatogr. A. 1139 (2007) 143–151.
[16] P.G. Muijselaar, H.A. Claessens, C.A. Cramers, Migration behaviour of monovalent weak acids in micellar electrokinetic chromatography mobility model versus retention model, J. Chromatogr. A. 765 (1997) 295–306.
[17] D.J. Bailey, J.G. Dorsey, pH effects on micelle-water partitioning determined by micellar electrokinetic chromatography, J. Chromatogr. A. 852 (1999) 559–571.
[18] Y. Ishihama, Y. Oda, N. Asakawa, A hydrophobicity scale based on the migration index from microemulsion electrokinetic chromatography of anionic solutes, Anal. Chem. 68 (1996) 1028–1032.
[19] Y. Ishihama, Y. Oda, N. Asakawa, Hydrophobicity of cationic solutes measured by electrokinetic chromatography with cationic microemulsions, Anal. Chem. 68 (1996) 4281–4284.
[20] A. Fernández-Pumarega, S. Amézqueta, S. Farré, L. Muñoz-Pascual, M.H. Abraham, E. Fuguet, M. Rosés, Modeling aquatic toxicity through chromatographic systems, Anal. Chem. 89 (2017) 7996–8003.
[21] A. Fernández-Pumarega, S. Amézqueta, E. Fuguet, M. Rosés, Tadpole toxicity prediction using chromatographic systems, J. Chromatogr. A. 1418 (2015) 167–176.
[22] S. Soriano-Meseguer, E. Fuguet, A. Port, M. Rosés, Estimation of skin permeation by liquid chromatography, ADMET DMPK 6 (2018) 140–152.
[23] M. Hidalgo-Rodríguez, S. Soriano-Meseguer, E. Fuguet, C. Ràfols, M. Rosés, Evaluation of the suitability of chromatographic systems to predict human skin permeation of neutral compounds, Eur. J. Pharm. Sci. 50 (2013) 557–568.
[24] M. Hidalgo-Rodríguez, E. Fuguet, C. Ràfols, M. Rosés, Modeling nonspecific toxicity of organic compounds to the fathead minnow fish by means of chromatographic systems, Anal. Chem. 84 (2012) 3446–3452.
[25] E. Fuguet, C. Ràfols, E. Bosch, M. Rosés, Solute-solvent interactions in micellar electrokinetic chromatography: IV. Characterization of electroosmotic flow and micellar markers, Electrophoresis 23 (2002) 56–66.
[26] E. Grunwald, A differential potentiometric method of measuring acid and base dissociation constants, J. Am. Chem. Soc. 73 (1951) 4934–4938.
[27] B. Saxton, H.F. Meier, The ionization constants of benzoic acid and of the three monochlorobenzoic acids, at 25°, from conductance measurements, J. Am. Chem. Soc. 56 (1934) 1918–1921.
[28] J.A. Cleveland Jr., M.H. Benko, S.J. Gluck, Y.M. Walbroehl, Automated pKa determination at low solute concentratrions by capillary electrophoresis, J. Chromatogr. A. 652 (1993) 301–308.
[29] F.G. Brockman, M. Kilpatrick, The thermodynamic dissociation constant of benzoic acid from conductance measurements, J. Am. Chem. Soc. 56 (1934) 1483–1486.
[30] F.H. Clarke, N.M. Cahoon, Ionization constants by curve fitting: determination of partition and distribution coefficients of acids and bases and their ions, J. Pharm. Sci. 76 (1987) 611–620.
[31] B. Slater, A. McCormack, A. Avdeef, J.E.A. Comer, pH-metric log P. 4. Comparison of partition coefficients determined by HPLC and potentiometric methods to literature values, J. Pharm. Sci. 83 (1994) 1280–1283.
[32] J.F.J. Dippy, R.H. Lewis, Chemical constitution and the dissociation constants of monocarboxylic acids. Part V. Further substituted benzoic and phenylacetic acids, J. Chem. Soc. (1936) 644–649.
[33] T. Degim, V. Zaimoglu, C. Akay, Z. Degim, pH-Metric logK calculations of famotidine, naproxen, nizatidine, ranitidine and salicylic acid, Farmaco 56 (2001) 659–663.
[34] S. Winiwarter, N.M. Bonham, F. Ax, A. Hallberg, H. Lennernäs, A. Karlén, Correlation of human jejunal permeability (in vivo) of drugs with experimentally and theoretically derived parameters. A multivariate data analysis approach, J. Med. Chem. 41 (1998) 4939–4949.
[35] Y. Ishihama, M. Nakamura, T. Miwa, T. Kajima, N. Asakawa, A rapid method for pKa determination of drugs using pressure-assisted capillary electrophoresis

with photodiode array detection in drug discovery, J. Pharm. Sci. 91 (2002) 933–942.
[36] M. Shalaeva, J. Kenseth, F. Lombardo, A. Bastin, Measurement of dissociation constants (pKa values) of organic compounds by multiplexed capillary electrophoresis using aqueous and cosolvent buffers, J. Pharm. Sci. 97 (2008) 2581–2606.
[37] M. Meloun, S. Bordovská, L. Galla, The thermodynamic dissociation constants of four non-steroidal anti-inflammatory drugs by the least-squares nonlinear regression of multiwavelength spectrophotometric pH-titration data, J. Pharm. Biomed. Anal. 45 (2007) 552–564.
[38] K. Schellenberg, C. Leuenberger, R.P. Schwarzenbach, Sorption of chlorinated phenols by natural sediments and aquifer materials, Environ. Sci. Technol. 18 (1984) 652–657.
[39] E. Fuguet, C. Ràfols, M. Rosés, E. Bosch, Critical micelle concentration of surfactants in aqueous buffered and unbuffered systems, Anal. Chim. Acta 548 (2005) 95–100.
[40] D.R. Baker, Capillary Electrophoresis, Wiley, New York (USA), 1995.
[41] L.M. Kushner, B.C. Duncan, J.I. Hoffman, A viscometric study of the micelles of sodium dodecyl sulfate in dilute solutions, J. Res. Natl. Bur. Stand. 49 (1952) 85–90.
[42] M.A. Motin, M.A. Hafiz Mia, A.K.M. Nasimul Islam, K.M. Salim Reza, M.A. Yousuf, Effect of sodium dodecyl sulfate on viscometric properties of methanol, ethanol, n-propanol, and iso-propanol at different temperatures, J. Bangladesh Chem. Soc. 25 (2012) 110–123.
[43] T. Ito, H. Mizutani, The Viscosity of Aqueous Sodium Dodecyl sulfate solution and the effect of inorganic electrolytes on it, J. Jpn. Oil Chem. Soc. 17 (1968) 246–248.
[44] M.V. Ionin, T.V. Sherstneva, G.N. Koleboshin, Phase equilibria in the system butanol-1-water-dioxane, Zh. Obs. Khim. 39 (1969) 23–25.
[45] J. Gregorowicz, A. Bald, A. Szejgis, A. Chmielewska, Gibbs energy of transfer and conductivity properties of NaI solutions in mixtures of water with butan-1-ol at 298.15 K, and some physicochemical properties of mixed solvent, J. Mol. Liq. 84 (2000) 149–160.
[46] C.M. Romero, E. Moreno, J.L. Rojas, Apparent molal volumes and viscosities of DL-α-alanine in water-alcohol mixtures, Thermochim. Acta 328 (1999) 33–38.
[47] C. Magallanes, A. Catenaccio, H. Mechetti, Relaxation time and viscosity of several n-alcohol/heptane systems, J. Mol. Liq. 40 (1989) 53–63.
[48] N. Gulyaeva, A. Zaslavsky, P. Lechner, A. Chait, B. Zaslavsky, pH dependence of the relative hydrophobicity and lipophilicity of amino acids and peptides measured by aqueous two-phase and octanol-buffer partitioning, J. Pept. Res. 61 (2003) 71–79.

ARTICLE IV

Comparison of the retention of basic compounds in anionic and cationic microemulsion electrokinetic chromatographic systems

Alejandro Fernández-Pumarega, Laura Olmo, Susana Amézqueta, Elisabet Fuguet, and Martí Rosés

Manuscrit en preparació

Comparison of the Retention of Basic Compounds in Anionic and Cationic Microemulsion Electrokinetic Chromatographic Systems

Alejandro Fernández-Pumarega[1], Laura Olmo[1], Susana Amézqueta[1], Elisabet Fuguet[1,2,*], Martí Rosés[1].

[1]Departament d'Enginyeria Química i Química Analítica and Institut de Biomedicina (IBUB), Facultat de Química, Universitat de Barcelona, Martí i Franquès 1-11, 08028, Barcelona, Spain. [2]Serra Húnter Programme. Generalitat de Catalunya. Spain

** Corresponding author*

Abstract

Retention of ionizable bases in microemulsion electrokinetic chromatography (MEEKC) has been studied using two different systems with anionic and cationic microemulsions. Microemulsion pseudostationary phase is composed of heptane (oil), 1-butanol (cosurfactant) and sodium dodecyl sulfate (SDS, anionic system) or tetradecyltrimethylammonium bromide (TTAB, cationic system) as surfactant.

In contrast to micellar electrokinetic chromatography (MEKC) where the retention of neutral compounds is very different in the two micellar pseudostationary phases (SDS and TTAB, respectively); in MEEKC, neutral compounds present very similar log *k* values in SDS and TTAB microemulsion pseudostationary phases.

However, the retention *k vs.* p*H* profiles of protonable bases are very different in the two MEEKC systems. In TTAB system, retention increases with p*H* because of neutralization of the protonated base and partition of the neutral form into the microemulsion. However, a reversed trend is observed in SDS system. Retention decreases with p*H* because of formation of an ionic pair between the protonated base and the anionic SDS much more retained than the neutral base.

Thus, it is demonstrated that the two systems behave very similar in the retention of neutral bases, but completely different for retention of protonated bases.

Keywords: Retention factor, Bases, Microemulsion, MEEKC, Chromatography, Ion pair interaction

Introduction

Capillary electrophoresis (CE) is a powerful separation technique able to separate compounds with different charge/size ratios. In order to separate both charged and neutral solutes new approaches of the technique, such as micellar and microemulsion electrokinetic chromatographies (MEKC and MEEKC, respectively), were developed [1–3]. In this case a pseudostationary phase (e.g. a charged micelle or microemulsion (ME) with its own mobility) is added into the buffer solution. Therefore, the elution of the compounds not only depends on their charge to size ratio, but also on their affinity to the pseudostationary phase. In contrast with MEKC where the pseudostationary phase is simply a surfactant, in MEEKC the pseudostationary phase is a ME composed of small oil droplets which are stabilized by a surfactant and a cosurfactant [4]. Due to their properties, MEs have been used in different applications in both research and industry (for example in cosmetics and pharmacy) [5]. Moreover, MEEKC systems have been used as surrogates for the estimation of lipophilicity of compounds. The octanol-water partition coefficient ($P_{o/w}$) has been estimated through the retention factor (k) of the compounds in a specific MEEKC system [6–10].

Whereas the retention processes in MEKC are well-known [2,3,11–13], retention in MEEKC has been scarcely studied and usually it is assumed to be similar to MEEKC. Thus, the same equations developed for MEKC are used [6,8]. However, it is clear that micellar and microemulsion systems have different properties. For instance, we have demonstrated that the addition of the oil and cosurfactant, needed to form the microemulsion, change significantly the viscosity of the surfactant solution, and the usual MEKC equation used to calculate the retention factor of partially ionized acids has to be corrected for this change of viscosity [14]. Also, the solvation properties of MEKC systems strongly depend on the surfactant used to form the micelle

[15–18]. However, Ishihama *et al.* [19] showed that in MEEKC, the nature of the surfactant does not affect the partition of neutral compounds between the aqueous buffer and the microemulsion, probably because the surfactants are shielded by the oil and the cosurfactant.

In a previous work [14], we studied the effect of the ionization of acids in a MEEKC system with a ME composed of heptane, 1-butanol and sodium dodecyl sulfate (SDS, an anionic surfactant), a system which showed to be a good surrogate for the determination of octanol-water partition coefficients [6–10]. However, the study of the retention of partially protonated bases was not intended because additional interactions, other than partition of the neutral form of the base into the ME, were expected. In the case of basic compounds, the retention mechanism into the SDS microemulsion can be more complex. The literature reports some studies based on micellar electrokinetic chromatography (MEKC) where an electrostatic interaction is observed when compounds and surfactant present opposite charges [11,13,20–22]. Actually, Quang *et al.* obtained higher retention factors (*k*) for the ionized bases than for the neutral compounds, meaning that apart from hydrophobicity other equilibria, such as ion pairing, must exist, enhancing retention of cationic ionized bases [13]. Moreover, the presence of other ions in the media (such as buffer components) can also interfere and influence the ion pair interaction between opposite charged test compounds and charged surfactants [22].

The purpose of this work is to study the retention of ionizable bases in two different MEEKC systems (anionic and cationic) and to compare the retention behaviour of the neutral and ionized forms of the bases in the two systems. The anionic system will be the same used previously [14] with a ME composed of heptane, 1-butanol and sodium dodecyl sulfate (SDS). The cationic systems will have the same composition, but changing SDS for tetradecyltrimethylammonium bromide (TTAB).

Theory

Calculation of retention factors in MEKC and MEEKC

In MEKC, retention factors are calculated from the well-known Eq. 1:

$$k = \frac{\mu - \mu_0}{\mu_{mc} - \mu} \quad (1)$$

where μ is the overall electrophoretic mobility of the compound in the MEKC system, μ_{mc} the electrophoretic mobility of the micellar pseudostationary phase (measured by the micellar marker) and μ_0 the electrophoretic mobility of the compound in capillary zone electrophoresis (CZE), where the electrophoretic mobility is measured using only the same aqueous buffer as for the MEKC system.

The same type of equation can be applied to MEEKC with the introduction of a correction factor that accounts for the change of viscosity between the microemulsion MEEKC system and the CZE plain buffer (Eq. 2):

$$k = \frac{\mu - \left(\frac{\mu}{\mu_0}\right)_{unretained\ solute} \cdot \mu_0}{\mu_{ME} - \mu} \quad (2)$$

Where μ_{ME} is the electrophoretic mobility of the ME (measured by the ME marker) and $\left(\frac{\mu}{\mu_0}\right)_{unretained\ solute}$ is the correction factor for the change of viscosity between the water/surfactant/cosurfactant/oil MEEKC system and the water CZE system (which cannot be reproduced with the same components than the microemulsion). The viscosity correction factor is calculated measuring the ratio of mobilities, in MEEKC (μ) and CZE (μ_0), of a compound that does not interact with the ME phase. In the case of the SDS-MEEKC system, benzoate ion

was used as compound for viscosity correction because it is a small, polar compound and easily detected [14]. The value of the correction for the studied SDS system is $\left(\frac{\mu}{\mu_0}\right)_{benzoate\ ion}$ = 0.76.

Influence of pH on mobility and retention factors

Mobility (μ) and retention (k) will change trough the measured p*H* range depending on the degree of ionization of the compound. Khaledi *et al.* [12] proposed a model to relate k of acidic compounds to p*H*. This expression can also be used to predict the behavior of basic compounds. k of a monoprotic basic compound can be defined as:

$$k = \alpha_B k_B + \alpha_{BH+} k_{BH+} \quad (3)$$

Where k_B and k_{BH+} are, respectively, the retention factor of the neutral and the fully ionized forms of the base, and α_B and α_{BH+} are, respectively, their mole fractions, which can be calculated using the apparent acidity constant (K_a') as follows:

$$\alpha_B = \frac{K_a'}{[H^+]+K_a'} \quad (4)$$

$$\alpha_{BH+} = \frac{[H^+]}{[H^+]+K_a'} \quad (5)$$

Finally, combining Eqs. 3-5 and organizing the terms Eq. 6 is obtained, which relates the retention factor of a monoprotic basic compound to p*H*.

$$k = \frac{k_{BH+}+k_B \cdot 10^{pH-pK_a'}}{1+10^{pH-pK_a'}} \quad (6)$$

The same equation can be derived for μ:

$$\mu = \frac{\mu_{BH+}+\mu_B \cdot 10^{pH-pK_a'}}{1+10^{pH-pK_a'}} \quad (7)$$

where μ_B and μ_{BH+} are the mobilities of the neutral and fully ionized species of the basic compound, respectively. Since the neutral base is uncharged, μ_B is equal to 0 and Eq. 7 can be simplified to Eq. 8.

$$\mu = \frac{\mu_{BH+}}{1+10^{pH-pK_a'}} \quad (8)$$

Experimental section

Equipment

A CE system equipped with a diode array from Agilent technologies (Santa Clara, CA, USA) was used to perform the electrophoretic measurements. The fused-silica capillary utilized was from Polymicro Technologies (Lisle, IL, USA) and presented an effective and a total length of 30 and 38.5 cm, respectively.

A p*H*-meter GLP 22 from Crison (Barcelona, Spain) was used to determine the p*H* of the solutions.

Reagents

Hydrochloric acid (1N Tritisol™), sodium hydroxide (0.5N Tritisol™), sodium dihydrogen phosphate monohydrate (≥99%), dimethyl sulfoxide (DMSO) (≥99.9%), and ammonium chloride (>99.8%) were from Merck (Darmstadt, Germany). Methanol (HPLC-grade) was obtained from Thermo Fisher Scientific (Waltham, MA, USA). Heptane (99%), dodecanophenone (98%), SDS (≥99%), TTAB (>99%), 1-butanol (≥99.7%), 2-[bis(2-hydroxyethyl)amino]-2-(hydroxymethyl)propane-1,3diol (BISTRIS) (>99%), 2-amino-2-(hydroxymethyl)propane-1,3diol (TRIS) (>99.8%), sodium phosphate dodecahydrate (>98%), and borax decahydrate (>99.5%) were from Sigma-Aldrich (St. Louis, MO, USA). Disodium hydrogen phosphate (99.5%) and sodium acetate anhydrous (99.6%) were from Baker (Center Valley, PA, US). Water was purified using a Milli-Q plus system from Millipore (Bedford, MA, US), with a resistivity of 18.2 MΩ cm.

Ephedrine, alprenolol, nadolol, oxprenolol, penbutolol, pindolol, propranolol and trimethoprim were supplied from Carlo Erba (Milan, Italy), and Sigma-Aldrich.

Analysis conditions

- *Buffer preparation*

Two sets of buffers were prepared: in the first set, acidic compounds were used to prepare the buffers in the 4.0-12.0 p*H* range maintaining, in all the cases, the ionic strength (I) constant at 0.05 M. These solutions were prepared using 0.2 M stock solutions of the buffer salts and the p*H* was adjusted using hydrochloric acid 1.0 M or sodium hydroxide 0.5 M. Anhydrous sodium acetate was used to prepare the buffers at approximately p*H* 4.0 and 5.0, the buffers at approximately p*H* 6.0, 7.0, and 8.0 were prepared using a mixture of sodium dihydrogen phosphate monohydrate and disodium hydrogen phosphate. Borax decahydrate was utilized for the preparation of the acidic buffers at approximately p*H* 9.0, and 10.0, and finally for the rest of the p*H* values (p*H* 11.0, and 12.0) a mixture of disodium hydrogen phosphate and sodium phosphate dodecahydrate was used.

In the second set, basic compounds were used to prepare buffers in the 5.0-10.5 p*H* range, also maintaining I at 0.05 M. Protonated BISTRIS adjusted with sodium hydroxide was used to prepare the buffers at approximately p*H* 5.0, 6.0 and 7.0. A solution of protonated TRIS also adjusted with sodium hydroxide was used to prepare the buffer at approximately p*H* 8.0. For the other two buffer solutions, approximately p*H* 9.0 and 10.0, an ammonium chloride solution adjusted with sodium hydroxide was used.

- *ME preparation*

Two different MEs were prepared in this study. In both cases the procedure followed was the same. First, the surfactant was dissolved in around 70 mL of the corresponding buffer solution (1.30 g of SDS, anionic ME, or 1.70 g of TTAB, cationic ME). Then, 8.15 mL of 1-butanol were added, finishing with the addition of 1.15 mL of heptane. The cosurfactant and the oil were added under continuous magnetic stirring, and if the solution remained turbid, it was sonicated until clarification [8]. Once all the components were added, buffer was added up to a total volume of 100 mL. The final concentration of each component was: 1.30 w/v of SDS or 1.70 w/v of TTAB for, respectively, the anionic and cationic ME, 8.15% v/v of 1-butanol, and 1.15% v/v of heptane.

- *Instrumental parameters*

Temperature was set at 25ºC for all the measurements. The analysis conditions varied depending on the ME used and the p*H* of work in order to obtain the appropriate electrophoretic window. For the SDS-ME system the applied voltage varied between 8.5-15 kV and the separation pressure varied in the 0-50 mbar range. In the case of the TTAB-ME system the voltage applied was negative, and it ranged between -11.5 to -14 kV, and the separation pressure was between 0 and 25 mbar. For the analysis performed in CZE the applied voltage varied between 8.5-15 kV and the separation pressure varied in the 0-50 mbar range.

To perform the MEEKC analysis the compounds were dissolved at 200 mg·L^{-1} in a 9:1 ME:methanol mixture, and in the CZE analysis, the solutes were dissolved in a 9:1 buffer:methanol mixture. The compounds were injected applying a pressure of 50 mbar during 5s, and they were detected at λ=200, 214 or 254 nm (depending on the absorbance profile of the solutes). The ME marker was dodecanophenone (at 200 mg·L^{-1}and detected at λ = 254 nm). The electroosmotic flow marker was DMSO (at a concentration of 0.2% v/v and detected at λ = 214 nm) when the ME was based on SDS, and methanol (at a concentration of 10% v/v and detected at λ = 254 nm) when the ME was based on TTAB [23].

- *Data calculation*

Electrophoretic mobility have been calculated from the migration time using the well-known Eq. 9:

$$\mu = \left[\frac{1}{t_r} - \frac{1}{t_0}\right] \cdot \left[\frac{L_T L_D}{V}\right] \quad (9)$$

where, t_r is the migration time of the analyte, t_o the migration time of the electroosmotic flow marker, L_T and L_D are the total and the effective length of the capillary, respectively, and V the voltage applied.

TableCurve 2D v5.01 from Systat Software Inc. (San Jose, CA, USA) was used to fit the *k*-p*H* profiles. Excel from Microsoft (Redmond, WA, USA) was used to perform all the data calculations. Bio-Loom database v1.7 from BioByte Corporation (Claremont, CA, USA) was utilized to obtain the log $P_{o/w}$ values of the tested compounds.

Results and discussion

Microemulsion vs. micelle selectivity for neutral solutes

In a previous study [16,17], the solute solvent-interactions and the selectivity of the two surfactants studied, among others, in MEKC was characterized. Results showed that TTAB is much more hydrogen bond acceptor, and less donator, than SDS. Consequently, the selectivity of the two systems is different. Hydrogen bond donors will be much more retained in TTAB than in SDS. Thus, the selectivity of the two systems is different and the correlation between the two retentions, presented in Eq. 10 and Figure 1A (data taken from [16,17]), is not very good.

$$\log k_{(TTAB-MEKC)} = -0.01(\pm 0.05) + 0.80(\pm 0.06) \cdot \log k_{(SDS-MEKC)} \quad (10)$$

n= 56; R^2 = 0.793; SD = 0.34; F = 207

where n is the number of data points, R^2 the determination coefficient, SD the standard deviation, and F the Fisher's F parameter. Standard deviations of the fitting parameters (slope and intercept) are in brackets.

In MEEKC, the retention in the two equivalent systems considered (indicated by SDS-MEEKC and TTAB-MEEKC subscripts) has been also compared from literature [24,25] and experimental data of a set of neutral compounds (Table 1). The results are presented in Eq. 11 and Figure 1B.

$$\log k_{(TTAB-MEEKC)} = 0.11(\pm 0.03) + 0.99(\pm 0.04) \cdot \log k_{(SDS-MEEKC)} \quad (11)$$

n= 22; R^2 = 0.973; SD = 0.11; F = 727

Correlation is much better than that of MEKC and the slope is not statistically different from 1 at 95% confidence level of Student's t-test. The intercept is not zero, but its value should depend on the amount of pseudostationary phase. Consequently, it can be concluded that the selectivity of the two systems is practically the same. These results support the theory of Ishihama *et al.* [19], that surfactants may be shielded by the oil and the cosurfactant, so the nature of the surfactant does not affect the partition of neutral compounds between the aqueous buffer and the ME.

Table 1. log *k* values determined in the SDS-MEEKC and TTAB-MEEKC systems.

Compound	log $k_{(SDS-MEEKC)}$ [a]	log $k_{(TTAB-MEKC)}$ [b]
Acetaminophen	-0.80	-0.56 [c]
Acetanilide	-0.30	-0.17
Acetophenone	-0.05	-0.03
Antipyrine	-0.59	-0.67
Butyrophenone	0.60	0.68
Caffeine	-0.89	-0.77
Carbamazepine	0.46	0.48 [c]
Corticosterone	0.59	0.65
Coumarin	-0.09	0.00 [c]
Dexamethasone	0.44	0.78 [c]
Estradiol	1.13	1.35
Naphthalene	1.13	1.21
Hydrocortisone	0.30	0.39
Hydrocortisone-21-acetate	0.47	0.65 [c]
Lormetazepam	1.03	0.90 [c]
Prednisolone	0.32	0.49 [c]
Progesterone	1.32	1.44 [c]
Propiophenone	0.26	0.35
Testosterone	0.97	1.07 [c]
Valerophenone	0.98	1.05
3-nitroaniline	-0.15	0.07
Thymol	0.96	1.20

a) Data from [24]; b) Data from [25]; c) Measured in this work.

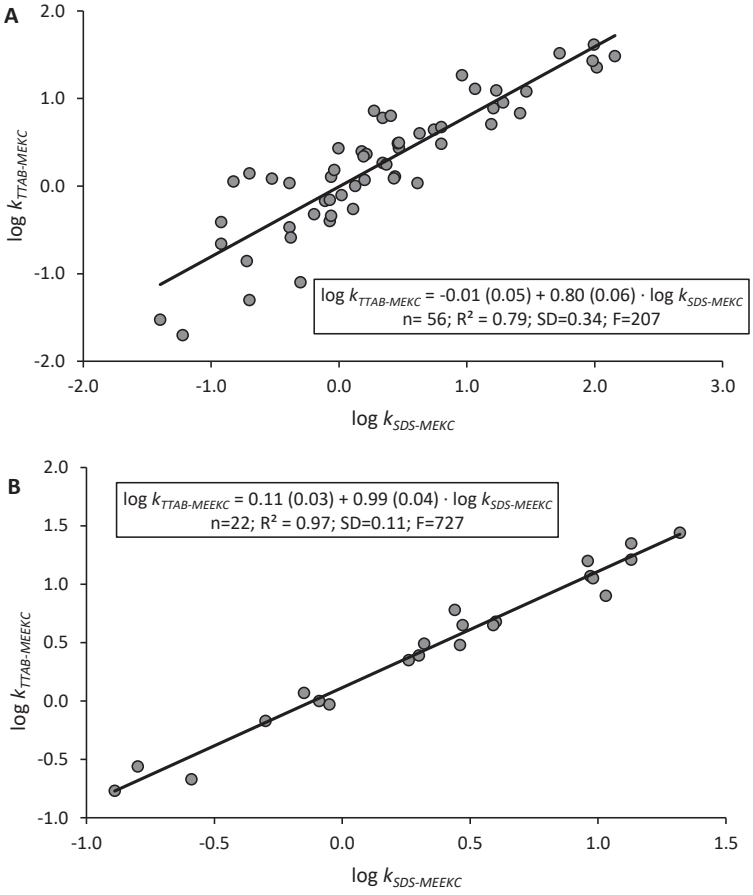

Figure 1. Correlations between log *k* of neutral compounds determined in different systems. A) Effect of surfactant change in MEKC. B) Effect of surfactant change in MEEKC.

Mobility and retention of protonated bases in MEEKC

The compounds selected for this work act as monoprotic bases in the p*H* range of work, presenting pK_a values inside the working electrophoretic p*H* range (2.0-12.0), have different lipophilicity according its log $P_{o/w}$ value, and can be detected by the UV-vis detector (absorb in the UV-vis range). The physicochemical properties (log $P_{o/w}$ and pK_a) of the eight selected bases are detailed in Table 2 [26–30]. The concentration pK_a constant (pK_a^c) of the bases, which can be calculated through Eq. 12, was determined at 25ºC through potentiometric methods.

$$K_a^c = \frac{[B]\cdot[H^+]}{[BH^+]} \quad (12)$$

In order to calculate the thermodynamic pK_a constant (pK_a) the next equation is used:

$$K_a = \frac{a_B \cdot a_{H+}}{a_{BH+}} = \frac{[B]\cdot[H^+]}{[BH^+]} \frac{\gamma_B \cdot \gamma_{H+}}{\gamma_{BH+}} \quad (13)$$

Then, substituting Eq. 12 into Eq. 13, it is obtained:

$$K_a = K_a^c \frac{\gamma_B \cdot \gamma_{H+}}{\gamma_{BH+}} \quad (14)$$

So, since γ_B is equal to 1 (as it is a neutral compound), and γ_{H+} and γ_{BH+} cancels each other, pK_a^c is the same as thermodynamic pK_a.

Table 2. Physicochemical parameters of the selected bases [26–30].

Compound	pK_a [a)]	log $P_{o/w}$ [b)]
Alprenolol	9.59	2.89
Ephedrine	9.64	0.93
Nadolol	9.69	0.71
Oxprenolol	9.57	2.10
Penbutolol	9.92	4.06
Pindolol	9.54	1.75
Propranolol	9.53	2.98
Trimethoprim	7.14	0.91

[a)] I = 0; 25ºC; [b)] In neutral form.

Calculation of the retention of the bases totally or partially protonated according to Eq. 2 requires the determination of its mobility in the microemulsion (MEEKC mode) and also in plain buffer, i.e. without microemulsion (CZE mode). Thus, the variation of the mobility of the bases with p*H* of the buffer has been studied in three different systems: MEEKC with SDS, MEEKC with TTAB, and CZE with plain buffer in water. The obtained mobilities together with the p*H* and nature of the buffers studied are presented in Table 3.

- *Mobility vs. pH profiles of bases in CZE mode*

First of all, μ_0 of the selected bases has been measured at several p*H* values in the 4.0-12.0 p*H* range in CZE, and the data obtained has been fitted to Eq. 8. The parameters and the statistics obtained from these fittings are presented in Table 4, and the μ_0 vs. p*H* obtained profiles are shown in Figure 2. Good μ_0-p*H* profiles have been obtained in all the cases and, as expected in CZE for cationic solutes, it is observed that all the bases behave in a similar way regardless of the buffer type used: mobility decreases from positive values down to zero when p*H* increases, according to the decrease in the ionization degree of the bases. Furthermore, the pK_a' obtained in these fittings (I=0.05 M) are of the same order as the ones presented in the literature determined by potentiometric methods (Table 2). Slight differences between both set of data can be seen as different conditions (such as buffer, and I) have been utilized when measuring the pK_a.

Table 3. μ, μ_0, μ_{ME} ($\cdot 10^5$, $cm^2\ s^{-1}\ V^{-1}$) of the bases determined in CZE, SDS-MEEKC, and TTAB-MEEKC systems at different p*H* values.

Compound	type of μ\p*H*	SDS-MEEKC system															TTAB-MEEKC system						
		4.1[a]	5.1[a]	5.8[a]	6.9[a]	7.9[a]	9.2[a]	10.1[a]	10.8[a]	11.7[a]	5.3[b]	6.4[b]	7.5[b]	8.4[b]	9.5[b]	10.4[b]	5.4[b]	6.3[b]	7.3[b]	8.3[b]	9.4[b]	10.2[b]	11.4[a]
Alprenolol	μ_0	17.5	17.7	17.6	16.5	16.0	12.5	4.3	1.6	0.0	17.6	18.0	17.4	16.9	12.1	3.9	17.4	17.6	16.8	16.5	12.6	4.0	0.0
	μ	-24.7	-23.8	-23.6	-25.6	-25.9	-24.4	-24.2	-25.5	-25.6	-23.1	-23.9	-25.0	-24.1	-25.1	-24.9	17.1	17.2	18.0	16.8	19.6	21.4	17.0
	μ_{ME}	-26.8	-25.8	-25.8	-27.9	-28.1	-26.6	-26.6	-27.8	-28.2	-25.2	-26.1	-27.4	-26.0	-27.5	-27.3	21.1	21.9	22.5	18.9	21.9	23.3	18.5
Ephedrine	μ_0	22.0	22.3	21.7	20.3	19.6	16.1	6.3	2.2	0.0	22.2	22.6	21.9	21.5	16.3	6.0	21.8	21.7	21.5	21.0	17.9	6.7	0.0
	μ	-12.8	-11.4	-11.9	-13.4	-14.3	-11.6	-9.8	-11.0	-9.6	-10.4	-11.7	-12.3	-12.1	-11.9	-11.1	18.2	17.9	-	17.3	15.7	11.1	7.3
	μ_{ME}	-27.1	-25.7	-26.6	-28.0	-28.7	-26.6	-26.5	-27.9	-28.1	-24.9	-25.9	-27.7	-26.0	-27.5	-26.9	21.3	21.4	-	18.8	22.2	22.7	19.5
Nadolol	μ_0	14.8	15.2	15.0	14.1	13.8	9.5	2.1	2.1	0.0	15.1	15.4	14.9	14.7	11.7	5.0	14.8	14.5	14.7	14.3	12.6	5.3	0.0
	μ	-12.6	-11.2	-11.7	-12.5	-14.1	-11.5	-12.0	-13.7	-13.5	-9.9	-10.8	-11.9	-10.7	-11.9	-12.2	12.8	12.6	12.5	11.7	12.2	11.3	9.0
	μ_{ME}	-27.0	-25.8	-26.4	-27.2	-28.8	-26.6	-26.6	-27.8	-28.1	-24.6	-25.9	-27.4	-26.1	-28.0	-27.1	21.3	22.1	21.9	18.7	22.2	22.7	19.2
Oxprenolol	μ_0	17.1	17.3	17.1	16.1	15.4	12.3	4.2	1.4	0.0	17.2	17.6	17.0	16.5	12.0	4.3	17.2	17.2	16.9	16.0	13.0	4.4	0.0
	μ	-21.7	-20.5	-21.3	-22.5	-23.3	-21.1	-20.1	-21.0	-20.8	-19.7	-20.3	-21.7	-20.6	-21.9	-21.0	15.2	15.2	15.4	14.7	16.0	16.7	14.2
	μ_{ME}	-27.0	-25.8	-26.6	-27.8	-28.8	-26.6	-26.5	-27.6	-28.0	-24.9	-25.8	-27.5	-26.0	-27.9	-27.0	21.4	21.6	21.9	18.7	22.0	22.7	19.3
Penbutolol	μ_0	15.7	15.9	15.8	14.8	14.5	12.4	4.9	1.7	0.0	15.4	16.2	15.6	15.5	12.3	4.9	15.7	15.6	15.1	12.8	11.7	4.6	0.0
	μ	-	-	-25.6	-27.0	-27.6	-25.9	-25.7	-27.0	-27.4	-	-	-26.0	-25.3	-26.7	-26.4	19.1	19.4	20.5	17.7	22.0	22.2	19.0
	μ_{ME}	-	-	-26.4	-27.8	-28.4	-26.7	-26.5	-27.6	-28.0	-	-	-26.8	-26.0	-27.5	-27.1	20.9	21.6	22.6	18.6	22.5	22.6	19.3
Pindolol	μ_0	17.8	18.2	17.8	16.8	16.4	12.9	4.5	1.7	0.0	18.1	18.5	17.7	17.4	12.7	4.6	17.6	18.1	17.6	16.9	13.7	4.8	0.0
	μ	-13.7	-13.1	-13.5	-15.3	-16.1	-14.2	-14.5	-15.7	-15.6	-12.2	-13.0	-14.2	-13.1	-14.2	-14.5	15.7	15.3	15.7	14.8	15.5	16.0	13.6
	μ_{ME}	-25.7	-25.9	-26.2	-27.9	-28.3	-26.7	-26.6	-27.7	-28.1	-24.7	-25.8	-27.6	-26.3	-27.9	-27.0	21.5	21.9	22.2	18.9	21.9	22.6	19.2
Propranolol	μ_0	17.5	17.6	17.4	16.2	15.7	11.9	3.9	1.4	0.0	17.5	17.9	17.1	16.7	11.6	3.9	16.8	17.2	16.7	15.4	11.7	3.9	0.0
	μ	-24.5	-24.4	-24.3	-26.3	-26.3	-25.0	-24.6	-26.0	-26.0	-23.7	-24.2	-25.9	-24.4	-26.2	-25.3	18.2	17.9	18.5	16.9	20.2	21.1	18.1
	μ_{ME}	-25.8	-25.9	-26.1	-27.9	-27.9	-26.7	-26.5	-27.9	-28.1	-25.5	-25.9	-27.7	-26.2	-28.1	-27.1	21.7	21.7	22.2	18.7	22.0	22.6	19.2
Trimethoprim	μ_0	17.2	17.3	15.2	7.2	1.9	0.0	0.0	0.0	0.0	17.1	15.0	5.3	1.2	0.0	0.0	17.0	16.2	9.0	1.5	0.0	0.0	0.0
	μ	-14.1	-14.3	-13.5	-14.2	-12.6	-9.7	-9.7	-10.4	-10.5	-12.8	-13.0	-12.6	-10.0	-9.6	-9.5	14.0	12.8	10.3	7.6	8.2	8.7	7.2
	μ_{ME}	-26.1	-26.3	-26.0	-28.0	-28.6	-26.7	-26.5	-28.1	-28.0	-25.5	-25.8	-27.6	-26.4	-27.5	-27.2	21.7	22.2	22.2	19.0	22.2	23.1	19.2

[a] Buffers prepared employing acidic compounds; [b] buffers prepared employing basic compounds.

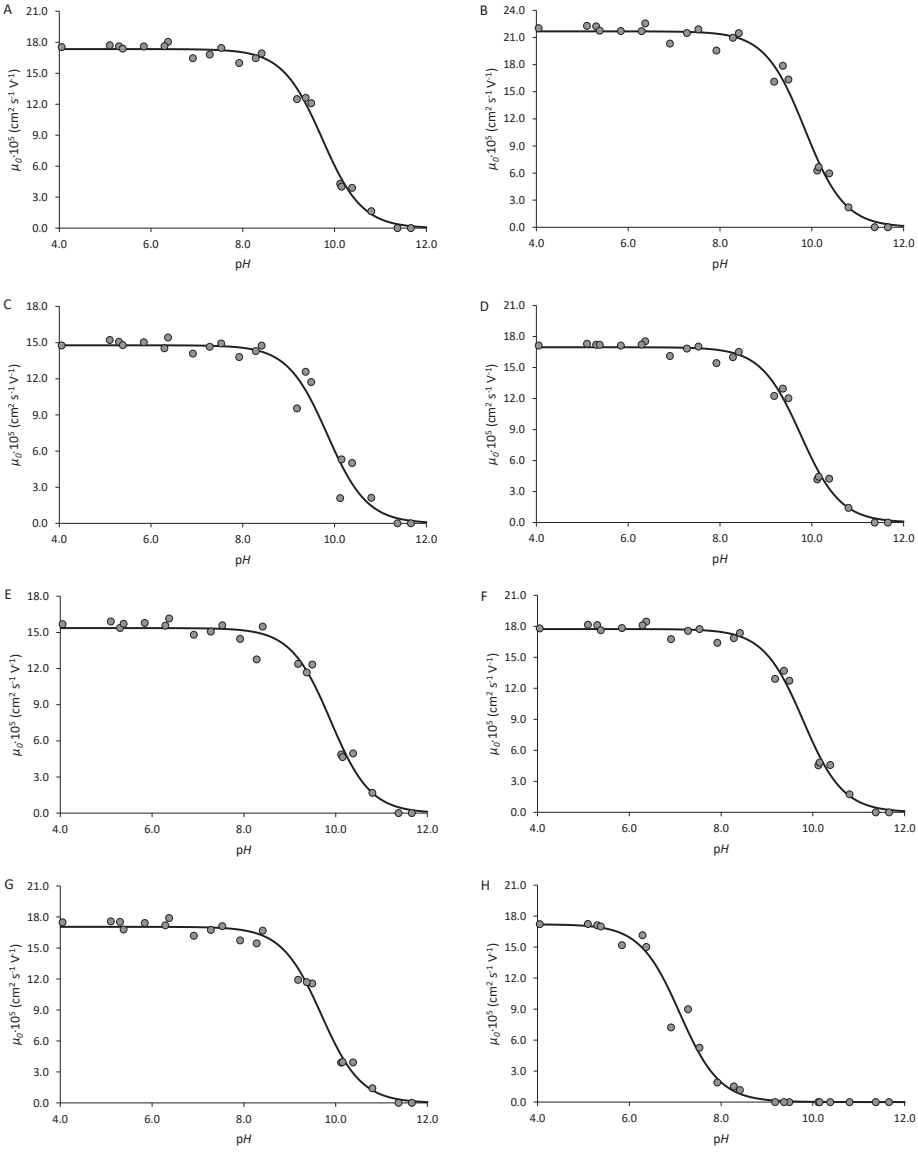

Figure 2. μ_0-p*H* profiles in CZE mode: A) alprenolol, B) ephedrine, C) nadolol, D) oxprenolol, E) penbutolol, F) pindolol, G) propranolol, and H) trimethoprim.

Table 4. Values of μ_{BH+} ($\cdot 10^5$, $cm^2\ s^{-1}\ V^{-1}$), pK_a', and statistics for the fit of Eq. 8 to electrophoretic mobilities determined in CZE (μ_0).

Compounds	pK_a' (SD)	μ_{BH+} (SD)	R^2	SD	F
Alprenolol	9.73 (0.03)	17.34 (0.18)	0.992	0.62	2385
Ephedrine	9.85 (0.04)	21.68 (0.26)	0.987	0.95	1524
Nadolol	9.84 (0.07)	14.78 (0.32)	0.960	1.15	479
Oxprenolol	9.76 (0.04)	16.97 (0.19)	0.990	0.66	1983
Penbutolol	9.89 (0.05)	15.36 (0.22)	0.981	0.80	1055
Pindolol	9.79 (0.04)	17.74 (0.19)	0.990	0.69	2005
Propranolol	9.69 (0.04)	17.05 (0.19)	0.990	0.67	1993
Trimethoprim	7.10 (0.06)	17.21 (0.43)	0.984	0.98	1196

- *Effect of buffer pH in mobility of bases in the SDS and TTAB MEEKC systems*

Next, the mobilities of the bases have been measured in the MEEKC systems with SDS and TTAB at the same p*H* values than in CZE. The measured μ values in both systems are plotted in Figure 3 against the aqueous buffer p*H*. It can be observed that the variation with p*H* is small in both cases, but the values are completely different. Mobilities in TTAB are positive, which correspond to cations as expected in protonated bases. Mobilities vary when p*H* increases from the mobility of the fully protonated base, scarcely partitioned into the microemulsion, to the mobility of the neutral base partially partitioned into the microemulsion. That is to say, the mobility can change between the mobility of the fully protonated base in CZE mode (corrected for the variation in viscosity) to the mobility of the neutral base partitioned into the TTAB microemulsion, moderated by the degree of partition of both species (protonated and unprotonated base). However, mobilities in SDS are negative, which indicates that an anionic species is formed, regardless of the nature of the buffer used (anionic or cationic), and thus the anionic species has to be an aggregate of the protonated base with the surfactant molecules. In this case, the variation observed is between the mobility of the anionic aggregate and that of the neutral base partitioned into the SDS microemulsion.

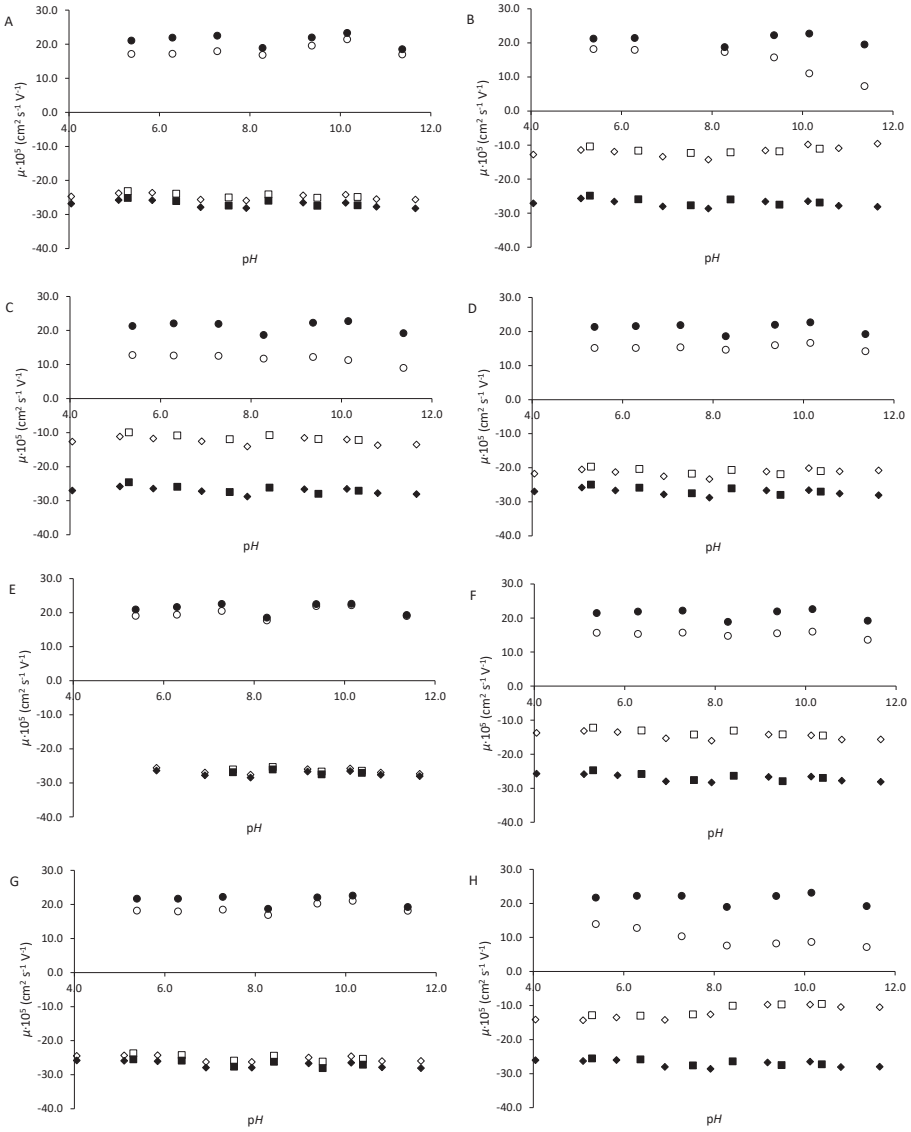

Figure 3. μ-p*H* profiles in MEEKC mode: TTAB (○), SDS with acidic buffers (◊), SDS with basic buffers (□). A) Alprenolol, B) ephedrine, C) nadolol, D) oxprenolol, E) penbutolol, F) pindolol, G) propranolol, and H) trimethoprim. The full symbols correspond to μ_{ME} determined in each of the respective conditions.

- *Effect of buffer pH in retention of bases in the SDS and TTAB MEEKC systems*

From the measured mobilities, *k* has been calculated through Eq. 2 and the results have been fitted to Eq. 6. For the analysis in the TTAB system, ephedrine ion was selected to correct the mobilities in CZE due to the different viscosity of the two media. When ephedrine is fully ionized it has a very low lipophilicity (log $P_{(BH+)}$ = -1.36; determined at p*H* = 4.5 and by the reference

shake-flask method [31]) and it is a small and polar compound. Therefore, it is not supposed to interact with the ME. With this aim, the ratio between the mobilities of ephedrine in the TTAB-MEEKC system and CZE at approximately p*H* 5.0 was calculated, which provided a mobility correction value of 0.84. In this case, benzoate ion has not been used, since it could interact electrostatically with the cationic surfactant monomers of TTAB. The parameters and statistics resulting from these fittings are shown in Tables 5-6 for the SDS and TTAB systems, respectively. In addition, these profiles are plotted in Figure 4.

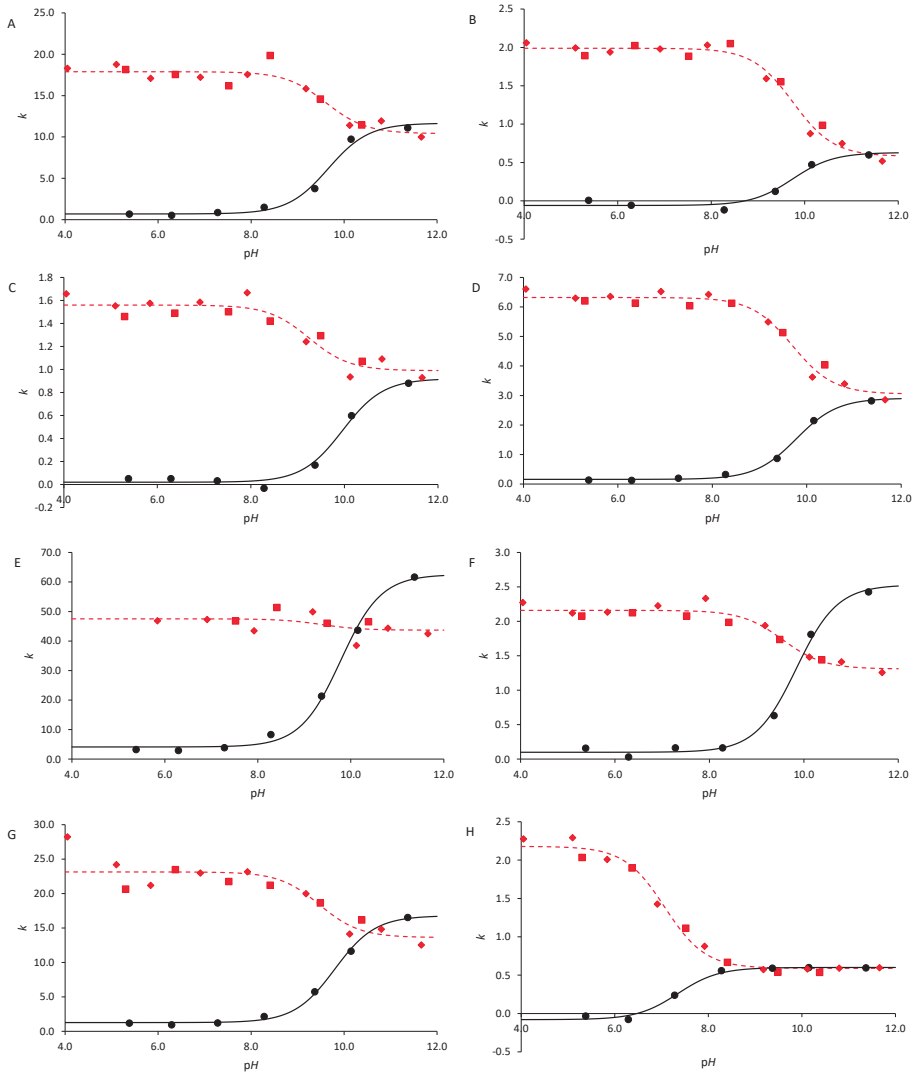

Figure 4. *k*-p*H* profiles in MEEKC. Symbols as in Figure 3. Dotted and solid lines correspond to *k*-p*H* profiles determined in the SDS-MEEKC and TTAB-MEEKC systems, respectively. A) alprenolol, B) ephedrine, C) nadolol, D) oxprenolol, E) penbutolol, F) pindolol, G) propranolol, and H) trimethoprim.

Table 5. Values of k_B, k_{BH+}, pK_a', and statistics for the fit of Eq. 6 to retention factor (k) determined at different pH values using the SDS-MEEKC system.

Compounds	pK_a' (SD)	k_{BH+} (SD)	k_B (SD)	R^2	SD	F
Alprenolol	9.61 (0.21)	17.89 (±0.35)	10.40 (±0.73)	0.906	1.03	58
Ephedrine	9.75 (0.10)	1.99 (0.03)	0.58 (0.07)	0.975	0.09	238
Nadolol	9.24 (0.23)	1.56 (0.03)	0.99 (0.05)	0.901	0.09	55
Oxprenolol	9.70 (0.11)	6.32 (0.08)	3.05 (0.17)	0.973	0.23	215
Penbutolol	9.37 (1.36)	47.53 (1.65)	43.67 (2.13)	0.269	3.36	1.47
Pindolol	9.55 (0.16)	2.16 (0.03)	1.31 (0.06)	0.947	0.09	107
Propranolol	9.47 (0.31)	23.14 (0.68)	13.63 (1.29)	0.820	1.96	27
Trimethoprim	7.07 (0.08)	2.18 (0.04)	0.59 (0.03)	0.988	0.08	490

Table 6. Values of k_B, k_{BH+}, pK_a', and statistics obtained through the fit of Eq. 6 to k determined at different pH values in a TTAB-MEEKC system.

Compounds	pK_a' (SD)	k_{BH+} (SD)	k_B (SD)	F	SD	R^2
Alprenolol	9.66 (±0.10)	0.69 (±0.29)	11.67 (±0.57)	188	0.57	0.989
Ephedrine	9.74 (0.20)	-0.06 (0.04)	0.63 (0.07)	49	0.07	0.970
Nadolol	9.96 (0.11)	0.02 (0.02)	0.92 (0.05)	156	0.05	0.987
Oxprenolol	9.78 (0.05)	0.16 (0.03)	2.91 (0.07)	841	0.07	0.998
Penbutolol	9.78 (0.06)	4.13 (0.86)	62.54 (1.76)	578	1.68	0.997
Pindolol	9.84 (0.07)	0.10 (0.04)	2.53 (0.09)	420	0.08	0.995
Propranolol	9.80 (0.05)	1.27 (0.19)	16.78 (0.39)	854	0.36	0.998
Trimethoprim	7.35 (0.11)	-0.08 (0.03)	0.60 (0.02)	218	0.04	0.991

Good fittings have been obtained for the k-pH profiles obtained using the TTAB-MEEKC system (Table 6 and solid lines in Figure 4). All eight compounds show low retention at the lowest pH values, where the solutes are in their cationic form, and k increases with pH. This fact means that the neutral species of the compounds interacts much more with the pseudostationary phase than the ionized species of the bases do. Note that k_{BH+} values are very low, almost zero for most of the compounds, and in case of showing some retention, it is in all cases less than 10% the retention of the neutral form. This tendency is the same observed when k-pH profiles of acidic compounds were measured using a ME formed by SDS, 1-butanol, and heptane [14].

However, a reversed trend is observed for the k-pH profiles determined in the SDS system (Table 5 and dotted lines in Figure 4), where high retention is observed at low pH values that decrease when pH increase. In all the profiles k_{BH+} is always higher than k_B, when we would expect the contrary if only hydrophobic partition would take place. The neutral species of the ionizable compounds (B) are more lipophilic than the ionized species (BH+) and thus, we expect them to partition better into the ME. The higher k of ionic species points out that, as it has been seen before from the μ-pH profiles, there is an electrostatically interaction between the cationic bases

and SDS monomers leading to ion aggregation, which increases retention even to a larger value than *k* of the neutral form.

Analyzing pK_a from Tables 5-6 it can be seen that generally similar values have been obtained in both approaches except for nadolol and penbutolol. Note that for penbutolol a poorly fitted *k*-p*H* profile was obtained in the SDS-MEEKC system. Furthermore, obtained pK_a' values are consistent with the ones reported in Table 2, and the slight differences observed between both set of pK_a' values can be due to the experimental conditions selected (different medium and/or ion strength).

- *Conjoint comparison of the retention of neutral and ionic species in MEEKC.*

To compare the retention of neutral and ionic species in the two systems, the log *k* determined in the SDS-MEEKC system (log $k_{(SDS\text{-}MEEKC)}$) have been correlated against log *k* values determined in the TTAB-MEEKC system (log $k_{(TTAB\text{-}MEEKC)}$) for both neutral (log k_B) and fully protonated (log k_{BH+}) forms. The equations of the resulting correlations, which are plotted in Figure 5, are:

$$\log k_{B(SDS\text{-}MEEKC)} = -0.04\ (\pm 0.05) + 0.94\ (\pm 0.05) \log k_{B(TTAB\text{-}MEEKC)} \quad (15)$$

$n = 8$; $R^2 = 0.981$; SD = 0.10; F = 309

$$\log k_{BH+(SDS\text{-}MEEKC)} = 1.28\ (\pm 0.07) + 0.69\ (\pm 0.08) \log k_{BH+(TTAB\text{-}MEEKC)} \quad (16)$$

$n = 6$; $R^2 = 0.952$; SD = 0.15; F = 79.

Eq. 15 is not significally different from Eq. 11 at a 95% confidence interval, confirming that both ME systems are equivalent for the neutral species of the bases. However, a different trend is observed when the bases are completely ionized (Eq. 16), where the charge of the surfactant modifies completely the retention behavior of ionic forms leading to totally different profiles in SDS than in TTAB. The intercept of Eq. 16 is higher than 0 as expected from the additional retention by ion aggregation in SDS. However, the slope is lower than 1 showing that the hydrophobicity of the compound has a lower effect in the aggregation than in the partition.

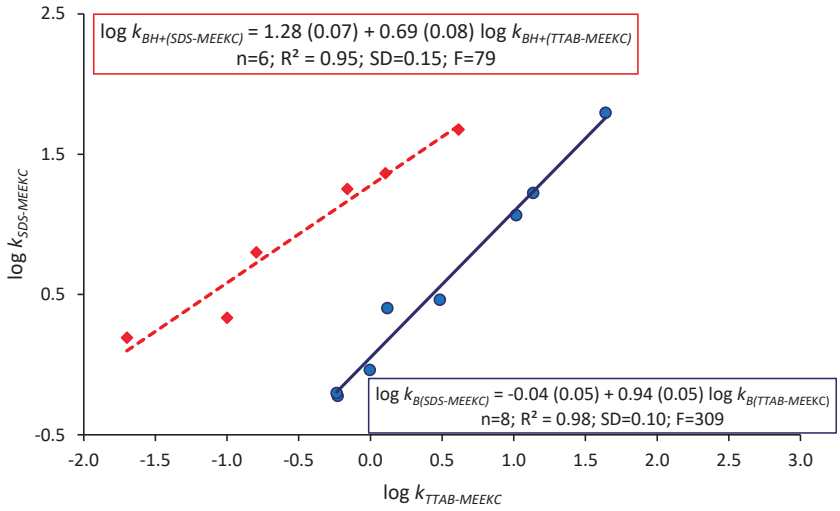

Figure 5. Comparison of the retention of neutral (●) and protonated (♦) forms of the bases in SDS and TTAB microemulsions. Eqs. 15 and 16 are represented as solid and dotted lines, respectively.

The effect of the additional retention by aggregation of cations with SDS can be also observed in Figure 6, where the retention of the ionic species has been plotted vs. the retention of the neutral forms of bases. The plot also includes retention of acids in SDS-MEEKC obtained in a previous work [14]. As expected from the similarity of both systems, retention of acids in SDS-MEEKC and bases in TTAB-MEEKC can be assembled in the same straight line, described in Eq. 17.

$$\log k_{ionized} = -1.27\ (\pm 0.12) + 1.01\ (\pm 0.11) \log k_{neutral} \quad (17)$$

n = 12; R^2 = 0.876; SD = 0.23; F = 79.

However, retention of protonated bases in SDS-MEEKC is higher because of the extra-retention by aggregation, described by a straight line (Eq. 18) with a higher intercept and a lower slope than Eq. 17.

$$\log k_{ionized} = 0.38\ (\pm 0.06) + 0.81\ (\pm 0.07) \log k_{neutral} \quad (18)$$

n = 8; R^2 = 0.953; SD = 0.13; F = 142.

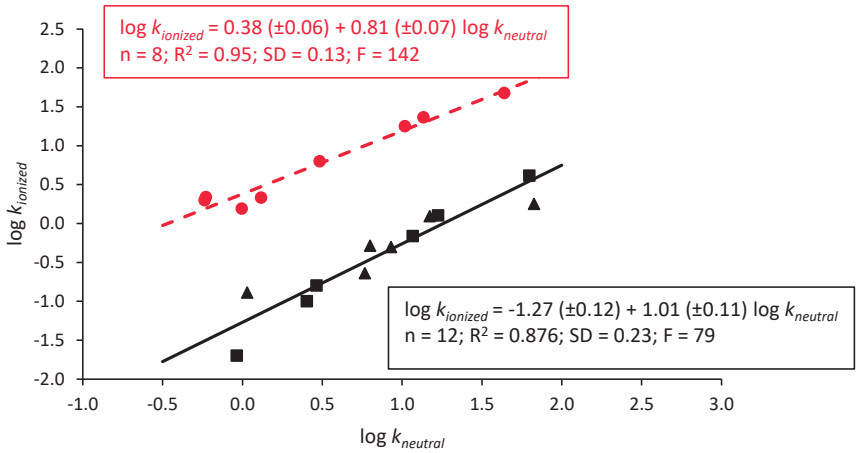

Figure 6. Comparison of the retention of ionized vs. neutral forms of ionizable acids and bases in SDS (▲ and ●, respectively) and bases in TTAB (■) microemulsions. Eqs. 17 and 18 are represented as solid and dotted lines, respectively.

Concluding remarks

In contrast with MEKC where the retention strongly depends on the surfactant used, retention of neutral compounds in two MEEKC systems with different surfactant (SDS or TTAB) and the same oil (heptane) and cosurfactant (butanol) is very similar, indicating that the surfactant used does not alter significantly the selectivity of the microemulsions.

However, higher retention for protonated bases is observed in the SDS-MEEKC system with regards to the TTAB-MEEKC system because of the aggregation between the cationic protonated base and the anionic surfactant. The use of basic or acidic compounds to prepare the buffers does not affect the mobilities obtained, indicating that aggregation is mainly caused by the SDS surfactant. This extra-retention for protonated bases is not observed in the TTAB-MEEKC system because cationic TTAB cannot form ionic aggregates with the protonated bases.

Acknowledgements

Financial support from the Ministerio de Economía y Competitividad from the Spanish Government (CTQ2017-88179-P) and the Catalan Government (2017SGR1074) is acknowledged. AFP wishes to thank the University of Barcelona for his APIF PhD fellowship.

Conflict of interest

The authors declare no competing financial interest.

References

[1] H. Watarai, Microemulsion capillary electrophoresis, Chem. Lett. 20 (1991) 391–394.

[2] S. Terabe, K. Otsuka, T. Ando, Electrokinetic chromatography with micellar solution and open-tubular capillary, Anal. Chem. 57 (1985) 834–841.

[3] S. Terabe, K. Otsuka, K. Ichikawa, A. Tsuchiya, T. Ando, Electrokinetic separations with micellar solutions and open-tubular capillaries, Anal. Chem. 56 (1984) 111–113.

[4] R. Ryan, K. Altria, E. McEvoy, S. Donegan, J. Power, A review of developments in the methodology and application of microemulsion electrokinetic chromatography, Electrophoresis. 34 (2013) 159–177.

[5] B.K. Paul, S.P. Moulik, Uses and applications of microemulsions, Curr. Sci. 80 (2001) 990-1001.

[6] M.H. Abraham, C. Treiner, M. Roses, C. Rafols, Y. Ishihama, Linear free energy relationship analysis of microemulsion electrokinetic chromatographic determination of lipophilicity, J. Chromatogr. A. 752 (1996) 243–249.

[7] S.K. Poole, D. Durham, C. Kibbey, Rapid method for estimating the octanol – water partition coefficient (log P_{ow}) by microemulsion electrokinetic chromatography, J. Chromatogr. B. 745 (2000) 117–126.

[8] X. Subirats, H.P. Yuan, V. Chaves, N. Marzal, M. Rosés, Microemulsion electrokinetic chromatography as a suitable tool for lipophilicity determination of acidic, neutral, and basic compounds, Electrophoresis. 37 (2016) 2010–2016.

[9] S.K. Poole, S. Patel, K. Dehring, H. Workman, J. Dong, Estimation of octanol-water partition coefficients for neutral and weakly acidic compounds by microemulsion electrokinetic chromatography using dynamically coated capillary columns, J. Chromatogr. B. 793 (2003) 265–274.

[10] J. Øtergaard, S.H. Hansen, C. Larsen, C. Schou, N.H.H. Heegaard, Determination of octanol-water partition coefficients for carbonate esters and other small organic molecules by microemulsion electrokinetic chromatography, Electrophoresis. 24 (2003) 1038–1046.

[11] J.K. Strasters, M.G. Khaledi, Migration behavior of cationic solutes in micellar electrokinetic capillary chromatography, Anal. Chem. 63 (1991) 2503–2508.

[12] M.G. Khaledi, S.C. Smith, J.K. Strasters, Micellar electrokinetic capillary chromatography of acidic solutes: migration behavior and optimization strategies, Anal. Chem. 63 (1991) 1820–1830.

[13] C. Quang, J.K. Strasters, M.G. Khaledi, Computer-assisted modeling, prediction, and multifactor optimization in micellar electrokinetic chromatography of ionizable compounds, Anal. Chem. 66 (1994) 1646–1653.

[14] A. Fernández-Pumarega, S. Amézqueta, E. Fuguet, M. Rosés, Determination of the retention factor of ionizable compounds in microemulsion electrokinetic chromatography, Anal. Chim. Acta. 1078 (2019) 221-230.

[15] M. Rosés, C. Ràfols, E. Bosch, A.M. Martínez, M.H. Abraham, Solute–solvent interactions in micellar electrokinetic chromatography: characterization of sodium dodecyl sulfate–Brij 35 micellar systems for quantitative structure–activity relationship modelling, J. Chromatogr. A. 845 (1999) 217–226.

[16] E. Fuguet, C. Ràfols, E. Bosch, M.H. Abraham, M. Rosés, Solute-solvent interactions in micellar electrokinetic chromatography: III. Characterization of the selectivity of micellar electrokinetic chromatography systems, J. Chromatogr. A. 942 (2002) 237–248.

[17] E. Fuguet, C. Ràfols, E. Bosch, M.H. Abraham, M. Rosés, Erratum to "solute-solvent interactions in micellar electrokinetic chromatography. III. Characterization of the selectivity of micellar electrokinetic systems", J. Chromatogr. A. 942 (2002) 237–248.

[18] M.D. Trone, M.G. Khaledi, Influence of ester and amide-containing surfactant headgroups on selectivity in micellar electrokinetic chromatography, Electrophoresis. 21 (2000) 2390–2396.

[19] Y. Ishihama, Y. Oda, N. Asakawa, Hydrophobicity of cationic solutes measured by electrokinetic chromatography with cationic microemulsions, Anal. Chem. 68 (1996) 4281–4284.

[20] T. Kaneta, S. Tanaka, M. Taga, H. Yoshida, Migration behavior of inorganic anions in micellar electrokinetic capillary chromatography using cationic surfactant, Anal. Chem. 64 (1992) 798–801.

[21] C.E. Lin, I.J. Fang, Y. Deng, W.S. Liao, H.T. Cheng, W.P. Huang, Capillary electrophoretic studies on the migration behavior of cationic solutes and the influence of interactions of cationic solutes with sodium dodecyl sulfate on the formation of micelles and critical micelle concentration, J. Chromatogr. A. 1051 (2004) 85–94.

[22] I. Orentaité, A. Maruska, U. Pyell, Regulation of the retention factor for weak acids in micellar electrokinetic chromatography with cationic surfactant via variation of the chloride concentration, Electrophoresis. 32 (2011) 604–613.

[23] E. Fuguet, C. Ràfols, E. Bosch, M. Rosés, Solute-solvent interactions in micellar electrokinetic chromatography: IV. Characterization of electroosmotic flow and micellar markers, Electrophoresis. 23 (2002) 56–66.

[24] A. Fernández-Pumarega, S. Amézqueta, E. Fuguet, M. Rosés, Estimation of the octanol-water distribution coefficient of acidic compounds by microemulsion electrokinetic chromatography, J. Pharmaceut. Biomed. 179 (2020).

[25] A. Fernández-Pumarega, B. Martín-Sanz, S. Amézqueta, E. Fuguet, M. Rosés, Estimation of the octanol-water distribution coefficient of basic compounds by a cationic microemulsion electrokinetic chromatography system, ADME & DMPK. (2020). Manuscript submitted.

[26] Bio−Loom, BioByte Corp. (Claremont, CA, USA), http://www.biobyte.com Version 1.7.

[27] A. Avdeef, Absorption and drug development: solubility, permeability, and charge state, Second edi, John Wiley & Sons, Inc., Hoboken, NJ, USA, 2012.

[28] G. Caron, G. Steyaert, A. Pagliara, F. Reymond, P. Crivori, P. Gaillard, P.A. Carrupt, A. Avdeef, J. Comer, K.J. Box, H.H. Girault, B. Testa, Structure-lipophilicity relationships of neutral and protonated b-blockers, part I, intra- and intermolecular effects in isotropic solvent systems, Helv. Chim. Acta. 82 (1999) 1211-1222.

[29] K. Takács-Novák, K.J. Box, A. Avdeef, Potentiometric p*K(a)* determination of water-insoluble compounds: validation study in methanol/water mixtures, Int. J. Pharm. 151 (1997) 235–248.

[30] A. Avdeef, C.M. Berger, p*H*-metric solubility. 3. Dissolution titration template method for solubility determination, Eur. J. Pharm. Sci. 14 (2001) 281–291.

[31] N. Gulyaeva, A. Zaslavsky, P. Lechner, M. Chlenov, A. Chait, B. Zaslavsky, Relative hydrophobicity and lipophilicity of beta-blockers and related compounds as measured by aqueous two-phase partitioning, octanol–buffer partitioning, and HPLC, Eur. J. Pharm. Sci. 17 (2002) 81–93.

ARTICLE V

Estimation of the Octanol–Water Distribution Coefficient of Acidic Compounds by Microemulsion Electrokinetic Chromatography

Alejandro Fernández-Pumarega, Susana Amézqueta, Elisabet Fuguet, and Martí Rosés

Journal of Pharmaceutical and Biomedical Analysis (2020), volum: 179

DOI: 10.1016/j.jpba.2019.112981

Journal of Pharmaceutical and Biomedical Analysis 179 (2020) 112981

Contents lists available at ScienceDirect

Journal of Pharmaceutical and Biomedical Analysis

journal homepage: www.elsevier.com/locate/jpba

Estimation of the octanol–water distribution coefficient of acidic compounds by microemulsion electrokinetic chromatography

Alejandro Fernández-Pumarega [a], Susana Amézqueta [a,*], Elisabet Fuguet [a,b], Martí Rosés [a]

[a] Departament d'Enginyeria Química i Química Analítica and Institut de Biomedicina (IBUB), Facultat de Química, Universitat de Barcelona, Martí i Franquès 1-11, 08028, Barcelona, Spain
[b] Serra Húnter Programme. Generalitat de Catalunya, Spain

ARTICLE INFO

Article history:
Received 20 September 2019
Received in revised form 4 November 2019
Accepted 9 November 2019
Available online 11 November 2019

Keywords:
Octanol-water distribution coefficient
EKC
MEEKC
Lipophilicity
Ionizable compounds

ABSTRACT

The feasibility of extending the determination of the lipophilicity of partially ionized acids (log $D_{o/w}$) by microemulsion electrokinetic chromatography (MEEKC) is tested. Theoretical considerations predict that a linear log $D_{o/w}$ vs. log k correlation can be obtained only when the neutral and ionic forms of an acid follow the same correlation equation and the slope of the correlation is unity. In practice, since the lipophilicity of the neutral acid is much higher than that of the ionic form and the correlation slope is not very different from 1, the general linear correlation for neutral compounds can be applied across most of the ionization range of the acid.

The linear correlation between log $P_{o/w}$ and log k of 20 neutral solutes (calibration curve) has been established and extended to 6 acids used as models, tested across their full ionization range. log $D_{o/w}$-pH, and log k-pH profiles have been obtained for these 6 acids, and plotted log $D_{o/w}$ against log k for any acid at any degree of ionization. Furthermore, the log $D_{o/w}$ of the acids has been estimated from the calibration curve and log k-pH profile, and compared to values in the literature determined using reference methods such as the shake-flask one. Accurate values have been obtained using the MEEKC method when the acids are in their neutral form or partially ionized (ionization degree, $\alpha < 0.995$). However, this parameter is overestimated when the acids are highly or fully ionized ($\alpha \approx 1$). Finally, in order to test the applicability of this method, we have applied the same procedure to estimate log $D_{o/w}$ at pH = 7.4 (blood physiological pH) of a set of 30 additional compounds (including partially and fully ionized acids). The results at this pH follow the same trend observed in the 6 model acids, and validate the application of the method for $D_{o/w}$ determination, except when α is very close to 1.

1. Introduction

The drug development process is a lengthy procedure that is expected to conclude with the release of a new drug onto the market. The process begins with thousands of drug candidates whose physicochemical properties are tested and evaluated, to select the most promising for preclinical and clinical testing [1]. One of the most important properties evaluated in the drug discovery process is the capacity of a compound, once in the bloodstream, to penetrate biological membranes, constituted mainly of lipid bilayers. This biological property is clearly related to lipophilicity, which can be described as the easiness of a compound to be dissolved in fats or non-polar solvents [2].

To evaluate the lipophilicity of a substance, the most widely accepted parameter is the octanol–water partition coefficient ($P_{o/w}$). The octanol–water system is widely used because of the similarity of 1-octanol to lipids (it contains a polar head and a hydrophobic chain), and its low water saturation [3].

The octanol–water partition coefficient (for neutral and fully ionized compounds) can be directly determined through the shake-flask procedure [4]. This method measures the ratio of the concentrations of the test solute in the two immiscible phases at equilibrium, according to Eq. 1, where $C_{n\text{-octanol}}$ is the concentration of the compound in the organic phase, and C_{water} is that in the aqueous phase:

$$P_{o/w} = \frac{C_{n-octanol}}{C_{water}} \quad (1)$$

* Corresponding author at: Departament d'Enginyeria Química i Química Analítica and Institut de Biomedicina (IBUB), Facultat de Química, Universitat de Barcelona, c/ Martí i Franquès 1-11, 08028, Barcelona, Spain.
E-mail address: samezqueta@ub.edu (S. Amézqueta).

https://doi.org/10.1016/j.jpba.2019.112981
0731-7085/

For partially ionized compounds, this parameter is called the octanol–water distribution coefficient ($D_{o/w}$). In this case, the coefficient is determined using the same analytical procedure but at a buffered p*H*.

Although the shake-flask method provides a direct way to determine the log $P_{o/w}$ value, it is a tedious and time-consuming procedure. Furthermore, it is not automated. These drawbacks have led to the development of alternative methods. The most popular for acid–base compounds is the potentiometric dual phase p*H*-metric titration technique [5]. Here, the partition coefficient is calculated by considering the differences between the pK_a values obtained for two titrations performed in the presence and absence of octanol [6,7].

In the case of chromatography, the lipophilicity of a compound is correlated with the retention factor (k) in a chromatographic system [8]. Ishihama et al. [9] developed a method capable of estimating the lipophilicity of a compound that uses microemulsion electrokinetic chromatography (MEEKC). Compared to the reference shake-flask method, MEEKC is fast and simple. It is also automated and does not require large amounts or a high purity of the compounds, as it is a separation technique. These characteristics make it an ideal tool for routine analysis in the drug discovery process.

In the MEEKC technique, based on capillary electrophoresis (CE), a microemulsion (ME)-based pseudostationary phase (a charged ME with its own electrophoretic mobility) is added to the buffer solution filling the capillary. Then the compounds migrate, depending on the electrophoretic conditions and also on their partition between the ME and the aqueous phase. The ME is composed of oil droplets (the core) which are stabilized by a surfactant and a cosurfactant, whose polar heads are in contact with the aqueous phase and whose apolar tails are orientated towards the inner part of the ME [10]. The ME employed by Ishihama and coworkers [9] contained heptane as the oil (0.82 %, w/w), sodium dodecyl sulfate (SDS) as the surfactant (1.44 %, w/w), and 1-butanol as the cosurfactant (6.49 %, w/w).

Further studies [11–15] have confirmed the correlation between the logarithm of the octanol–water partition coefficient (log $P_{o/w}$) of neutral compounds and the logarithm of the retention factor in MEEKC systems (log k). Abraham et al. [11] correlated log $P_{o/w}$ to log k measured in the same ME as Ishihama et al., obtaining the following equation:

$$\log P_{o/w} = 1.542 + 1.276 \log k$$
$$R^2 = 0.99;\ SD = 0.096;\ n = 53 \quad (2)$$

where R^2 is the determination coefficient, SD the standard deviation, and n the number of compounds.

Subirats et al. [12] performed the same procedure but with an ME formed of 1.30 % (w/v) SDS, 8.15 % (v/v) 1-butanol, 1.15 % (v/v) heptane, and 5 % (v/v) acetonitrile (at p*H* 7.4, in a 10 mM phosphate buffer). Acetonitrile was added to avoid co-elution of the micellar marker with highly hydrophobic compounds. The resulting correlation was:

$$\log P_{o/w} = 1.48(\pm 0.05) + 1.48(\pm 0.05) \log k$$
$$R^2 = 0.96;\ n = 32 \quad (3)$$

Analyzing Eq. 2 and Eq. 3, we can state that the MEEKC method is capable of emulating the octanol–water partition system and of estimating log $P_{o/w}$ of neutral solutes through chromatographic determinations. Nevertheless, the majority of drugs released onto the market are acids or bases, which are partly or fully ionized depending on their pK_a and the medium p*H*. Some works have already estimated the log $P_{o/w}$ of acidic and basic solutes through MEEKC at a p*H* where they are not ionized [12,14]. But there are no studies regarding the estimation of log $D_{o/w}$ of totally or partially ionized compounds. Therefore, the aim of this work is to broaden the applicability of the MEEKC method to estimate, in addition to log $P_{o/w}$, the log $D_{o/w}$ value of partially and totally ionized species of acidic compounds.

Preliminary studies with a single model compound indicated that the MEEKC method might be capable of estimating log $D_{o/w}$ of partially ionized acid–base compounds under certain conditions [16].

For the present study, we selected 6 model monoprotic acids with a wide range of log $P_{o/w}$ values, and we studied the relationship between their retention factor and lipophilicity when the acids are partially or totally ionized. Then, to validate our results, the log $P_{o/w}$ and log $D_{o/w}$ values of a set of 30 solutes (including neutral solutes, and partially and totally ionized acids) at a p*H* equal to 7.4 (blood physiological p*H*) were estimated using the proposed method. Finally, we compared the estimated log $D_{o/w}$ values (in the case of partially ionized acids) and log $P_{o/w}$ values (for the neutral and fully ionized species) with values reported in the literature determined using classical methods (mainly shake-flask and potentiometric methods).

2. Theory

2.1. Estimation of log $P_{O/W}$ from MEEKC retention factors. Feasibility of the extension to partially ionized compounds

Previous work [11,12] has shown a linear relationship between log $P_{o/w}$ and log k for neutral compounds (Eqs. 2 and 3), which for a neutral acid, HA, can be generalized as:

$$\log P_{o/w(HA)} = q_{(HA)} + p_{(HA)} \log k_{(HA)} \quad (4)$$

where log $P_{o/w(HA)}$ and log $k_{(HA)}$ are the logarithms of the octanol–water partition coefficient and the retention factor of fully protonated acids, respectively; and $q_{(HA)}$ and $p_{(HA)}$ are the intercept and the slope of Eq. 4, respectively.

Extension of this equation to ionic or ionizable compounds is not straightforward. To the best of our knowledge, a similar (linear) relationship has not yet been established for ionic compounds. Even if such a linear relation exists, it will probably not have the same parameters as for neutral compounds, and we should write it as:

$$\log P_{o/w(A^-)} = q_{(A^-)} + p_{(A^-)} \log k_{(A^-)} \quad (5)$$

where log $P_{o/w(A^-)}$ and log $k_{(A^-)}$ are the logarithms of the octanol–water partition coefficient and the retention factor of the fully ionized acid, respectively; and $q_{(A^-)}$ and $p_{(A^-)}$ are the intercept and the slope of Eq. 5, respectively.

For partially ionized compounds, the relationship is even more complex.

Both, the retention factor and the octanol–water distribution coefficient of the compound can be computed from the degree of ionization of the compound (which can be easily calculated from the p*H* of the medium and the pK_a' of the solute, the apparent acidity constant), and the k or $P_{o/w}$ value of the pure species, according to Eqs. 6 and 7:

$$k = (1 - \alpha) k_{(HA)} + \alpha k_{(A^-)} \quad (6)$$

$$D_{o/w} = (1 - \alpha) P_{o/w(HA)} + \alpha P_{o/w(A^-)} \quad (7)$$

where:

$$\alpha = \frac{10^{pH - pK_a'}}{1 + 10^{pH - pK_a'}} \quad (8)$$

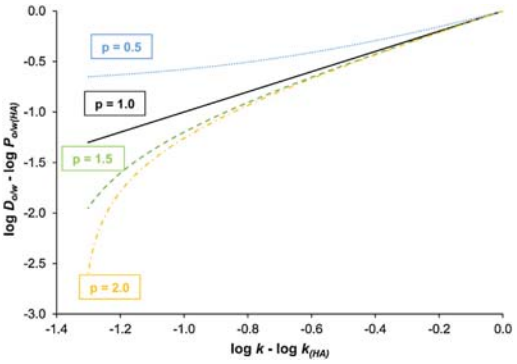

Fig. 1. Variation of the lipophilicity (log $D_{o/w}$ – log $P_{o/w(HA)}$) with the retention factor (log k – log $k_{(HA)}$) at different degrees of ionization for a hypothetical compound with a $k_{(HA)}/k_{(A^-)}$ ratio of 20, and different representative p values: 0.5 (···); 1.0 (—); 1.5 (—); and 2.0 (· – ·).

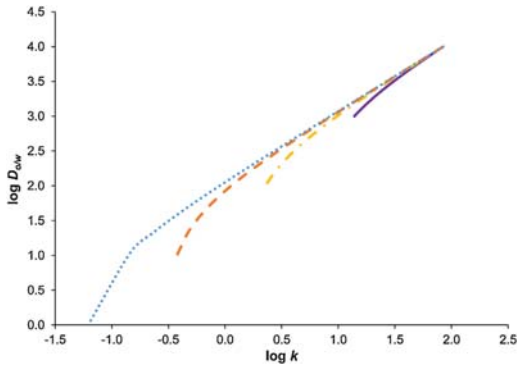

Fig. 2. Plots of log $D_{o/w}$ against log k for compounds with a $P_{o/w(HA)}$ of 4 and $P_{o/w(A^-)}$ of: 3, (—); 2 (· – ·); 1 (—); and 0 (···). We calculated the log k values using Eq. 2.

which lead to the well-known equations for the k vs. pH and $D_{o/w}$ vs. pH profiles:

$$k = \frac{k_{(HA)} + k_{(A^-)} \cdot 10^{pH-pK'_a}}{1 + 10^{pH-pK'_a}} \quad (9)$$

$$D_{o/w} = \frac{P_{o/w(HA)} + P_{o/w(A^-)} \cdot 10^{pH-pK'_a}}{1 + 10^{pH-pK'_a}} \quad (10)$$

or in their logarithmic forms:

$$\log k = \log\left(\frac{10^{\log k_{(HA)}} + 10^{\log k_{(A^-)}} \cdot 10^{pH-pK'_a}}{1 + 10^{pH-pK'_a}}\right) \quad (11)$$

$$\log D_{o/w} = \log\left(\frac{10^{\log P_{o/w(HA)}} + 10^{\log P_{o/w(A^-)}} \cdot 10^{pH-pK'_a}}{1 + 10^{pH-pK'_a}}\right) \quad (12)$$

Combining Eqs. 4, 5, and 7, we obtain the general relationship between $D_{o/w}$ and k (Eq. 13).

$$D_{o/w} = (1-\alpha)\, 10^{q_{(HA)}} k_{(HA)}^{p_{(HA)}} + \alpha\, 10^{q_{(A^-)}} k_{(A^-)}^{p_{(A^-)}} \quad (13)$$

It is evident that a linear relationship of the type:

$$\log D_{o/w} = q + p \log k \quad (14)$$

can be obtained only when $q_{(HA)} = q_{(A\text{-})} = q$, and $p_{(HA)} = p_{(A\text{-})} = p = 1$. That is to say, we would expect a linear correlation between log $D_{o/w}$ and log k for acids at any pH only when the correlation for ionic and neutral compounds are the same, but also only when the slope of the correlation is close to one. Fig. 1 shows an example of the variation of the lipophilicity (log $D_{o/w}$ – log $P_{o/w(HA)}$), Eq. 15, with the variation of the retention factor (log k – log $k_{(HA)}$), Eq. 16, at different degrees of ionization for a compound with a $k_{(HA)}/k_{(A\text{-})}$ ratio of 20. The effect of several representative p values (0.5, 1.0, 1.5, and 2.0) is shown. The plots presented are easily derived from Eqs. 4, 6 and 13, assuming $q_{(HA)} = q_{(A\text{-})}$, $p_{(HA)} = p_{(A\text{-})} = p$, and providing values of α.

$$\log D_{o/w} - \log P_{o/w(HA)} = \log\left[(1-\alpha) + \alpha\left(\frac{k_{(A^-)}}{k_{(HA)}}\right)^p\right] \quad (15)$$

$$\log k - \log k_{(HA)} = \log\left[(1-\alpha) + \alpha\left(\frac{k_{(A^-)}}{k_{(HA)}}\right)\right] \quad (16)$$

The same tendency is observed for other $k_{(HA)}/k_{(A\text{-})}$ ratios (data not shown). The relationship is completely linear only for $p = 1$, but it is close to linearity across a wide range of p values (mainly between 0.5 and 1.5, see for example Eqs. 2 and 3). The plot deviates from linearity for low values of log k (or log $D_{o/w}$), i.e., when the solute is highly ionized and the slope of the correlation is not equal to 1.

The deviation from linearity is produced when the contribution of the ionized form of the acid to log $D_{o/w}$ is significant. Since log $P_{o/w(A\text{-})}$ is much lower than log $P_{o/w(HA)}$ [17], the relationship between log $D_{o/w}$ and log k is close to that given by Eq. 4 for most of the ionization range. Fig. 2 represents the effect of the lipophilicity of the ionized form (log $P_{o/w(A\text{-})}$) on the linearity of the plot for a typical acid with log $P_{o/w(HA)} = 4$. If log $P_{o/w(A\text{-})} = 3$, linearity is lost when $\alpha > 0.67$; but as log $P_{o/w(A\text{-})}$ decreases, the α value increases, being approximately 0.86, 0.96, and 0.998 for log $P_{o/w(A\text{-})}$ values of 2, 1, and 0, respectively. The actual difference between log $P_{o/w(HA)}$ and log $P_{o/w(A\text{-})}$ can be between 1.5 and 4.5 log units, depending on the structure of the compound and measurement conditions, with a mean of about 3.15 [17]. Thus, we expect log $D_{o/w}$ vs. log k to be linear for a wide range of degrees of ionization. The extent of this range is tested in the experimental part of the present work.

3. Experimental section

3.1. Equipment

To perform the electrophoretic measurements, a CE 7100 system equipped with a diode array from Agilent Technologies (Santa Clara, CA, USA) was used. Fused-silica capillaries from Polymicro Technologies (Phoenix, AZ, USA), with an effective and total length of 30 cm and 38.5 cm, respectively, were used.

A GLP 22 pH meter from Crison (Barcelona, Spain) was used to measure the pH of the buffer solutions; and an ultrasonic bath from JP Selecta (Abrera, Spain) to favor the dissolution of some substances.

3.2. Reagents

Sodium dihydrogen phosphate monohydrate (≥99 %), dimethyl sulfoxide (≥99.9 %), hydrochloric acid (Tritisol™ 1 N), ammonium chloride (>99.8 %), and sodium hydroxide (Tritisol™ 0.5 N) were from Merck (Darmstadt, Germany). Methanol (HPLC grade) was from Thermo Fisher Scientific (Waltham, MA, USA). Sodium dodecyl sulfate (SDS, ≥99 %), 1-butanol (≥99.7 %), heptane (99 %), sodium phosphate dodecahydrate (>98 %), and dodecanophenone (98 %) were from Sigma-Aldrich (St. Louis, MO, USA). Disodium hydrogen phosphate (99.5 %) was from Baker (Phillipsburg, NJ, USA).

The solutes tested were of high purities and were acquired from Sigma-Aldrich, Baker, Merck, Carlo Erba (Milan, Italy), Fluka (St. Louis, MO, USA), Acros Organics (Geel, Belgium), and Riedel-de Haën (Seelze, Germany).

Water was purified using a Milli-Q plus system from Millipore (Burlington, MA, USA).

3.3. Buffer solutions

The buffer with a p*H* equal to 7.4 was prepared by mixing 0.2 M sodium dihydrogen phosphate and 0.2 M disodium hydrogen phosphate solutions. The p*H* 11.5 buffer was prepared by mixing 0.2 M disodium hydrogen phosphate and 0.2 M sodium phosphate dodecahydrate solutions. The buffer with a p*H* of 9.5 was prepared by adding 0.5 M sodium hydroxide to a 0.05 M ammonium chloride solution. The ionic strength of all the buffers was 0.05 M.

3.4. ME preparation

MEs were prepared following the procedure described elsewhere in the literature [18]. The concentrations of each component with respect the total volume of the ME were: 1.30 % (w/v) SDS, 8.15 % (v/v) 1-butanol, and 1.15 % (v/v) heptane.

3.5. Analysis conditions

We measured mobility by applying 13−14 kV. Detection was performed at λ = 200, 214, or 254 nm, depending on the chromophores of each compound. Injection was hydrodynamic, and a pressure of 50 mbar was applied for 5 s.

The compounds analyzed were dissolved in an ME:methanol solution (9:1) for MEEKC analysis, and in a water:methanol solution (9:1) for capillary zone electrophoresis (CZE) measurements, at a concentration of 200 mg L^{-1}. Dodecanophenone (200 mg L^{-1}) and dimethyl sulfoxide (0.2 % v/v) were added to the test compound vials as ME and electroosmotic flow markers, respectively [19].

3.6. Calculation methods

The physicochemical properties of the compounds were obtained from the Bio-Loom database of the BioByte Corporation (Claremont, CA, USA). Retention profiles were fitted with Table Curve 2D from Systat Software Inc. (San Jose, CA, USA). Data calculations were performed using Excel from Microsoft (Redmond, WA, USA).

Mobilities (μ_i) were calculated using the following expression:

$$\mu_i = [\frac{1}{t_r} - \frac{1}{t_0}][\frac{L_T L_D}{V}] \quad (17)$$

where t_r and t_o are, respectively, the migration times of the analyte and the electroosmotic flow marker; L_T and L_D are the total and the effective capillary length; and V is the applied voltage.

Retention factors of neutral compounds were calculated from the mobilities of the compound (μ) and ME marker (μ_{ME}) by the well-known Eq. 18:

$$k = \frac{\mu}{\mu_{ME} - \mu} \quad (18)$$

Application of Eq. 4 to totally or partially ionized compounds requires subtraction of the mobility of the compound in CZE, i.e., in the buffer without an ME (μ_0), according to Eq. 19:

$$k = \frac{\mu - \mu_0}{\mu_{ME} - \mu} \quad (19)$$

It is not feasible to reproduce the MEEKC system without a ME and so μ_0 is usually measured in an aqueous solution with the same p*H* buffer. However, the MEEKC medium contains not only the aqueous buffer but also the surfactant, the co-surfactant and the oil, which usually have viscosities very different from water. Thus, the presence of ME components changes the viscosity of the medium, leading to inaccurate k values, as demonstrated in previous work [18]. Note that the viscosity of the electrophoretic medium (η) and the mobility of a compound are inversely related, according to Eq. 20 [20]:

$$\mu = \frac{q}{6\pi\eta r} \quad (20)$$

where q is the charge of the ion, and r its radius.

We have proposed a viscosity correction obtained from the mobility of an ion that does not interact with the ME (the benzoate ion). The ratio of the mobilities of the benzoate ion in the ME and plain buffer ($(\frac{\mu}{\mu_0})_{benzoate\ ion}$) is equivalent to the ratio of viscosities, and the mobility of any other ion in a plain buffer can be corrected for the viscosity changes without the need to measure the viscosities. We then determined the correct retention factor from the following equation:

$$k = \frac{\mu - (\frac{\mu}{\mu_0})_{benzoate\ \ ion} \cdot \mu_0}{\mu_{ME} - \mu} \quad (21)$$

where $(\frac{\mu}{\mu_0})_{benzoate\ ion}$ has a value of 0.76, and was measured at p*H* 11.0, when benzoic acid is fully ionized.

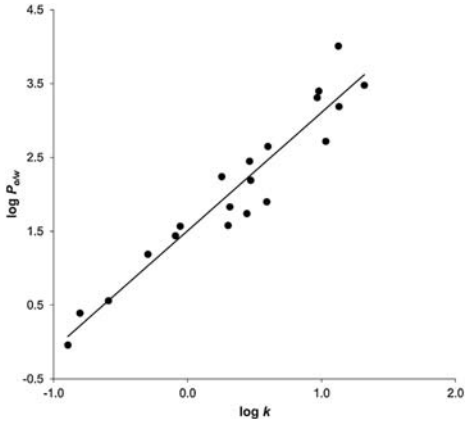

Fig. 3. Plot of log $P_{o/w}$ versus log k for the set of 20 neutral compounds selected for the calibration curve.

4. Results and discussion

4.1. log $P_{o/w}$ vs. log k correlation for neutral compounds

We established the correlation between log $P_{o/w}$ and log k of 20 neutral compounds, that present known and uniformly distributed log $P_{o/w}$ values [21–26] for the MEEKC system studied and the equation resulting from this correlation is:

$$\log P_{o/w} = 1.51(\pm 0.08) + 1.60(\pm 0.11)\log k \quad (22)$$

$$R^2 = 0.916;\ SD = 0.33;\ n = 20;\ F = 196$$

where F is Fisher's F parameter.

A graphical representation of this correlation can be seen in Fig. 3; while the solutes, and their log $P_{o/w}$ and log k values are

Table 1
Values of log $P_{o/w}$ and log k of the 20 solutes used for the calibration curve.

Compound	log $P_{o/w}$ [a)]	log k
Acetaminophen	0.39	−0.80
Acetanilide	1.19	−0.30
Acetophenone	1.57	−0.05
Antipyrine	0.56	−0.59
Butyrophenone	2.65	0.60
Caffeine	−0.04	−0.89
Carbamazepine	2.45	0.46
Corticosterone	1.90	0.59
Coumarin	1.44	−0.09
Dexamethasone	1.74	0.44
Estradiol	4.01	1.13
Naphthalene	3.19	1.13
Hydrocortisone	1.58	0.30
Hydrocortisone-21-acetate	2.19	0.47
Lormetazepam	2.72	1.03
Prednisolone	1.83	0.32
Progesterone	3.48	1.32
Propiophenone	2.24	0.26
Testosterone	3.31	0.97
Valerophenone	3.40	0.98

a) From references [21–26].

shown in Table 1. We obtained a good correlation, similar to that obtained for other SDS-MEEKC systems (Eqs. 2 and 3).

4.2. Influence of the degree of ionization on the estimation of log $D_{o/w}$

The compounds chosen to perform this study were benzoic acid, 3-bromobenzoic acid, naproxen, ketoprofen, ibuprofen, and 2,4,6-trichlorophenol. We selected them because they have known and well-defined lipophilicity-p*H* profiles (data provided in the supplementary information). Moreover, they have pK_a values in the working p*H* range, and are detectable by UV–vis.

Experimental *k*-p*H* profiles of the compounds were taken from a previous study [18] and the log *k*-p*H* profiles were obtained by fitting the data to Eq. 11. Values of log $k_{(HA)}$, log $k_{(A-)}$, and pK_a', as well as the statistics from the fits, are presented in Table 2. In addition, Fig. 4 offers a graphical representation of the profiles.

A similar procedure was followed when fitting log $D_{o/w}$ values determined at different p*H*s from the literature (data provided in the supplementary information) to Eq. 12. Note that data from the literature are obtained in different experimental conditions (nature of the buffers, concentration of the buffers, ionic strength, temperature, etc.) so some discrepancies can be observed, especially at low p*H* values, where ion-pairs between ionized acids and buffer components can be formed. Experimental conditions of literature data are also provided in Table SI-1 of the supplementary information. In the fits of the log $D_{o/w}$-p*H* profiles, pK_a' was fixed using the values obtained previously in the log *k*-p*H* profiles (Table 2). The estimated log $D_{o/w}$ vs. p*H* profiles are shown in Fig. 5, while the parameters and statistics resulting from these are in Table 3. The log $D_{o/w}$-p*H* fits have small SD, and high R^2 and F values for all the compounds studied.

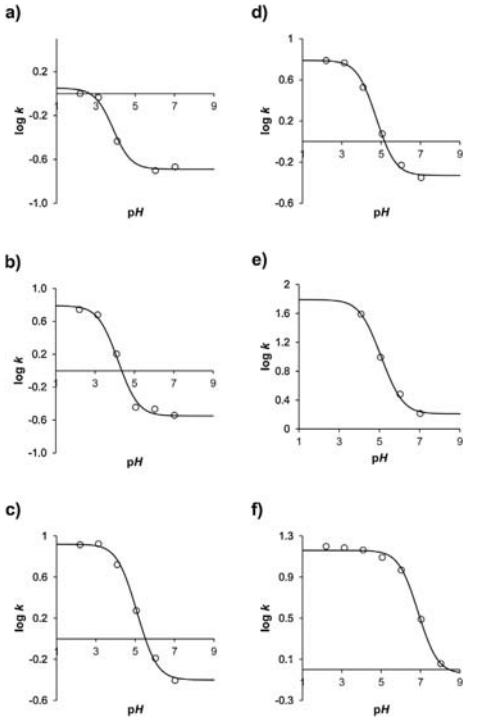

Fig. 4. log k – p*H* profiles obtained by fitting the data from [18] to Eq. 11: a) benzoic acid, b) 3-bromobenzoic acid, c) naproxen, d) ketoprofen, e) ibuprofen, f) 2,4,6-trichlorophenol.

Table 3
Parameters and statistics obtained from fitting log $D_{o/w}$ vs. p*H* through Eq. 12 (data taken from the literature). The standard deviation of each fitted parameter is shown in brackets. Experimental conditions of literature data are provided in Table SI-1 of the supplementary information.

Compound	log $P_{o/w(HA)}$	log $P_{o/w(A-)}$	R^2	F	SD
Benzoic acid	2.01 (0.07)	−1.37 (0.09)	0.992	880	0.15
3-Bromobenzoic acid	2.91 (0.04)	−0.44 (0.05)	0.999	2696	0.06
Naproxen	3.15 (0.05)	0.05 (0.10)	0.985	1056	0.16
Ketoprofen	3.10 (0.04)	−1.95 (4.47)	0.994	1604	0.10
Ibuprofen	4.16 (0.10)	0.10 (0.31)	0.894	161	0.41
2,4,6-Trichlorophenol	3.67 (0.08)	1.03 (0.16)	0.950	246	0.27

In Fig. 6, the log $P_{o/w}$ values of the neutral and fully ionized species of the 6 model acids are plotted against the corresponding log k values. It can clearly be seen that all the neutral species lie within the confidence interval of the calibration curve (Eq. 22). However, this is not the case for the fully ionized species, hence their estimation using this equation is not accurate.

Table 2
Parameters and statistics obtained from fitting log k vs. p*H* through Eq. 11 [18]. The standard deviation of each fitted parameter is shown in brackets.

Compound	pK_a'	log $k_{(A-)}$	log $k_{(HA)}$	R^2	F	SD
Benzoic acid	3.50 (0.15)	−0.69 (0.03)	0.05 (0.04)	0.991	116	0.04
3-Bromobenzoic acid	3.50 (0.14)	−0.55 (0.05)	0.79 (0.06)	0.992	188	0.07
Naproxen	4.43 (0.07)	−0.40 (0.04)	0.92 (0.03)	0.997	532	0.04
Ketoprofen	4.19 (0.07)	−0.33 (0.03)	0.79 (0.02)	0.997	589	0.03
Ibuprofen	4.30 (0.19)	0.21 (0.06)	1.79 (0.12)	0.997	151	0.06
2,4,6-Trichlorophenol	6.28 (0.07)	−0.04 (0.05)	1.16 (0.02)	0.996	510	0.03

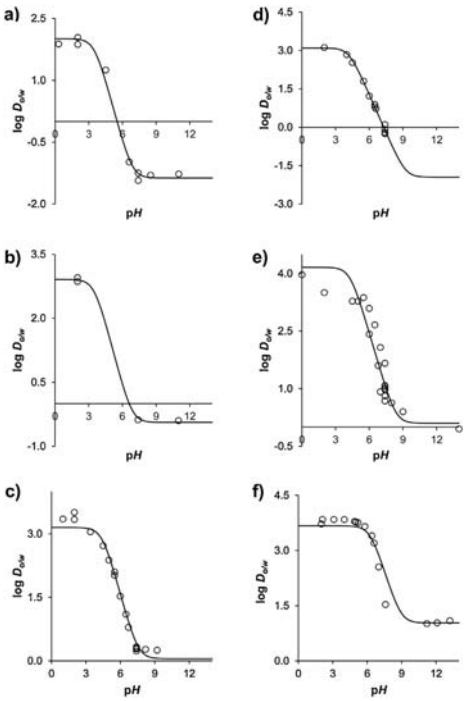

Fig. 5. log $D_{o/w}$ – p*H* profiles obtained by fitting the data from the literature to Eq. 12: a) benzoic acid, b) 3-bromobenzoic acid, c) naproxen, d) ketoprofen, e) ibuprofen, f) 2,4,6-trichlorophenol.

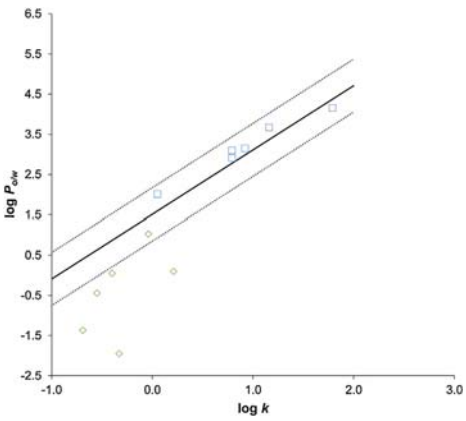

Fig. 6. Plot of log $P_{o/w}$ against log *k* for the neutral (□) and fully ionized (◊) species of the 6 model acids; calibration curve (Eq. 22) and ±2 SD (dotted lines) are also plotted.

Next, log $D_{o/w}$ and log *k* for all the acids have been determined at each degree of ionization through the log *k*-p*H* and log $D_{o/w}$-p*H* profiles (data from Tables 2 and 3). For a given degree of ionization, log $D_{o/w}$ is graphically represented against log *k* (Fig. 7a). The same figure also represents the neutral calibration curve obtained in the previous section, and two extra lines corresponding to the calibration curve ±2 SD (which corresponds to the 95 % confidence interval). Almost the entire set of log $D_{o/w}$ - log *k* values fall within this range, except for the lowest values that correspond to the highly or fully ionized species of the acids. Then we estimated log $D_{o/w}$ from the calibration curve and log *k* at each degree of ionization of the acid (log $D_{est.}$). The differences between the log $D_{o/w}$ values in the literature (log D_{lit}, Table 3) and the log D_{est} was calculated and plotted as a function of the ionization degree (Fig. 7b).

Table 4
The log $D_{o/w(7.4)}$ values estimated using the present method (log D_{est}) and in the literature (log D_{lit}) for compounds at different degrees of ionization.

Compound	Ionization degree (α)	log $D_{est.}$	log $D_{lit.}$ [a)]	log $D_{lit.}$-log D_{est}
3-nitroaniline	0	1.27	1.39	0.12
Aminopyrine	0	0.86	0.63	−0.23
Benzocaine	0	1.84	1.89	0.05
Bromazepam	0	2.13	1.65	−0.48
Diazepam	0	3.27	2.62 ± 0.28	−0.65
Griseofulvin	0	2.83	2.28 ± 0.13	−0.55
Hexanophenone	0	3.67	3.69	0.02
Isoniazid	0	−0.61	−0.75 ± 0.14	−0.14
Methoxsalen	0	2.02	1.97	−0.05
Thymol	0	3.04	3.34	0.30
Bumetanide	1	1.26	0.10 ± 0.30	−1.16
Diclofenac	1	1.86	1.17 ± 0.07	−0.69
Diflunisal	1	1.75	0.76	−0.99
Fenbufen	1	1.84	0.61 ± 0.03	−1.23
Flurbiprofen	1	1.70	0.89 ± 0.03	−0.81
Gemfibrozil	1	2.16	1.20	−0.96
Glyburide	1	2.21	2.19 ± 0.00	−0.02
Indomethacin	1	2.07	0.98 ± 0.13	−1.09
Mefenamic acid	1	2.20	2.03 ± 0.04	−0.17
Pentachlorophenol	1	2.59	1.83	−0.76
3-Nitrophenol	0.13	1.44	1.52	0.08
4-Nitrophenol	0.61	0.86	1.38	0.52
Butylparaben	0.20	3.23	3.32	0.09
Ethylparaben	0.13	2.03	2.44	0.41
Methylparaben	0.13	1.46	1.98	0.52
Omeprazole	0.10	1.98	2.30 ± 0.11	0.32
Phenobarbital	0.54	0.61	1.12 ± 0.03	0.51
Propylparaben	0.14	2.64	3.01	0.37
sulfamethazine	0.42	−0.56	−0.43	0.13
Theophylline	0.10	−0.33	−0.04 ± 0.01	0.29

a) References are provided in the supplementary information.

Our results show that accurate estimates are obtained if the acid is either in its neutral form or partially ionized. In both cases, the precision of the results is similar to that reported previously for neutral compounds (Section 4.1, SD = 0.33). However, the present method overestimates the $D_{o/w}$ of the highly or fully ionized species of the acids ($\alpha \geq 0.995$). It must be noted that log $P_{o/w(A-)}$ varies depending on the capacity of the ionized compound to form ion pairs with the ions of the buffer [17,27]. Thus, literature log $P_{o/w(A-)}$ data may differ if the buffer and the conditions used in their measurements are different (such as different concentrations of buffers or nature of counter-ions, among other possibilities). Nonetheless, in all the cases our method overestimated its value. Another reason for the observed differences could be the lower retention of ionized species in MEEKC compared to that of neutral ones, which causes higher experimental error in μ measurement. Also, the larger surface between the aqueous and the lipid phase in MEEKC, compared to the classical octanol–water partition system, may lead to a higher partition into the ME than in the octanol–water system.

4.3. Estimation of lipophilicity at physiological pH (log $D_{o/w(7.4)}$)

To validate our method, we estimated the log $D_{o/w}$ value at the blood physiological p*H* (log $D_{o/w(7.4)}$) for ten neutral compounds, ten partially ionized acids, and ten totally ionized acids. Their log

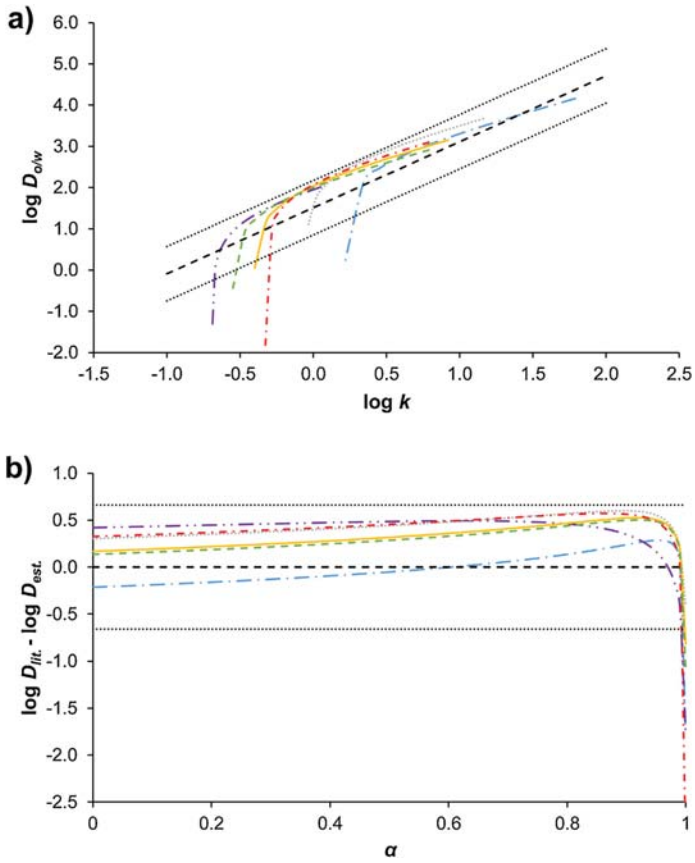

Fig. 7. a) Variation of log $D_{o/w}$ vs. log k at different degrees of ionization. Data for log $D_{o/w}$ and log k are taken from the profiles in Figs. 4 and 5, b) Difference between log $D_{o/w}$ in the literature (log D_{lit}) and the value of log $D_{o/w}$ estimated using our present method (log D_{est}) at different degrees of ionization. The calibration curve ±2 SD (Eq. 22) is also plotted. Each line corresponds to one of the six model acids: benzoic acid (—··); 3-bromobenzoic acid (—); naproxen (—); ketoprofen (· – ·); ibuprofen (·—·); and 2,4,6-trichlorophenol (···).

$D_{o/w(7.4)}$ values were estimated directly from their log k values using the calibration curve (Eq. 22). In the case of partially ionized acids, α was also measured via:

$$\alpha = \frac{\mu_{7.4}}{\mu_{(A^-)}} \tag{23}$$

where, $\mu_{7.4}$ is the electrophoretic mobility of the compound in CZE at a pH value of 7.4, and $\mu_{(A^-)}$ is the electrophoretic mobility of the fully ionized compound in CZE. The $\mu_{(A^-)}$ value of these compounds was determined at a pH where the fully ionized form was present (pH = 11.5, except for phenobarbital, for which it was measured at pH = 9.5, as it has other acid–base groups that can be ionized at pH = 11.5).

Table 4 shows the log $D_{o/w(7.4)}$ values of the 30 additional substances for which it was estimated using the present method, and their comparison with values reported in the literature determined using classical methods (mostly the shake-flask procedure) (data provided in the supplementary information). The log D_{lit} values were measured under different experimental conditions and usually at room temperature. Due to their variability, reported values that differ considerably from the rest of the published data were excluded, and they were not used to obtain the average value. In the case of pentachlorophenol, log $D_{o/w(7.4)}$ is not available. However, the compound is fully ionized at this pH value, so the log D_{lit} value is determined as an average of the log $D_{o/w}$ values determined at pH values higher than 7.4. As previously for the 6 model acid, log $D_{o/w(7.4)}$ vs. log k is represented for all the compounds together with the calibration curve (Eq. 22). Furthermore, we calculated log D_{lit} – log D_{est} and plotted it against the degree of ionization (Fig. 8). The values obtained via the MEEKC measurements are similar to those in the literature when the compounds are neutral or partially ionized (presenting differences of less than two times the SD from the calibration curve). However, when the compound is highly or fully ionized ($\alpha \approx 1$) larger differences are obtained between the estimated data and those reported in the literature.

5. Concluding remarks

We obtained a linear relationship between log $P_{o/w}$ and log k for neutral compounds that is not very different from those reported

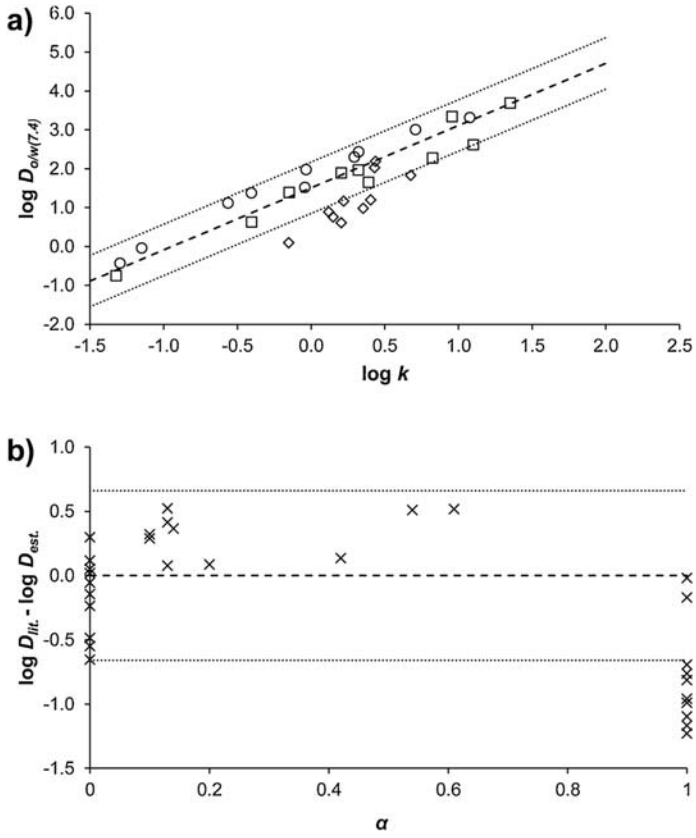

Fig. 8. a) Plot of log $D_{o/w(7.4)}$ against log k for a set of compounds including neutral (□), and both partially (○) and completely (◊) ionized acids. b) Difference between the log $D_{o/w(7.4)}$ in the literature (log D_{lit}) and the value of log $D_{o/w(7.4)}$ estimated using our present method (log D_{est}), according to the degree of ionization. The calibration curve ±2 SD (Eq. 22) is also plotted.

in literature for similar systems. Although theory predicts that accurate log $D_{o/w}$ estimation of partially ionized acids can only be performed when the slope of the calibration curve is equal to 1.0, in practice the linear correlation can be extended to most of the ionization range of the acids tested. Therefore, it is possible to estimate $D_{o/w}$ of partially ionized acids with only the determination of k at the pH value of interest. With the MEEKC method the log $D_{o/w}$ value of an acid can be estimated with an error equivalent to that of neutral compounds for a degree of ionization up to 0.995, which corresponds to a pH of pK_a+2. However, our method overestimates the lipophilicity of highly or fully ionized acids ($\alpha \approx 1$).

Declaration of Competing Interest

The authors declare no conflicts of interest.

Acknowledgements

Financial support from the Spanish *Ministerio de Economía y Competitividad* (CTQ2017-88179-P) and the Catalan Government (2017SGR1074) is acknowledged. AFP wishes to thank the University of Barcelona for his APIF PhD fellowship.

Appendix A. Supplementary data

Supplementary material related to this article can be found, in the online version, at doi:https://doi.org/10.1016/j.jpba.2019.112981.

References

[1] FDA, Learn About Drug and Device Approvals, 2018 (Accessed 25 October 2019) https://www.fda.gov/ForPatients/Approvals/default.htm.
[2] A. McNaught, A. Wilkinson, Compendium of Chemical Terminology, second ed., Blackwell science, Oxford, 1997.
[3] C. Giaginis, A. Tsantili-Kakoulidou, Alternative measures of lipophilicity: from octanol-water partitioning to IAM retention, J. Pharm. Sci. 97 (2008) 2984–3004, http://dx.doi.org/10.1002/jps.21244.
[4] OECD, Test No. 107: Partition Coefficient (n-octanol/water): Shake Flask Method, 1995 (Accessed 25 October 2019) http://www.oecd-ilibrary.org/environment/test-no-107-partition-coefficient-n-octanol-water-shake-flask-method_9789264069626-en.
[5] OECD, Partition Coefficient (n-octanol/water), pH-metric Method for Ionisable Substances, 2000 (Accessed 25 October 2019) http://www.oecd.org/chemicalsafety/testing/2731134.pdf.
[6] A. Avdeef, pH-metric log P. Part 1. Difference plots for determining ion-pair octanol-water partition coefficients of multiprotic substances, Quant, Struct. Relationships 11 (1992) 510–517, http://dx.doi.org/10.1002/qsar.2660110408.
[7] U. Franke, A. Munk, M. Wiese, Ionization constants and distribution coefficients of phenothiazines and calcium channel antagonists determined

by a pH-metric method and correlation with calculated partition coefficients, J. Pharm. Sci. 88 (1999) 89–95, http://dx.doi.org/10.1021/js980206m.
[8] OECD, Test No. 117: Partition Coefficient (n-octanol/water), HPLC Method, 2004 (Accessed 25 October 2019) http://www.oecd-ilibrary.org/environment/test-no-117-partition-coefficient-n-octanol-water-hplc-method_9789264069824-en.
[9] Y. Ishihama, Y. Oda, K. Uchikawa, N. Asakawa, Evaluation of solute hydrophobicity by microemulsion electrokinetic chromatography, Anal. Chem. 67 (1995) 1588–1595, http://dx.doi.org/10.1021/ac00105a018.
[10] R. Ryan, K. Altria, E. McEvoy, S. Donegan, J. Power, A review of developments in the methodology and application of microemulsion electrokinetic chromatography, Electrophoresis 34 (2013) 159–177, http://dx.doi.org/10.1002/elps.201200375.
[11] M.H. Abraham, C. Treiner, M. Roses, C. Rafols, Y. Ishihama, Linear free energy relationship analysis of microemulsion electrokinetic chromatographic determination of lipophilicity, J. Chromatogr. A 752 (1996) 243–249, http://dx.doi.org/10.1016/S0021-9673(96)00518-3.
[12] X. Subirats, H.P. Yuan, V. Chaves, N. Marzal, M. Rosés, Microemulsion electrokinetic chromatography as a suitable tool for lipophilicity determination of acidic, neutral, and basic compounds, Electrophoresis 37 (2016) 2010–2016, http://dx.doi.org/10.1002/elps.201600080.
[13] S.K. Poole, D. Durham, C. Kibbey, Rapid method for estimating the octanol – water partition coefficient (log P_{ow}) by microemulsion electrokinetic, Chromatography 745 (2000) 117–126.
[14] S.K. Poole, S. Patel, K. Dehring, H. Workman, J. Dong, Estimation of octanol-water partition coefficients for neutral and weakly acidic compounds by microemulsion electrokinetic chromatography using dynamically coated capillary columns, J. Chromatogr. B 793 (2003) 265–274, http://dx.doi.org/10.1016/S1570-0232(03)00321-0.
[15] J. Øtergaard, S.H. Hansen, C. Larsen, C. Schou, N.H.H. Heegaard, Determination of octanol-water partition coefficients for carbonate esters and other small organic molecules by microemulsion electrokinetic chromatography, Electrophoresis 24 (2003) 1038–1046, http://dx.doi.org/10.1002/elps.200390120.
[16] A. Fernández-Pumarega, S. Amézqueta, E. Fuguet, M. Rosés, Feasibility of the estimation of octanol-water distribution coefficients of acidic drugs by microemulsion electrokinetic chromatography, ADMET DMPK 6 (2018) 55–60, http://dx.doi.org/10.5599/admet.6.1.510.
[17] S.F. Donovan, M.C. Pescatore, Method for measuring the logarithm of the octanol-water partition coefficient by using short octadecyl-poly(vinyl alcohol) high-performance liquid chromatography columns, J. Chromatogr. A 952 (2002) 47–61, http://dx.doi.org/10.1016/S0021-9673(02)00064-X.
[18] A. Fernández-Pumarega, S. Amézqueta, E. Fuguet, M. Rosés, Determination of the retention factor of ionizable compounds in microemulsion electrokinetic chromatography, Anal. Chim. Acta 1078 (2019) 221–230, http://dx.doi.org/10.1016/j.aca.2019.06.007.
[19] E. Fuguet, C. Ràfols, E. Bosch, M. Rosés, Solute-solvent interactions in micellar electrokinetic chromatography: IV. Characterization of electroosmotic flow and micellar markers, Electrophoresis. 23 (2002) 56–66, http://dx.doi.org/10.1002/1522-2683(200201)23:1<56::AID-ELPS56>3.0.CO;2-7.
[20] D.R. Baker, Capillary Electrophoresis, Wiley, New York, 1995.
[21] A. Andrés, M. Rosés, C. Ràfols, E. Bosch, S. Espinosa, V. Segarra, J.M. Huerta, Setup and validation of shake-flask procedures for the determination of partition coefficients (log D) from low drug amounts, Eur. J. Pharm. Sci. 76 (2015) 181–191, http://dx.doi.org/10.1016/j.ejps.2015.05.008.
[22] S. Winiwarter, N.M. Bonham, F. Ax, A. Hallberg, H. Lennernäs, A. Karlén, Correlation of human jejunal permeability (in vivo) of drugs with experimentally and theoretically derived parameters. A multivariate data analysis approach, J. Med. Chem. 41 (1998) 4939–4949, http://dx.doi.org/10.1021/jm9810102.
[23] M. Kansy, H. Fischer, K. Kratzat, F. Senner, B. Wagner, I. Parrilla, High-throughput artificial membrane permeability studies in early drug discovery and development, in: B. Testa, H. Van de Waterbeemd, G. Folkers, R. Guy (Eds.), Pharmacokinetic Optimization in Drug Research: Biological, Physicochemical, and Computational Strategies, Verlag Helvetica Chimica Acta, Zürich, 2001, pp. 447–464.
[24] G. Camenisch, G. Folkers, H. Van De Waterbeemd, Comparison of passive drug transport through Caco-2 cells and artificial membranes, Int. J. Pharm. 147 (1997) 61–70, http://dx.doi.org/10.1016/S0378-5173(96)04796-5.
[25] F. Lombardo, M.Y. Shalaeva, K.A. Tupper, F. Gao, M.H. Abraham, ElogP(oct): a tool for lipophilicity determination in drug discovery, J. Med. Chem. 43 (2000) 2922–2928, http://dx.doi.org/10.1021/jm0000822.
[26] C. Zhu, L. Jiang, T.M. Chen, K.K. Hwang, A comparative study of artificial membrane permeability assay for high throughput profiling of drug absorption potential, Eur. J. Med. Chem. 37 (2002) 399–407, http://dx.doi.org/10.1016/S0223-5234(02)01360-0.
[27] C.S. Chen, S.T. Lin, Prediction of pH effect on the octanol-water partition coefficient of ionizable pharmaceuticals, Ind. Eng. Chem. Res. 55 (2016) 9284–9294, http://dx.doi.org/10.1021/acs.iecr.6b02040.

SUPPLEMENTARY INFORMATION

Estimation of the octanol–water distribution coefficient of acidic compounds by microemulsion electrokinetic chromatography

Alejandro Fernández-Pumarega[1], Susana Amézqueta[1,*], Elisabet Fuguet[1,2], Martí Rosés[1]

[1]Departament d'Enginyeria Química i Química Analítica and Institut de Biomedicina (IBUB), Facultat de Química, Universitat de Barcelona, Martí i Franquès 1-11, 08028, Barcelona, Spain

[2]Serra Húnter Programme. Generalitat de Catalunya. Spain

* Corresponding author: Susana Amézqueta Pérez

E-mail: samezqueta@ub.edu

Departament d'Enginyeria Química i Química Analítica and Institut de Biomedicina (IBUB), Facultat de Química, Universitat de Barcelona

c/ Martí i Franquès 1-11, 08028, Barcelona, Spain

Phone: (+34) 934021277

Fax: (+34) 934021233

Table SI-1. log $D_{o/w}$ compilation of the model acids determined at different p*H* values.

Compound	p*H*	log $D_{o/w}$	Experimental conditions	References
3-Bromobenzoic acid	2	2.95	0.15 M NaCl in 0.01 M universal buffer	[1,2]
	7.4	-0.38	"	
	11	-0.40	"	
	2	2.86	50 mM KCl-HCl at 25ºC	
2,4,6-trichlorophenol	2.1	3.84	0.1 M ionic strength, 0.1 M $NaClO_3$ aqueous solution	[3,4]
	3.1	3.84	"	
	4	3.84	"	
	4.9	3.79	"	
	5	3.77	"	
	5.2	3.76	"	
	5.8	3.65	"	
	6.4	3.40	"	
	6.6	3.20	"	
	7	2.55	"	
	7.6	1.53	"	
	11.2	1.01	"	
	12.1	1.03	"	
	13.2	1.09	"	
	2	3.72	0.01 M HCl at 20ºC	
Benzoic acid	2	1.87	0.15 M NaCl in 0.01 M universal buffer	[1,2,5,6]
	4.5	1.25	"	
	6.6	-0.98	"	
	7.4	-1.25	"	
	8.5	-1.30	"	
	11	-1.27	"	
	7.4	-1.43	0.1 N NaOH and HCl used as titrants	
	0.3	1.88	0.5 N HCl at 25ºC	
	2	2.04	50 mM KCl-HCl at 25ºC	
Ketoprofen	7.4	-0.09	0.02 M phosphate buffer at 20ºC	[7–13]
	7.4	0.1	0.15 M KCl solution	
	6.5	0.8	"	
	5.5	1.8	"	
	6	1.223	buffer of 100 mM D-mannitol, 100 mM KCl and 20 mM Mes/tris	
	2	3.12	buffer solutions at room temperature	
	4.5	2.53	"	
	7.4	-0.25	"	
	4	2.84	Buffer solutions at 37ºC	
	6.5	0.89	"	
	6.6	0.72	phosphate buffer	
	7.4	-0.20	phosphate buffer (0.16 M) at room temperature	

Compound	p*H*	log $D_{o/w}$	Experimental conditions	References
Naproxen	7.4	0.23	aqueous buffer 50 mM phosphate	[8,9,14–18]
	7.4	0.3	0.15 M KCl solution	
	6.5	1.1	"	
	5.5	2.1	"	
	1	3.35	phosphate or acetate buffer, 0.1 M NaCl adjuster at 20 ºC	
	2	3.34	"	
	3.4	3.05	"	
	4.5	2.72	"	
	5.5	2.02	"	
	6.7	0.79	"	
	7.4	0.33	"	
	8.2	0.27	"	
	9.2	0.25	"	
	7.4	0.28	phosphate buffer at 37ºC	
	2	3.51	0.05 M phosphate buffer or 0.01 M HCl at 20-22ºC	
	6	1.526	buffer of 100 mM D-mannitol, 100 mM KCl and 20 mM Mes/tris	
	7.4	0.30	phosphate buffer at room temperature	
	5	2.38	"	
Ibuprofen	5.5	3.37	25ºC	[7,10,26,14, 19–25]
	6	3.09	"	
	6.5	2.66	"	
	7	2.07	"	
	7.4	1.66	"	
	5	3.28	phosphate buffers at 25 ºC	
	6	2.42	"	
	7	0.92	"	
	8	0.63	"	
	2	3.50	buffer solutions at room temperature	
	4.5	3.28	"	
	7.4	1.07	"	
	9	0.40	0.01 N HCl or borate buffer	
	7.4	0.68	aqueous buffer 50 mM phosphate	
	7.4	0.81	0.15 M NaCl in 0.01 M universal buffer	
	7.4	1.02	0.01 M sodium phosphate buffer at 25ºC	
	7.4	0.98	0.02 M phosphate buffer at 20ºC	
	6.8	1.60	0.5 M HCl and 0.5 M KOH (used as titrants), (fixed ionic strength 0.1-0.3 M KNO_3)	
	7.4	1.08	100 mM K_2HPO_4	
	HA[a)]	3.97	0.5 M HCl or 0.5 M KOH (used as titrants) and 0.15 M KCl at 25ºC	
	A^{-}[b)]	-0.05	"	

a) neutral form of the acids; b) fully ionized acid.

Table SI-2. log $D_{o/w(7.4)}$ compilation of neutral solutes and partially and fully ionized acids.

Compound	log $D_{o/w(7.4)}$	References
3-nitroaniline	1.39	[27]
Aminopyrine	0.63	[28]
Benzocaine	1.89	[29]
Bromazepam	1.65	[30]
Diazepam	2.25	[7,28,30,31]
	2.58	
	2.79	
	2.87	
Griseofulvin	2.18	[14,23,28,31]
	2.23	
	2.23	
	2.47	
Hexanophenone	3.69	[32]
Isoniazid	-0.65	[33]
	-0.85	
Methoxsalen	1.97	[7]
Thymol	3.34	[32]
Bumetanide	-0.11	[7,14]
	0.31	
Diclofenac	1.09	[7,10,14,16,19,26,34]
	1.13	
	1.13	
	1.15	
	1.16	
	1.22	
	1.31	
Diflunisal	0.76	[10]
Fenbufen	0.59	[10,19]
	0.63	
Flurbiprofen	0.87	[19,23]
	0.91	
Gemfibrozil	1.20	[29]
Glyburide	2.19	[7,23]
	2.19	
Indomethacin	0.77	[7,10,14,16,22,23,28,34–36]
	0.89	
	0.91	
	0.93	
	1.00	
	1.00	
	1.00	
	1.00	
	1.03	
	1.26	
Mefenamic acid	2.05	[10,35]
	2.00	
Pentachlorophenol	1.83	[3]

Compound	log $D_{o/w(7.4)}$	References
3-Nitrophenol	1.52	[37]
4-Nitrophenol	1.38	[37]
Butylparaben	3.32	[38]
Ethylparaben	2.44	[38]
Methylparaben	1.98	[38]
Omeprazole	2.22 2.38	[39,40]
Phenobarbital	1.10 1.14	[25,41]
Propylparaben	3.01	[38]
sulfamethazine	-0.43	[42]
Theophylline	-0.05 -0.03 -0.03	[14,23,32]

REFERENCES

[1] N. Gulyaeva, A. Zaslavsky, P. Lechner, A. Chait, B. Zaslavsky, pH dependence of the relative hydrophobicity and lipophilicity of amino acids and peptides measured by aqueous two-phase and octanol-buffer partitioning, J. Pept. Res. 61 (2003) 71–79. doi:10.1034/j.1399-3011.2003.00037.x.

[2] Y.Z. Da, K. Ito, H. Fujiwara, Energy aspects of oil/water partition leading to the novel hydrophobic parameters for the analysis of quantitative structure-activity relationships, J. Med. Chem. 35 (1992) 3382–3387. doi:10.1021/jm0022357023448.

[3] B.E. Nowosielski, J.B. Fein, Experimental study of octanol-water partition coefficients for 2,4,6-trichlorophenol and pentachlorophenol: Derivation of an empirical model of chlorophenol partitioning behaviour, Appl. Geochemistry. 13 (1998) 893–904. doi:10.1016/S0883-2927(98)00015-8.

[4] K. Schellenberg, C. Leuenberger, R.P. Schwarzenbach, Sorption of chlorinated phenols by natural sediments and aquifer materials, Environ. Sci. Technol. 18 (1984) 652–657. doi:10.1021/es00127a005.

[5] F.H. Clarke, N.M. Cahoon, Partition coefficients by curve fitting: The use of two different octanol volumes in a dual-phase potentiometric titration, J. Pharm. Sci. 85 (1996) 178–183. doi:10.1021/js950230p.

[6] K. Nishimura, Y. Nozaki, A. Yoshimi, S. Nakamura, M. Kitagawa, N. Kakeya, K. Kitao, Studies on the promoting effects of carboxylic acid derivatives on the rectal absorption of β-lactam antibiotics in rats, Chem. Pharm. Bull. 33 (2002) 282–291. doi:10.1248/cpb.33.282.

[7] R.P. Austin, P. Barton, S.L. Cockroft, M.C. Wenlock, R.J. Riley, The influence of nonspecific microsomal binding on apparent intrinsic clearance, and its prediction from physicochemical properties, Drug Metab. Dispos. 30 (2002) 1497–1503. doi:10.1124/dmd.30.12.1497.

[8] S. Winiwarter, N.M. Bonham, F. Ax, A. Hallberg, H. Lennernäs, A. Karlén, Correlation of human jejunal permeability (in vivo) of drugs with experimentally and theoretically derived parameters. A multivariate data analysis approach, J. Med. Chem. 41 (1998) 4939–4949. doi:10.1021/jm9810102.

[9] M. Sugawara, Y. Takekuma, M. Kobayashi, K. Iseki, K. Miyazaki, Predicting the intestinal absorption of anionic drugs from their physicochemical properties, Pharm. Pharmacol. Commun. 1 (1995) 491–493. doi:10.1111/j.2042-7158.1995.tb00362.x.

[10] M.I. La Rotonda, G. Amato, F. Barbato, C. Silipo, A. Vittotia, Relationships between octanol-water partition data, chromatographic indices and their dependence on pH in a set of nonsteroidal anti-inflammatory drugs, Quant. Struct. Relationships. 2 (1983) 168–173. doi:10.1002/qsar.19830020405.

[11] A. Fini, I. Orienti, V. Zecchi, Analysis of a two- and three-phase dissolution process of ketoprofen, Acta Pharm. Technol. 34 (1988) 160–163.

[12] J.A. Cordero, L. Alarcon, E. Escribano, R. Obach, J. Domenech, A comparative study of the transdermal penetration of a series of nonsteroidal antiinflammatory drugs, J. Pharm. Sci. 86 (1997) 503–508. doi:10.1021/js950346l.

[13] J. Rautio, H. Taipale, J. Gynther, J. Vepsäläinen, T. Nevalainen, T. Jarvinen, In vitro evaluation of acyloxyalkyl esters as dermal prodrugs of ketoprofen and naproxen, J. Pharm. Sci. 87 (1998) 1622–1628. doi:10.1021/js970465w.

[14] C. Zhu, L. Jiang, T.M. Chen, K.K. Hwang, A comparative study of artificial membrane permeability assay for high throughput profiling of drug absorption potential, Eur. J. Med. Chem. 37 (2002) 399–407. doi:10.1016/S0223-5234(02)01360-0.

[15] F. Barbato, G. Caliendo, M.I. La Rotonda, C. Silipo, G. Toraldo, A. Vittoria, Distribution coefficients by curve fitting: application to ionogenic nonsteroidal antiinflammatory drugs, Quant. Struct. Relationships. 5 (1986) 88–95. doi:10.1002/qsar.19860050303.

[16] H.C. Atkinson, E.J. Begg, Relationship between human milk lipid–ultrafiltrate and octanol-water partition coefficients, J. Pharm. Sci. 77 (1988) 796–798. doi:10.1002/jps.2600770916.

[17] H. Bundgaard, N.M. Nielsen, Glycolamide esters as a novel biolabile prodrug type for non-steroidal anti-inflammatory carboxylic acid drugs, Int. J. Pharm. 43 (1988) 101–110. doi:10.1016/0378-5173(88)90064-6.

[18] J. Rautio, T. Nevalainen, H. Taipale, J. Vepsäläinen, J. Gynther, K. Laine, T. Järvinen, Synthesis and in vitro evaluation of novel morpholinyl- and methylpiperazinylacyloxyalkyl prodrugs of 2-(6-methoxy-2-naphthyl)propionic acid (naproxen) for topical drug delivery, J. Med. Chem. 43 (2000) 1489–1494. doi:10.1021/jm991149s.

[19] A. Chiarini, A. Tartarini, A. Fini, pH-solubility relationship and partition coefficients for some anti-inflammatory arylaliphatic acids, 317 (1984) 268–273.

[20] V. Sarveiya, J.F. Templeton, H.A. Benson, Ion-pairs of ibuprofen: increased membrane diffusion, J. Pharm. Pharmacol. 56 (2004) 717–724. doi:10.1211/0022357023448.

[21] G. Orzalesi, F. Mari, E. Bertol, R. Selleri, G. Pisaturo, Anti-inflammatory agents:

determination of ibuproxam and its metabolite humans. Correlation between bioavailability, tolerance and chemico-physical characteristics, Arzneimittelforschung. 30 (1980) 1607–1609.

[22] N. Gulyaeva, A. Zaslavsky, P. Lechner, M. Chlenov, O. McConnell, A. Chait, V. Kipnis, B. Zaslavsky, Relative hydrophobicity and lipophilicity of drugs measured by aqueous two-phase partitioning, octanol-buffer partitioning and HPLC. A simple model for predicting blood-brain distribution, Eur. J. Med. Chem. 38 (2003) 391–396. doi:10.1016/S0223-5234(03)00044-8.

[23] Y.W. Alelyunas, L. Pelosi-Kilby, P. Turcotte, M.B. Kary, R.C. Spreen, A high throughput dried DMSO Log D lipophilicity measurement based on 96-well shake-flask and atmospheric pressure photoionization mass spectrometry detection, J. Chromatogr. A. 1217 (2010) 1950–1955. doi:10.1016/j.chroma.2010.01.071.

[24] K. Balon, B.V. Riebesehl, B.W. Müller, Drug liposome partitioning as a tool for the prediction of human passive intestinal absorption, Pharm. Res. 16 (1999) 882–888. doi:10.1023/A:1018882221008.

[25] L. Hitzel, A.P. Watt, K.L. Locker, An increased throughput method for the determination of partition coefficients, Pharm. Res. 17 (2000) 1389–1395. doi:10.1023/A:1007546905874.

[26] A. Avdeef, K.J. Box, J.E.A. Comer, C. Hibbert, K.Y. Tam, pH-Metric logP 10. Determination of liposomal membrane-water partition coefficients of ionizable drugs, Pharm. Res. 15 (1998) 209–215. doi:10.1023/A:1011954332221.

[27] G.G. Briggs, Theoretical and experimental relationships between soil adsorption, octanol-water partition coefficients, water solubilities, bioconcentration factors, and the parachor, J. Agric. Food Chem. 29 (1981) 1050–1059. doi:10.1021/jf00107a040.

[28] M. Yazdanian, S.L. Glynn, J.L. Wright, A. Hawi, Correlating partitioning and Caco-2 cell permeability of structurally diverse small molecular weight compounds, Pharm. Res. 15 (1998) 1490–1494. doi:10.1023/A:1011930411574.

[29] A. Avdeef, Absorption and drug development: solubility, permeability, and charge state, Second ed., John Wiley & Sons, Inc., Hoboken, 2012.

[30] F. Lombardo, M.Y. Shalaeva, K.A. Tupper, F. Gao, M.H. Abraham, ElogP(oct): A tool for lipophilicity determination in drug discovery, J. Med. Chem. 43 (2000) 2922–2928. doi:10.1021/jm0000822.

[31] M. Kansy, H. Fischer, K. Kratzat, F. Senner, B. Wagner, I. Parrilla, High-throughput artificial membrane permeability studies in early drug discovery and development, in: B.

Testa, H. Van de Waterbeemd, G. Folkers, R. Guy (Eds.), Pharmacokinetic optimization in drug research: biological, physicochemical, and computational strategies. Verlag Helvetica Chimica Acta, Zürich, 2001: pp. 447–464.

[32] A. Andrés, M. Rosés, C. Ràfols, E. Bosch, S. Espinosa, V. Segarra, J.M. Huerta, Setup and validation of shake-flask procedures for the determination of partition coefficients (log D) from low drug amounts, Eur. J. Pharm. Sci. 76 (2015) 181–191. doi:10.1016/j.ejps.2015.05.008.

[33] C. Ràfols, E. Bosch, R. Ruiz, K.J. Box, M. Reis, C. Ventura, S. Santos, M.E. Araújo, F. Martins, Acidity and hydrophobicity of several new potential antitubercular drugs: Isoniazid and benzimidazole derivatives, J. Chem. Eng. Data. 57 (2012) 330–338. doi:10.1021/je200827u.

[34] P. Moser, A. Sallmann, I. Wiesenberg, Synthesis and quantitative structure-activity relationships of diclofenac analogues, J. Med. Chem. 33 (1990) 2358–2368. doi:10.1021/jm00171a008.

[35] R. Menassé, P.R. Hedwall, J. Kraetz, C. Pericin, L. Riesterer, A. Sallmann, R. Ziel, R. Jaques, Pharmacological properties of diclofenac sodium and its metabolites, Scand. J. Rheumatol. Suppl. (1978) 5–16. doi:10.3109/03009747809097211.

[36] J.A. Jona, L.W. Dittert, P.A. Crooks, S.M. Milosovich, A.A. Hussain, Design of novel prodrugs for the enhancement of the transdermal penetration of indomethacin, Int. J. Pharm. 123 (1995) 127–136. doi:10.1016/0378-5173(95)00061-M.

[37] N. El Tayar, R.S. Tsai, P. Vallat, C. Altomare, B. Testa, Measurement of partition coefficients by various centrifugal partition chromatographic techniques. A comparative evaluation, J. Chromatogr. A. 556 (1991) 181–194. doi:10.1016/S0021-9673(01)96220-X.

[38] L. Lacko, B. Wittke, G. Zimmer, Interaction of benzoic acid derivatives with the transport system of glucose in human erythrocytes, Biochem. Pharmacol. 30 (1981) 1425–1431. doi:10.1016/0006-2952(81)90362-2.

[39] A.L. Ungell, S. Nylander, S. Bergstrand, Å. Sjöberg, H. Lennernäs, Membrane transport of drugs in different regions of the intestinal tract of the rat, J. Pharm. Sci. 87 (1998) 360–366. doi:10.1021/js970218s.

[40] F. Lombardo, M.Y. Shalaeva, K.A. Tupper, F. Gao, ElogDoct: A tool for lipophilicity determination in drug discovery. 2. Basic and neutral compounds, J. Med. Chem. 44 (2001) 2490–2497. doi:10.1021/jm0100990.

[41] L. Rodriguez, V. Zecchi, M. Cini, In vitro study of the partition of drugs in triphasic

systems. II. Partition of various barbiturates and their sodium salts in the system: solution buffered at pH 7.4/n-octanol/solution buffered at pH 7.4, Farm. Ed. Prat. 34 (1979) 371–377.

[42] I.B. Glowinski, H.E. Radtke, W.W. Weber, Genetic variation in N-acetylation of carcinogenic arylamines by human and rabbit liver, Mol. Pharmacol. 14 (1978) 940–949.

ARTICLE VI

Estimation of the Octanol-Water Distribution Coefficient of Basic Compounds by a Cationic Microemulsion Electrokinetic Chromatography System

Alejandro Fernández-Pumarega, Belén Martín-Sanz, Susana Amézqueta, Elisabet Fuguet, and Martí Rosés

ADMET & DMPK, en revisió

ADMET & DMPK X(Y) (20xx) pp-pp; doi: ***http://dx.doi.org/10.5599/admet.0000.000***

ADMET

Open Access : ISSN : 1848-7718

http://www.pub.iapchem.org/ojs/index.php/admet/index

Original scientific paper

Estimation of the octanol-water distribution coefficient of basic compounds by a cationic microemulsion electrokinetic chromatography system

Alejandro Fernández-Pumarega[1], Belén Martín-Sanz[1], Susana Amézqueta[1,*], Elisabet Fuguet[1,2], Martí Rosés[1]

[1]*Departament d'Enginyeria Química i Química Analítica and Institut de Biomedicina (IBUB), Facultat de Química, Universitat de Barcelona, Martí i Franquès 1-11, 08028, Barcelona, Spain.*

[2]*Serra Húnter Programme. Generalitat de Catalunya. Spain*

*Corresponding Author: E-mail: samezqueta@ub.edu; Tel.: (+34) 934021277; Fax: (+34) 934021233

Received: MMMM DD, YYYY; Revised: MMMM DD, YYYY; Published: MMMM DD, YYYY

Abstract

The octanol-water partition coefficient ($P_{o/w}$), or the octanol-water distribution coefficient ($D_{o/w}$) for ionized compounds, is a key parameter in the drug development process. In a previous work, this parameter was estimated through the retention factor measurements in a sodium dodecyl sulfate (SDS)-MEEKC system for acidic compounds. Nonetheless, when ionized basic compounds were analyzed, undesirable ion-pairs were formed with the anionic surfactant and avoided a good estimation of log $D_{o/w}$. For this reason, an alternative MEEKC system based on a cationic surfactant has been evaluated to estimate $P_{o/w}$ or $D_{o/w}$ of neutral compounds and ionized bases. To this end, it has been characterized through the solvation parameter model (SPM) and compared to the octanol-water partition system. Results pointed out that both systems show a similar partition behaviour. Hence, the log $P_{o/w}$ of a set of neutral compounds has been successfully correlated against the logarithm of the retention factor (log k) determined in this MEEKC system. Then, the log $D_{o/w}$ of 6 model bases have been estimated at different pH values and they have been compared to data from the literature, determined by the reference shake-flask and potentiometric methods. Good agreement has been observed between the literature and the estimated values when the base is neutral or partially ionized (up to 99% of ionization).

Keywords

Lipophilicity; log $P_{o/w}$; log $D_{o/w}$; MEEKC; ionized bases; solvation parameter model; microemulsion; system surrogation.

Introduction

Chromatographic systems based on different techniques such as high performance liquid chromatography (HPLC) and electrokinetic chromatography (EKC) have been widely used to determine biopartitioning properties [1–6]. In these systems, the compounds experiment a partition between an aqueous phase and a stationary phase, for HPLC systems, or a pseudoestationary phase, for EKC systems, similar to the partition that compounds experiment in a biological system. Therefore, if the partition in the chromatographic system and in the biological one is similar enough, it is possible to estimate the biological property through a correlation like Eq. 1:

$$\log SP_{bio} = q + p \log SP_{chrom} \quad (1)$$

where, SP_{bio} is the solute biological property, SP_{chrom} the solute physicochemical property (generally the retention factor, *k*), and "*q*" and "*p*" are, respectively, the intercept and the slope of the resulting correlation between both parameters.

In previous works [3–6] Eq. 1 was applied to the determination of the octanol-water partition coefficient of neutral solutes ($P_{o/w}$) and the distribution coefficient of partially ionized acidic compounds ($D_{o/w}$) from microemulsion electrokinetic chromatography (MEEKC) measurements. A MEEKC system based on an anionic charged microemulsion (ME) constituted of heptane, 1-butanol, and sodium dodecyl sulfate (SDS) was used. The aim of the present study is to evaluate the applicability of MEEKC measurements to estimate the log $P_{o/w}$ and log $D_{o/w}$ of ionized basic compounds, which are positively charged in their ionized form.

However, the SDS-MEEKC system cannot be used for basic compounds since the formation of ion-pairs between the surfactant, negatively charged, and the protonated base, positively charged has been observed. Thus, the retention factor would be altered leading to wrong log $D_{o/w}$ estimated values. In this work, the replacement of the anionic surfactant (SDS) by a cationic one (tetradecyltrimethylammonium bromide, TTAB) is tested to solve this problem. So, as the only role of the surfactant is to stabilize the oil droplets, we think that the TTAB-MEEKC system should be able to estimate the $P_{o/w}$ or $D_{o/w}$ of basic solutes as well as the SDS-MEEKC does for acidic solutes. Actually, Ishihama *et al.* [7] evaluated 3 different surfactants and showed that neither the ionic groups nor the hydrocarbon chain lengths affected the selectivity of the ME for neutral compounds. Thus, the aim of the present work is to test this potential ability of the TTAB-MEEKC system.

Theory

The retention factor of an ionized base can be calculated through Eq. 2 [8]:

$$k = \frac{\mu - \left(\frac{\mu}{\mu_0}\right)_{ephedrine\ cation} \cdot \mu_0}{\mu_{ME} - \mu} \quad (2)$$

where, μ and μ_0 are the electrophoretic mobility of the compound in MEEKC and in plain buffer (capillary zone electrophoresis, CZE), respectively. μ_{ME} is the electrophoretic mobility of the ME marker in the MEEKC analysis, and $(\mu/\mu_0)_{ephedrine\ cation}$ is the viscosity correction factor (whose value is 0.84). This correction needs to be introduced since two solutions with quite different viscosities (η) are employed in *k* calculation, and μ is inversely related to η [9]. Therefore, the mobility in CZE is corrected to make it equivalent to the one measured in MEEKC.

μ values can be obtained from:

$$\mu = \left[\frac{1}{t_r} - \frac{1}{t_0}\right] \cdot \left[\frac{L_T L_D}{V}\right] \quad (3)$$

where, t_r and t_0 are the elution times of the compound and the electroosmotic flow marker, respectively. L_T and L_D are the total and the effective length of the capillary, respectively, and *V* is the voltage applied during the separation.

Similarly to acidic solutes [10], the retention factor of a monoprotic basic compound in a MEEKC system varies with the p*H* of the media through:

$$k = \frac{k_{(BH^+)} + k_{(B)} \cdot 10^{\mathrm{pH} - \mathrm{p}K'_a}}{1 + 10^{\mathrm{pH} - \mathrm{p}K'_a}} \quad (4)$$

where $k_{(B)}$ and $k_{(BH+)}$ are the retention factor of the neutral and the fully ionized base, respectively, and the pK_a' is the apparent acidity constant of the base.

Experimental

Equipment

All the analysis were performed with a capillary electrophoresis (CE) 7100 equipped with a UV diode array detector from Agilent technologies (Santa Clara, CA, USA). The fused-silica capillaries employed were from Polymicro Technologies (Phoenix, AZ, USA). The capillaries used presented a 50 µm internal diameter.

Water was purified by a Milli-Q plus system from Millipore (Burlington, MA, USA) with a resistivity of 18.2 MΩ·cm. To determine the pH of the solutions a pH-meter GLP 22 from Crison (Barcelona, Spain) was used.

Reagents

Hydrochloric acid (1N Tritisol™), and sodium hydroxide (0.5N Tritisol™) were acquired from Merck (Darmstadt, Germany). Methanol (HPLC-grade) was obtained from Thermo Fisher Scientific (Waltham, MA, USA). Heptane (99%), dodecanophenone (98%), TTAB (>99%), 1-butanol (≥99.7%), 2-[Bis(2-hydroxyethyl)amino]-2-(hydroxymethyl)propane-1,3diol (Bis-tris) (>99%), and sodium phosphate dodecahydrate (>98%) were purchased from Sigma-Aldrich (St. Louis, MO, USA). Disodium hydrogen phosphate (99.5%) was from Baker (Phillipsburg, NJ, USA).

Test compounds with high purities were supplied from different manufacturers: Sigma-Aldrich, Merck, Baker, Carlo Erba (Milan, Italy), Fluka (St. Louis, MO, USA), Riedel-de Häen (Seelze, Germany), and Scharlab (Barcelona, Spain).

Analysis conditions

- *Buffer preparation*

To prepare the buffers at pH 5.4 and pH 7.0, an aliquot of a 0.2 M protonated solution of bis-tris adjusted with NaOH was employed, while to prepare the buffer at pH 11.4 a mixture of a 0.2 M disodium hydrogen phosphate solution and a 0.2 M sodium phosphate dodecahydrate was employed. All the buffers were prepared maintaining the ionic strength at 0.05 M.

- *ME preparation*

To prepare the ME 1.70 g of TTAB were dissolved in around 70 mL of the corresponding buffer solution. Then, 8.15 mL of 1-butanol were added, finishing by the addition of 1.15 mL of heptane. The cosurfactant and the oil were added under continuous magnetic stirring, and if the solution remained turbid, it was sonicated until clarification [4]. Finally, buffer was added up to a total volume of 100 mL. The concentrations of each component with respect the total volume of the ME were: 1.70% (w/v) TTAB, 8.15% (v/v) 1-butanol, and 1.15% (v/v) heptane.

- *Instrumental parameters*

All the measurements were performed keeping the temperature at 25ºC and using a fused-silica capillary with an effective length of 30 cm and a total length of 38.5 cm. The voltage applied in MEEKC measurements was negative and between -11.5 and -14 kV. Regarding the internal pressure applied, it ranged between 0 and 25 mbar. The analysis conditions were different depending on the p*H* to obtain the best electrophoretic window possible. In the case of CZE measurements, the analyses were performed employing positive voltages.

Most compounds were dissolved at 200 $mg \cdot L^{-1}$ in a 9:1 ME:methanol mixture in the MEEKC analysis and in a 9:1 buffer:methanol mixture in the CZE analysis. The alcohol solutes (with low absorptivity) were analyzed at a concentration of 10% (v/v).

The injection of the compounds was performed applying during 5 s an internal pressure of 50 mbar. The

detection of the solutes was performed at λ=200, 214 or 254 nm (depending on the absorbance profile of the compounds). The ME marker used was dodecanophenone (200 mg·L^{-1}, detected at λ = 254 nm), while the electroosmotic flow marker was methanol (10% v/v, detected at λ = 200 nm) [11].

Comparison of systems characterized by the solvation parameter model

The TTAB-MEEKC system has been characterized through the solvation parameter model (SPM) to check its suitability to surrogate the octanol-water partition system [12]. SPM relates a free energy solvation property (in this work the log $P_{o/w}$ or the log k) to five different solute descriptors. The equation resulting from the characterization of a system through the SPM model has the following structure:

$$log\ SP = c + eE + sS + aA + bB + vV \quad (5)$$

where *SP* is the solute property in a given partitioning system; *E*, *S*, *A*, *B* and *V* are the Abraham solute descriptors (which are specific for each compound), and the coefficients *e*, *s*, *a*, *b* and *v* provide the characteristics of the partition system. *E* is the excess molar refraction, *S* the solute dipolarity/polarizability, *A* and *B* are, respectively, the solute hydrogen-bond acidity and basicity descriptors, and *V* the McGowan's volume of the molecule. Each of the system coefficients are complementary to their respective solute descriptor. The system coefficients can be calculated by a multiple linear regression between the depending solute property of a set of representative neutral compounds and their solute descriptors [13].

The similarity between different systems can be determined by comparing the coefficients resulting from the characterization of the systems by the SPM. Lazaro, *et al.* [14] proposed the distance parameter *d* to compare two different systems (i and j) through their normalized SPM coefficients (Eqs. 6-10).

$$\boldsymbol{e_u} = \frac{\boldsymbol{e}}{\boldsymbol{l}} \quad (6)$$

$$\boldsymbol{s_u} = \frac{\boldsymbol{s}}{\boldsymbol{l}} \quad (7)$$

$$\boldsymbol{a_u} = \frac{\boldsymbol{a}}{\boldsymbol{l}} \quad (8)$$

$$\boldsymbol{b_u} = \frac{\boldsymbol{b}}{\boldsymbol{l}} \quad (9)$$

$$\boldsymbol{v_u} = \frac{\boldsymbol{v}}{\boldsymbol{l}} \quad (10)$$

Where e_u, s_u, a_u, b_u, v_u are the normalized coefficients (or coefficients of the unitary vector) and *l* is the length of the coefficients vector; which is calculated as follows:

$$\boldsymbol{l} = \sqrt{\boldsymbol{e^2} + \boldsymbol{s^2} + \boldsymbol{a^2} + \boldsymbol{b^2} + \boldsymbol{v^2}} \quad (11)$$

then, the *d* parameter is calculated by Eq. 12.

$$\boldsymbol{d} = \sqrt{(\boldsymbol{e_{ui}} - \boldsymbol{e_{uj}})^2 + (\boldsymbol{s_{ui}} - \boldsymbol{s_{uj}})^2 + (\boldsymbol{a_{ui}} - \boldsymbol{a_{uj}})^2 + (\boldsymbol{b_{ui}} - \boldsymbol{b_{uj}})^2 + (\boldsymbol{v_{ui}} - \boldsymbol{v_{uj}})^2} \quad (12)$$

The smaller the *d* parameter, the more similar will be the systems compared. As a practical convention, if the distance between the systems compared is below 0.25, it can be concluded that these systems are analogous [15].

Moreover, the precision of the correlation (Eq. 13) between log $P_{o/w}$ and log *k* in the TTAB-MEEKC system has been estimated following the approach published elsewhere [15].

The overall precision of the correlation (SD_{corr}^2) can be estimated by the sum of three different contributions:

$$SD_{corr}^2 = SD_{P_{o/w}}^2 + (p \cdot SD_{MEEKC})^2 + SD_d^2 \quad (13)$$

$SD_{Po/w}$ and SD_{MEEKC} are the standard deviations (SD) obtained from the characterization through the SPM of the octanol-water partition system and the TTAB-MEEKC system, respectively. SD_d and "p" are the SD and the slope obtained from the correlation of the log $P_{o/w}$ and log k values of a set of representative solutes. The values of the parameters were calculated using the equations resulting from the SPM characterization and the descriptors of the solutes. By using these equations, $SD_{Po/w}$ and SD_{MEEKC} are equal to 0. So, the SD of this correlation can be attributed uniquely to the dissimilarity between the systems.

Data analysis

Table Curve 2D from Systat Software Inc. (San Jose, CA, USA) was employed to obtain the log $D_{o/w}$-p*H* profiles of the basic compounds. Data calculations were performed using Excel 2010 from Microsoft (Redmond, WA, USA).

Results and Discussion

Suitability of the TTAB-MEEKC system to estimate log $P_{o/w}$ values

- *Characterization of the MEEKC system by the SPM*

The TTAB-MEEKC system has been characterized through the SPM in order to later evaluate its similarity with the octanol-water partition system. To obtain accurate solvation coefficients of the model, representative analytes have been selected to characterize the system. In 2001, Fuguet, *et al.* [13] proposed 71 compounds from a 2975 solute data base, selected according to their solute-solvent interactions, as a good set to characterize chromatographic systems by the SPM.

The retention factors of the proposed set of compounds in the TTAB-MEEKC system have been measured at pH 7.0, where all compounds are neutral. During the characterization, some of the compounds have been discarded since they are not lipophilic enough and elute with the EOF marker (propan-1,3-diol, butan-1,4-diol, and pentan-1,5-diol), they are too lipophilic and they coelute with the ME marker (butylbenzene, and α-pinene), or they present other experimental troubles in the TTAB-MEEKC system (myrcene, pentan-1-ol and pentan-3-ol). The retention factor of neutral compounds can be calculated using Eq. 2, being μ_0 equal to 0 as they are uncharged. Table 1 lists the compounds used in the characterization together with their solute descriptors, and the log k in the TTAB-MEEKC system. Moreover, the log $P_{o/w}$ values of each compound reported in the literature are also listed [16–30].

Table 1. Abraham solute descriptors, log k and log $P_{o/w}$ of the chosen neutral analytes.

Compound	*E*	*S*	*A*	*B*	*V*	log *k*	log $P_{o/w}$ [a)]
Propan-1-ol	0.236	0.42	0.37	0.48	0.5900	-0.71	0.30
Propan-2-ol	0.212	0.36	0.33	0.56	0.5900	-0.79	0.05
Butan-1-ol	0.224	0.42	0.37	0.48	0.7309	0.08	0.88
Pentan-1-ol	0.219	0.42	0.37	0.48	0.8718	-	1.56
Pentan-3-ol	0.218	0.36	0.33	0.56	0.8718	-	1.21
Propan-1,3-diol	0.397	0.91	0.77	0.85	0.6487	-	-1.04
Butan-1,4-diol	0.395	0.93	0.72	0.90	0.7860	-	-0.83
Pentan-1,5-diol	0.388	0.95	0.72	0.91	0.9305	-	-0.43
Thiourea	0.840	0.82	0.77	0.87	0.5696	-1.06	-1.02
Benzene	0.610	0.52	0.00	0.14	0.7164	0.36	2.13
Toluene	0.601	0.52	0.00	0.14	0.8573	0.77	2.69

Compound	*E*	*S*	*A*	*B*	*V*	log *k*	log $P_{o/w}$ [a)]
Ethylbenzene	0.613	0.51	0.00	0.15	0.9982	1.10	3.15
Propylbenzene	0.604	0.50	0.00	0.15	1.1391	1.53	3.68
Butylbenzene	0.600	0.51	0.00	0.15	1.2800	-	4.38
p-Xylene	0.613	0.52	0.00	0.16	0.9982	1.12	3.15
Naphthalene	1.340	0.92	0.00	0.20	1.0854	1.21	3.37
Chlorobenzene	0.718	0.65	0.00	0.07	0.8388	0.85	2.90
Bromobenzene	0.882	0.73	0.00	0.09	0.8914	0.99	2.99
Anisole	0.708	0.75	0.00	0.29	0.9160	0.28	2.11
Benzaldehyde	0.820	1.00	0.00	0.39	0.8730	-0.10	1.47
Acetophenone	0.818	1.01	0.00	0.48	1.0139	-0.03	1.58
Propiophenone	0.804	0.95	0.00	0.51	1.1548	0.35	2.24
Butyrophenone	0.797	0.95	0.00	0.51	1.2957	0.68	2.65
Valerophenone	0.795	0.95	0.00	0.50	1.4366	1.05	3.40
Heptanophenone	0.720	0.95	0.00	0.50	1.7184	1.88	4.41
Benzophenone	1.447	1.50	0.00	0.50	1.4808	1.02	3.18
Methyl benzoate	0.733	0.85	0.00	0.46	1.0726	0.35	2.12
Benzyl benzoate	1.264	1.42	0.00	0.51	1.6804	1.49	3.97
Benzonitrile	0.742	1.11	0.00	0.33	0.8711	-0.06	1.56
Aniline	0.955	0.96	0.26	0.50	0.8162	-0.28	0.90
o-Toluidine	0.970	0.90	0.23	0.59	0.9751	-0.04	1.32
3-Chloroaniline	1.050	1.10	0.30	0.36	0.9390	0.47	1.88
4-Chloroaniline	1.060	1.10	0.30	0.35	0.9390	0.41	1.84
2-Nitroaniline	1.180	1.37	0.30	0.36	0.9904	0.25	1.79
3-Nitroaniline	1.200	1.71	0.40	0.35	0.9904	0.07	1.32
4-Nitroaniline	1.220	1.91	0.42	0.38	0.9904	0.11	1.39
Nitrobenzene	0.871	1.11	0.00	0.28	0.8906	0.16	1.85
2-Nitroanisole	0.965	1.34	0.00	0.38	1.0902	0.17	1.73
Benzamide	0.990	1.50	0.49	0.67	0.9728	-0.39	0.64
4-Aminobenzamide	1.340	1.94	0.80	0.94	1.0726	-0.86	-0.41
Acetanilide	0.870	1.36	0.46	0.69	1.1137	-0.17	1.19
4-Chloroacetanilide	0.980	1.50	0.64	0.51	1.2357	0.51	2.12
Phenol	0.805	0.89	0.60	0.30	0.7751	0.05	1.48
3-Methylphenol	0.822	0.88	0.57	0.34	0.9160	0.38	2.02
2,3-Dimethylphenol	0.850	0.90	0.52	0.36	1.0569	0.64	-
2,4-Dimethylphenol	0.840	0.80	0.53	0.39	1.0569	0.71	2.42
Thymol	0.822	0.79	0.52	0.44	1.3387	1.20	3.34
4-Chlorophenol	0.915	1.08	0.67	0.20	0.8975	0.79	2.39
Catechol	0.970	1.10	0.88	0.47	0.8338	-0.09	0.88
Resorcinol	0.980	1.00	1.10	0.58	0.8338	-0.18	0.80
Hydroquinone	1.000	1.00	1.16	0.60	0.8338	-0.43	0.58
2-Naphthol	1.520	1.08	0.61	0.40	1.1441	1.04	2.84
1,2,3-Trihydroxybenzene	1.165	1.35	1.35	0.62	0.8925	-0.29	-
Furan	0.369	0.53	0.00	0.13	0.5363	-0.31	1.34
2,3-Benzofuran	0.888	0.83	0.00	0.15	0.9053	0.71	2.67
Quinoline	1.268	0.97	0.00	0.51	1.0443	0.20	2.15

Compound	*E*	*S*	*A*	*B*	*V*	log *k*	log $P_{o/w}$ [a)]
Pyrrole	0.613	0.73	0.41	0.29	0.5774	-0.44	0.75
Pyrimidine	0.606	1.00	0.00	0.65	0.6342	-1.03	-0.40
Antipyrine	1.320	1.50	0.00	1.48	1.5502	-0.67	0.56
Caffeine	1.500	1.60	0.00	1.33	1.3632	-0.77	-0.01
Corticosterone	1.860	3.43	0.40	1.63	2.7389	0.65	1.90
Cortisone	1.960	3.50	0.36	1.87	2.7546	0.23	1.47
Hydrocortisone	2.030	3.49	0.71	1.90	2.7975	0.39	1.53
Estradiol	1.800	3.30	0.88	0.95	2.1988	1.35	4.01
Estratriol	2.000	3.36	1.40	1.22	2.2575	0.67	2.45
Monuron	1.140	1.50	0.47	0.78	1.4768	0.32	1.94
Myrcene	0.483	0.29	0.00	0.21	1.3886	-	4.17
α-Pinene	0.446	0.14	0.00	0.12	1.2574	-	4.83
Geraniol	0.513	0.63	0.39	0.66	1.4903	1.07	-

[a)] From references [16-30].

To obtain the SPM coefficients of the TTAB MEEKC system, butan-1-ol, and thiourea were considered as outliers and discarded, as they presented standard residues higher than 2.5. Estradiol had a standard residue slightly greater than 2.5, but to discard it had no big influence on the result, so it was not considered as outlier.

The parameters and statistics (F, Fisher's F parameter; SD, standard deviation; R^2, determination coefficient; n, number of compounds) resulting from the system characterization are:

$$log\ k = -0.96(\pm 0.05) + 0.44(\pm 0.08)E\ - 0.63(\pm 0.06)S + 0.20(\pm 0.05)A - 2.13(\pm 0.07)B + 2.36(\pm 0.06) \quad (14)$$

R^2 = 0.972, SD = 0.12, F = 368, n = 59.

The large values of the coefficients *b* and *v* show that the hydrogen bond basicity and the volume of the solute are the more important parameters. The *v* coefficient is positive, meaning that it is easier to form a cavity to place the solute in the ME phase than in the aqueous one. A negative *b* coefficient is obtained indicating a higher hydrogen bonding acidity of the aqueous phase with respect to the ME phase. The *e* coefficient is positive, so the ME is more polarizable than the aqueous phase. The negative value of the *s* coefficient indicates that the ME system is less dipolar than the aqueous phase. The coefficient *a* is close to zero, showing that hydrogen bonding basicities of ME and aqueous phases are similar, and the variation of solute hydrogen bond acidity has a small effect on the system.

- *Model comparison*

The TTAB-MEEKC system has been compared to the octanol-water partition system and the SDS-MEEKC system. The last system was used in other research studies to estimate the log $P_{o/w}$ of ionizable acids [5,6].

The normalized coefficients obtained from the characterization of the TTAB-MEEKC, the octanol-water partition [31], and the SDS-MEEKC [3] (calculated using Eqs. 6-11), and the *d* distance parameter (Eq. 12) are summarized in Table 2.

Table 2. Normalized coefficients and "*d*" distances of the compared systems.

System	e_u	s_u	a_u	b_u	v_u	n	SD	R^2	*d*	Ref.
TTAB MEEKC	0.13	-0.19	0.06	-0.65	0.72	59	0.12	0.972	-	This work
Octanol-water	0.11	-0.20	0.01	-0.65	0.72	613	0.12	0.994	0.06	[31]
SDS MEEKC	0.07	-0.16	-0.01	-0.67	0.72	53	0.09	0.988	0.11	[3]

The normalized coefficients of the three systems are very similar, being for all of them the *b* and *v* coefficients the most important ones. Furthermore, the *d* parameter between TTAB-MEEKC and octanol-water partition is much smaller than 0.25, meaning that the TTAB-MEEKC system is a good approximation to surrogate the octanol-water partition one, and consequently, lipophilicity. The *d* parameter obtained between TTAB-MEEKC and SDS-MEEKC is also below 0.25, therefore TTAB is a good substitute of SDS for log $P_{o/w}$ determination.

The chromatographic precision of the correlation between log *k* in the TTAB-ME and the octanol-water partition has also been calculated. As explained before and elsewhere in the literature [15], the overall precision results can be estimated from a sum of three different contributions ($SD_{Po/w}^2$, $(p{\cdot}SD_{MEEKC})^2$, SD_d^2). Here, the largest contribution to the overall precision comes from the chromatographic data ($(p{\cdot}SD_{MEEKC})^2$ = 0.034) and the dissimilarity between the two systems (SD_d^2 = 0.013) is similar than the variance of the biopartitioning data ($SD_{Po/w}^2$ = 0.013). However, the calculated overall precision (SD_{corr}^2 = 0.061) is low. Therefore, the correlation obtained between the TTAB-MEEKC and octanol-water systems should be good, meaning that, the TTAB-MEEKC system is a good candidate to estimate satisfactorily the lipophilicity of neutral compounds.

- *Correlation between log $P_{o/w}$ and log k.*

A linear correlation between the log $P_{o/w}$ and the log *k* of 58 solutes presented in Table 1 has been established. The correlation between log $P_{o/w}$ and log *k* is plotted in Figure 1. The equation and statistics obtained are as follows:

$$log\ P_{o/w} = 1.68(\pm 0.05) \cdot log\ k + 1.35(\pm 0.04) \quad (15)$$

R^2=0.954; SD=0.25; F=1174; n=58;

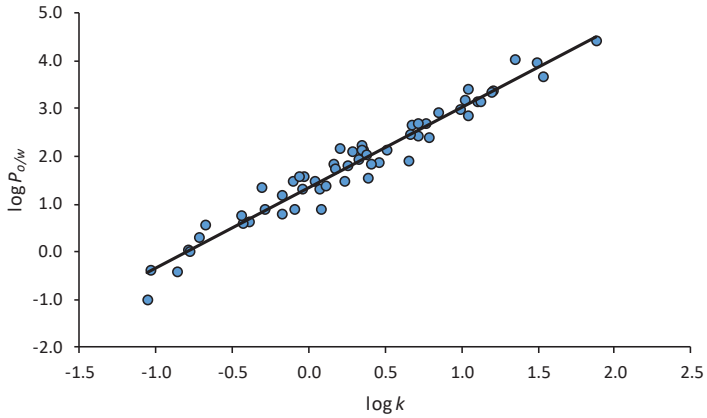

Figure 1. log $P_{o/w}$ vs log *k* correlation with the compounds from Table 1 (Eq. 15).

which is not significantly different from the log $P_{o/w}$ – log *k* correlation obtained for the SDS-MEEKC system employing a set of neutral compounds (Eq. 16) [6].

$$log\ P_{o/w} = 1.60(\pm 0.11) \cdot log\ k + 1.51(\pm 0.08) \quad (16)$$

R^2 = 0.916; SD = 0.33; n = 20; F = 196

Good statistics have been obtained for the correlation: R^2 value close to 1, and a small SD value of the regression, whereby the TTAB-MEEKC system has been proved to provide a good estimation of the log $P_{o/w}$ of neutral compounds, as already pointed out through the model comparison tools. Therefore, Eq. 15 is going to be used as calibration curve for the estimation of $D_{o/w}$ of ionized bases in the following section.

log $D_{o/w}$ estimation of ionized basic compounds.

With the aim to extent the applicability of the method to ionizable bases, the log $D_{o/w}$ of six basic compounds (alprenolol, nadolol, oxprenolol, penbutolol, pindolol, and propranolol) have been estimated at different pH values, thus at different ionization degrees and compared to literature experimental values. All these compounds are used as pharmaceutical drugs and present a basic group with a pK_a inside the electrophoretic p*H* working range (2-12) [27].

Similarly to *k* (Eq. 4), the log $D_{o/w}$ of ionized bases depends on the pK_a' of the base and the p*H* of the ME through:

$$\log D_{o/w} = \log\left(\frac{10^{log\ P_{o/w(BH^+)}} + 10^{logP_{o/w(B)}} \cdot 10^{\mathrm{pH}-\mathrm{p}K_a'}}{1+10^{\mathrm{pH}-\mathrm{p}K_a'}}\right) \quad (17)$$

where log $P_{o/w(BH+)}$ and log $P_{o/w(B)}$ are the logarithms of the octanol–water partition coefficient of the fully ionized and neutral base, respectively. log $D_{o/w}$ – p*H* profiles for each of the model compounds have been calculated fitting to Eq. 17 log $D_{o/w}$ values determined at different values of p*H* taken from the literature [32–37]. The log $D_{o/w}$ values compiled have been determined using the reference shake-flask, and the p*H*-metric titration methods. The profiles, the parameters and the statistics resulting from these fittings can be found in Figure 2 and Table 3.

Table 3. Parameters resulting from the fit of Eq. 17 to log $D_{o/w}$ vs p*H* data. $k_{(BH+)}$ and $k_{(B)}$ have been experimentally determined in the TTAB-MEEKC system.

Compound	pK_a' (SD)	log $P_{o/w(BH+)}$ (SD)	log $P_{o/w(B)}$ (SD)	R^2	SD	F	$k_{(BH+)}$	$k_{(B)}$
Alprenolol	9.63 (0.28)	-0.46 (0.16)	3.20 (0.23)	0.939	0.36	116	0.67	11.09
Nadolol	9.31 (0.21)	-2.05 (0.11)	0.83 (0.15)	0.975	0.21	156	0.05	0.88
Oxprenolol	9.38 (0.16)	-1.43 (0.10)	2.14 (0.13)	0.985	0.18	328	0.14	2.82
Penbutolol	9.37 (0.31)	1.23 (0.24)	4.06 (0.24)	0.987	0.24	37	3.20	61.64
Pindolol	9.32 (0.17)	-1.39 (0.10)	1.79 (0.13)	0.970	0.23	243	0.16	2.43
Propranolol	9.24 (0.26)	-0.17 (0.15)	2.99 (0.21)	0.908	0.37	94	1.19	16.51

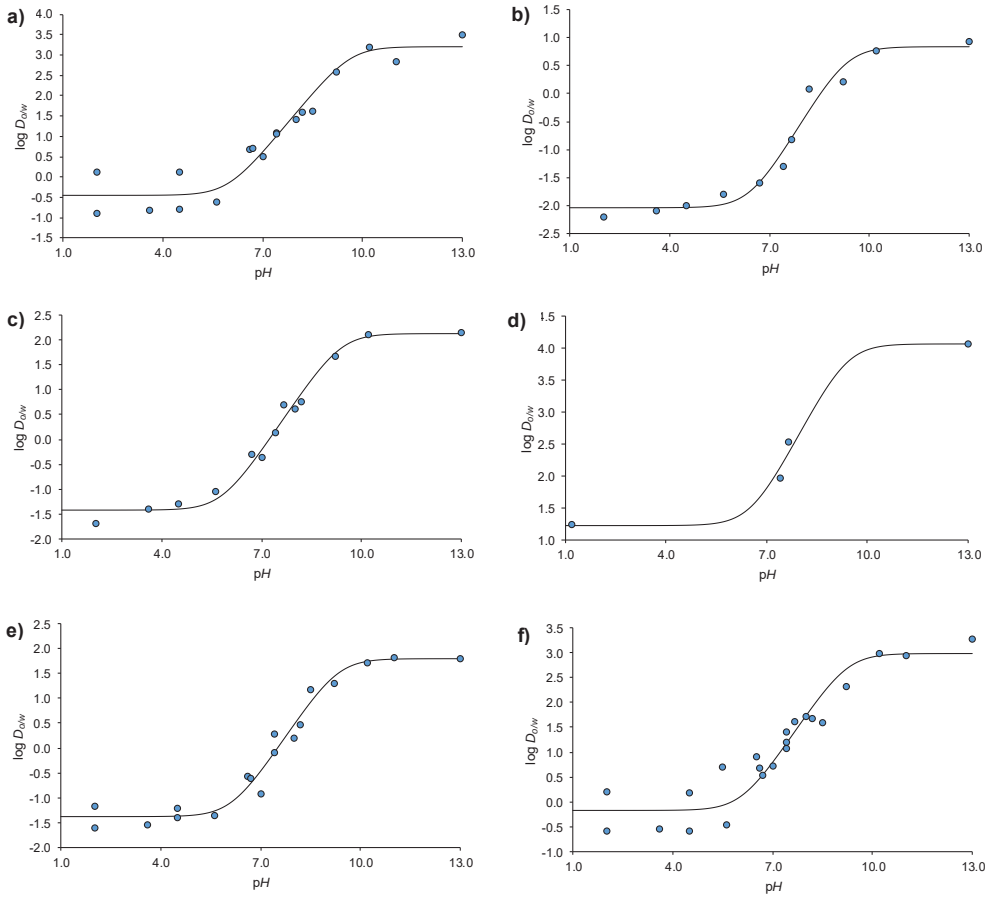

Figure 2. log $D_{o/w}$ – p*H* profiles obtained adjusting the data from the literature (•) to Eq. 17. a) alprenolol, b) nadolol, c) oxprenolol, d) penbutolol, e) pindolol, f) propranolol.

Then, the $k_{(BH+)}$ and $k_{(B)}$ of the bases have been determined in the TTAB-MEEKC system at pH 5.4 and 11.4, respectively (Table 3). The retention factors and the pK_a' of each of the bases have been used in Eq. 4 to estimate *k* values at the p*H* of interest. Then, log $D_{o/w}$ has been estimated through Eq. 15. The log $D_{o/w}$ from the literature [32–37] and the estimated values are summarized in Table 4. The ionization degree ($\alpha_{(BH+)}$) of the bases at each p*H* value (calculated using Eq. 18) are also provided.

$$\alpha_{(BH^+)} = \frac{10^{pK_a'-pH}}{1+10^{pK_a'-pH}} \quad (18)$$

Figure 3 compares the estimated and the experimental data from Table 4 for bases neutral or fully ionized (Figure 3A) or partially ionized, from 1 to 99% (Figure 3B). The same figure also represents a line with a slope of 1 and an intercept of 0, and two extra lines showing the 95% confidence interval (±2SD) of the calibration curve for neutral compounds.

Table 4. Differences between literature (log $D_{lit.}$) and estimated (log $D_{est.}$) values of the bases at different p*H* values.

Compound	p*H*	*α*	log $D_{lit.}$ [a)]	log $D_{est.}$	log $D_{lit.}$ – log $D_{est.}$
Alprenolol	2.0	1.00	0.13	1.06	-0.93
	2.0	1.00	-0.89	1.06	-1.95
	3.6	1.00	-0.80	1.06	-1.86
	4.5	1.00	0.14	1.06	-0.92
	4.5	1.00	-0.77	1.06	-1.83
	5.6	1.00	-0.60	1.06	-1.66
	6.6	1.00	0.68	1.07	-0.39
	6.7	1.00	0.73	1.07	-0.34
	7.0	1.00	0.51	1.08	-0.57
	7.4	0.99	1.09	1.12	-0.03
	7.4	0.99	1.08	1.12	-0.04
	8.0	0.98	1.44	1.28	0.16
	8.2	0.96	1.60	1.38	0.22
	8.5	0.93	1.63	1.59	0.04
	9.2	0.73	2.59	2.26	0.33
	10.2	0.21	3.20	2.94	0.26
	11.0	0.04	2.84	3.08	-0.24
	13.0	0.00	3.50	3.11	0.39
Nadolol	2.0	1.00	-2.20	-0.84	-1.36
	3.6	1.00	-2.10	-0.84	-1.26
	4.5	1.00	-2.00	-0.84	-1.16
	5.6	1.00	-1.80	-0.83	-0.97
	6.7	1.00	-1.60	-0.81	-0.79
	7.4	0.99	-1.30	-0.70	-0.60
	7.65	0.98	-0.82	-0.61	-0.21
	8.2	0.93	0.08	-0.26	0.34
	9.2	0.56	0.22	0.70	-0.48
	10.2	0.11	0.76	1.17	-0.41
	13.0	0.00	0.93	1.26	-0.33
Oxprenolol	2.0	1.00	-1.70	-0.08	-1.62
	3.6	1.00	-1.40	-0.08	-1.32
	4.5	1.00	-1.30	-0.08	-1.22
	5.6	1.00	-1.04	-0.08	-0.96
	6.7	1.00	-0.30	-0.06	-0.24
	7.0	1.00	-0.37	-0.03	-0.34
	7.4	0.99	0.13	0.05	0.08
	7.65	0.98	0.69	0.13	0.56
	8.0	0.96	0.61	0.33	0.28
	8.2	0.94	0.76	0.49	0.27
	9.2	0.60	1.67	1.49	0.18
	10.2	0.13	2.10	2.01	0.09
	13.0	0.00	2.16	2.11	0.05

Compound	p*H*	*α*	log $D_{lit.}$ [a)]	log $D_{est.}$	log $D_{lit.}$ – log $D_{est.}$
Penbutolol	1.2	1.00	1.24	2.20	-0.96
	7.4	0.99	1.97	2.33	-0.36
	7.65	0.98	2.53	2.41	0.12
	13.0	0.00	4.06	4.36	-0.30
Pindolol	2.0	1.00	-1.17	0.01	-1.18
	2.0	1.00	-1.60	0.01	-1.61
	3.6	1.00	-1.55	0.01	-1.56
	4.5	1.00	-1.40	0.01	-1.41
	4.5	1.00	-1.22	0.01	-1.23
	5.6	1.00	-1.35	0.01	-1.36
	6.6	1.00	-0.56	0.03	-0.59
	6.7	1.00	-0.62	0.04	-0.66
	7.0	1.00	-0.92	0.06	-0.98
	7.4	0.99	0.29	0.13	0.16
	7.4	0.99	-0.10	0.13	-0.23
	8.0	0.95	0.19	0.38	-0.19
	8.2	0.93	0.46	0.52	-0.06
	8.5	0.87	1.18	0.78	0.40
	9.2	0.57	1.29	1.45	-0.16
	10.2	0.12	1.72	1.91	-0.19
	11.0	0.02	1.82	1.98	-0.16
	13.0	0.00	1.80	2.00	-0.20
Propranolol	2.0	1.00	0.20	1.48	-1.28
	2.0	1.00	-0.58	1.48	-2.06
	3.6	1.00	-0.55	1.48	-2.03
	4.5	1.00	0.18	1.48	-1.30
	4.5	1.00	-0.59	1.48	-2.07
	5.5	1.00	0.7	1.5	-0.8
	5.6	1.00	-0.46	1.48	-1.94
	6.5	1.00	0.9	1.50	-0.6
	6.6	1.00	0.68	1.50	-0.82
	6.7	1.00	0.54	1.50	-0.96
	7.0	0.99	0.73	1.53	-0.80
	7.4	0.99	1.4	1.6	-0.2
	7.4	0.99	1.20	1.60	-0.40
	7.4	0.99	1.07	1.60	-0.53
	7.65	0.97	1.62	1.68	-0.06
	8.0	0.95	1.72	1.86	-0.14
	8.2	0.92	1.67	2.01	-0.34
	8.5	0.85	1.60	2.27	-0.67
	9.2	0.52	2.32	2.91	-0.59
	10.2	0.10	2.98	3.33	-0.35
	11.0	0.02	2.94	3.38	-0.44
	13.0	0.00	3.28	3.40	-0.12

a) From references [32–37].

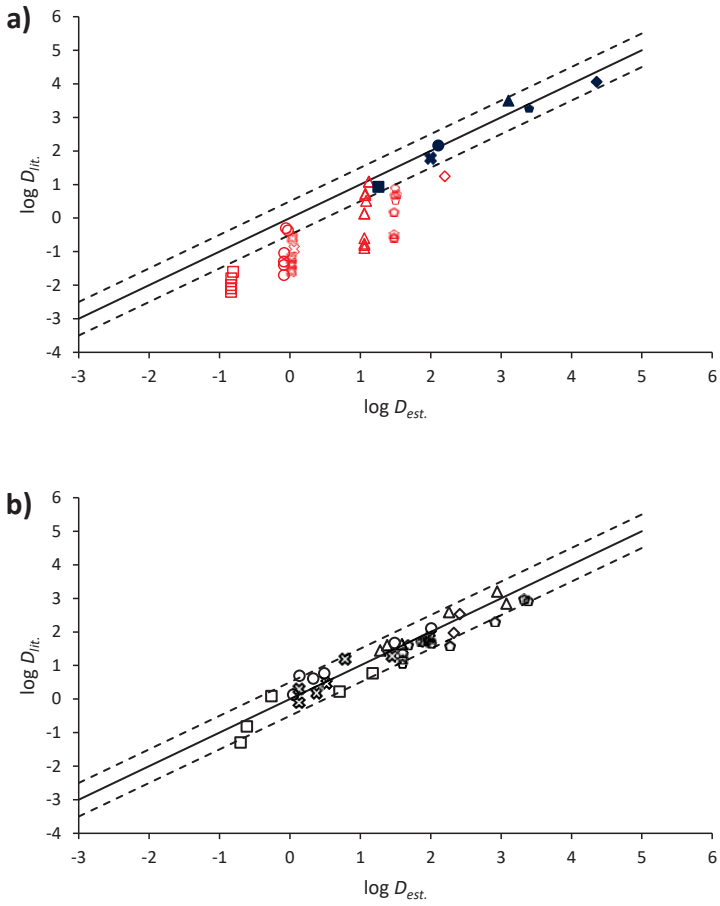

Figure 3. Correlation between the log $D_{o/w}$ from the literature (log $D_{lit.}$) and the log $D_{o/w}$ estimated through the present method (log $D_{est.}$) at different degrees of ionization. Alprenolol (▲), nadolol (■), oxprenolol (●), penbutolol (♦), pindolol (✖), and propranolol (⬟). a) Comparison of the data when the bases are in their neutral form (0-1% of ionization, blue full symbol) or fully ionized (≥99% of ionization, red empty symbol). b) Comparison of the data when the bases are partially ionized (1-99% of ionization). In addition, a line with a slope of 1 and an intercept of 0, and two extra lines corresponding to ±2 SD of the calibration curve (Eq. 15) (which corresponds to the 95% confidence interval) are also shown.

Analysing the results from Figure 3 and Table 4, it can be concluded that, generally, accurate estimated log $D_{o/w}$ values are obtained especially when the compound is in its neutral or partially ionized forms. The error obtained is similar to the one obtained for neutral compounds, as indicated by the error bars. Nonetheless, when the bases are highly or totally ionized ($\alpha \approx 1$) an overestimation of the parameter is observed. Note that when the compound is completely ionized the results are less comparable due to the high dependence of the log $P_{o/w(BH+)}$ value with the solution medium (nature of counter-ions and concentrations as usually ion pairs are formed).

The results obtained in this work agree with the ones published before for acidic compounds when a SDS-MEEKC system was employed [6].

Conclusions

The TTAB-MEEKC system characterized through the solvation parameter model shows great similarity with the octanol-water partition and the SDS-MEEKC systems. Thus, both ME-based systems can be used for log $P_{o/w}$ estimation of neutral solutes.

A good correlation has been obtained between log $P_{o/w}$ data and log k measured in the TTAB-MEEKC system for neutral compounds. Moreover, the applicability of the method has been widen to the estimation of log $D_{o/w}$ of partially ionized bases. Accurate estimated values have been obtained when the compound is neutral or partially ionized (up to a 99% of ionization).

***Acknowledgements**: Financial support from the Ministerio de Economía y Competitividad from the Spanish Government (CTQ2017-88179-P) and the Catalan Government (2017SGR1074) is acknowledged. AFP wishes to thank the University of Barcelona for his APIF PhD fellowship.*

Conflict of interest*: The declare no conflict of interest.*

References

[1] A. Fernández-Pumarega, S. Amézqueta, S. Farré, L. Muñoz-Pascual, M.H. Abraham, E. Fuguet, M. Rosés, Modeling aquatic toxicity through chromatographic systems, *Analytical Chemistry* **89** (2017) 7996–8003.

[2] S. Soriano-Meseguer, E. Fuguet, A. Port, M. Rosés, Estimation of skin permeation by liquid chromatography, *ADMET & DMPK* **6** (2018) 140–152.

[3] M.H. Abraham, C. Treiner, M. Roses, C. Ràfols, Y. Ishihama, Linear free energy relationship analysis of microemulsion electrokinetic chromatographic determination of lipophilicity, *Journal of Chromatography A* **752** (1996) 243–249.

[4] X. Subirats, H.P. Yuan, V. Chaves, N. Marzal, M. Rosés, Microemulsion electrokinetic chromatography as a suitable tool for lipophilicity determination of acidic, neutral, and basic compounds, *Electrophoresis* **37** (2016) 2010–2016.

[5] A. Fernández-Pumarega, S. Amézqueta, E. Fuguet, M. Rosés, Feasibility of the estimation of octanol-water distribution coefficients of acidic drugs by microemulsion electrokinetic chromatography, *ADMET & DMPK* **6** (2018) 55–60.

[6] A. Fernández-Pumarega, S. Amézqueta, E. Fuguet, M. Rosés, Estimation of the octanol-water distribution coefficient of acidic compounds by microemulsion electrokinetic chromatography, *Journal of pharmaceutical and biomedical analysis* (Accepted manuscript).

[7] Y. Ishihama, Y. Oda, N. Asakawa, Hydrophobicity of cationic solutes measured by electrokinetic chromatography with cationic microemulsions, *Analytical Chemistry* **68** (1996) 4281–4284.

[8] A. Fernández-Pumarega, S. Amézqueta, E. Fuguet, M. Rosés, Determination of the retention factor of ionizable compounds in microemulsion electrokinetic chromatography, *Analytica Chimica Acta* **1078** (2019) 221–230.

[9] D.R. Baker, *Capillary electrophoresis*, Wiley, Hoboken, NJ, USA, 1995.

[10] M.G. Khaledi, S.C. Smith, J.K. Strasters, Micellar electrokinetic capillary chromatography of acidic solutes: migration behavior and optimization strategies, *Analytical Chemistry* **63** (1991) 1820–1830.

[11] E. Fuguet, C. Ràfols, E. Bosch, M. Rosés, Solute-solvent interactions in micellar electrokinetic chromatography: IV. Characterization of electroosmotic flow and micellar markers, *Electrophoresis* **23** (2002) 56–66.

[12] M.H. Abraham, Scales of solute hydrogen-bonding: their construction and application to physicochemical and biochemical processes, *Chemical Society Reviews* **22** (1993) 73–83.

[13] E. Fuguet, C. Ràfols, E. Bosch, M.H. Abraham, M. Rosés, Solute-solvent interactions in micellar

electrokinetic chromatography: III. Characterization of the selectivity of micellar electrokinetic chromatography systems, *Journal of Chromatography A* **942** (2002) 237–248.

[14] E. Lázaro, C. Ràfols, M.H. Abraham, M. Rosés, Chromatographic estimation of drug disposition properties by means of immobilized artificial membranes (IAM) and C18 columns, *Journal of Medicinal Chemistry* **49** (2006) 4861–4870.

[15] M. Hidalgo-Rodríguez, E. Fuguet, C. Ràfols, M. Rosés, Estimation of biological properties by means of chromatographic systems: evaluation of the factors that contribute to the variance of biological-chromatographic correlations, *Analytical Chemistry* **82** (2010) 10236–10245.

[16] E.O. Dillingham, R.W. Mast, G.E. Bass, J. Autian, Toxicity of methyl- and halogen-substituted alcohols in tissue culture relative to structure—activity models and acute toxicity in mice, *Journal of Pharmaceutical Sciences* **62** (1973) 22–30.

[17] Bio−Loom, BioByte Corp. (Claremont, CA, USA), http://www.biobyte.com Version 1.7.

[18] T. Sotomatsu, M. Shigemura, Y. Murata, T. Fujita, Octanol/water partition coefficient of ortho-substituted aromatic solutes, *Journal of Pharmaceutical Sciences* **82** (1993) 776–781.

[19] S. Banerjee, S.H. Yalkowsky, C. Valvani, Water solubility and octanol/water partition coefficients of organics. Limitations of the solubility-partition coefficient correlation, *Environmental Science and Technology* **14** (1980) 1227–1229.

[20] J. Li, E.M. Perdue, S.G. Pavlostathis, R. Araujo, Physicochemical properties of selected monoterpenes, *Environment International* **24** (1998) 353–358.

[21] P.R. Rich, R. Harper, Partition coefficients of quinones and hydroquinones and their relation to biochemical reactivity, *FEBS Letters* **269** (1990) 139–144.

[22] D.E. Leszczynski, R.M. Schafer, Nonspecific and metabolic interactions between steroid hormones and human plasma lipoproteins, *Lipids* **25** (1990) 711–718.

[23] D.M. Miller, Evidence that interfacial transport is rate-limiting during passive cell membrane permeation, *Biochimica et Biophysica Acta (BBA) - Biomembranes* **1065** (1991) 75–81.

[24] T. Fujita, J. Iwasa, C. Hansch, A new substituent constant, π, derived from partition coefficients, *Journal of the American Chemical Society* **86** (1964) 5175–5180.

[25] J. Iwasa, T. Fujita, C. Hansch, Substituent constants for aliphatic functions obtained from partition coefficients, *Journal of Medicinal Chemistry* **8** (1965) 150–153.

[26] J. De Bruijn, F. Busser, W. Seinen, J. Hermens, Determination of octanol/water partition coefficients for hydrophobic organic chemicals with the "slow-stirring" method, *Environmental Toxicology and Chemistry* **8** (1989) 499–512.

[27] A. Avdeef, *Absorption and Drug Development: Solubility, Permeability, and Charge State, 2nd edition,* Wiley, Hoboken, NJ, USA, 2012.

[28] A. Andrés, M. Rosés, C. Ràfols, E. Bosch, S. Espinosa, V. Segarra, J.M. Huerta, Setup and validation of shake-flask procedures for the determination of partition coefficients (log D) from low drug amounts, *European Journal of Pharmaceutical Sciences* **76** (2015) 181–191.

[29] L. Hitzel, A.P. Watt, K.L. Locker, An increased throughput method for the determination of partition coefficients, *Pharmaceutical Research* **17** (2000) 1389–1395.

[30] C. Hansch, S.M. Anderson, The effect of intramolecular hydrophobic bonding on partition coefficients, *Journal of Organic Chemistry* **32** (1967) 2583–2586.

[31] M.H. Abraham, H.S. Chadha, G.S. Whiting, R.C. Mitchell, Hydrogen bonding. 32. An analysis of water-octanol and water-alkane partitioning and the Δlog P parameter of seiler, *Journal of Pharmaceutical Sciences* **83** (1994) 1085–1100.

[32] S. Winiwarter, N.M. Bonham, F. Ax, A. Hallberg, H. Lennernäs, A. Karlén, Correlation of human jejunal

permeability (in vivo) of drugs with experimentally and theoretically derived parameters. A multivariate data analysis approach, *Journal of Medicinal Chemistry* **41** (1998) 4939–4949.

[33] F. Barbato, G. Caliendo, M.I. La Rotonda, P. Morrica, C. Silipo, A. Vittoria, Relationships between octanol-water partition data, chromatographic indices and their dependence on pH in a set of beta-adrenoceptor blocking agents, *Farmaco* **45** (1990) 647–663.

[34] M. Recanatini, Partition and distribution coefficients of aryloxypropanolamine β-adrenoceptor antagonists, *Journal of Pharmacy and Pharmacology* **44** (1992) 68–70.

[35] H.S. Huang, R.D. Schoenwald, J.L. Lach, Corneal penetration behavior of β-blocking agents II: assessment of barrier contributions, *Journal of Pharmaceutical Sciences* **72** (1983) 1272–1279.

[36] D. Hellenbrecht, B. Lemmer, G. Wiethold, H. Grobecker, Measurement of hydrophobicity, surface activity, local anaesthesia, and myocardial conduction velocity as quantitative parameters of the non-specific membrane affinity of nine β-adrenergic blocking agents, *Naunyn-Schmiedeberg's Archives of Pharmacology* **277** (1973) 211–226.

[37] N. Gulyaeva, A. Zaslavsky, P. Lechner, M. Chlenov, A. Chait, B. Zaslavsky, Relative hydrophobicity and lipophilicity of β-blockers and related compounds as measured by aqueous two-phase partitioning, octanol – buffer partitioning, and HPLC, *European Journal of Pharmaceutical Sciences* **17** (2002) 81–93.

ARTICLE VII

A Comprehensive Investigation of the Peak Capacity for the Reversed-Phase Gradient Liquid-Chromatographic Analysis of Intact Proteins using a Polymer-Monolithic Capillary Column

Alejandro Fernández-Pumarega, José Luís Dores-Sousa, and Sebastiaan Eeltink

Journal of Chromatography A (2020), volum: 1609

DOI: 10.1016/j.chroma.2019.460462

Journal of Chromatography A 1609 (2020) 460462

Contents lists available at ScienceDirect

Journal of Chromatography A

journal homepage: www.elsevier.com/locate/chroma

A comprehensive investigation of the peak capacity for the reversed-phase gradient liquid-chromatographic analysis of intact proteins using a polymer-monolithic capillary column☆

Alejandro Fernández-Pumarega[a,1], José Luís Dores-Sousa[b,1], Sebastiaan Eeltink[b,*]

[a] Departament d'Enginyeria Química i Química Analítica and Institut de Biomedicina (IBUB), Facultat de Química, Universitat de Barcelona, Barcelona, Spain
[b] Vrije Universiteit Brussel (VUB), Department of Chemical Engineering, Pleinlaan 2, B-1050 Brussels, Belgium

ARTICLE INFO

Article history:
Received 19 July 2019
Revised 13 August 2019
Accepted 16 August 2019
Available online 17 August 2019

Keywords:
Kinetic performance
Van Deemter
Ion-pairing agent
Loadability
Top-down proteomics

ABSTRACT

The present study reports on the analysis of different factors affecting the magnitude of the peak capacity for intact protein separations conducted in gradient reversed-phase liquid chromatography. Experiments were conducted using a 200 µm i.d. capillary styrene-*co*-divinylbenzene monolithic column that was developed in-house and was characterized by a mode globule cluster size of 1.2 µm and a mode macropore size of 1.0 µm (based on scanning electron microscopy). The monolith yielded a minimum plate-height value of 13.3 µm for uracil. The use of trifluoroacetic acid instead of formic acid as ion-pairing agent generally led to better peak symmetry, narrower peak widths which effect is protein-dependent, and improved loadability characteristics. The peak capacity has been systematically assessed at different flow rates and gradient duration. The highest peak capacity of 247 was obtained at a flow rate of 1 µL min^{-1} and a gradient time of 120 min, which corresponds to an optimal t_G/t_0 ratio of ~60. While the optimum van Deemter velocity for intact proteins was approximated to be 0.065 µL min^{-1}, the highest peak capacity was achieved at approximately 20-fold higher flow rate, depending on the gradient duration applied and the molecular weight of the proteins. The optimum velocity increased with decreasing gradient time and is a compromise between the magnitude of the mass-transfer contribution (decreasing the peak capacity with velocity) affected by molecular diffusion, and the increase in peak capacity induced by the more favorable gradient-volume ratio.

1. Introduction

The chromatographic analysis of intact proteins is becoming increasingly important. This is in part because of regulatory guidelines that demand for the comprehensive characterization of emerging biotherapeutics, such as monoclonal antibodies and antibody-drug conjugates, with respect to the primary sequence, impurity profiles including posttranslational modifications, and also higher order structures [1–3]. Reversed-phase gradient LC is the workhorse for protein analysis, allowing the analysis of proteins that cover broad hydrophobicity range and that adequately considers the steep dependency of retention factor and mobile-phase composition using columns that are packed with large-pore (300–1000 Å) silica C_4-modified particles [4,5]. Capillary column formats are readily interfaced to mass spectrometry via electrospray interfacing. Furthermore, current top-down mass-spectrometry approaches, which provide reliable sequence information and databases enabling automated protein identifications, are rapidly expanding [6]. Examples of the current state-of-the-art intact protein separations comprise the work of Wagner et al. who designed superficially porous C_4-particles with wide large-pores (1000 Å) for separation of large biomolecules [4], Shen et al. reported the use of ≥ 1 m-long C_4-core–shell (200–300 Å) columns for top-down proteomics, obtaining high-resolution separations of the proteoforms of a microbial lysate [7], and Kirkland et al., showing fast separations of protein mixtures of 9 and 5 different proteins in less than 2 and 0.33 min, respectively, using core–shell particle packed columns [8].

Polymer-monolithic stationary phases, characterized by interconnected (micro)globular support structure percolated with macropores, have been introduced in 1989 as a viable alternative for protein analysis with packed columns [9]. In this year Svec et al. also demonstrated separation of four intact proteins in 30 s operating large column conduits in RP-LC mode applying a flow rate of 25 mL/min in 1993 [10]. The development of capillary column formats containing poly(styrene-*co*-divinylbenzene)

☆ 48TH International Symposium on High-Performance Liquid Phase Separations and Related Techniques, 16–20 June 2019 in Milan, Italy.

* Corresponding author.
E-mail address: sebastiaan.eeltink@vub.be (S. Eeltink).

[1] These authors contributed equally to this work.

https://doi.org/10.1016/j.chroma.2019.460462
0021-9673/

entities by Huber et al. yielding exquisite separation efficiency is considered a breakthrough in technology, allowing hyphenation of monolith chromatography to mass spectrometric detection [11,12]. In 2014, Vaast et al. demonstrated the development of polymer monolithic nanomaterials compatible with ultra-high pressures allowing for high-resolution protein and peptide gradient separations within sub-minute analysis times [13,14].

To assess the separation performance in gradient mode, peak capacity has been introduced as metric, which is defined as the number of peaks that fit within the gradient window with a fixed resolution [15]. However, to resolve 98% of the analytes that are randomly distributed over the gradient window, the peak capacity must exceed the number of components in the sample by a factor of 100 [16–18]. In an excellent paper, Neue derived a general theoretical model to describe peak capacity for small molecule separations in isocratic and gradient reversed-phase LC mode based on the linear solvent strength (LSS) retention model and peak dispersion induced by the eddy dispersion (*A*-term), longitudinal diffusion (*B*-term), and mass-transfer (*C*-term) contributions [19]. This model was then extended to describe the peak capacity for a wide range of analytes, including peptides, oligonucleotides and oligomers [20–22]. Different experimental studies have been performed in RP-LC mode aiming at maximizing the peak capacity for biomolecule separation [22–25]. Marchetti et al. optimized gradient RP-LC analysis of peptides and concluded that to operate in the relatively low optimal velocity (u_{opt}) also relatively low gradient volume should be applied [23]. In contrast, Wang et al. reported the maximum peak capacity is generated when applying a flow rate higher than u_{opt} [24] and this observation was later confirmed by Petersson et al. for small-molecule and peptide separations [25], and also Neue and Gilar for oligonucleotide separations [22].

The current study focusses on the comprehensive characterization and optimization of the gradient performance for intact protein separations with respect to peak capacity using a capillary polymer-monolithic column prepared from polystyrene and divinylbenzene. First, optimization of system conditions and effect of ion-pairing agents (type and concentration) are discussed. Next, the effects of flow rate and gradient volume on resulting peak capacity were assessed and the validity of Neue's peak capacity model for intact protein analysis was investigated. The effect of molecular weight on the selection of optimal gradient conditions is discussed. Finally, the potential of monolith chromatography for profiling intact proteins and degradation products is demonstrated at optimal gradient conditions.

2. Materials and methods

2.1. Chemicals and materials

2,2′-azobis(2-methylpropionitrile) (AIBN, 98%), 1-decanol (≥ 98%), divinylbenzene (DVB, 80%), styrene (S, ≥ 99%), tetrahydrofuran (THF, anhydrous, inhibitor-free, ≥ 99.9%), toluene (anhydrous, 99.8%), 3-(trimethoxysilyl)propyl methacrylate (98%), and proteins including carbonic anhydrase from bovine erythrocytes (≥ 95%), cytochrome *c* from bovine heart (≥ 95%), cytochrome *c* from equine heart (≥ 95%), insulin from bovine pancreas, lysozyme from chicken egg white (≥ 90%), myoglobin from equine heart (≥ 90%), and ribonuclease A from bovine pancreas were purchased from Sigma-Aldrich (Zwijndrecht, The Netherlands). Aluminum oxide (90 active neutral), hydrochloric acid (32%) and sodium hydroxide pellets, and uracil were purchased from Merck (Darmstadt, Germany). Acetonitrile (ACN, HPLC supra-gradient quality), formic acid (FA, 99%) and trifluoroacetic acid (TFA, 99%) were purchased from Biosolve (Valkenswaard, The Netherlands). Deionized water (18.2 MΩ cm) was purified in-house using a Milli-Q water-purification system (Millipore, Molsheim, France). Polyimide-coated fused-silica capillary tubing (200 µm i.d. × 350 µm o.d.) was purchased from Polymicro Technologies (Molex B.V, Eindhoven, The Netherlands).

2.2. Synthesis of polymer-monolithic capillary columns

To establish a covalent link between the monolithic entity and the capillary wall preventing channeling effects, a surface-modification procedure was followed as previously described in [26]. In summary, the procedure includes i) regeneration of silanol groups by flushing the capillary subsequently with 1 M sodium hydroxide solution during 30 min at 2 µL min^{-1}, flushing with water, and flushing with 1 M hydrochloric acid solution at 2 µL min^{-1} during 30 min; ii) surface modification by flushing the capillary with a solution containing 10% (v/v) 3-(trimethoxysilyl)propyl methacrylate diluted in toluene during 1 h at 2 µL min^{-1}; and iii) removal of unreacted monomer by flushing with toluene. After each flushing step the capillary was dried with air. After completing surface modification, the capillary was filled with the monolithic precursor mixture, composed of 2 wt% AIBN (the initiator), 20 wt% S and 20 wt% DVB (the monomer and the crosslinking monomer, respectively), and a solution of THF and 1-decanol (the porogen), with a monomer to porogen ratio of 40:60 wt%. The polymerization reaction was carried out in a water bath maintained at 70 °C for 24 h to reach complete conversion. After completion of the polymerization reaction, the column was rinsed with ACN.

2.3. Instrumentation and LC conditions

Gradient LC experiments were performed employing an Ultimate 3000 HPLC system (Thermo Fisher Scientific, Germering, Germany) consisting on a dual-ternary pump with a degasser module, a column oven equipped with a 1:100 flow splitter, a well-plate autosampler, and a UV detector with a 3 nL detector flow cell. The connections between the flow splitter, the injection valve and the column were established using 20 µm i.d. fused-silica capillaries. Mobile phase A consisted of 0.1% (v/v) aqueous TFA or FA and mobile phase B of 80:20% (v/v) ACN:water with 0.08% (v/v) TFA or FA. The protein test mixture contained 1–2 µg mL^{-1} of ribonuclease A, insulin, myoglobin, lysozyme, carbonic anhydrase, and cytochrome *c* from bovine and equine, dissolved in mobile phase A. The gradient window was from 25% to 60%B, corresponding to $\Delta c = 0.28$.

All gradient separations were performed using a "direct injection" set-up applying a 1 µL full-loop injection. The column was placed in the column oven thermostated at 37 °C. UV detection was performed at 210 nm, with a 20 Hz data collection rate and 0.12 s response time. Isocratic experiments were conducted to determine the separation efficiency with a 20 nL injection valve and direct attachment of the column on to the valve stator. The capillary column was connected to a 3 nL flow cell equipped with 20 µm i.d. × 100 mm long inlet tubing. Uracil was used as a void (t_0) marker applying 100% mobile phase B.

3. Results and discussion

A polymer styrene-*co*-divinylbenzene monolithic entity was synthesized *in-situ* in a capillary column format with 200 µm i.d., applying a thermally initiated free-radical polymerization. Fig. 1 shows the interconnected globular structure of a high-porosity monolith prepared with a monomer to porogen ration of 40/60 wt%. The monolith, covalently linked to the column wall, spans the cross section and a seemingly homogeneous structure has been obtained. Based on scanning electron micrographs we estimate that the interconnected polymer agglomerates are

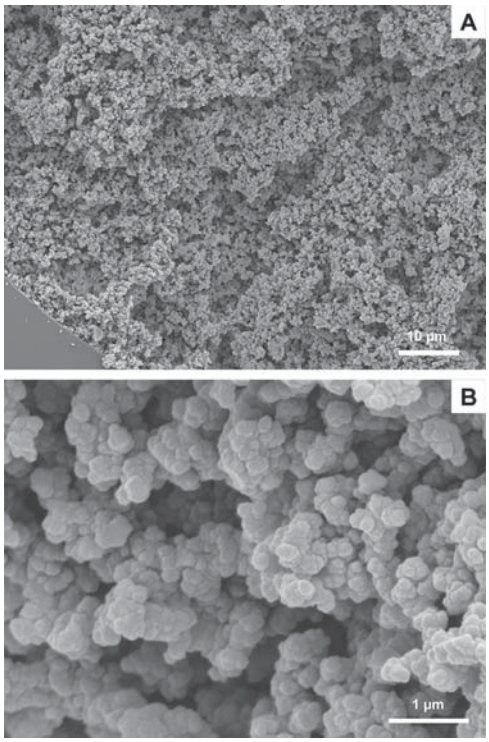

Fig. 1. Scanning electron microscopy (SEM) images of the cross section of a 200 µm i.d. monolithic poly(styrene-*co*-divinylbenzene) capillary column (A) prepared by thermal initiation at 70 °C and composed of a monomer to porogen ratio of 40:60 wt% and a zoom-in (B).

approximately 1.2 µm in diameter and the macropores 1.0 µm obtained from at least 100 measurements, see Fig. S1. The minimum plate height (H_{min}) was determined by injection of uracil used as void marker to be 13.3 µm, with van Deemter characteristics A = 5.9 µm, B = 1.8 mm^2/s, and C_m = 7.1 ms, as determined via non-linear regression, see Fig. S2. The Van Deemter curve for an intact protein with a molecular weight of 22.7 kDa was reconstructed taking into account the molecular diffusion coefficient. The permeability ($K_{v,0}$) was determined based on the Darcy equation to be 7.73×10^{-15} m^2.

Ion-pairing chromatography in RP-LC mode is commonly used to retained ionized biomolecules by the hydrophobic stationary phase. First, the tubing i.d. and flow-cell volume were optimized to minimize the extra-column contribution to band broadening. The effects of type (FA *versus* TFA) and concentration of the ion-pairing agent on protein retention, peak shape, and peak width are demonstrated in Fig. 2. Fig. 2A shows the effect of type of ion-pairing agent applying the same concentration (0.1%) and gradient span (Δc = 0.28). Applying TFA instead of FA increases protein retention, due to the formation of strong ion pairs, which is expected based on the pK_a values (0.23 for TFA *versus* 3.75 for FA). Note, the peak profile of lysozyme was significantly degraded, when FA was used. This seems to be a protein specific effect. Compared to columns packed with porous particles the surface area of polymer monoliths is significantly lower a factor 6 up to 8 depending on the size, number, and agglomeration level of the polymer globules [27], which impairs the loadability. Fig. 2B shows a zoom-in of peak profiles obtained when increasing the injected protein concentration from 1 ppm, to 5 ppm, up to 10 ppm (applying 1 µL full-loop injections). Up to 2.5 ppm the peak width was not affected. Above this threshold the peak width increases linearly with protein mass, but symmetric peak shape was still observed up to 10 ppm. Even when injecting 50 ppm, no carry-over could be detected in the UV trace of subsequent blank gradient runs, which is independent of the type of ion-pairing agent applied. The use of FA negatively influences mass loadability; when injecting 10 ppm insulin an 81% increase in peak width was observed when using 0.1% FA, while only a 19% increase in peak width was observed using TFA as the ion-pairing agent (data not shown).

A model to approximate the peak capacity (n_c) of peptides in gradient mode derived by Neue shows that the peak capacity depends on the gradient steepness defined as the ratio of the

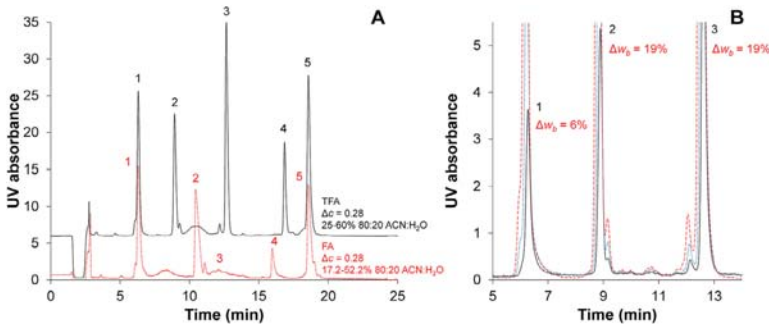

Fig. 2. (A) Separation of (1) ribonuclease A, (2) insulin, (3) lysozyme, (4) myoglobin, and (5) carbonic anhydrase, applying a mobile phase A consisting of 0.1% (v/v) aqueous TFA (black chromatogram) or FA (red dotted chromatogram) and mobile phase B of 80:20% (v/v) ACN:H_2O with 0.08% (v/v) TFA or FA; with a gradient window from 25% to 60% of B when TFA was used, or from 17.2% to 52.2% of B when FA was used (B) Zoom-in of peak profiles of (1) ribonuclease A, (2) insulin, and (3) lysozyme, obtained when injecting protein concentration of 2.5 ppm (black), 5 ppm (blue), and 10 ppm (red), applying a mobile phase A consisting of 0.1% (v/v) aqueous TFA and mobile phase B of 80:20% (v/v) ACN:H_2O with 0.08% (v/v) TFA, gradient window from 25% to 60% of B, injection volume of 1 µL, column temperature at 37 °C, and detection at 210 nm. The Δw_b refers to the difference in the peak width at the base, between the protein concentration of 10 and 2.5 ppm. (For interpretation of the references to color in this figure legend, the reader is referred to the web version of this article.)

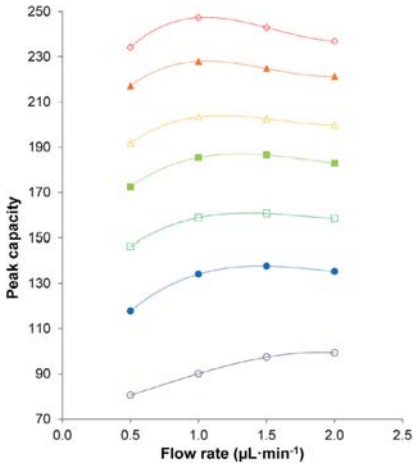

Fig. 3. Effect of gradient time and flow rate on the average peak capacity measured on a 200 µm i.d. × 100 mm long monolithic poly(styrene-*co*-divinylbenzene) capillary column. Experimental conditions similar as in Fig. 2B with 0.1% TFA in the mobile phase. The average peak-capacity values were calculated using equation $n_c = (t_G/W_b)+1$, applying gradient times of 10 min. (○), 20 min. (●), 30 min. (□), 45 min. (■), 60 min. (△), 90 min. (▲), 120 min. (◊).

gradient time and the column dead time (t_G/t_0) the solvent-strength parameter (S), and of the column efficiency (N), according to [22]:

$$n_c = 1 + \frac{\sqrt{N}}{4} \cdot \frac{S \cdot \Delta c}{S \cdot \Delta c \cdot \frac{t_0}{t_g} + 1} \quad (1)$$

where S is defined as the slope of the linear dependency of ln k *versus* the volume fraction of organic solvent in the mobile phase. S values ranged between 131.9 for carbonic anhydrase (MW ~ 30.0 kDa) and 48.5 for insulin (MW ~ 5.8 kDa), respectively, see Fig. S3. The isocratic plate count (N) can be expressed as a function of operating parameter, *i.e.*, column length (L), and domain size (d_{dom}) approximated as the sum of the mode globule size and mode macropore size, and the (reduced) a-, b-, and c_m-term contributions of the van Deemter equation:

$$N = \frac{L}{a \cdot d_{dom} + \frac{b \cdot D_m \cdot t_0}{L} + c_m \cdot \frac{{d_{dom}}^2}{D_m} \cdot \frac{L}{t_0}} \quad (2)$$

where D_m is the diffusion coefficient. Note that the convective transport in a monolith (or any support structure operated at laminar flow conditions) occurs parallel with the surface. Also, the stationary-phase mass-transfer contribution (C_s-term) is merely absent, since this type of polymer monolith contains a very limited fraction of meso- and micropores, and these pores are generally not accessible for large molecules [28].

The gradient performance was assessed for the separation of a mixture of intact proteins with molecular weights ranging between 5.8 and 22.7 kDa, yielding diffusion coefficients between 12 and 9 × 10^{-11} m^2 s^{-1}, based on the methodology of laminar flow analysis [29]. The gradient time and flow rate were systematically varied and the corresponding experimental peak capacities were determined from the average peak width at half height ($W_{1/2}$) recorded for mixture of 7 proteins. A linear increase in peak width was obtained as function of gradient time (independent of flow rate), resulting in a steep initial increase in peak capacity between t_G 5 and 60 min, and at longer gradient times the peak capacity increase levels off, see Fig S4. A maximum peak capacity of approximately 250 was observed applying a gradient time of 120 min. Although the peak capacity can be moderately increased by using longer gradient duration, such a gain in overall performance can only obtained at the expense of a significantly lower peak production rate (peak-capacity-per-unit time). Fig. 3 shows the average peak capacity as function of the flow rate and applying different gradient duration (between 10 min and 120 min). Fig. S5A and B shows the data for carbonic anhydrase and insulin. The trendline has been constructed based on Eqs. (1) and (2) with the van Deemter parameters, determined for uracil and recalculated based on reduced a-, b-, and c-terms and considering the diffusion coefficients and experimentally-determined S value. Neue's model provides a reasonable estimation for carbonic anhydrase, however the experimental peak capacities for insulin are much higher than predicted for insulin. Note that Neue's model assumes the validity of the linear solvent-strength (LSS) model to describe protein retention, which may lead to a significant underestimation of S, which in turn leads to an underestimation of n_c.

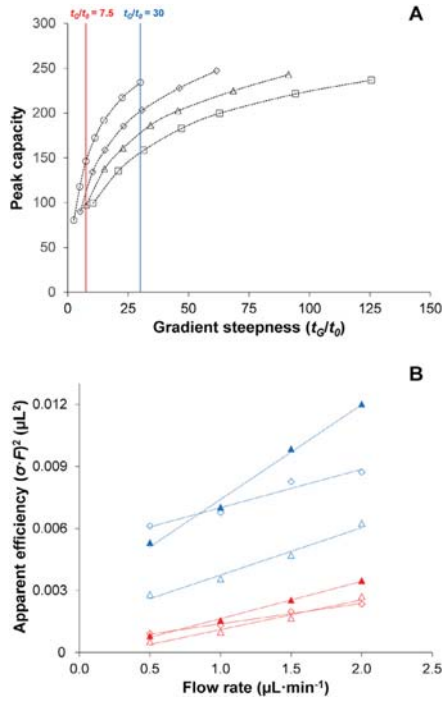

Fig. 4. Effect of gradient volume on separation performance as function of flow rate. (A) Shows the average peak capacity as function of t_G/t_0 employing different flow rates: 0.5 µL min^{-1} (circles), 1.0 µL min^{-1} (diamonds), 1.5 µL min^{-1} (triangles), 2.0 µL min^{-1} (squares). The vertical lines indicate performance data for t_G/t_0 = 7.5 and 30, respectively. (B) Depicts the effect of diffusion coefficients of intact proteins on apparent efficiency (C-term effect) as a function of flow rate for t_G/t_0 = 7.5 and 30. Solid triangles = carbonic anhydrase, open triangles = ribonuclease A, open diamonds = insulin. Experimental conditions similar as in Fig. 2B with 0.1% TFA in the mobile phase.

Fig. 3 shows that fixing the flow rate and increasing t_G leads to a higher peak capacity, as predicted by Eq. (1). The representation depicted in Fig. 3 also shows that the maximum peak capacities are reached when applying flow rates of 1 µL min^{-1} or higher, and that the optimal mobile-phase velocity yielding maximum peak capacity strongly depends on gradient duration applied. The

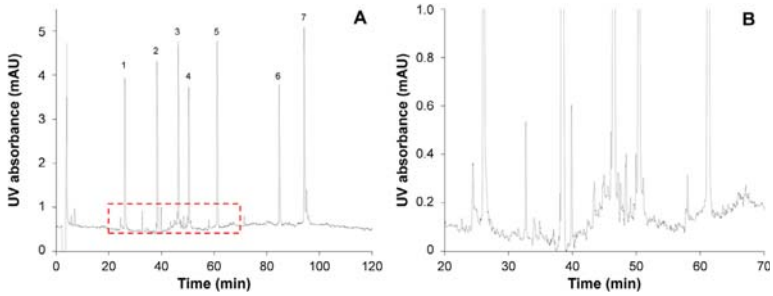

Fig. 5. Separation of a mixture of intact proteins and its degradation products at a flow rate of 1 µL min^{-1} and gradient time of 120 min with $\Delta c = 0.28$ and a column temperature at 37 °C (A) and a zoom-in of the peak profiles (B). Peak identification: (1) ribonuclease A, (2) insulin, (3) cytochrome *c* equine, (4) cytochrome *c* bovine, (5) lysozyme, (6) myoglobin, and (7) carbonic anhydrase.

optimum flow rate at a gradient duration of 120 min was obtained at a flow rate of 1 µL min^{-1}, which corresponds to an optimal t_G/t_0 ratio of ~60. The optimum velocity increases with decreasing gradient time. The optimal volumetric flow rate (F_{opt}) when applying a gradient of 10 min was observed at 2 µL min^{-1}, which corresponds to an optimal t_G/t_0 ratio of ~10. The effect of flow rate on peak capacity was also assessed for individual proteins, *i.e.*, carbonic anhydrase (MW = 30.0 kDa), ribonuclease A (MW = 13.7 kDa), and insulin (MW = 5.8 kDa). The optimal mobile-phase velocity depends on the molecular weight. With increasing molecular weight D_m decreases and the optimal flow velocity (F_{opt}) shifts to low velocity, as can be expected based on the van Deemter curve.

To assess the effect of flow rate on *N*, which in turn affects the magnitude of n_c the average peak capacity is plotted as function of t_G/t_0, while operating the column at different flow rates, see Fig. 4A. When comparing the performance at a fixed t_G/t_0 value, *i.e.*, $t_G/t_0 = 30$, it is observed that the peak capacity decreases when applying higher flow rates. This effect can be mainly attributed to the effect of mobile-phase velocity on the magnitude of the mobile-phase mass-transfer (C_m-term) contribution. Based on the van Deemter data depicted in Fig. S2 it is anticipated that the optimum van Deemter flow rate for intact proteins is reached at a flow rate below 0.1 µL min^1. Hence, at flow rates of 0.5 µL min^{-1} and above, the column is operated in the *C*-term region of the van Deemter curve. When plotting the $(\sigma \cdot \text{flow rate})^2$ values, that are proportional to apparent plate height, as function of flow rate (see Fig. 4B) an increase in the slope is observed, representing the resistance to mass transfer (*C*-term) contributions in gradient mode for three individual proteins, *i.e.*, carbonic anhydrase, ribonuclease A, and insulin. With increasing molecular weight an increase in slope is observed, as the plate height in the *C*-term region of the van Deemter curve is inversely proportional to D_m. Note that the molecular-diffusion coefficients do not correlate with the apparent efficiency, see also Fig. S6 for a wider range of intact proteins. Fig. 4B also demonstrates that the gradient volume, defined by the gradient span (Δc) and the t_G/t_0 ratio, has a large effect on the resulting peak variance.

Fig. 5 shows the potential of the capillary polymer-monolithic columns for profiling intact proteins and their impurities/degradation products, yielding an average peak capacity of 247. The separation was conducted at a flow rate of 1 µL min^{-1}, applying a gradient time of 120 min, and optimizing Δc (= 0.28) to maximize peak coverage within the gradient span. The zoom-in between the 30- and 70-min timeslot demonstrates the very-high resolving power.

4. Concluding remarks

The peak capacity in gradient LC is a trade-off between, on the one hand, the flow rate affecting the peak capacity via the plate number, and on the other hand the effect of flow rate affecting the gradient volume, defined by t_G/t_0. To maximize the peak capacity in gradient mode the use of faster than optimal (van Deemter) flow rates is encouraged, since this effectively leads to shallower gradients. In our study, the highest peak capacity for intact proteins in gradient mode applying the monolithic capillary column was achieved at flow rates a factor 10–20 higher than u_{opt}. By using a highly-efficient monolithic column, the mass transfer (C-term) contribution to band broadening is relatively low. Hence, the loss in efficiency at elevated flow rates is only modest, and also depends on the diffusion coefficient of the proteins. Note that the resulting peak capacity also depends on gradient slope. At a flow rate of 1 µL min^{-1} and a gradient time of 120 min, the magnitude of the peak capacity is dominated by the effect of gradient volume. When increasing the flow rate further, the peak capacity decreases because of the dominating *C*-term contribution to band broadening. When applying short 10 min gradients the optimal gradient flow rate is reached at 2 µL min^{-1}. With other words, for very shallow gradients, the optimal flow rate approaches the optimal van Deemter flow rate as measured in isocratic mode.

Declaration of Competing Interest

None.

Acknowledgments

JLDS and SE acknowledge grants of the Research Foundation Flanders (FWO – grant no. G025916N and G033018N). AFP wishes to thank the University of Barcelona for his APIF PhD fellowship. The authors thank Dr. Martin Gilar (Waters Corporation, Milford, USA) for helpful discussions.

Supplementary materials

Supplementary material associated with this article can be found, in the online version, at doi:10.1016/j.chroma.2019.460462.

References

[1] A. Wagh, H. Song, M. Zeng, L. Tao, T.K. Das, Challenges and new frontiers in analytical characterization of antibody-drug conjugates, MAbs 10 (2018) 222–243.

[2] European Medicines Agency, Guideline on development, production, characterisation and specification for monoclonal antibodies and related products. https://www.ema.europa.eu/en/development-production-characterisation-specifications-monoclonal-antibodies-related-products, 2016 (accessed Accessed 01 May 2019).
[3] M. Tassi, J. De Vos, S. Chatterjee, F. Sobott, J. Bones, S. Eeltink, Advances in native high-performance liquid chromatography and intact mass spectrometry for the characterization of biopharmaceutical products, J. Sep. Sci. 41 (2018) 125–144.
[4] B.M. Wagner, S.A. Schuster, B.E. Boyes, T.J. Shields, W.L. Miles, M.J. Haynes, R.E. Moran, J.J. Kirkland, M.R. Schure, Superficially porous particles with 1000 Å pores for large biomolecule high performance liquid chromatography and polymer size exclusion chromatography, J. Chromatogr. A 1489 (2017) 75–85.
[5] S.A. Schuster, B.M. Wagner, B.E. Boyes, J.J. Kirkland, Optimized superficially porous particles for protein separations, J. Chromatogr. A 1315 (2013) 118–126.
[6] J.S. Cottrell, Protein identification using MS/MS data, J. Proteom. 74 (2011) 1842–1851.
[7] Y. Shen, N. Tolić, P.D. Piehowski, A.K. Shukla, S. Kim, R. Zhao, Y. Qu, E. Robinson, R.D. Smith, L. Paša-Tolić, High-resolution ultrahigh-pressure long column reversed-phase liquid chromatography for top-down proteomics, J. Chromatogr. A 1498 (2017) 99–110.
[8] J.J. Kirkland, F.A. Truszkowski, C.H. Dilks Jr., G.S. Engel, Superficially porous silica microspheres for fast high-performance liquid chromatography of macromolecules, J. Chromatogr. A 890 (2000) 3–13.
[9] F. Svec, Monolithic columns: a historical overview, Electrophoresis 38 (2017) 2810–2820.
[10] Q.C. Wang, F. Svec, J.M.J. Fréchet, Macroporous polymeric stationary-phase rod as continuous separation medium for reversed-phase chromatography, Anal. Chem. 65 (1993) 2243–2248.
[11] H. Oberacher, C.G. Huber, Capillary monoliths for the analysis of nucleic acids by high-performance liquid chromatography-electrospray ionization mass spectrometry, TrAC – Trends Anal. Chem. 21 (2002) 166–174, doi:10.1016/S0165-9936(02)00304-7.
[12] A. Premstaller, H. Oberacher, W. Walcher, A.M. Timperio, L. Zolla, J. Chervet, N. Cavusoglu, A. Van Dorsselaer, C.G. Huber, High-performance liquid chromatography – electrospray ionization mass spectrometry using monolithic capillary columns for proteomic studies, Anal. Chem. 73 (2001) 2390–2396.
[13] A. Vaast, E. Tyteca, G. Desmet, P.J. Schoenmakers, S. Eeltink, Gradient-elution parameters in capillary liquid chromatography for high-speed separations of peptides and intact proteins, J. Chromatogr. A 1355 (2014) 149–157.
[14] A. Vaast, H. Terryn, F. Svec, S. Eeltink, Nanostructured porous polymer monolithic columns for capillary liquid chromatography of peptides, J. Chromatogr. A 1374 (2014) 171–179, doi:10.1016/j.chroma.2014.11.063.
[15] L.R. Snyder, J.W. Dolan, High-Performance Gradient Elution: The Practical Application of the Linear-Solvent-Strength Model, Wiley, Hoboken, NJ, USA, 2007.
[16] J.C. Giddings, Sample dimensionality: a predictor of order-disorder in component peak distribution in multidimensional separation, J. Chromatogr. A 703 (1995) 3–15.
[17] J.M. Davis, P.W. Carr, Effective saturation: a more informative metric for comparing peak separation in one- and two-dimensional separations, Anal. Chem. 81 (2009) 1198–1207.
[18] J.M. Davis, J.C. Giddings, Origin and characterization of departures from the statistical model of component-peak overlap in chromatography, J. Chromatogr. A 289 (1984) 277–298.
[19] U.D. Neue, Theory of peak capacity in gradient elution, J. Chromatogr. A 1079 (2005) 153–161.
[20] H. Liu, J.W. Finch, J.A. Luongo, G.Z. Li, J.C. Gebler, Development of an on-line two-dimensional nano-scale liquid chromatography/mass spectrometry method for improved chromatographic performance and hydrophobic peptide recovery, J. Chromatogr. A 1135 (2006) 43–51.
[21] H. Liu, J.W. Finch, M.J. Lavallee, R.A. Collamati, C.C. Benevides, J.C. Gebler, Effects of column length, particle size, gradient length and flow rate on peak capacity of nano-scale liquid chromatography for peptide separations, J. Chromatogr. A 1147 (2007) 30–36.
[22] M. Gilar, U.D. Neue, Peak capacity in gradient reversed-phase liquid chromatography of biopolymers. Theoretical and practical implications for the separation of oligonucleotides, J. Chromatogr. A 1169 (2007) 139–150.
[23] N. Marchetti, A. Cavazzini, F. Gritti, G. Guiochon, Gradient elution separation and peak capacity of columns packed with porous shell particles, J. Chromatogr. A 1163 (2007) 203–211.
[24] X. Wang, D.R. Stoll, A.P. Schellinger, P.W. Carr, Peak capacity optimization of peptide separations in reversed-phase gradient elution chromatography: fixed column format, Anal. Chem. 78 (2006) 3406–3416.
[25] P. Petersson, A. Frank, J. Heaton, M.R. Euerby, Maximizing peak capacity and separation speed in liquid chromatography, J. Sep. Sci. 31 (2008) 2346–2357.
[26] J. Courtois, M. Szumski, E. Byström, A. Iwasiewicz, A. Shchukarev, K. Irgum, A study of surface modification and anchoring techniques used in the preparation of monolithic microcolumns in fused silica capillaries, J. Sep. Sci. 29 (2006) 14–24.
[27] S. Eeltink, J.M. Herrero-Martinez, G.P. Rozing, P.J. Schoenmakers, W.T. Kok, Tailoring the morphology of methacrylate ester-based monoliths for optimum efficiency in liquid chromatography, Anal. Chem. 77 (2005) 7342–7347.
[28] S. Wouters, T. Hauffman, M.C. Mittelmeijer-Hazeleger, G. Rothenberg, G. Desmet, G.V. Baron, S. Eeltink, Comprehensive study of the macropore and mesopore size distributions in polymer monoliths using complementary physical characterization techniques and liquid chromatography, J. Sep. Sci. 39 (2016) 4492–4501.
[29] R.R. Walters, J.F. Graham, R.M. Moore, D.J. Anderson, Protein diffusion coefficient measurements by laminar flow analysis: method and applications, Anal. Biochem. 140 (1984) 190–195.

Supplementary information for:

A comprehensive investigation of the peak capacity for the reversed-phase gradient liquid-chromatographic analysis of intact proteins using a polymer-monolithic capillary column

Alejandro Fernández-Pumarega[1‡], José Luís Dores-Sousa[2‡], Sebastiaan Eeltink[2,*]

[1]Departament d'Enginyeria Química i Química Analítica and Institut de Biomedicina (IBUB), Facultat de Química, Universitat de Barcelona, Barcelona, Spain

[2]Vrije Universiteit Brussel (VUB), Department of Chemical Engineering, Brussels, Belgium

(‡) These authors contributed equally to this work.

(*) Corresponding author

Pleinlaan 2, B-1050, Brussels, Belgium

Tel.: +32 (0)2 629 3324, Fax: +32 (0)2 629 3248, E-mail: sebastiaan.eeltink@vub.be

The frequency distribution of the globule size and pore diameter depicted in Fig. S1 was estimated based on scanning electron micrographs. Cross sections of monolithic capillary columns were sputtered with 6 nm of Pt-Pd using a 208 HR sputter coater equipped with a Cressington mtm 20 Thickeness Controller (Cressington Scientific Instruments, Watford, UK). A JSM-6400 field emission scanning electron microscope (JEOL, Tokyo, Japan) was operated at acceleration voltages of 5 kV.

To determine the globule sizes, the SEM pictures were uploaded in ImageJ (NIH, USA) and straight lines ($n \geq 100$), corresponding to the diameter of the globules were manually drawn. The length of the straight lines was subsequently analyzed via the software. This procedure was repeated to determine the macropore size. Note, that this is only a rough estimation of the characteristic feature size.

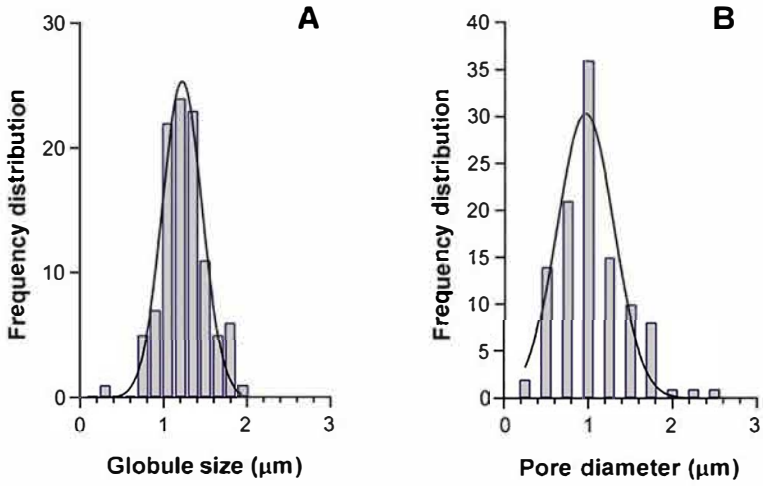

Figure S1. Frequency distribution of the globule size (A) and pore diameter (B) estimated based on scanning electron micrographs (SEM), obtained from $n \geq 100$. The line shows a fitted Gaussian distribution based on the frequency distribution with 95% confidence interval.

The separation efficiency as function of flow rate (van Deemter curve) was recorded by injecting uracil as the t_0-marker applying a mobile phase of 80:20% (v/v) ACN:H_2O, see Fig. S2. Note the experimental was set-up to minimize the extra-column dispersion, *i.e.* using a 4 nL injection valve, the column directly connected at the stator, and applying a 3 nL UV flow cell. The van Deemter curve representing a protein was constructed by reducing the plate height based on the domain size (sum of the mode globule and macropore size) of the monolithic column and applying the diffusion coefficient of a protein with a molecular weight of 22.7 kDa. This corresponds to a diffusion coefficient of 9×10^{-11} $m^2 \cdot s^{-1}$, based on the methodology of laminar flow analysis [1]. Based on this transformation it can be observed that the optimal flow velocity for a protein is a factor 7 lower than that of a small molecule, *i.e.*, uracil.

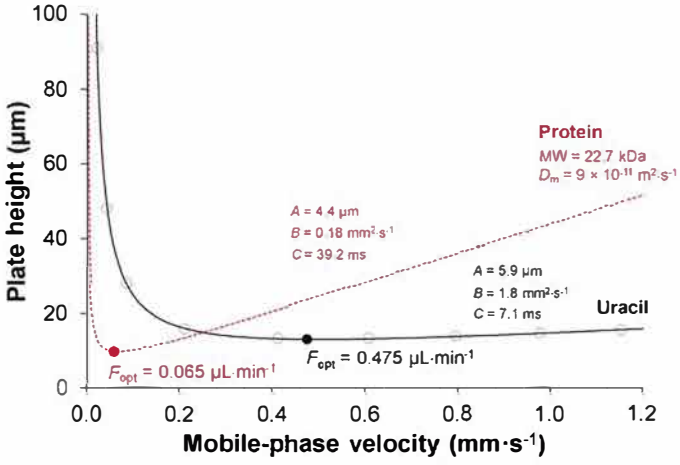

Figure S2. Van Deemter curve recorded for uracil while applying 80:20% (v/v) ACN:H_2O on the poly(styrene-*co*-divinylbenzene) monolithic column. The van Deemter curve for the protein was reconstructed considering the difference in molecular diffusion coefficient.

Fig. S3 shows the ln k vs. ϕ plots of insulin and carbonic anhydrase recorded in isocratic mode applying a flow rate of 1.5 $\mu L \cdot min^{-1}$. The S value is analyte depended and is the slope of this curve.

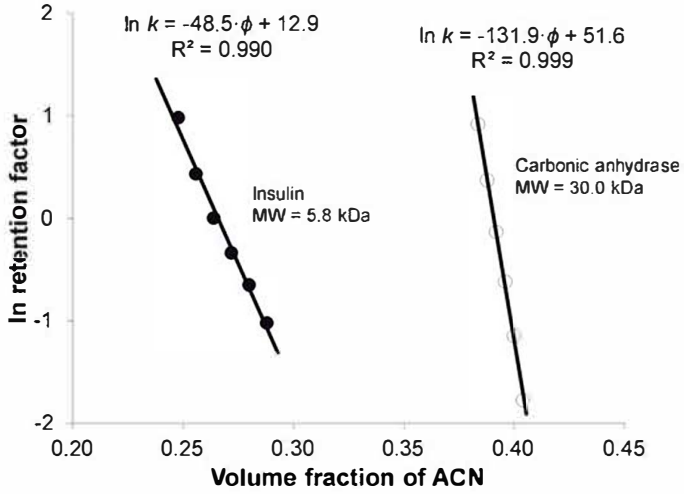

Figure S3. Plots of natural logarithm of retention factor (ln k) as function of the volume fraction, ϕ, of ACN in the mobile phase of insulin (closed symbols) and carbonic anhydrase (open symbols).

Fig. S4 shows the experimental peak capacity recoreded for intact proteins on a monolithic column as function of flow rate and gradient time. The peak capacty was calculated according $n_c = t_G/W + 1$.

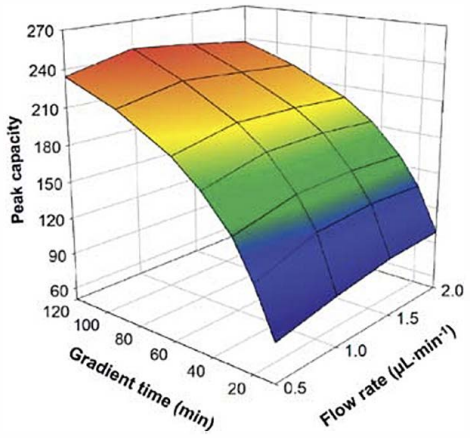

Figure S4. The experimental peak capacites recorded on a poly(styrene-*co*-divinylbenzene) monolithic column as function of flow rate and gradient time using 0.1% TFA as ion pairing agent.

Fig. S5 shows the fit of experimental data applying Neue's model (Eqs. 1 and 2 in the main manuscript). While a reasonable first estimation was obtained for carbonic anhydrase the experimental values for insulin were significantly higher than that predicted with Neue's model. This may be due to an underestimation of the magnitude of the S value. When doubling the S value for insulin 48.5 (experimentally determined) to 97 to fit appears more the fit appears to be a better predictor.

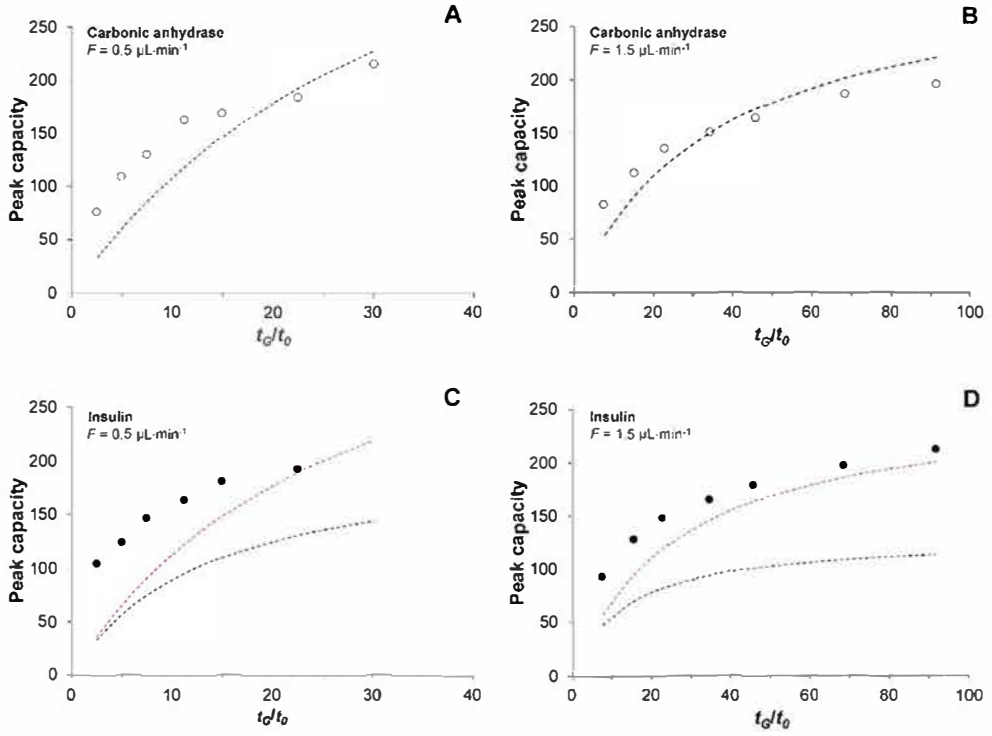

Figure S5. Experimental peak capacity data for carbonic anhydrase and insulin applying flow rates of 0.5 and 15 µL·min^{-1} respectively. The black fits (dotted lines) were obtained applying S values experimentally determined and reported in Fig S3. The red fit (dotted line for insulin only) was obtained by doubling the experimental S value.

Fig. S6 shows the gradient performance for individual proteins as function of flow rate visualizing the effect of mass-transfer (C-term) contribution to the efficiency in gradient mode. Note that the molecular-diffusion coefficients do not directly correlate to the apparent efficiency

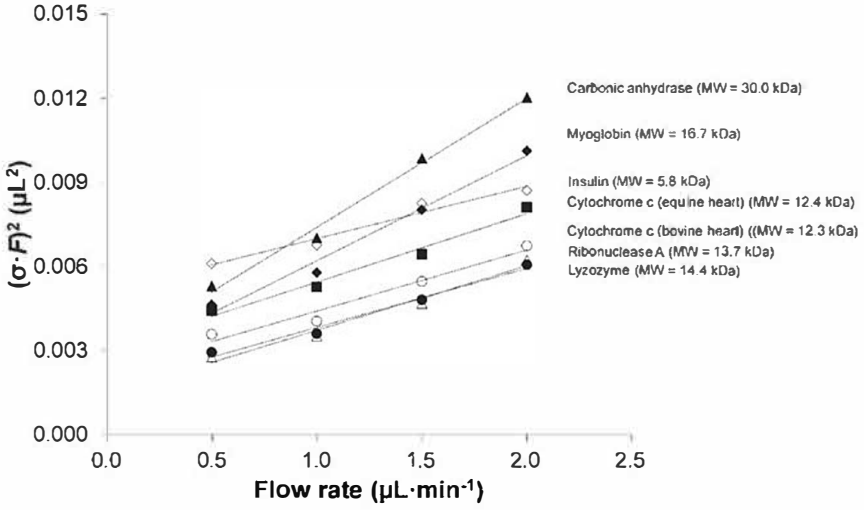

Figure S6. Effect of flow rate on apparent efficiency, corresponding to the volumetric peak variance, as measured in gradient mode for individual proteins

Reference

[1] R.R. Walters, J.F. Graham, R.M. Moore, D.J. Anderson, Protein diffusion coefficient measurements by laminar flow analysis: Method and applications, Anal. Biochem. 140 (1984) 190–195

RESULTATS I DISCUSSIÓ

6.1 Estimació de propietats de biopartició de substàncies neutres.

6.1.1 Caracterització de nous sistemes de partició cromatogràfics a partir del model de paràmetres de solvatació

L'estimació de propietats de biopartició de compostos neutres a partir de sistemes fisicoquímics, com s'ha dit anteriorment, és d'un gran interès ambiental i farmacèutic. Per aquest motiu, el desenvolupament i caracterització per un mateix model (com podria ser el SPM) de nous sistemes cromatogràfics és important. Durant els últims anys s'han caracteritzat a partir del SPM una gran quantitat de sistemes cromatogràfics i electrocinètics (especialment sistemes basats en MEKC), alguns dels quals es mostren a la Taula 2. Per això, en aquest treball s'ha buscat desenvolupar i caracteritzar nous sistemes fisicoquímics, principalment sistemes basats en MEs i en preparats liposòmics, que puguin tenir diferents selectivitats, i que permetin l'emulació de sistemes de biopartició. En aquest treball s'han desenvolupat i caracteritzat 4 sistemes de partició cromatogràfics addicionals: un sistema LEKC (basat en preparats liposòmics de lecitina de soja), 2 sistemes MEEKC (un basat en lecitina de soja i l'altre utilitzant TTAB com a tensioactiu), i finalment un sistema MELC (basat també en microemulsions preparades a partir de lecitina de soja). S'han caracteritzat aquests sistemes, ja que, per una banda, els sistemes basats en preparats de lecitina de soja (dissenyats per preparar o bé liposomes o bé microemulsions) són senzills, ràpids de preparar i la seva composició és molt similar a la de les membranes biològiques cel·lulars i, per l'altra, no hi ha molts sistemes basats en microemulsions caracteritzats a partir del SPM.

Per caracteritzar els nous sistemes de partició s'ha utilitzat un grup representatiu de 71 soluts neutres a p*H* 7,0 dels quals es coneixen els seus descriptors [78,79]. La propietat de partició dels sistemes cromatogràfics caracteritzats en aquest treball és el factor de retenció, que s'ha calculat a partir de les Eqs. 4 i 11, respectivament, per sistemes EKC i MELC. Seguidament, a partir d'una regressió lineal múltiple entre *k* i els descriptors dels soluts, s'han obtingut els coeficients dels sistemes. A la Taula 4 es mostren els paràmetres obtinguts en la caracterització pel model SPM d'aquests 4 sistemes de partició, les dades estadístiques i els coeficients normalitzats calculats

a partir de les Eqs. 13-18. A més, a la Taula 5 s'inclouen les distàncies calculades entre els sistemes caracteritzats de la Taula 4 a partir de l'Eq. 19.

Tal com s'observava per altres sistemes cromatogràfics caracteritzats a partir del SPM (Taula 2), els principals coeficients que defineixen la partició dels soluts entre les dues fases dels sistemes són el volum de McGowan (*v*) i l'acidesa per pont d'hidrogen (*b*). La resta de coeficients presenten també la mateixa tendència, valors de *e* positius i *s* negatius; és amb el coeficient *a* on una altra vegada es veu una major variabilitat. Els sistemes TTABME, LMEEKC i LLEKC tenen coeficients *a* positius que indiquen que la fase pseudoestacionària té una major basicitat per pont d'hidrogen que no pas la fase aquosa. En canvi, en el sistema LMELC, que presenta valors negatius, passa al contrari. La lecitina, que forma part de la fase mòbil, presenta un caràcter més bàsic que no pas la columna C18 que conforma la fase estacionària.

Pel que fa als sistemes basats en lecitina de soja, encara que en LMEEKC i LLEKC la lecitina conforma la fase pseudoestacionària i en LMELC la lecitina forma part de la fase mòbil, s'observen uns coeficients normalitzats molt similars entre si i un paràmetre de distància *d* inferior a 0,25, que evidencien una gran similitud entre aquests sistemes. Aquesta similitud indica que la lecitina podria recobrir la superfície de les cadenes d'octadecilsilà de la columna C18 i actuar com a fase estacionària. En relació al sistema TTABME, aquest mostra també una gran similitud amb els sistemes preparats a partir de la lecitina de soja. Això no és estrany, ja que les microemulsions de TTAB estan formades per components com l'oli que tenen trets estructurals similars als dels fosfolípids.

6.1.2 Comparació dels sistemes caracteritzats amb altres sistemes fisicoquímics

Primerament, s'han comparat els sistemes caracteritzats en aquest treball (Taula 4) amb un conjunt de sistemes fisicoquímics diversos compilats a la Taula 2, que inclouen sistemes basats en cadascuna de les tècniques següents: RP-LC, MEKC, MEEKC, LEKC, VEKC, poly-EKC i MELC. Els sistemes han estat comparats considerant els coeficients normalitzats (Eqs. 13-18) a partir del càlcul paràmetre de

Taula 4. Dades estadístiques i coeficients dels sistemes cromatogràfics caracteritzats a partir del model SPM. Entre parèntesis es mostra la desviació estàndard de cadascun dels coeficients.

Sistema de partició	*SP*	Coeficients						Coeficients normalitzats					Paràmetres estadístics			
		c	***e***	***s***	***a***	***b***	***v***	e_u	s_u	a_u	b_u	v_u	**n**	**R^2**	**SD**	**F**
TTAB MEEKC (TTABME)	log k_{EKC}	-0,96 (0,05)	0,44 (0,08)	-0,63 (0,06)	0,20 (0,05)	-2,13 (0,07)	2,36 (0,06)	0,13	-0,19	0,06	-0,65	0,72	59	0,972	0,12	368
Lecitina MELC (LMELC)	log k_{HPLC}	0,53 (0,05)	0,25 (0,07)	-0,59 (0,04)	-0,21 (0,04)	-1,98 (0,06)	2,08 (0,06)	0,09	-0,20	-0,07	-0,67	0,71	39	0,984	0,08	410
Lecitina MEEKC (LMEEKC)	log k_{EKC}	-2,22 (0,10)	0,43 (0,10)	-0,62 (0,07)	0,33 (0,07)	-3,71 (0,16)	3,32 (0,12)	0,09	-0,12	0,07	-0,74	0,66	47	0,937	0,13	246
Lecitina LEKC (LLEKC)	log k_{EKC}	-1,87 (0,08)	0,89 (0,12)	-0,81 (0,08)	0,34 (0,07)	-2,87 (0,11)	2,81 (0,09)	0,21	-0,19	0,08	-0,68	0,67	46	0,968	0,13	241

Taula 5. Paràmetre de distància *d* entre els sistemes de partició cromatogràfics de la Taula 4.

Sistema de partició	TTABME	LLEKC	LMEEKC	LMELC
TTABME	-	0,10	0,13	0,14
LLEKC	0,10	-	0,15	0,20
LMEEKC	0,13	0,15	-	0,18
LMELC	0,14	0,20	0,18	-

distància *d* (Eq. 19), d'un dendrograma (Figura 16) i d'un PCA (Figura 17). Per una banda, el paràmetre de distància *d* ens permet comparar individualment la similitud dels sistemes caracteritzats en aquest treball amb cadascun dels sistemes cromatogràfics escollits, i, per l'altra, a partir del dendrograma i del PCA es pot veure com s'agrupen aquells sistemes que presenten selectivitats similars. A l'hora d'establir el dendrograma, s'han agrupat els sistemes en funció del paràmetre de distància *d* (distància euclidiana) i el mètode *weighted-linkage*.

Taula 6. Paràmetre de distància *d* calculat entre els sistemes caracteritzats en aquest treball (Taula 4) i altres sistemes cromatogràfics (Taula 2). Els valors inferiors a 0,25 es troben en negreta.

Sistema de partició	TTABME	LLEKC	LMEEKC	LMELC
RP18	**0,18**	**0,22**	**0,20**	**0,05**
IAM	**0,08**	**0,04**	**0,12**	**0,18**
PLM	**0,06**	**0,10**	**0,07**	**0,16**
SDS	**0,23**	0,29	0,33	**0,22**
SLN	**0,12**	**0,18**	**0,18**	**0,23**
STC	**0,09**	**0,06**	**0,11**	**0,20**
TTAB	**0,18**	**0,14**	**0,23**	0,32
SDSbrij	**0,07**	**0,09**	**0,11**	**0,18**
SDS0.8	0,48	0,50	0,50	0,36
SDS1.6	0,66	0,69	0,69	0,54
Brij C18	0,40	0,45	0,42	0,27
BrijSDS C18	0,47	0,50	0,48	0,34
SDSME	**0,10**	**0,18**	**0,13**	**0,07**
DGDCChol	**0,10**	**0,12**	**0,05**	**0,17**
DGDC	**0,15**	**0,17**	**0,10**	**0,25**
PAAU	0,34	0,41	0,42	0,32
PSUA	0,44	0,48	0,42	0,44
DHP	**0,08**	**0,15**	**0,11**	**0,18**
DHPChol	**0,06**	**0,11**	**0,08**	**0,17**
POPC/PS	**0,13**	**0,11**	**0,11**	**0,15**
AGESS	**0,08**	**0,13**	**0,11**	**0,17**

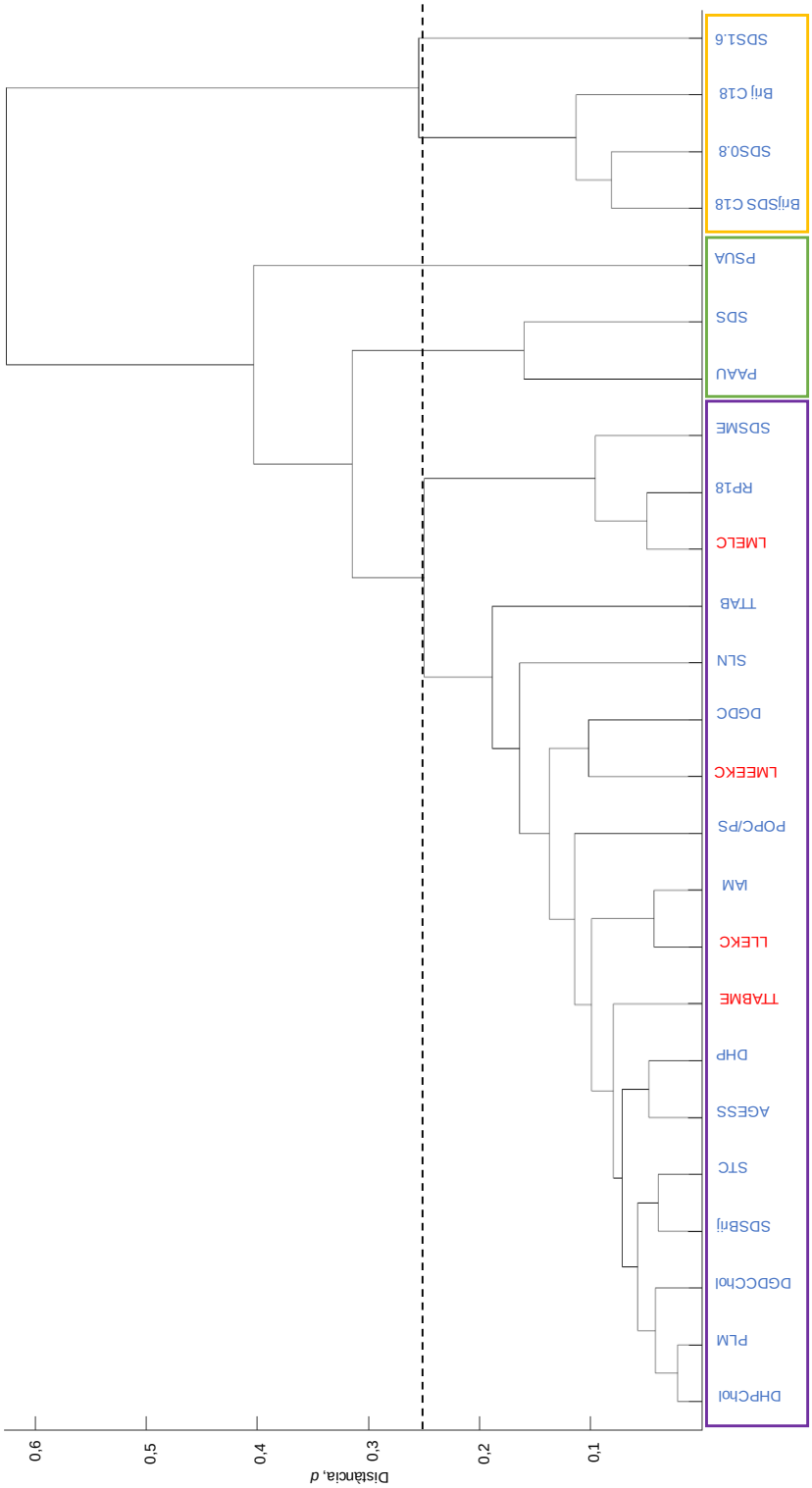

Figura 16. Dendrograma establert a partir dels coeficients normalitzats dels sistemes de partició de les Taules 2 (blau) i 4 (vermell).

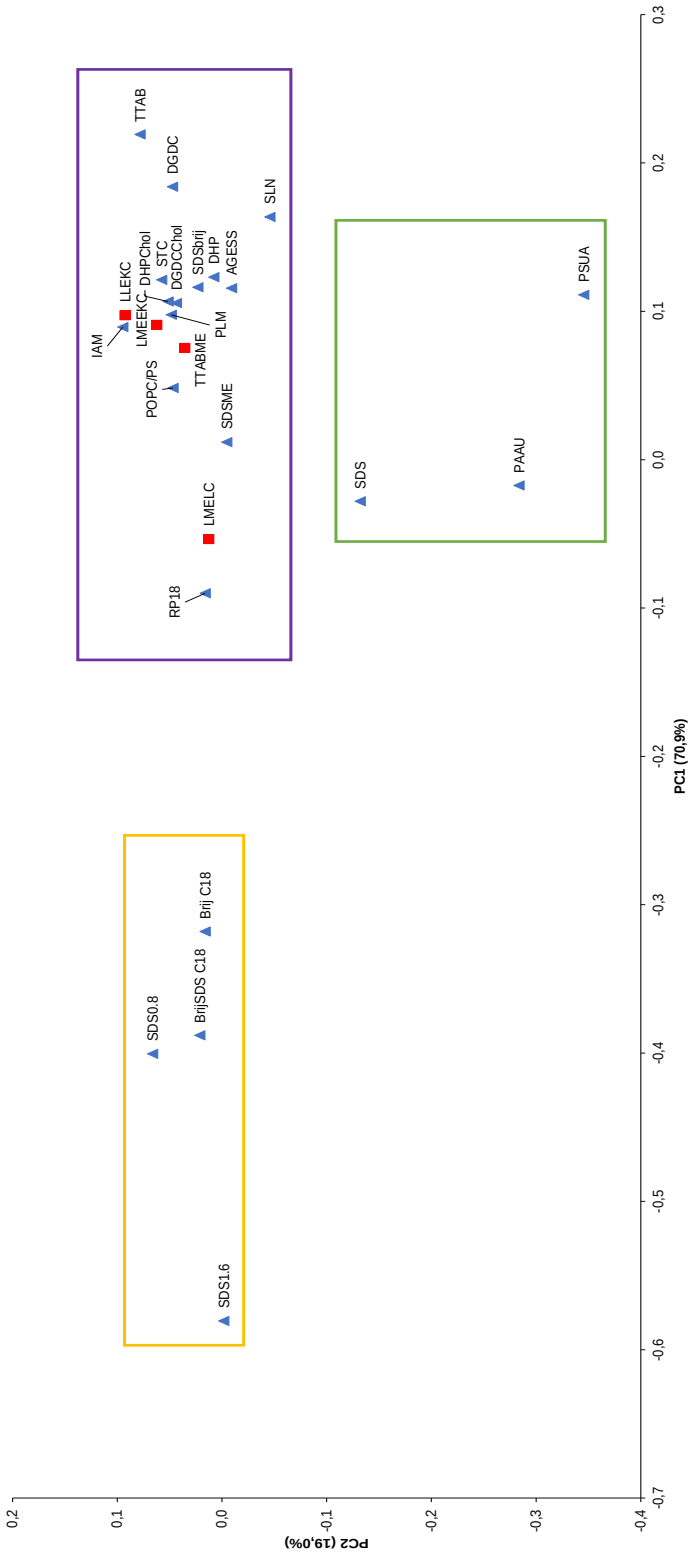

Figura 17. PCA establert a partir dels coeficients normalitzats dels sistemes de partició de les de les Taules 2 (triangle, blau) i 4 (quadrat, vermell).

A partir de les Figures 16-17 es pot veure que els sistemes fisicoquímics s'organitzen principalment en 3 grups diferents: Un majoritari (lila) en el qual es troben la majoria de sistemes analitzats, incloent-hi els 4 caracteritzats en aquest apartat, un segon (verd) format pels sistemes PAAU, SDS i PSUA i un tercer (groc) format per quasi la totalitat dels sistemes MELC (SDS1.6, SDS0.8, BrijSDS C18, Brij C18). Els resultats obtinguts amb el dendrograma i el PCA concorden amb les distàncies calculades entre els sistemes de les Taules 5 i 6, on aquestes són, pràcticament en tots els casos, inferiors a 0,25 pels sistemes que formen part del clúster lila.

Respecte als sistemes basats en preparats desenvolupats a partir de lecitina de soja (LLEKC, LMEEKC, LMELC), es pot veure com són força semblants als altres sistemes basats en fosfolípids (DGDC, DGDCChol, DHP, DHPChol, POPC/PS, IAM i PLM). Aquests formen part del mateix clúster en el dendrograma (Figura 16), es troben molt a prop en el PCA (Figura 17), i, a més, entre aquests sistemes sempre s'observen distàncies calculades inferiors a 0,25 (Taula 6). Tot i això, no es veuen aquestes similituds amb els sistemes PAAU i PSUA (sistemes LEKC), segurament per la naturalesa (polímers sintètics) de les fases pseudoestacionàries d'aquests sistemes. Contràriament al que s'esperaria, el sistema LMELC no forma part del mateix clúster dels altres sistemes MELC basats en tensioactius (BrijSDS C18, SDS0.8, Brij C18, SDS1.6) i a més les distàncies calculades són molt superiors a 0,25. Això és així, ja que possiblement la lecitina s'adsorbeix a la superfície de la fase estacionaria presentant més similituds amb els sistemes IAM i PLM. També s'observa una gran similitud d'aquest sistema amb el sistema RP18, ja que la fase estacionària del LMELC és una columna C18.

Per últim, el sistema TTABME mostra una gran similitud amb l'altre sistema MEEKC analitzat (SDSME). Aquests es troben molt a prop en el PCA i, a més, tenen entre ells un paràmetre de distància d'aproximadament 0,10. S'ha de tenir en compte que ambdós sistemes estan formats pels mateixos cotensioactiu i oli (respectivament, 1-butanol i heptà) que segurament tinguin un pes més gran en la selectivitat del sistema que no pas el tensioactiu utilitzat. Per tant, possiblement el sistema TTABME pot ser una alternativa clara al sistema SDSME en l'estimació de propietats de biopartició.

6.1.3 Similitud entre sistemes de biopartició i sistemes cromatogràfics

A continuació s'han comparat els sistemes cromatogràfics de les Taules 2 i 4 amb un conjunt de sistemes de biopartició (Taula 3) amb l'objectiu de poder emular-los i determinar les propietats d'interès biològic a partir de mesures cromatogràfiques. Primerament, s'ha establert un PCA amb els coeficients normalitzats de tot aquest conjunt de sistemes (Figura 18).

A la Figura 18, tal com passava amb els sistemes fisicoquímics, els diferents sistemes de partició s'organitzen principalment en un gran clúster amb valors de PC1 negatius o molt propers a 0. S'ha de tenir en compte que el pes del PC1 (que explica el 69,3% de la informació total) és molt més elevat que no pas el del PC2 (al qual li correspon el 16,4% de la informació total). Per tant, la variància entre els diferents sistemes s'explicarà principalment per la seva situació en l'eix d'abscisses. Clarament hi ha 3 sistemes de biopartició que no poden emular-se per cap dels sistemes cromatogràfics considerats (IA, AP i BBD). El sistema SDS1.6 basat en MELC seria, *a priori*, la millor opció per a la subrogació del sistema BBP. En estudis previs s'han correlacionat ambdós paràmetres de partició obtenint bons resultats [122].

A continuació, s'han descartat els sistemes IA, AP, BBD, BBP, SDS1.6, SDS0.8, Brij C18, BrijSDS C18. Segons aquest estudi, a diferència de treballs anteriors [108], els sistemes basats en preparats de lecitina de soja no serien òptims per a la subrogació de l'absorció intestinal.

Amb la resta de sistemes de partició (situats dintre del quadrat lila a la Figura 18), tal com s'ha procedit a la secció 6.1.2, s'han tornat a establir un dendrograma (Figura 19) i un PCA (Figura 20) i, a més, s'han calculat les distàncies (Eq. 19) entre la resta de sistemes de biopartició i cromatogràfics considerats (Taula 7).

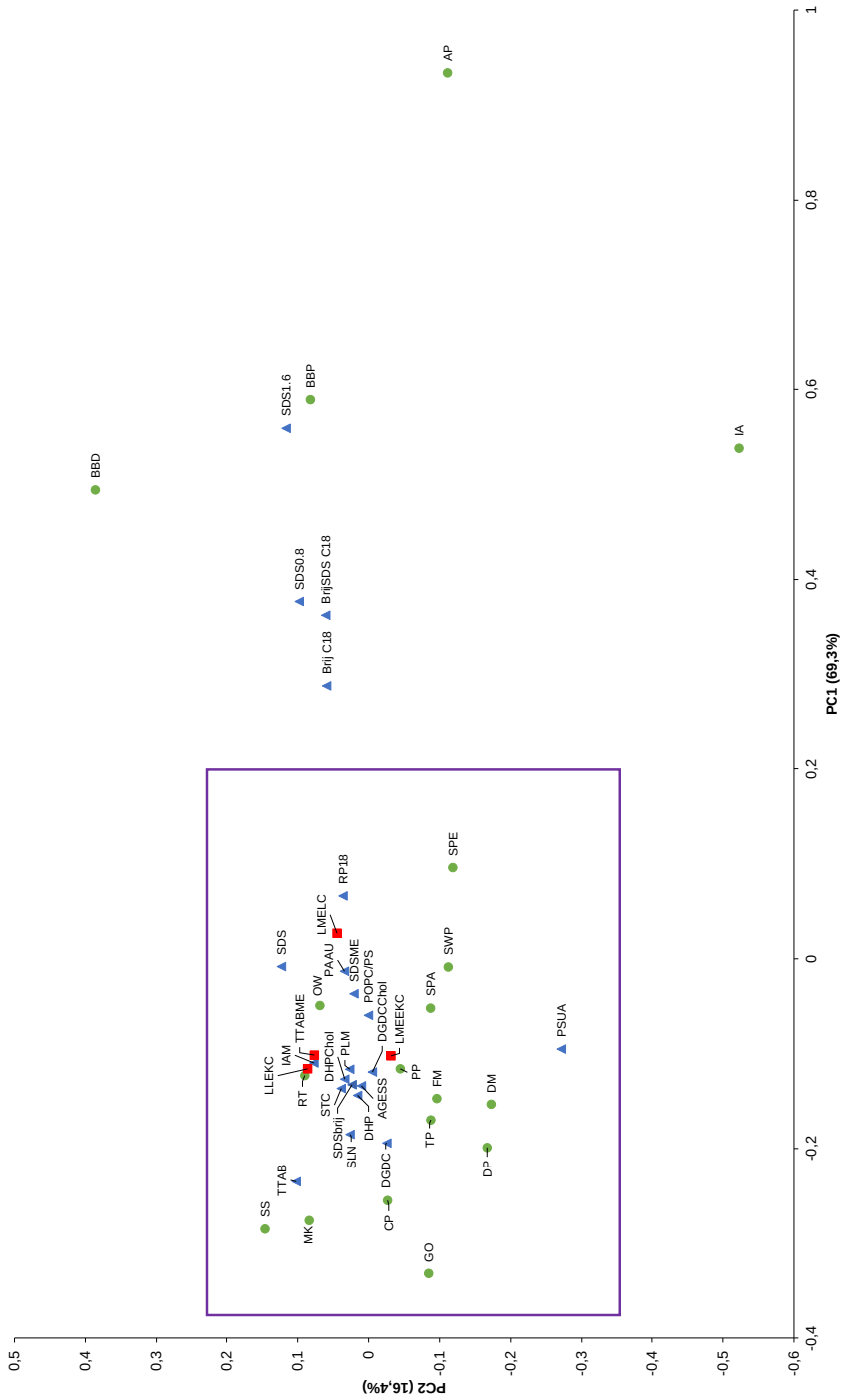

Figura 18. PCA establert a partir dels coeficients normalitzats dels sistemes de partició de les Taules 2 (triangles, blau), 3 (cercles, verd), i 4 (quadrats, vermell).

Taula 7. Paràmetre de distància *d* entre sistemes de biopartició i sistemes fisicoquímics calculat a partir dels coeficients normalitzats dels sistemes de partició de les Taules 2, 3 i 4. Els valors inferiors a 0,25 es troben en negreta.

Sistema de partició	SPA	SPE	RT	FM	GO	MK	DM	DP	TP	CP	PP	SS	SWP	OW
RP18	**0,19**	**0,20**	**0,22**	0,26	0,48	0,40	0,31	0,34	0,28	0,45	0,33	0,42	**0,24**	**0,13**
IAM	**0,18**	0,32	**0,14**	**0,19**	0,36	**0,23**	0,26	0,28	**0,21**	0,34	0,31	0,26	0,28	**0,12**
PLM	**0,14**	0,28	**0,13**	**0,13**	0,33	**0,24**	**0,20**	**0,22**	**0,15**	0,34	0,29	0,28	0,26	**0,09**
SDS	0,34	0,41	**0,17**	0,35	0,42	0,35	0,40	0,39	0,31	0,37	**0,24**	0,34	0,33	**0,21**
SLN	**0,23**	0,37	**0,11**	**0,16**	**0,25**	**0,20**	**0,22**	**0,20**	**0,12**	0,28	**0,24**	**0,22**	0,31	**0,16**
STC	**0,16**	0,32	**0,13**	**0,15**	0,31	**0,20**	**0,22**	**0,23**	**0,16**	0,30	0,28	**0,24**	**0,25**	**0,13**
TTAB	0,29	0,46	**0,18**	**0,25**	0,27	**0,09**	0,31	0,30	**0,24**	0,26	0,32	**0,12**	0,35	**0,24**
SDSbrij	**0,15**	0,31	**0,11**	**0,13**	0,30	**0,21**	**0,20**	**0,21**	**0,13**	0,29	**0,25**	**0,25**	**0,24**	**0,11**
SDSME	**0,16**	**0,23**	**0,16**	**0,18**	0,39	0,33	**0,24**	0,26	**0,19**	0,40	0,30	0,35	0,26	**0,06**
DGDCChol	**0,12**	0,27	**0,16**	**0,10**	0,32	**0,25**	**0,17**	**0,20**	**0,13**	0,33	0,29	0,29	**0,24**	**0,12**
DGDC	**0,18**	0,33	**0,20**	**0,09**	0,28	**0,23**	**0,16**	**0,17**	**0,12**	0,33	0,32	0,27	0,30	**0,19**
PAAU	0,41	0,47	0,28	0,40	0,42	0,43	0,43	0,40	0,35	0,40	**0,25**	0,43	0,38	0,32
PSUA	0,38	0,46	0,41	0,35	0,35	0,48	0,32	0,28	0,30	0,37	0,26	0,52	0,33	0,44
DHP	**0,18**	0,30	**0,13**	**0,12**	0,31	**0,25**	**0,20**	**0,20**	**0,12**	0,34	0,29	0,27	0,29	**0,11**
DHPChol	**0,16**	0,29	**0,14**	**0,13**	0,33	**0,24**	**0,21**	**0,23**	**0,15**	0,34	0,30	0,27	0,28	**0,10**
POPC/PS	**0,09**	0,26	**0,17**	**0,15**	0,36	0,28	**0,21**	**0,25**	**0,18**	0,33	0,27	0,32	**0,18**	**0,13**
AGESS	**0,16**	0,31	**0,10**	**0,12**	0,29	**0,23**	**0,19**	**0,19**	**0,11**	0,30	**0,24**	0,26	**0,25**	**0,11**
TTABME	**0,19**	0,31	**0,09**	**0,18**	0,35	**0,24**	0,26	0,27	**0,18**	0,34	0,29	0,26	0,28	**0,06**
LLEKC	**0,19**	0,34	**0,14**	**0,21**	0,35	**0,21**	0,27	0,29	**0,22**	0,32	0,30	**0,24**	0,27	**0,14**
LMEEKC	**0,10**	**0,23**	**0,20**	**0,09**	0,36	0,30	**0,16**	**0,20**	**0,15**	0,38	0,33	0,34	**0,25**	**0,14**
LMELC	**0,18**	**0,21**	**0,19**	**0,23**	0,45	0,37	0,29	0,32	**0,25**	0,43	0,32	0,39	0,26	**0,08**

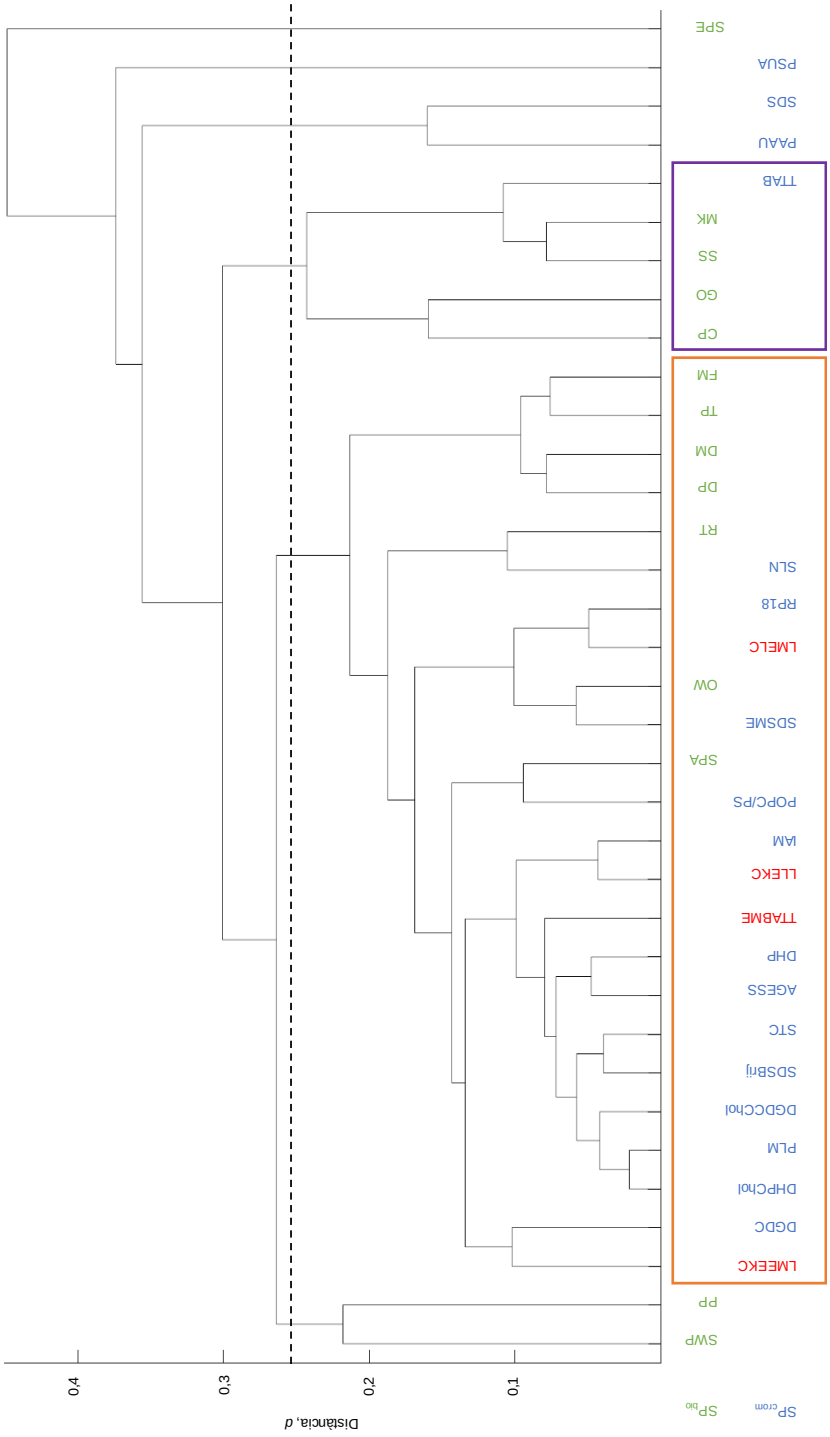

Figura 19. Dendrograma establert a partir dels coeficients normalitzats dels sistemes de partició de les Taules 2 (blau), 3 (verd), i 4 (vermell). En aquest cas només s'han tingut en compte aquells sistemes que estiguessin dintre del clúster lila de la Figura 18.

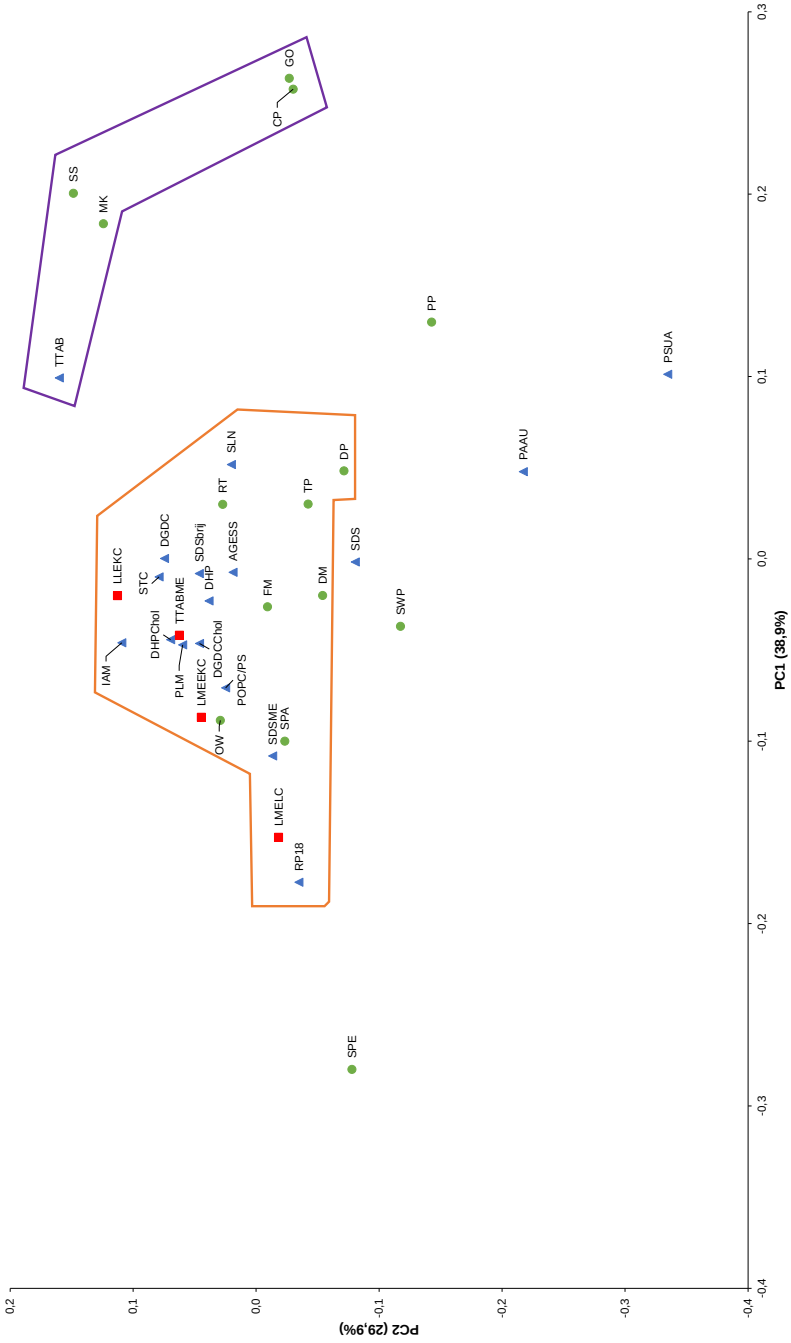

Figura 20. PCA establert a partir dels coeficients normalitzats dels sistemes de partició de les Taules 2 (triangles, blau), 3 (cercles, verd), i 4 (quadrats, vermell). En aquest cas només s'han tingut en compte aquells sistemes que estiguessin dintre del clúster lila de la Figura 18.

Analitzant les Figures 19 i 20 es pot veure com els sistemes de partició analitzats es divideixen en: i) un primer gran clúster (taronja) format tant per sistemes de biopartició (SPA, OW, RT, DP, DM, TP, FM) com d'un gran ventall de sistemes de partició cromatogràfics (DGDC, DHPChol, PLM, DGDCChol, SDSBrij, STC, AGESS, DHP, IAM, POPC/PS, SDSME, RP18 i SLN) i tots els sistemes de la Taula 4 (LMEEKC, TTABME, LLEKC i LMELC); ii) un segon clúster (lila) amb valors de PC1 positius format per un sistema cromatogràfic basat en MEKC (TTAB) i un conjunt de sistemes de toxicitat aquàtica (MK, SS, CP i GO); iii) altres sistemes tant de biopartició (SPE, SWP i PP) com cromatogràfics (SDS, PAAU, PSUA) que, *a priori* per almenys una de les dues eines de comparació, no formarien part dels clústers anteriors. Sí que és veritat que en el PCA (Figura 20) l'SDS queda molt a prop del clúster I (taronja), però això no es veu en el dendrograma (Figura 19). En canvi, segons el PCA els sistemes de biopartició SWP i PP, per una banda, i els sistemes EKC SDS i PAAU, per l'altre, no serien gaire semblants, però fixant-se en el dendrograma (Figura 19) això no seria així. S'ha de tenir en compte que tant el dendrograma com el PCA ens aporten informació complementària, ja que en la representació PC2 *vs.* PC1 es perd informació i en el dendrograma la formació de subgrups pot variar en funció del mode d'agrupació.

A partir de la informació obtinguda de les Figures 19 i 20 i de la Taula 7, s'avaluarà la possibilitat d'emular la toxicitat aquàtica, la partició a la pell i la partició octanol-aigua a partir de sistemes fisicoquímics. L'emulació dels altres sistemes de biopartició (SPE i SWP) ja han estat avaluats en treballs previs del grup de recerca [66,67,123].

6.1.3.1 Toxicitat aquàtica

La determinació de la toxicitat per a diferents organismes aquàtics permet saber quins compostos poden ser contaminants i tenir un efecte nociu pel medi ambient i la cadena tròfica. Actualment, segons el reglament REACH [124] és obligatori identificar i gestionar els riscs tant per la salut humana com pel medi ambient de les substàncies que es fabriquin i es comercialitzin a la Unió Europea. Per tant, la subrogació de la toxicitat envers diferents organismes aquàtics a partir de sistemes cromatogràfics és d'un gran interès. Fins data d'avui, s'han publicat una sèrie de

treballs on s'abordava la subrogació de la toxicitat aquàtica en la Rana Tadpole i Fathead Minnow a partir de sistemes fisicoquímics [52,53]. Tot i això, hi ha una major quantitat d'organismes aquàtics que s'utilitzen amb aquesta fi i per tant també té interès la seva subrogació.

Amb aquesta fi, s'ha avaluat la possibilitat d'emular la toxicitat aquàtica envers 8 organismes aquàtics diferents (FM, GO, RT, DM, TP, CP, SS i PP). Aquest conjunt ha estat seleccionat, ja que és un grup de sistemes representatiu, de tots ells se'n disposa de dades de toxicitat per un grup elevat i variat de substàncies i, a més, s'hi troben organismes de diferents regnes representats (peixos: FM i GO, capgrossos: RT, puces d'aigua: DM, protozous: TP i CP i bacteris: SS i PP).

Segons el dendrograma i el PCA establert a les Figures 19 i 20 i les distàncies calculades a la Taula 7, tots els sistemes fisicoquímics que formin part del primer i segon clúster (taronja i lila) serien bons candidats per a subrogació d'almenys d'algun dels sistemes de toxicitat aquàtica. També segons les distàncies *d* calculades, el sistema SDS, situat molt a prop del primer clúster al PCA (taronja), podria ser una bona opció per a l'emulació dels sistemes RT i PP. Del conjunt de sistemes fisicoquímics en principi aptes per emular la toxicitat en organismes aquàtics se n'han escollit 4 per a la seva avaluació: 1 sistema HPLC (IAM) i 3 MEKC (STC, TTAB, SDSBrij), els quals mostren valors de distància *d* per sota de 0,25 per més d'un sistema de toxicitat aquàtica. Els altres sistemes cromatogràfics s'han descartat, ja que absorbeixen força a la franja UV-vis dificultant la detecció dels anàlits (SLN), estan formats per vesícules o liposomes que són difícils de preparar (DHP, DHPChol, POPC/PS, DGDC, DGDCChol) o no són tan prometedors com els sistemes seleccionats (SDSME, RP18). PLM i AGESS encara que semblen sistemes prometedors, no són tan fàcils d'adquirir com els altres esmentats. En el moment en el qual es va realitzar aquest estudi encara no s'havien desenvolupat els sistemes LLEKC, LMEEKC, LMELC i TTABME. A partir dels resultats obtinguts en aquest estudi global també podrien ser prometedors, especialment pels sistemes de toxicitat aquàtica FM (LMEEKC) i RT (TTABME, LLEKC i LMELC).

A continuació, s'ha estimat la variància de la correlació ($SDcorr^2$) entre els sistemes de toxicitat aquàtica i els sistemes cromatogràfics seleccionats, tal com s'indica a la introducció. Els valors estimats es mostren a la Taula 8.

Taula 8. SD_{corr}^2 estimades a partir de l'Eq. 21 entre diferents sistemes de toxicitat aquàtica i els sistemes cromatogràfics seleccionats.

Sistemes de biopartició	Sistemes cromatogràfics			
	IAM	**STC**	**SDSBrij**	**TTAB**
RT	0.201	0.141	0.141	0.172
FM	0.145	0.140	0.114	0.188
GO	0.318	0.204	0.241	0.205
DM	0.181	0.135	0.117	0.144
TP	0.087	0.074	0.066	0.112
CP	0.383	0.303	0.307	0.227
PP	0.242	0.144	0.176	0.169
SS	0.137	0.114	0.120	0.107

Observant les dades de la Taula 8, es pot veure com, *a priori*, els millors sistemes per emular el RT seria l'STC i el SDSBrij, ja que mostren baixes SD_{corr}^2, mentre que pel FM seria l'SDSBrij, encara que també es podrien obtenir bones correlacions pels sistemes IAM i STC. DM i TP serien ben emulades pel sistema SDSBrij, mentre que CP i SS ho serien pel TTAB. Pel que fa als sistemes de toxicitat aquàtica restants (GO i PP), aquests mostren les menors variàncies calculades pels sistemes MEKC STC i TTAB.

6.1.3.2 Partició a la pell

La partició a la pell esdevé de gran importància en l'àmbit farmacèutic o cosmètic per determinar com particionen en aquesta diferents compostos que podrien ser emprats com a potencials fàrmacs o cosmètics. Tal com s'ha esmentat a la

introducció, la composició de fosfolípids de les cèl·lules de la pell és molt similar a la de la lecitina de soja [106,107], per tant, els sistemes basats en preparats de lecitina de soja poden resultar adients per subrogar aquest sistema de biopartició. A més, a diferència d'altres sistemes on s'incorporen fosfolípids a la fase pseudoestacionària o estacionària, aquests es poden preparar *in situ*, d'una manera fàcil i ràpida.

Dels 3 sistemes preparats a partir de la lecitina de soja, observant les Figures 19 i 20 i la Taula 7, de tots 3 el que sembla que pot subrogar millor la partició en la pell (SPA) és el sistema LMEEKC. Ambdós sistemes es troben a prop al PCA (pràcticament amb el mateix PC1), formen part del mateix clúster en el dendrograma i presenten un paràmetre de distància més petit que 0,25, en concret 0,10 (el valor més petit entre els 3 sistemes de lecitina). A més a més, la SD_{corr}^2 calculada entre els sistemes SPA i LMEEKC (SD_{corr}^2= 0,062) és més petita que l'obtinguda per les correlacions SPA-LLEKC (SD_{corr}^2= 0,067) i SPA-LMELC (SD_{corr}^2= 0,079).

6.1.3.3 Partició octanol-aigua

El coeficient de partició octanol-aigua, paràmetre de referència per avaluar la lipofilicitat d'un compost, ha estat estimat en treballs anteriors [54–58] a partir del sistema SDSME. Observant el dendrograma, el PCA (Figures 19 i 20) i les distàncies *d* (Taula 7), el sistema OW s'assembla molt als sistemes basats en microemulsions (SDSME, TTABME, LMEEKC i LMELC). Sobretot es poden destacar els baixos valors del paràmetre de distància *d* pels sistemes SDSME (0,06) i TTABME (0,06). Aquests resultats indiquen que la contribució del tensioactiu escollit a les propietats de la ME és negligible a favor de l'oli i cotensioactiu utilitzats [125]. Per tant, el sistema TTABME podria estimar el $P_{o/w}$ tal com ja s'ha comprovat pel sistema SDSME. El valor calculat de SD_{Corr}^2 entre els sistemes OW i TTABME és baix (0,061) sent, segons això, plausible l'estimació del log $P_{O/W}$ a partir del log *k* determinat en el sistema TTABME.

6.1.4 Correlacions establertes entre els sistemes de biopartició i els cromatogràfics

A continuació s'ha comprovat experimentalment si és possible emular els sistemes de biopartició considerats a partir dels sistemes cromatogràfics, *a priori*, més semblants. Amb aquesta fi, s'han correlacionat la propietat de biopartició [6–19,126–146] amb el logaritme del factor de retenció per a cada sistema fisicoquímic. Les correlacions experimentals obtingudes es mostren a la Taula 9 i Figura 21. A part a la mateixa taula, també s'inclou la correlació log $P_{o/w}$ – log k establerta entre els sistemes OW i SDSME que ja es va observar, en estudis anteriors [54–58], una molt bona correlació entre ambdós paràmetres. En el cas del sistema RT, com es disposa de dades de toxicitat per dues espècies de capgrossos diferents, a les correlacions s'ha incorporat un flag descriptor corresponent a l'espècie *Rana japonica* (I_{jap}), assignant un valor d'1 si el valor de toxicitat correspon a aquesta espècie o 0 si les dades corresponen a l'espècie *Rana temporaria*.

A la Taula 9 i la Figura 21 s'observen, en la majoria de casos, bones correlacions experimentals entre les propietats de biopartició i cromatogràfiques. Els 3 sistemes MEKC (STC, SDSBrij i TTAB) i el sistema HPLC (IAM) poden emular satisfactòriament la majoria dels sistemes de toxicitat aquàtica considerats (RT, FM, DM, TP i SS; Figura 21A - 21H). Per GO, CP i PP (Figura 21I – 21K), on el sistema TTAB és el que sembla el més prometedor, no han anat gaire bé. En el cas de CP i PP s'obtenen unes correlacions amb un error més elevat que la resta mentre que en el cas del GO no s'ha obtingut una correlació dolenta però es disposa de molt pocs punts experimentals. Per determinar la toxicitat per aquestes espècies aquàtiques caldrien nous sistemes fisicoquímics que presentessin diferents selectivitats als considerats en aquest estudi.

En les correlacions RT-STC i RT-SDSBrij (respectivament, Figura 21A i 21B), el *flag descriptor* introduït per l'espècie *Rana japonica* no té significat estadístic per un interval de confiança del 95% (±2SD). Per tant, es pot concloure que les dues espècies de *Rana Tadpole* (*Rana temporaria* i *Rana japonica*) són igual de sensibles envers la toxicitat aquàtica.

Taula 9. Correlacions experimentals establertes entre les propietats de partició dels sistemes de biopartició emulats i els sistemes cromatogràfics seleccionats.

Sistema de biopartició	**Sistema fisicoquímic**	***q*** **(SD)**	***p*** **(SD)**	l_{jap} **(SD)**	SD_{corr}^2	**n**	R^2	**F**
RT	STC	3,21 (0,05)	1,24 (0,06)	0,08 (0,07)	0,065	56	0,90	231
	SDSBrij	2,40 (0,05)	1,00 (0,05)	0,10 (0,08)	0,067	57	0,90	232
FM	STC	3,77 (0,04)	0,93 (0,06)		0,072	54	0,84	273
DM	IAM	3,58 (0,07)	2,74 (0,16)		0,197	47	0,87	289
	SDSBrij	2,61 (0,12)	1,42 (0,12)		0,237	32	0,82	135
TP	SDSBrij	-0,71 (0,04)	1,09 (0,05)		0,054	45	0,93	571
SS	SDSBrij	-1,50 (0,08)	0,77 (0,06)		0,055	24	0,88	160
	TTAB	-1,57 (0,08)	0,82 (0,07)		0,055	23	0,87	142
GO	TTAB	2,93 (0,11)	1,20 (0,16)		0,194	18	0,78	57
CP	TTAB	3,16 (0,14)	1,10 (0,27)		0,323	17	0,52	16
PP	TTAB	3,41 (0,09)	1,02 (0,15)		0,209	26	0,67	48
SPA	LMEEKC	1,29 (0,06)	0,71 (0,08)		0,049	24	0,79	82
OW	TTABME	1,35 (0,04)	1,68 (0,05)		0,063	58	0,95	1174
	SDSME	1,51 (0,08)	1,60 (0,11)		0,109	20	0,92	196

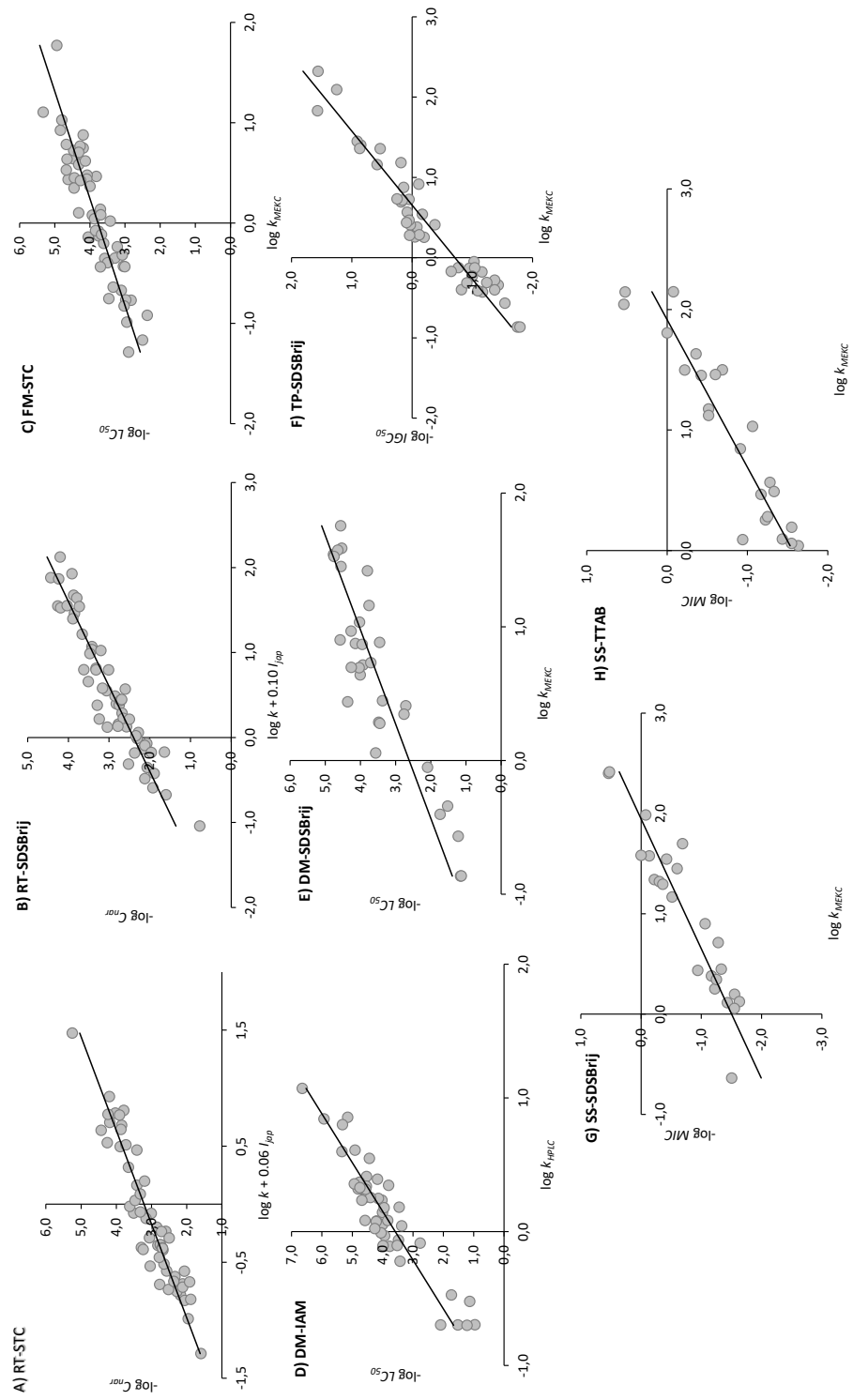
A) RT-STC
-log C_{nar}
log k + 0.06 I_{pp}
B) RT-SDSBrij
-log C_{nar}
log k + 0.10 I_{pp}
C) FM-STC
-log LC_{50}
log k_{MEKC}
D) DM-IAM
-log LC_{50}
log k_{HPLC}
E) DM-SDSBrij
-log LC_{50}
log k_{MEKC}
F) TP-SDSBrij
-log LC_{50}
log k_{MEKC}
G) SS-SDSBrij
-log MIC
log k_{MEKC}
H) SS-TTAB
-log MIC
log k_{MEKC}

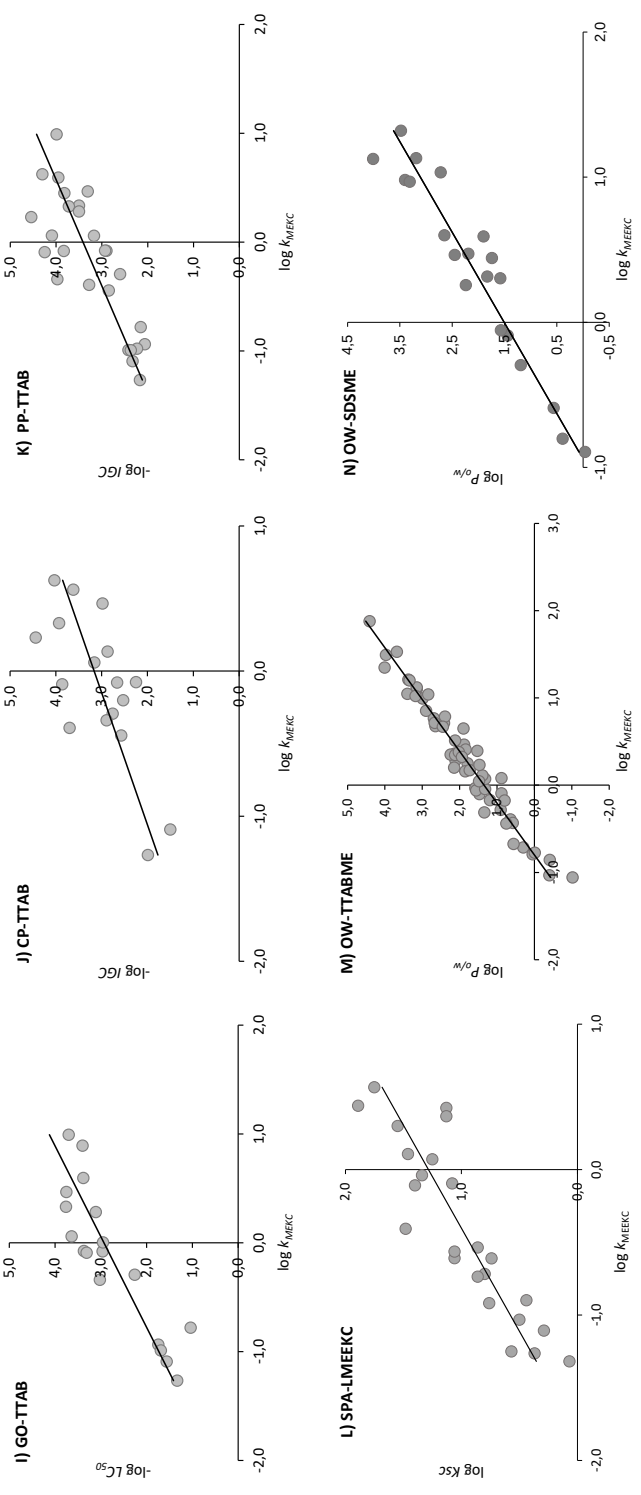

Figura 21. Millors correlacions establertes entre les propietats de partició dels sistemes de biopartició emulats i els sistemes cromatogràfics seleccionats. a) RT-STC; b) RT-SDSBrij; c) FM-STC; d) DM-IAM; e) DM-SDSBrij; f) TP-SDSBrij; g) SS-SDSBrij; h) SS-TTAB; i) GO-TTAB; j) CP-TTAB, k) PP-TTAB; l) SPA-LMEEKC; m) OW-TTABME; n) OW-SDSME. (Articles I, II, V i VI)

En referència a la partició a la pell, la millor correlació obtinguda ha estat emprant com a sistema fisicoquímic el LMEEKC (Figura 21L), tal com indicaven les eines de comparació entre sistemes. Els altres dos sistemes considerats no semblaven presentar grans diferències amb aquest, tot i que, el sistema LMELC seria menys aconsellable, ja que és un sistema més tediós on s'utilitza més volum de microemulsió i és necessari un sistema de neteja rigorós per tal d'evitar embrutar molt la columna cromatogràfica emprada.

En referència a la subrogació del sistema de partició octanol-aigua, s'han obtingut unes molt bones correlacions (R^2>0,9) pels dos sistemes basats en MEEKC avaluats (SDSME i TTABME; Figura 21M i 21N), amb unes equacions molt similars entre si. Finalment, es pot concloure que el sistema TTABME és una alternativa clara al sistema SDSME per subrogar la partició octanol-aigua de substàncies neutres.

Per tant, a partir d'aquests resultats es pot concloure que les eines de comparació són efectives, ja que ens permeten saber amb anterioritat quins sistemes són, *a priori*, els que millor emularan el sistema de biopartició objecte d'estudi.

6.2 Estimació de propietats de biopartició de substàncies àcid-base

En l'apartat anterior s'han estimat diferents propietats de biopartició de compostos neutres. Al llarg dels darrers anys s'han publicat nombrosos estudis sobre aquest tema [53,54,67], però hi ha una manca de treballs relacionats amb l'estimació de propietats de biopartició de compostos ionitzables, concretament quan aquests estan parcialment o total ionitzats i, per tant, carregats. Tenint en compte que la majoria dels fàrmacs són compostos amb grups funcionals àcids o bàsics i que la forma iònica d'un compost presenta habitualment un comportament biològic i químic diferent del de la corresponent forma neutra, estimar la biopartició dels compostos en la seva forma iònica esdevé de gran interès. En treballs anteriors [54–58], s'ha demostrat que, per a substàncies neutres, és possible estimar el coeficient de partició octanol-aigua a partir del factor de retenció dels compostos en un sistema MEEKC específic (format per: tampó, butanol, heptà i el tensioactiu SDS). A més a més, la correlació entre ambdós paràmetres s'ha corroborat a l'apartat 6.1.4. Per tant, en

aquest treball s'ha estudiat la possibilitat d'ampliar l'aplicació del mètode per a substàncies àcid-base ionitzades.

6.2.1 Establiment dels perfils *k*-p*H* en sistemes electrocinètics

Per poder estimar el log $D_{o/w}$ de compostos parcialment i total ionitzats es necessita estudiar com varia el factor de retenció en funció del p*H* i del grau de ionització del compost àcid-base. En aquesta secció s'han establert els perfils *k*-p*H* d'un conjunt de compostos àcid-base monopròtics (o que almenys actuïn com a tal a l'interval de p*H* de treball), que absorbeixin a la regió UV-vis i que tinguin un perfil lipofílic ben definit i variat a la literatura [25,127,131,141,147–173]. Entre els compostos seleccionats hi ha 6 àcids (àcid benzoic, àcid 3-bromobenzoic, naproxèn, ketoprofèn, ibuprofèn i 2,4,6-triclorofenol) i 8 bases (alprenolol, efedrina, nadolol, oxprenolol, penbutolol, pindolol, propranolol i trimetoprim).

6.2.1.1 Perfils k-pH en el sistema SDS MEEKC

Per cadascun dels compostos seleccionats, s'ha calculat el factor de retenció a partir de l'Eq. 5 a diferents valors de p*H*, dintre de l'interval de p*H* de treball electroforètic (2,0-12,0). A continuació, les Eqs. 9-10 s'han ajustat a les dades experimentals, en funció de si el compost és àcid (Eq. 9) o bàsic (Eq. 10), i s'han establert els perfils *k*-p*H* pel sistema SDSME. Els perfils obtinguts es mostren a la Figura 22.

Els perfils *k*-p*H* obtinguts pels compostos àcids presenten la màxima retenció a aquells valors de p*H* en els quals el compost es troba en la seva forma neutra (p*H*s baixos), mentre que a mesura que augmenta el grau de ionització dels compostos la retenció comença a disminuir fins a arribar al seu mínim quan l'àcid es troba totalment desprotonat. Clarament, tal com passa amb el log $P_{o/w}$, els compostos neutres seran d'entrada més lipòfils i tindran una major afinitat per particionar a la fase pseudoestacionària que no pas la forma ionitzada. Tot i això, *k* per l'espècie totalment ionitzada de l'àcid, per pràcticament tots els casos, presenta valors negatius. Aquest fenomen no té cap significat químic, ja que, com a mínim, el valor de *k* hauria de ser 0.

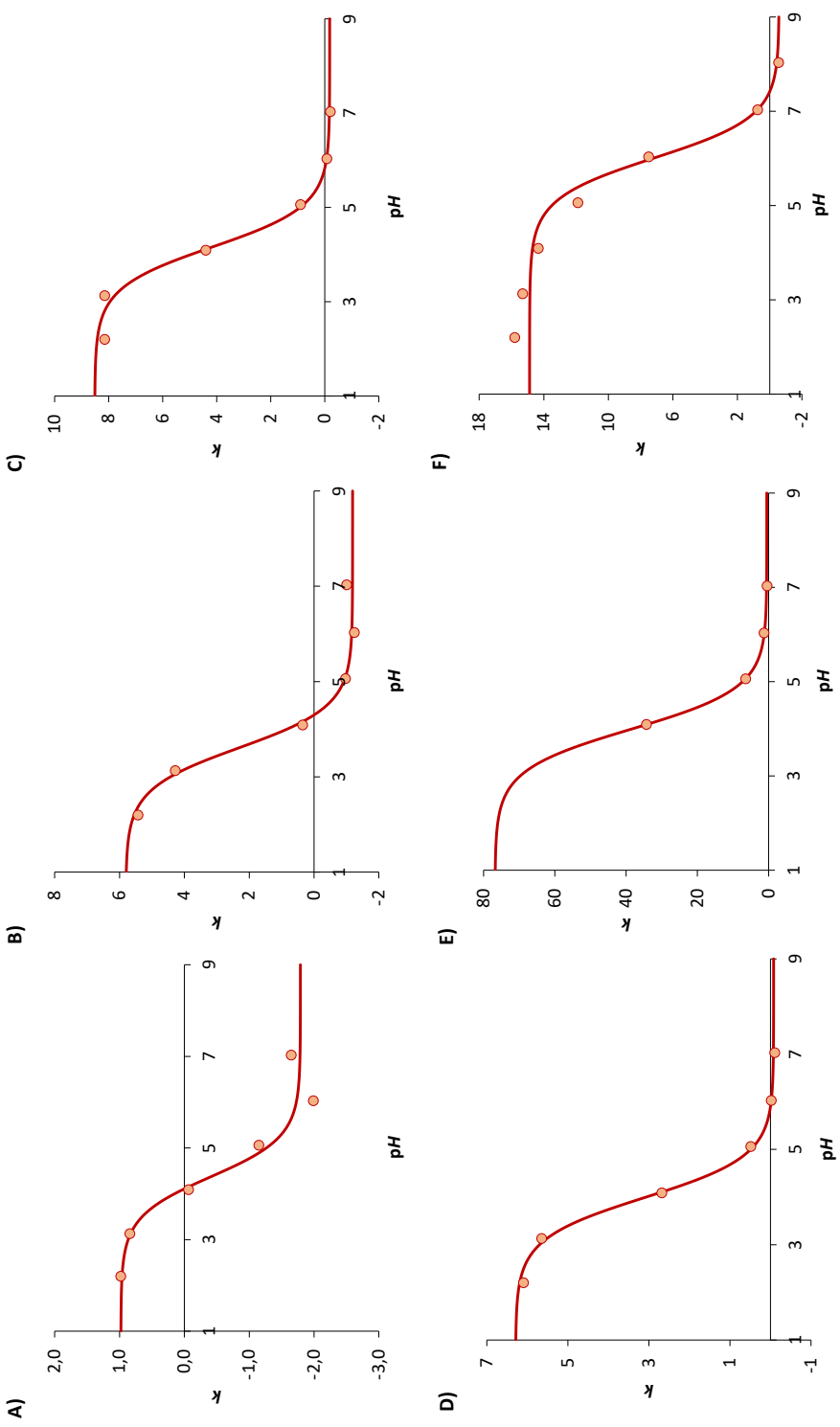
A)
B)
C)
D)
E)
F)
pH
k

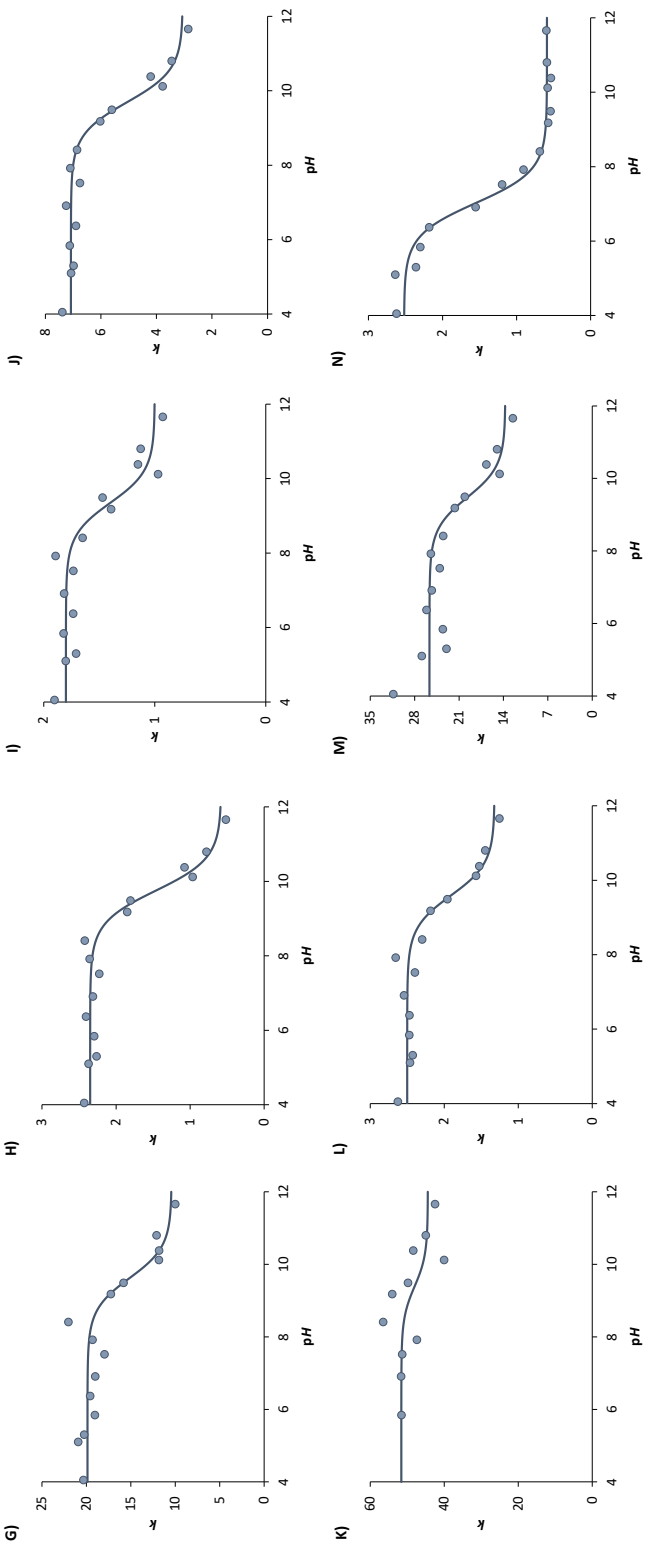

Figura 22. Perfils *k*-p*H* obtinguts en el sistema SDSME resultant de l'ajust de les Eqs. 9-10 a les dades experimentals, per respectivament compostos àcids i bàsics. A) àcid benzoic; B) àcid 3-bromobenzoic; C) naproxèn; D) ketoprofèn; E) ibuprofèn; F) 2,4,6-triclorofenol; G) alprenolol; H) efedrina; I) nadolol; J) oxprenolol; K) penbutolol; L) pindolol; M) propranolol; N) trimetoprim.

En el cas dels perfils *k*-p*H* dels compostos bàsics aquest fet no s'observa, en tots els casos *k* és positiva. Tot i això, i a diferència dels àcids, s'observa que els valors de *k* més grans corresponen a l'espècie totalment ionitzada. Per tant, en el cas de les substàncies bàsiques, a part de la partició dels compostos a la fase pseudoestacionària en funció de les seves hidrofobicitats, han d'haver-hi altres reaccions paràsites que contribueixen a la interacció de les bases ionitzades amb la microemulsió.

Per entendre què és el que està passant, a la Figura 23 es mostren els perfils μ-p*H* de les mobilitats que intervenen en el càlcul de *k* (μ, μ_0 i μ_{fp}, Eq. 5) per l'àcid benzoic i l'efedrina.

Les formes totalment ionitzades d'aquests compostos tenen valors de log $P_{o/w}$ molt baixos (log $P_{o/w(ió\ benzoat)}$ = -1,30 [25], log $P_{o/w(ió\ efedrina)}$ = -1,36 [167]). Per tant, quan aquests compostos es troben totalment ionitzats són molt poc hidrofòbics, i pràcticament no haurien de particionar amb la microemulsió. És a dir, teòricament, *k* hauria de ser aproximadament 0 i, per tant, μ i μ_0 haurien de ser pràcticament iguals, fet que no s'observa a la Figura 23.

En el cas de l'àcid benzoic μ_0 és més gran en valor absolut que no pas μ a p*H*s superiors a 4,0 (quan l'àcid es troba ionitzat), de manera que quan es calcula *k*, a partir de l'Eq. 5, s'obtenen valors negatius (s'ha de tenir en compte que el denominador "μ_{fp}-μ" sempre és negatiu). Aquest fet no té cap significat químic, ja que el valor de *k* ha de ser un valor positiu o, com a mínim, aproximadament 0.

Per altra banda, en els perfils obtinguts per l'efedrina a la Figura 23 s'observa com μ pràcticament no varia en els diferents p*H*s, en canvi μ_0 sí que ho fa. Quan es calcula *k* a partir de l'Eq. 5, s'obtenen valors més alts per l'espècie ionitzada que no pas per la neutra (Figura 22H). Això indica que quan el compost es troba ionitzat (catió) segurament forma un parell iònic i augmenta la seva partició a la microemulsió. Els diferents perfils μ-p*H* de les bases s'han determinat utilitzant tampons preparats a partir de compostos tant àcids com bàsics. Com que els resultats obtinguts no han variat en funció del tampó usat, es pot concloure que l'efedrina estableix un parell iònic amb l'SDS present a la fase aquosa.

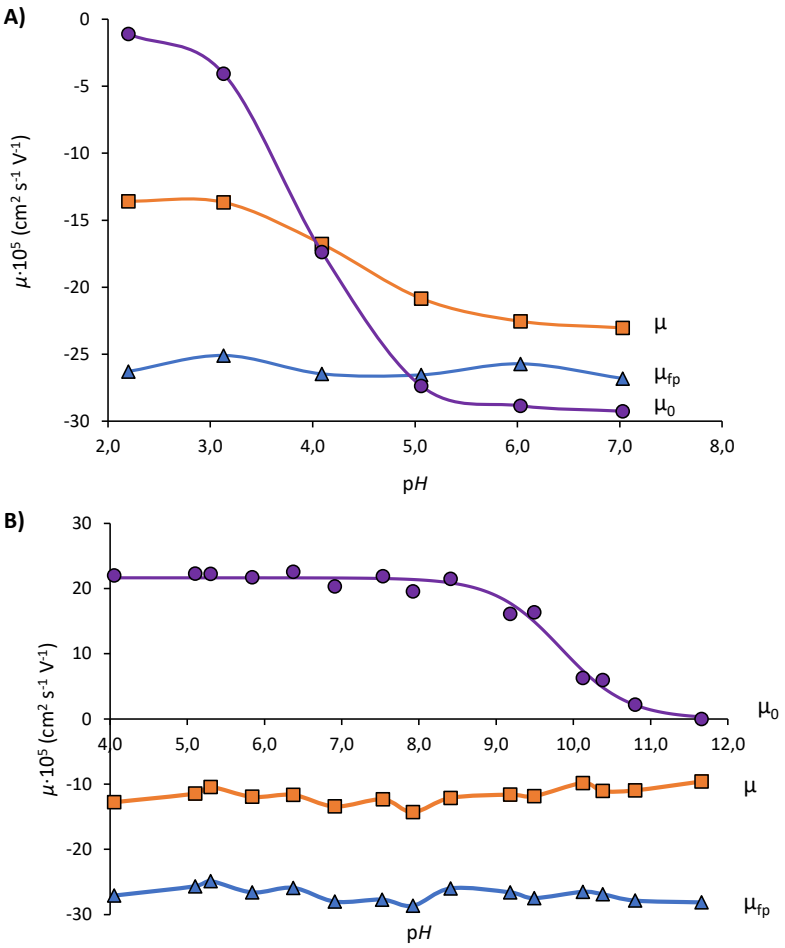

Figura 23. Efecte del p*H* en la mobilitat de la microemulsió, μ_{fp} (▲), i del compost en CZE, μ_0 (●) i MEEKC, μ (■) determinada en el sistema SDS MEEKC. A) Àcid benzoic; B) efedrina.

En el cas de l'ió benzoat, la formació de parells iònics amb el tensioactiu no és possible, ja que es troben carregats amb el mateix signe. Per tant, hi han d'haver altres factors que poden afectar a les mobilitats i, com a conseqüència, al càlcul de *k*.

Un dels factors que pot alterar la mobilitat electroforètica és la viscositat. Aquestes dues propietats estan inversament relacionades segons l'Eq. 3, i l'ús de dissolucions amb diferents viscositats pot afectar el valor de la mobilitat corresponent i, indirectament, *k*. S'ha de tenir en compte que pel càlcul de *k* cal fer dos mesures en

MEEKC i CZE. En les anàlisis en MEEKC, a part del tampó aquós hi ha un tensioactiu, SDS, i concentracions importants de dos dissolvents (1-butanol, i heptà). En canvi, en CZE només hi ha tampó.

A la Figura 24 es mostra com evoluciona la viscositat de mescles d'aigua amb diferents proporcions d'1-butanol [174–176] i a diferents concentracions de SDS [177]. En tots dos casos aquesta s'incrementa amb la concentració d'aquests components. La viscositat d'una solució aigua/butanol al 8,15% (v/v) és almenys un 30% més gran que la d'aigua pura, mentre que una solució aquosa d'SDS al 1,3% (p/v) presenta una viscositat aproximadament el 5% més gran que la solució aquosa sense el tensioactiu. A part s'ha vist que l'heptà, que es troba a una concentració de 1,15% (v/v) a la microemulsió, disminueix la viscositat quan augmenta la seva proporció en mescles heptà/1-butanol [178] (Figura 5C de l'article III). Per tant el fet de combinar a l'Eq. 5 mobilitats determinades en MEEKC i CZE, medis amb viscositat força diferent, pot afectar el càlcul de *k* i, per tant, ser la causa d'obtenir valors més petits que 0.

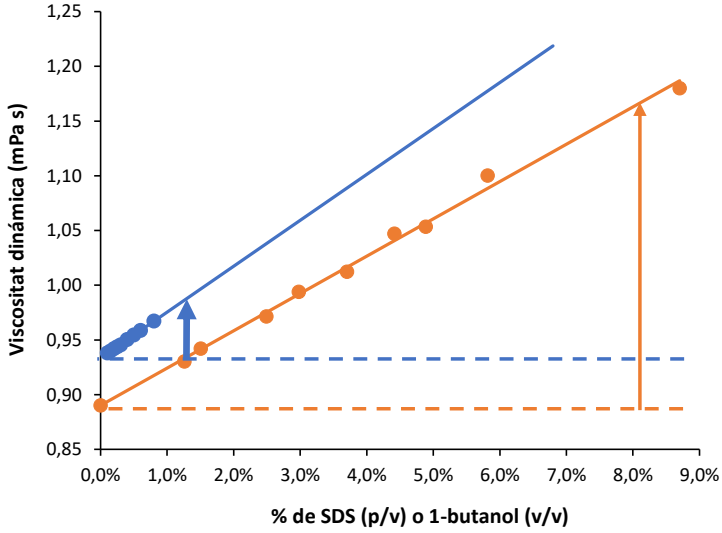

Figura 24. Efecte de la concentració de SDS (blau; [NaCl]=0,05M) i la d'1-butanol (taronja) en la viscositat de solucions aquoses. Les fletxes indiquen l'augment de la viscositat esperat tenint en compte la concentració d'SDS i 1-butanol a la microemulsió.

A la Figura 25 es mostra com evoluciona la mobilitat electroforètica de l'ió benzoat (p*H* 11,0) en mescles ME/tampó aquós. En principi l'ió benzoat no hauria de particionar a la fase pseudoestacionària, i la mobilitat hauria de ser la mateixa a qualsevol percentatge de ME. Tot i això, la mobilitat de l'ió benzoat disminueix un 24% (en valor absolut) al passar de tampó aquós a la solució MEEKC. Per tant, clarament la viscositat del medi afecta la mobilitat dels àcids ionitzats.

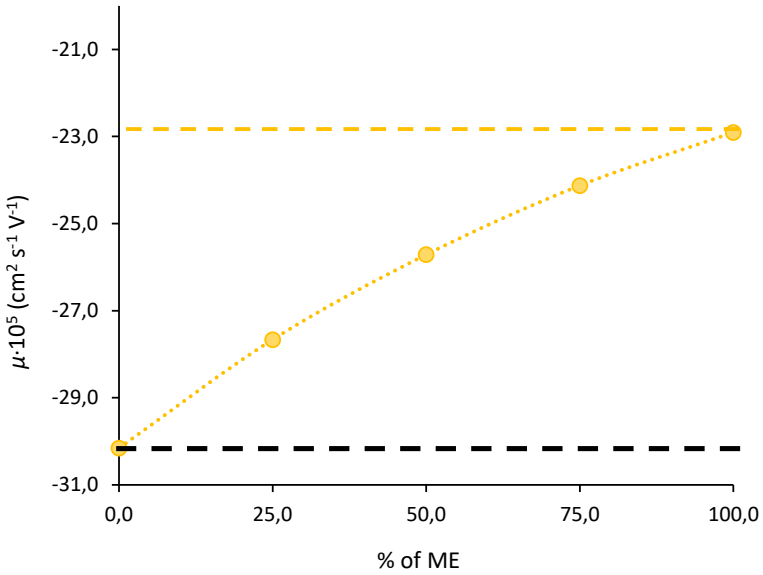

Figura 25. Efecte de la quantitat de ME en el tampó electroforètic sobre la mobilitat de l'ió benzoat.

A causa d'això, les mobilitats del numerador de l'Eq. 5 (μ-μ_0) no es poden restar directament, ja que s'han mesurat en medis que presenten diferent viscositat.

L'Eq. 3 es pot simplificar en l'Eq. 27.

$$\mu = \frac{C}{\eta} \qquad \text{Eq. 27}$$

On el paràmetre *C* agrupa els termes constants que no varien entre MEEKC i CZE. Així la diferència en mobilitats i viscositats determinades en MEEKC i CZE es poden relacionar a partir de l'equació següent:

$$\frac{\mu}{\mu_0} = \frac{\eta_0}{\eta} \qquad \text{Eq. 28}$$

Per tant, la diferència de mobilitats deguda a la viscositat pot ser corregida a partir de la relació de viscositats entre els medis, tal com es pot veure a l'Eq. 29.

$$k = \frac{\mu - \left(\frac{\eta_0}{\eta}\right) \cdot \mu_0}{\mu_{fp} - \mu} \qquad \text{Eq. 29}$$

Ara bé, no és necessari mesurar la relació de viscositats experimentals, ja que segons l'Eq. 28, aquesta és inversament proporcional a la relació de mobilitat d'un compost no retingut (com seria l'ió benzoat). Per tant, *k* es podria calcular a partir de l'Eq. 30.

$$k = \frac{\mu - \left(\frac{\mu}{\mu_0}\right)_{benzoat} \cdot \mu_0}{\mu_{fp} - \mu} \qquad \text{Eq. 30}$$

El valor de μ/μ_0 per l'àcid benzoic és de 0,76. Aquesta aproximació és necessària, ja que no es pot simular la microemulsió en CZE.

6.2.1.2 Perfils k-pH en el sistema TTAB MEEKC.

En el cas de l'efedrina, i per tant de la resta de bases, es forma un parell iònic entre l'SDS i el compost ionitzat. Per solucionar aquest problema s'ha decidit substituir el tensioactiu per un de catiònic com és el TTAB. Aquest ha estat seleccionat, ja que s'ha vist a l'apartat 6.1.4 una bona correlació entre els valors de log $P_{o/w}$ i els de log *k* que s'han determinat en aquest sistema.

Per tant en el sistema TTABME, μ, μ_0 i μ_{fp} s'han determinat per les bases a diferents valors de p*H*, dintre de l'interval de p*H* de treball electroforètic (2,0-12,0). A la Figura 26, es mostren els tres perfils μ-p*H* determinats per l'efedrina en aquest sistema.

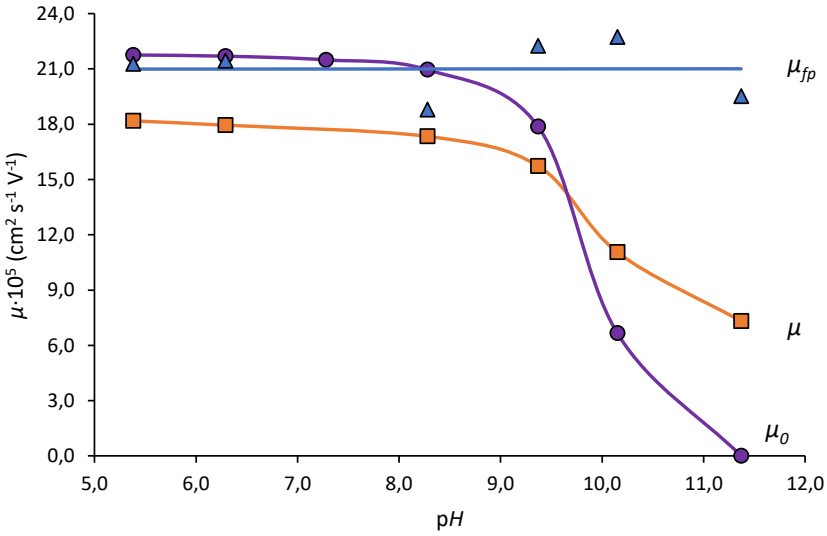

Figura 26. Efecte del p*H* en la mobilitat de la microemulsió (▲), i del compost en CZE (●) i MEEKC (■) determinada en el sistema TTAB MEEKC per l'efedrina.

Els resultats obtinguts són similars als de l'àcid benzoic al sistema SDS MEEKC (Figura 23A), i com era d'esperar en aquest cas les mobilitats obtingudes són positives. També s'aprecia que quan l'efedrina està totalment ionitzada μ_0 és major que μ, sent necessari realitzar també una correcció del valor de les mobilitats a causa de la diferència entre viscositats. L'efedrina protonada no particiona gairebé amb la microemulsió, de manera que la seva relació de mobilitats en zona i MEEKC es pot utilitzar per calcular el factor de retenció de les substàncies catiòniques a partir de l'Eq. 31.

$$k = \frac{\mu - \left(\frac{\mu}{\mu_0}\right)_{efedrina} \cdot \mu_0}{\mu_{fp} - \mu} \qquad \text{Eq. 31}$$

On μ/μ_0 per l'efedrina és de 0,84.

6.2.1.3 Perfils k-pH corregits

Pels 14 àcids i bases seleccionats, s'han calculat els factors de retenció a diferents valors de p*H* en els respectius sistemes MEEKC utilitzant les Eqs. 30-31. A continuació, s'han ajustat les Eqs. 9-10 als valors obtinguts obtenint per cadascun dels compostos el corresponent perfil *k*-p*H* (Figura 27). A la Taula 10 es mostren els paràmetres de l'ajust i les dades estadístiques pels àcids i les bases escollides.

Analitzant els perfils de la Figura 27 i els paràmetres resultants dels ajustos (Taula 10) es pot concloure que tant per àcids com per bases s'han obtingut bons perfils *k*-p*H*, amb valors de R^2 superiors a 0,90 i, fins i tot, per molts compostos amb valors molt propers a 1,0. En relació a la SD obtinguda a l'ajust, aquesta és petita si es compara amb el factor de retenció de l'espècie neutre dels compostos. A més a més, els pK_a' obtinguts en els ajustos concorden amb els obtinguts a la bibliografia. Poden haver-hi petites diferències entre els valors comparats, ja que aquests s'han determinat utilitzant medis diferents amb força iònica diferent.

En tots els casos, la retenció de l'espècie neutra és sempre més gran que no pas la de l'espècie ionitzada, tal com s'esperaria segons les seves hidrofobicitats, i, a diferència del que passava anteriorment, ara no s'obtenen factors de retenció negatius per l'espècie totalment ionitzada dels àcids. Per l'efedrina i pel trimetoprim sí que s'observen valors de $k_{(BH+)}$ lleugerament negatius, però que en cap dels casos aquest valor és diferent de 0 per un interval de confiança del 95% (±2SD). L'efedrina i l'àcid benzoic han sigut els escollits per calcular el factor de correcció de viscositats, però altres compostos com per exemple el trimetoprim o el nadolol, on l'espècie totalment ionitzada pràcticament no particiona a la ME, també es podrien utilitzar amb aquesta fi.

Per tant, a partir dels perfils *k*-p*H* de la Figura 27 i de la Taula 10 es podrà calcular el valor de *k* a qualsevol p*H*. Això serà d'utilitat de cara a veure si el log *k* correlaciona amb el log $D_{o/w}$ a qualsevol p*H* i grau de ionització del compost.

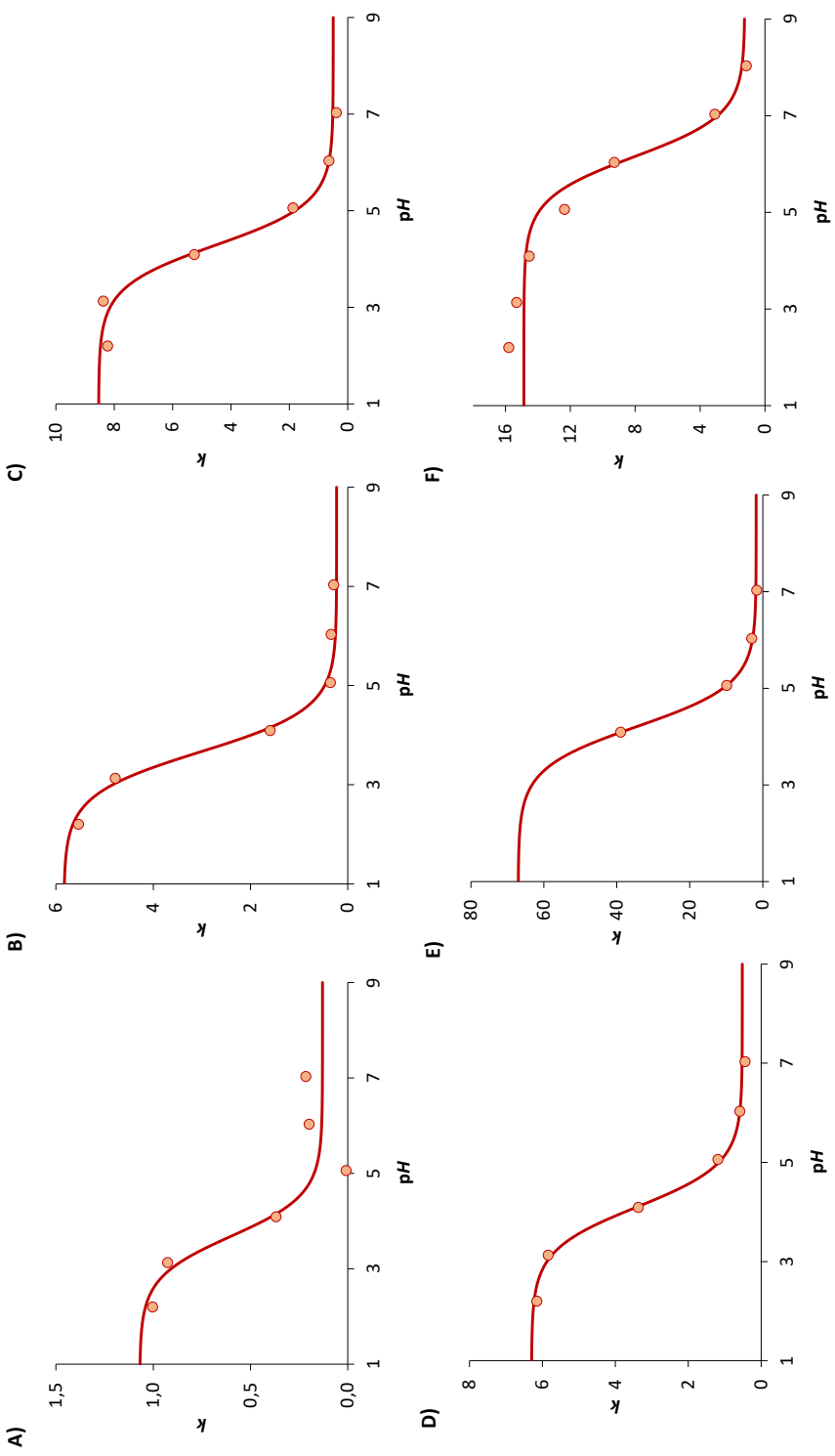
A)
B)
C)
D)
E)
F)
k
pH

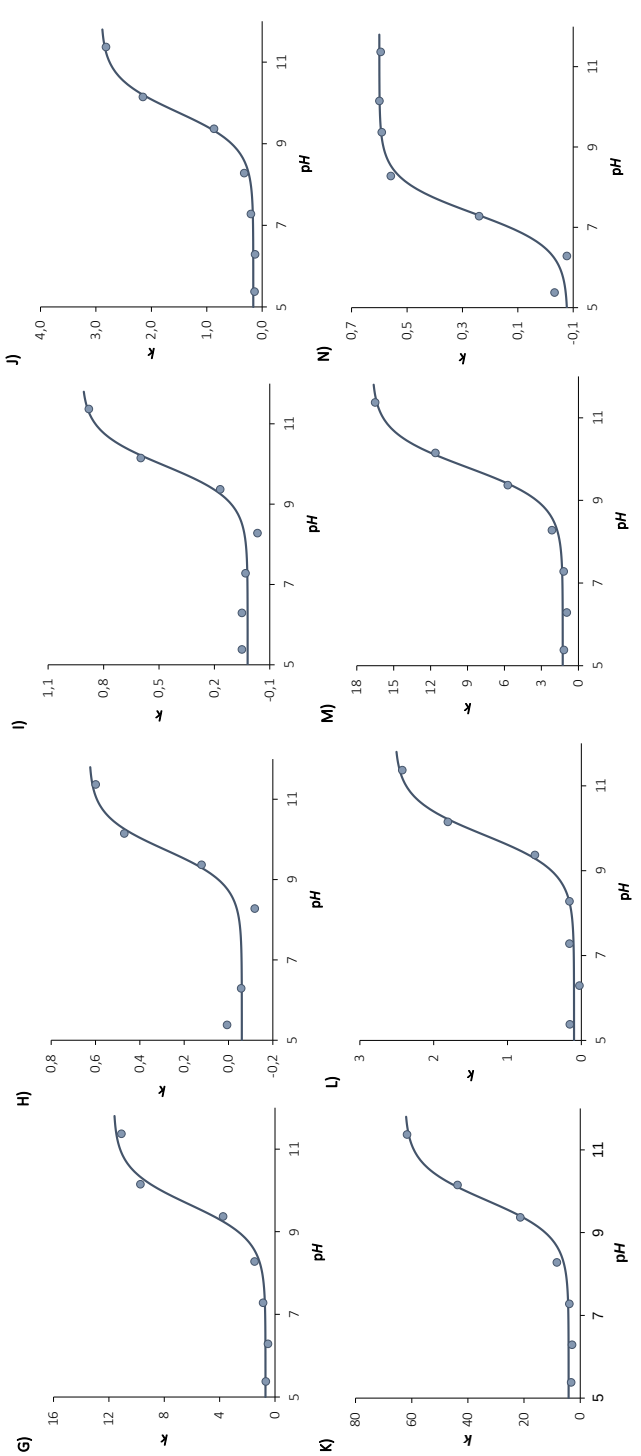

Figura 27. Perfils *k*-p*H* obtinguts en el sistema SDSME (àcids), i TTABME (bases), resultants de l'ajust de les Eqs. 9-10 a les dades experimentals, després de realitzar la correcció de la viscositat. A) àcid benzoic; B) àcid 3-bromobenzoic; C) naproxèn; D) ketoprofèn; E) ibuprofèn; F) 2,4,6-triclorofenol; G) alprenolol; H) efedrina; I) nadolol; J) oxprenolol; K) penbutolol; L) pindolol; M) propranolol; N) trimetoprim.

Taula 10. Paràmetres i dades estadístiques de l'ajust de les Eqs. 9-10 a les dades experimentals. La desviació estàndard es troba entre parèntesis. a) pK_a termodinàmic [127,140,166,179–192].

Compost	pK_a'	$k_{(A-)}$	$k_{(HA)}$	$k_{(BH+)}$	$k_{(B)}$	R^2	SD	F	pK_a[a)]
2,4,6-triclorofenol	6,15 (0,14)	1,24 (0,82)	14,87 (0,51)			0,983	0,94	119	6,17
Àcid 3-bromobenzoic	3,66 (0,08)	0,23 (0,11)	5,84 (0,19)			0,996	0,19	415	3,81
Àcid benzoic	3,68 (0,30)	0,13 (0,07)	1,07 (0,13)			0,948	0,12	28	4,19
Alprenolol	9,66 (0,10)			0,69 (0,29)	11,67 (0,57)	0,989	0,57	188	9,59
Efedrina	9,74 (0,20)			-0,06 (0,04)	0,63 (0,07)	0,970	0,07	49	9,64
Ibuprofèn	4,21 (0,05)	1,79 (0,28)	67,04 (3,55)			1,000	0,36	3448	4,36
Ketoprofèn	4,10 (0,04)	0,52 (0,07)	6,30 (0,09)			0,999	0,11	1424	4,13
Nadolol	9,96 (0,11)			0,02 (0,02)	0,92 (0,05)	0,987	0,05	156	9,69
Naproxèn	4,29 (0,08)	0,50 (0,21)	8,54 (0,25)			0,996	0,30	360	4,24
Oxprenolol	9,78 (0,05)			0,16 (0,03)	2,91 (0,07)	0,998	0,07	841	9,57
Penbutolol	9,78 (0,06)			4,13 (0,86)	62,54 (1,76)	0,997	1,68	578	9,92
Pindolol	9,84 (0,07)			0,10 (0,04)	2,53 (0,09)	0,995	0,08	420	9,54
Propranolol	9,80 (0,05)			1,27 (0,19)	16,78 (0,39)	0,998	0,36	854	9,53
Trimetoprim	7,35 (0,11)			-0,08 (0,03)	0,60 (0,02)	0,991	0,04	218	7,14

6.2.2 Estimació del coeficient de distribució octanol-aigua mitjançant MEEKC

A partir dels perfils *k*-p*H* optimitzats a l'apartat anterior, es pretén estimar el coeficient de distribució octanol-aigua dels compostos àcid-base a diferents valors de p*H* a partir dels dos sistemes MEEKC (SDSME i TTABME).

6.2.2.1 Viabilitat del mètode per l'estimació de $D_{o/w}$ per compostos àcid-base ionitzats.

Pels sistemes MEEKC SDSME i TTABME, tal com s'ha vist a l'apartat 6.1.4, el log $P_{o/w}$ correlaciona satisfactòriament amb el log *k* de substàncies neutres amb una equació del tipus:

$$\log P_{\mathrm{o/w}} = \mathrm{q} + \mathrm{p}\ \log k \qquad \text{Eq. 32}$$

En el cas de substàncies àcid-base, aquesta relació s'establirà per una banda per l'espècie neutra (que ja s'ha vist que s'obtenen bones correlacions) i, per l'altra, per l'espècie totalment ionitzada (de la qual es desconeix si existeix una correlació lineal similar). Aquestes dues equacions (Eqs. 33-34) no tenen per què ser iguals:

$$\log P_{\mathrm{o/w(AB)}} = \mathrm{q_{(AB)}} + \mathrm{p_{(AB)}} \log k_{\mathrm{(AB)}} \qquad \text{Eq. 33}$$

$$\log\ P_{\mathrm{o/w(AB\pm)}} = \mathrm{q_{(AB\pm)}} + \mathrm{p_{(AB\pm)}}\ \log\ k_{\mathrm{(AB\pm)}} \qquad \text{Eq. 34}$$

log $P_{o/w(AB)}$, log $k_{(AB)}$, $q_{(AB)}$ i $p_{(AB)}$ són els paràmetres relacionats amb l'espècie neutra i log $P_{o/w(AB\pm)}$, log $k_{(AB\pm)}$, $q_{(AB\pm)}$ i $p_{(AB\pm)}$ els que tenen relació amb l'espècie totalment ionitzada.

En cas de tenir espècies parcialment ionitzades, tant *k* com $D_{o/w}$ depenen del grau de ionització del compost (α) en funció de, respectivament, les Eqs. 6 i 35.

$$D_{o/w} = (1 - \alpha)\, P_{o/w(AB)} + \alpha\, P_{o/w(AB\pm)} \qquad \text{Eq. 35}$$

on α es calcula segons les Eqs. 36-37 per, respectivament, àcids i bases.

$$\alpha = \frac{10^{pH-pK'_a}}{1+10^{pH-pK'_a}}$$ Eq. 36

$$\alpha = \frac{10^{pK'_a-pH}}{1+10^{pK'_a-pH}}$$ Eq. 37

Combinant les Eqs. 33-35 s'obté la següent relació entre $D_{o/w}$ i k:

$$D_{o/w} = (1 - \alpha)\, 10^{q_{(AB)}}\, k_{(AB)}{}^{p_{(AB)}} + \alpha\, 10^{q_{(AB\pm)}}\, k_{(AB\pm)}{}^{p_{(AB\pm)}}$$ Eq. 38

Per tant, per tenir una relació lineal del tipus:

$$\log D_{o/w} = \mathrm{q} + \mathrm{p} \log\ k$$ Eq. 39

es necessari que $q_{(AB)} = q_{(AB\pm)} = q$ i que $p_{(AB)} = p_{(AB\pm)} = p = 1{,}0$. Per tant, les dues correlacions haurien de ser iguals, i a més, el pendent de la correlació entre la propietat de biopartició i la fisicoquímica hauria de ser 1 (això s'ha demostrat numèricament a la Figura 1 de l'article V). Com que el valor de $p_{(AB)}$ de les correlacions obtingudes a la secció 6.1.4, a partir d'un conjunt de substàncies neutres, no és massa diferent d'1,0 (Taula 9) es considerarà el seu efecte negligible i es comprovarà la seva aplicabilitat a substàncies ionitzades.

De tota manera cal remarcar que si les correlacions per a substàncies neutres i substàncies iòniques no fossin iguals (Eq. 33 i 34), l'estimació del log $D_{o/w}$ només a partir de la recta corresponent als compostos neutres (Taula 9) seria possible pràcticament per tots els valors α. Això és degut a que, segons l'Eq. 35, el log $D_{o/w}$ es calcula a partir dels log $P_{o/w}$ tant de l'espècie neutra com de la iònica. Ara bé, la contribució al valor del log $D_{o/w}$ de la part iònica és molt més petita que no pas la de la part neutra fins a un elevat grau de ionització dels compostos. De fet, a mode de simulacre, a la Figura 28 s'ha avaluat la linealitat entre el log $D_{o/w}$ i el valor de log k (segons l'Eq. 33) per valors de log $P_{o/w(AB)}$ iguals a 4 i valors de log $P_{o/w(AB\pm)}$ de 3 (lila), 2 (taronja), 1 (blau) i 0 (vermell).

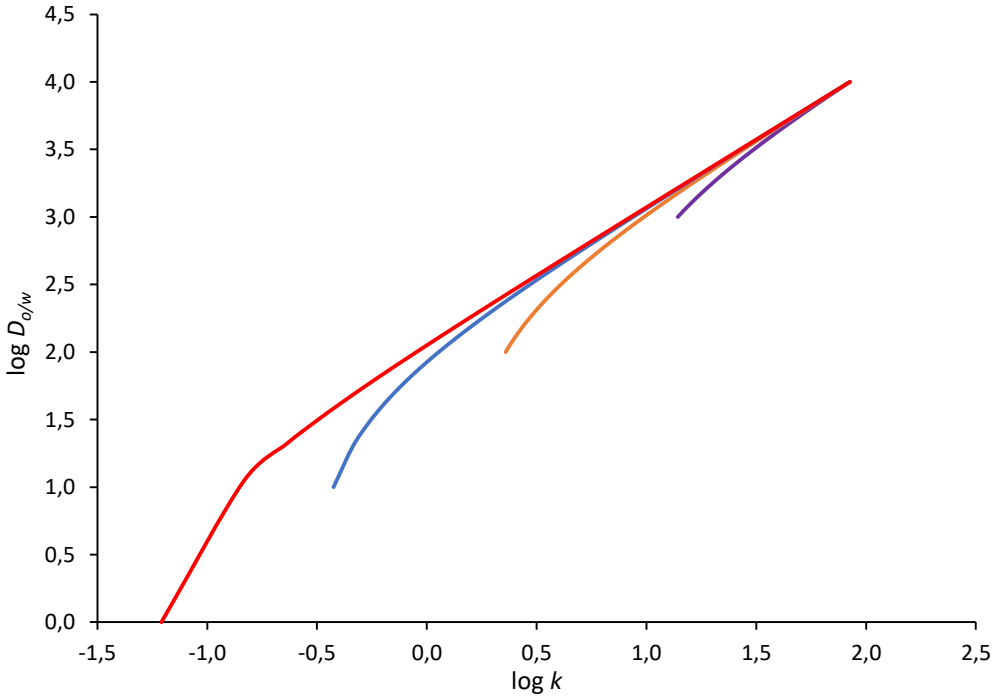

Figura 28. log $D_{o/w}$ vs. log k amb un log $P_{o/w(AB)}$ igual a 4 i valors de log $P_{o/w(AB\pm)}$ de 3 (lila), 2 (taronja), 1 (blau) i 0 (vermell). (Article V)

Pel primer dels casos (log $P_{o/w(AB+)}$ = 3) la linealitat entre el log k i el log $D_{o/w}$ es perd quan α>0,67. En canvi, per la resta això passa a valors de α superiors, sent: 0,86 per quan log $P_{o/w(AB+)}$ = 2, 0,96 pel log $P_{o/w(AB+)}$ = 1 i 0,998 pel log $P_{o/w(AB+)}$ = 0. Tal com es pot observar, com més diferència hi ha entre el log $P_{(AB)}$ i el log $P_{(AB\pm)}$, la correlació entre el log k i el log $D_{o/w}$ és lineal per a un interval de α més gran. Tenint en compte que la diferència mitjana entre el valor de log $P_{o/w(AB)}$ i de log $P_{o/w(AB\pm)}$ és de 3,15 unitats [193], s'espera una linealitat en la correlació log $D_{o/w}$ *vs.* log k fins a un elevat grau de ionització per a la majoria de compostos amb propietats àcid-base.

6.2.2.2 Estimació del log $D_{o/w}$ dels compostos model a partir dels sistemes MEEKC

Considerant que per a la gran majoria de compostos estudiats (àcids i bases) la diferència entre el log $P_{o/w}$ de la forma neutra i el log $P_{o/w}$ de la forma ionitzada és al voltant de 3 unitats o més, s'ha comprovat fins a quin punt es pot determinar el log $D_{o/w}$ només a partir de la correlació entre el log $P_{o/w}$ i el log *k* de la forma neutra. A tal efecte, el log $D_{o/w}$ s'ha estimat a aquells valors de p*H* d'on es disposa de dades a la literatura (log $D_{lit.}$) (determinades mitjançant els mètodes tradicionals i de referència, principalment a partir del mètode *shake-flask*) [25,127,131,141,147–173]. Per fer aquesta estimació (log $D_{est.}$), primer s'ha calculat *k* a aquells p*H*s d'interès a partir dels perfils *k*-p*H* de la Taula 10 i Figura 27, i, a continuació, s'ha calculat el valor de log $D_{o/w}$ a partir de les correlacions log $P_{o/w}$ *vs.* log *k* establertes a la Taula 9 pels sistemes SDSME (en el cas de compostos àcids, Eq. 40) i TTABME (en el cas de compostos bàsics, Eq. 41).

$$log\ P_{o/w} = 1{,}60(\pm 0{,}11) \cdot log\ k + 1{,}51(\pm 0{,}08) \qquad \text{Eq. 40}$$

$$log\ P_{o/w} = 1{,}68(\pm 0{,}05) \cdot log\ k + 1{,}35(\pm 0{,}04) \qquad \text{Eq. 41}$$

L'efedrina i el trimetoprim no s'han utilitzat en aquest apartat, ja que presentaven retencions negatives per les espècies totalment ionitzades. A la Figura 29 es representa log $D_{lit.}$ – log $D_{est.}$ en funció del grau de ionització del compost. En aquesta figura també s'inclouen dues línies addicionals corresponents a ±2 vegades la desviació estàndard obtinguda en cadascuna de les correlacions log $P_{o/w}$ – log *k* (de les Eqs. 40-41), les quals delimiten l'interval de confiança per una probabilitat del 95%.

A la Figura 29 es pot veure com tant per àcids com per bases log D_{lit} – log D_{est} es troba dintre de l'interval de confiança amb una probabilitat del 95% per la majoria de graus de ionització. Només es troben fora d'aquest interval aquells valors corresponents a quan el compost està altament o completa ionitzat (α>0.99).

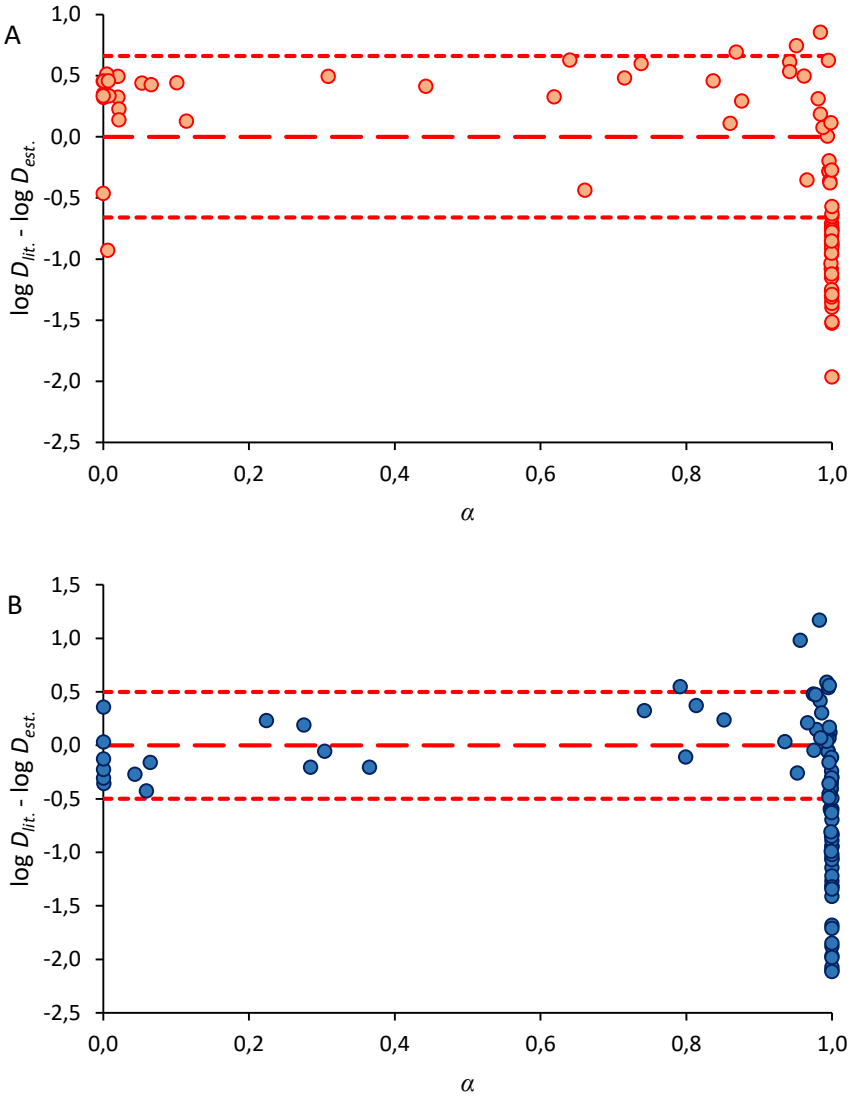

Figura 29. log $D_{lit.}$ – log $D_{est.}$ en funció del grau de ionització per compostos: A) àcids; B) bàsics.

Per tant, es pot concloure que el log $D_{o/w}$ de substàncies àcid-base parcialment ionitzades pot estimar-se a partir de mesures en MEEKC fins al 99% de ionització dels compostos. Quan aquests es troben totalment o alta ionitzats generalment se sobreestima el seu valor. Això pot ser degut al fet que el valor de log $P_{o/w}$ de

compostos totalment ionitzats depèn força del contraió del tampó i de la seva concentració, ja que poden formar parells iònics que facin variar la partició del compost. També és possible que aquesta sobreestimació vingui deguda al fet que la superfície existent entre la fase lipídica i aquosa en MEEKC és més gran en comparació a l'observada en el clàssic sistema de partició octanol-aigua.

La metodologia desenvolupada en aquest apartat és aplicable també a àcids i base polipròtics, i a compostos amfòters. En l'únic cas on hi podria haver algun problema seria per compostos zwitteriònics, que previsiblement al estar carregats positivament i negativa podrien formar parells iònics amb els tensioactius. Tot i això, aquestes hipòtesis s'haurien de demostrar en treballs futurs.

6.3 Disseny i estudi de noves columnes monolítiques

Un altre dels objectius del treball ha estat el desenvolupament de noves fases estacionàries basades en columnes monolítiques. Aquesta tasca ha estat realitzada durant una estada predoctoral a la *Universiteit Vrije Brussel*, a Brussel·les (Bèlgica).

6.3.1 Característiques de la columna desenvolupada

En aquest treball s'ha desenvolupat i avaluat una columna monolítica basada en un polímer d'estirè-*co*-divinilbenzè que ha estat preparada en un capil·lar de 200 µm de diàmetre. Aquest tipus de columnes són especialment usades en l'anàlisi de proteïnes per RP-LC per formació de parells iònics utilitzant el mode gradient. La columna s'ha sintetitzat a partir d'una mescla de polimerització que consisteix en AIBN (l'iniciador de la polimerització) dos monòmers (estirè i divinilbenzè, sent el segon el monòmer d'entrecreuament) i un porogen format per una mescla d'1-decanol i THF (sent el segon el "bon" dissolvent del porogen). La proporció de cadascun dels monòmers respecte al total de la mescla de polimerització ha estat d'aproximadament el 20% p/p, mentre que el restant 60% p/p el conforma el porogen. Aquesta proporció monòmer:porogen del 40:60 en percentatge p/p ha

sigut àmpliament utilitzada a la literatura seguint la recepta original desenvolupada per Svec i Fréchet [194–197]. A la Figura 30 es mostra una imatge SEM (microscòpia electrònica de rastreig, en anglès *Scanning electron microscope*) de l'estructura globular interconnectada de la columna.

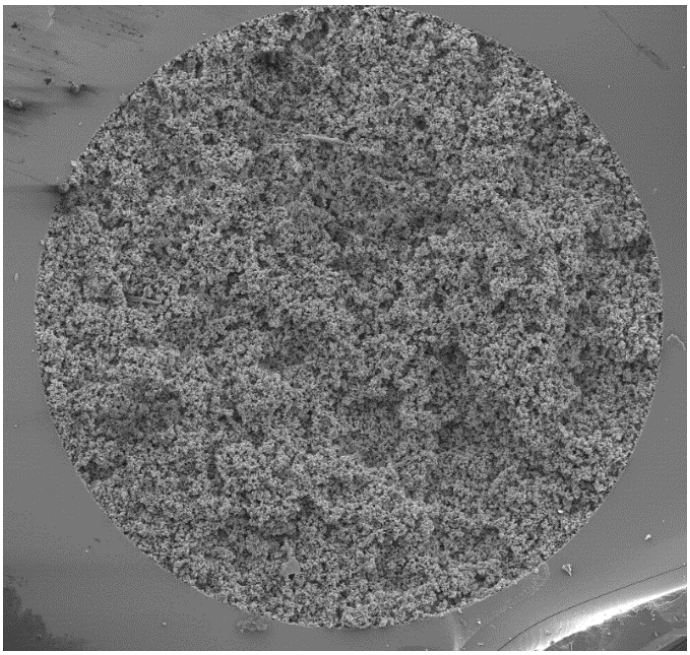

Figura 30. Imatge SEM d'una secció de la columna monolítica capil·lar basada en un polímer d'estirè-co-divinilbenzè i preparada en un capil•lar de 200 µm de diàmetre.

A la imatge es pot veure que l'estructura és homogènia i que el polímer recobreix la superfície interna del capil·lar amb el qual estableix una unió covalent. A més, s'han mesurat la mida mitjana dels microglòbuls (1.2 µm de diàmetre) i dels macroporus (1.0 µm de diàmetre) a partir de vàries imatges SEM de la columna.

Les propietats de la fase estacionària i l'eficàcia de la columna sintetitzada han estat avaluades cromatograficament utilitzant l'uracil. S'ha escollit aquest compost, ja que, quan s'utilitza una fase mòbil al 80:20 (v:v) d'ACN:aigua, aquest no queda retingut a la fase estacionària, fet pel qual és també idoni per utilitzar-

lo com a marcador del temps mort. Amb aquesta fi, s'ha calculat *H*, per mitjà de l'Eq. 25, a diferents cabals entre 0,025 i 1,500 μL·min^{-1} amb una fase mòbil al 80:20 (v:v) d'ACN:aigua, i s'ha obtingut el valor mínim de *H* (13.3 μm) a un cabal de 0.500 μL.min^{-1}. A la Figura 31 (línia negra) es mostra el perfil obtingut després d'ajustar l'Eq. 22 a aquestes dades. Els paràmetres de l'equació de Van Deemter obtinguts són els següents: *A* = 5,9 μm, *B* = 1,8 mm^2/s i *C* = 7,1 ms.

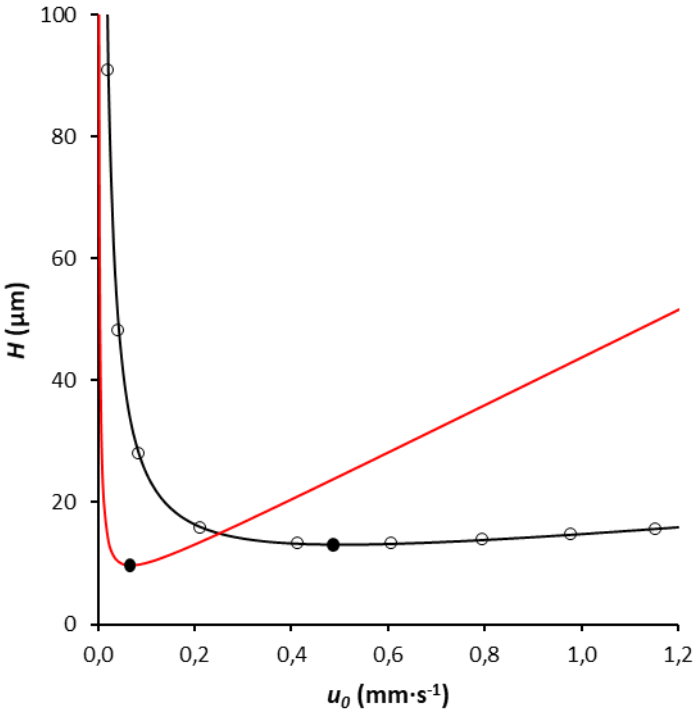

Figura 31. Perfil de l'equació de van Deemter per l'uracil (línia negra) i per una proteïna model amb un pes molecular de 22.7 kDa i amb un coeficient de difusió d'aproximadament 9·10^{-11} m^2/s [198] (línia vermella). En cada cas es troba marcat el mínim de l'equació de Van Deemter (•). (Article VII)

A partir d'aquests paràmetres i sabent el coeficient de difusió de l'uracil (D_M), s'ha estimat el perfil de Van Deemter d'una proteïna model, amb un pes molecular de 22.7 kDa i amb un coeficient de difusió d'aproximadament 9·10^{-11} m^2/s [198], a partir de l'equació següent:

$$H = a \cdot d_{dom} + \frac{b \cdot D_M}{u_0} + C_m \cdot \frac{d_{dom}^2}{D_M} \cdot u_0 \qquad \text{Eq. 42}$$

Aquesta equació és anàloga a l'Eq. 22, on *a*, *b* i *c* són els paràmetres reduïts de Van Deemter i d_{dom} és defineix com la suma de la mida mitjana dels microglòbuls i dels macroporus. El perfil estimat per la proteïna model es mostra a la Figura 31 (perfil vermell) on es pot veure que el cabal on s'observa el valor mínim de *H*, corresponent al u_{opt}, és inferior a 0,1 µL.min^{-1}.

6.3.2 Paràmetres que afecten n_c per a la separació de proteïnes

Hi ha molts paràmetres experimentals, a part del disseny de la fase estacionària, que poden afectar la capacitat separativa d'una columna cromatogràfica. Per aquest motiu, la columna monolítica desenvolupada ha estat caracteritzada utilitzant com a model 7 proteïnes que presenten pesos moleculars en el rang 6-30 KDa (ribonucleasa A, insulina, citocrom c equí, citocrom c boví, lisozim, mioglobina, i anhidrasa carbònica). Per a dur a terme la caracterització s'han avaluat els paràmetres següents:

6.3.2.1 Efecte del formador del parell iònic

Tal com s'ha comentat anteriorment, aquest tipus de columnes són especialment usades en l'anàlisi de proteïnes per RP-LC per formació de parells iònics utilitzant el mode gradient. Per tant, s'ha avaluat la influència de 2 àcids utilitzats com a agents formadors de parell iònic (l'àcid trifluoroacètic, TFA, i l'àcid fòrmic, FA) sobre la retenció de les proteïnes i la forma i amplada dels pics cromatogràfics resultants.

En primer lloc, s'han analitzat 5 de les 7 proteïnes escollides (ribonucleasa A, insulina, lisozim, mioglobina, i anhidrasa carbònica) amb la mateixa concentració de cadascun dels formadors de parells iònics a la fase mòbil (aproximadament 0,1% v/v) (Figura 32). Per realitzar el gradient s'han utilitzat 2 solucions diferents: i) solució A que consisteix en una solució aquosa amb 0,1% (v/v) de TFA o FA; ii) solució B que consisteix en 80:20 (v/v) ACN:H20 amb 0,08% (v/v) de TFA o FA.

Per poder comparar l'efecte d'ambdós àcids s'ha mantingut el mateix interval de gradient (Δc=0,28) i s'ha intentat que la proteïna menys i més retinguda eluïssin al mateix temps. Amb aquesta fi quan s'ha utilitzat TFA la finestra de gradient aplicada ha estat del 25 al 60% de solució B, mentre que pel FA ha estat del 17,2 al 52,2% de solució B.

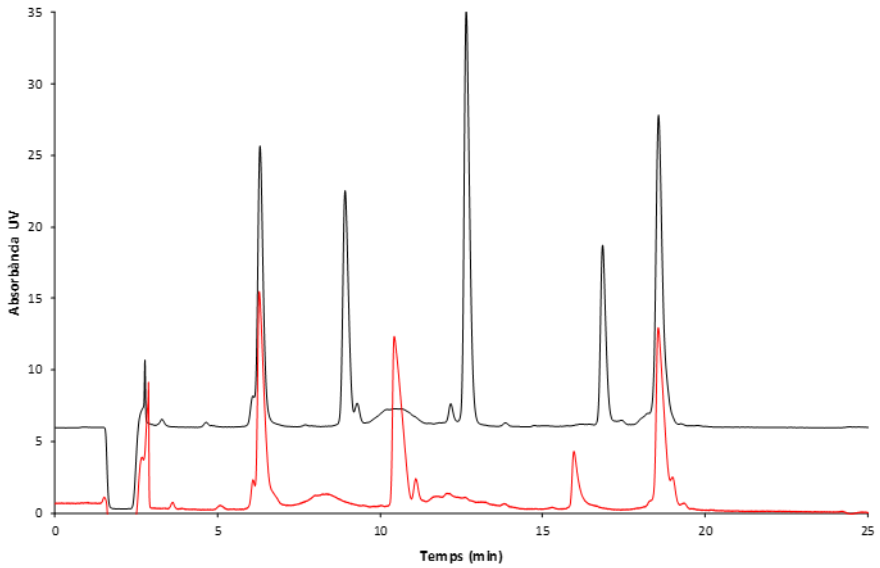

Figura 32. Separació de (1) ribonucleasa A, (2) insulina, (3) lisozim, (4) mioglobina, i (5) anhidrasa carbònica amb una fase mòbil amb aproximadament 0,08-0,10% (v/v) de TFA (negre) o FA (vermell). (Article VII)

Els resultats mostrats a la Figura 32 indiquen que el TFA incrementa la retenció de les proteïnes, ja que els compostos elueixen a continguts d'ACN més elevats, i els pics obtinguts són més estrets i gaussians que no pas amb el FA. Això indica que el TFA forma parells iònics més forts amb les proteïnes que no pas el FA.

Per tant, a partir de l'ús del TFA com a agent formador de parell iònic s'esperen obtenir separacions amb n_c més elevades. Tot i això, l'ús del TFA com a agent formador de parells iònics pot estar limitat, ja que aquest suprimeix la senyal quan es realitzen anàlisis per espectrometria de masses [199].

6.3.2.2 Capacitat de càrrega

En segon lloc, s'ha avaluat la capacitat de càrrega de la columna sintetitzada. S'ha de tenir en compte que la superfície de les columnes monolítiques és de 6 a 8 vegades menor que la de les columnes empaquetades [200], per tant, aquestes tindran una capacitat de càrrega inferior. A concentracions per sobre de la capacitat de càrrega de les columnes, s'obtindran pics cromatogràfics més amples obtenint una pitjor eficàcia a la separació.

Per determinar a partir de quina concentració de les proteïnes els pics cromatogràfics comencen a eixamplar-se, s'han analitzat aquestes a diferents concentracions utilitzant com a agent de formador de parell iònic el TFA. A la Figura 33 es mostren els pics cromatogràfics obtinguts per 3 de les proteïnes analitzades (ribonucleasa A, insulina i lisozim) a 3 concentracions diferents (2,5 ppm, 5 ppm i 10 ppm).

L'amplada dels pics cromatogràfics roman constant fins a una concentració de les proteïnes de 2,5 ppm. A concentracions superiors, tal com es pot veure a la Figura 33, l'amplada de pic augmenta de manera gradual. Els resultats mostrats corresponen als obtinguts quan s'utilitza TFA com a agent formador de parell iònic. Quan s'utilitza FA aquest efecte és més important (dades no mostrades).

Per tant en aquesta columna, per poder arribar al valor màxim de n_c és important treballar a concentracions inferiors a 2,5 ppm.

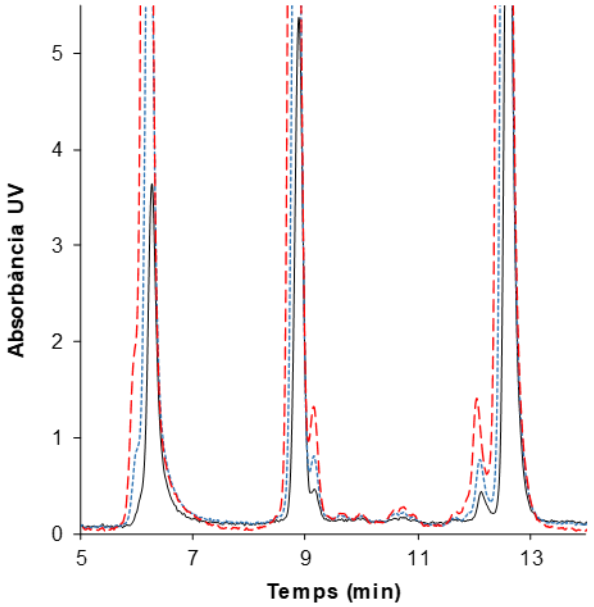

Figura 33. Pics cromatogràfics obtinguts per (1) ribonucleasa A, (2) insulina, i (3) lisozim, quan s'utilitza una fase mòbil formada per: A (solució aquosa 0,1% (v/v) de TFA) i B (80:20 (v/v) ACN:H_20 amb 0,08% (v/v) de TFA) amb una finestra de gradient del 25 al 60% de solució B. La concentració de les proteïnes és de 2,5 ppm (negre), 5 ppm (blau) i 10 ppm (vermell). (Article VII)

6.3.2.3 Efecte del temps de gradient i del cabal

A part dels factors anteriors, també s'ha avaluat com afecta el temps de gradient i el flux usat en n_c. Amb aquest objectiu, s'ha analitzat la mescla de 7 proteïnes a diferents temps de gradient (10-120 min) i a diferents cabals de fase mòbil (0,5-2,0 $\mu L \cdot min^{-1}$). En tots els casos l'agent de formador del parell iònic (TFA), la finestra de gradient (Δc = 0,28) i la temperatura (37ºC) han estat els mateixos. Per cadascuna de les condicions, s'ha calculat n_c a partir de l'Eq. 23, on *w* és la mitjana de les amplades de la base dels pics cromatogràfics de totes les proteïnes que s'han analitzat. Els resultats obtinguts es poden veure a la Figura 34.

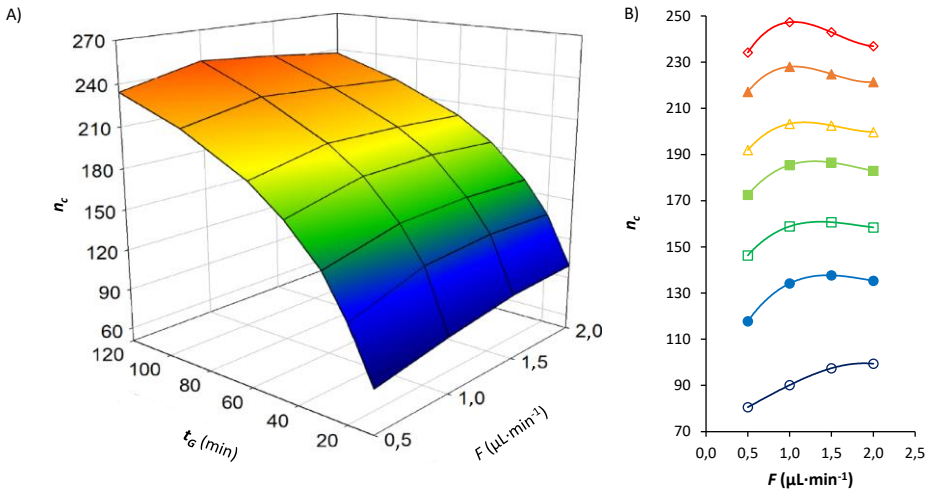

Figura 34. Efecte del cabal (0,5, 1,0, 1,5 i 2,0 µL/min) i del temps de gradient en n_c. A) Gràfic en 3 dimensions. B) Gràfic en 2 dimensions on t_G és 10 min (◦), 20 min (•), 30 min (□), 45 min (■), 60 min (△), 90 min (▲) i 120 min (◊). (Article VII)

A la Figura 34A s'observa com la capacitat de pics augmenta per tots els cabals amb el temps de gradient, sent aquest augment més pronunciat per temps de gradient més baixos (entre 10-60 min). A partir d'un gradient de 120 min el valor de n_c comença a anivellar-se. En referència al u_{opt}, cabal amb el valor més alt de n_c, a la Figura 34B es pot observar com aquest varia en funció del temps de gradient utilitzat. u_{opt} és més gran quan s'utilitzen temps de gradient més baixos, en canvi, a mesura que augmenta el temps de gradient el u_{opt} disminueix assemblant-se cada cop més a l'obtingut en condicions isocràtiques (sent aquest 1,0 µL·min^{-1} per t_G = 120 min).

Segons la Figura 31 l'eficàcia de la separació hauria de disminuir a mesura que es treballa amb cabals per sobre del $u_{opt,}$ però això no s'observa en aquest cas, on per tots els gradients estudiats, el cabal en el qual s'ha obtingut el valor màxim de n_c és sempre molt superior a l'estimat de manera isocràtica per una proteïna model (<0,1 µL.min^{-1}). Com que a la Figura 34 es presenten 2 variables diferents que influeixen en n_c (temps de gradient i el cabal), a la Figura 35 s'ha correlacionat n_c en funció de t_G/t_0.

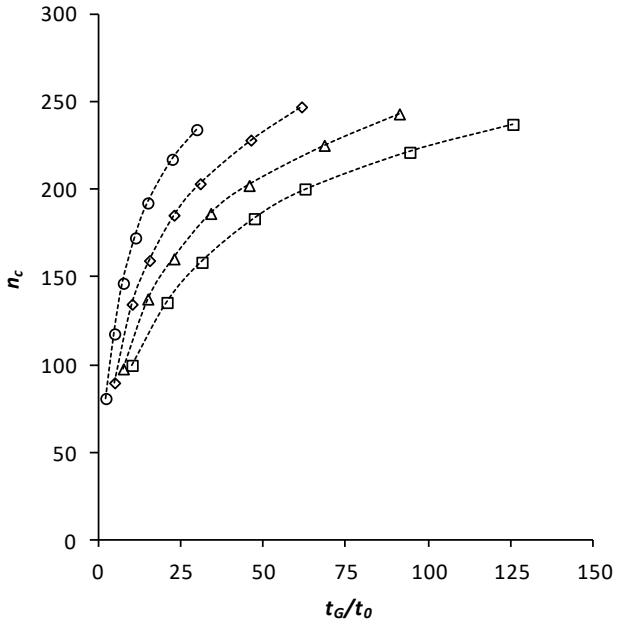

Figura 35. Efecte del pendent de gradient (t_G/t_0) en n_c aplicant diferents cabals ((○) 0,5 µL.min^{-1}; (◊) 1,0 µL.min^{-1}; (Δ) 1,5 µL.min^{-1}; (□) 2,0 µL.min^{-1}). (Article VII)

En aquesta figura, per un mateix valor de t_G/t_0 es pot observar com n_c augmenta a mesura que el flux és més petit i s'assembla més al u_{opt} determinat de manera isocràtica. Per tant, hi ha d'haver un factor addicional que faci que u_{opt} en mode gradient sigui 10-20 vegades superior al determinat de manera isocràtica.

Aquest fenomen també es va observar en estudis anteriors [201] i es pot explicar mitjançant l'Eq. 24 desenvolupada per Neue *et al.* [120]. Aquesta equació diu que si es manté el mateix interval de gradient (Δc) i s'utilitzen els mateixos compostos (S), per una banda n_c variarà en funció de N, disminuint a mesura que augmentem el flux (relacionat amb el terme C de l'equació de Van Deemter, ja que es treballa a cabals superiors al u_{opt}), però n_c augmentarà per l'efecte del volum de gradient (valor de t_G/t_0 més gran), ja que aquestes propietats estan inversament relacionades. Per aquest motiu serà possible treballar a cabals superiors d'una manera més ràpida, que impliquen temps d'anàlisi més curts i eficaços, ja que u_{opt} serà més elevat.

A partir d'aquests resultats, es pot concloure que en RP-LC la capacitat de pics depèn de molts altres factors a part del disseny de la fase estacionària, ja que les condicions utilitzades en les separacions cromatogràfiques poden també afectar a la capacitat separativa de la columna cromatogràfica utilitzada.

CONCLUSIONS

1. When different partitioning systems are characterized through the solvation parameter model, they can be compared through their normalized coefficients. With this aim, different comparison tools such as the distance *d* parameter, other chemometric tools (PCA and dendrogram) and the calculation of the correlation precision can be used.

2. The comparison between the aquatic systems used to evaluate aquatic toxicity indicate that most of them show similar toxicity information. Among all, 8 of them (Rana tadpole, Fathead minnow, Golden orfe, *Daphnia magna (24h)*, *Tetrahymena pyriformis*, *Chilomonas paramecium*, *Pseudomonas putida*, and *Streptococus sobrinus*) have been selected as representative.

3. Aquatic toxicity to RT, FM, DM, TP or PP of neutral compounds can be surrogated through 4 physicochemical systems, 3 based on MEKC (using as surfactants STC, TTAB, and a mixture of SDS and Brij 35), and another system based on RP-LC (employing as a stationary phase an IAM column). The results agree with the initial predictions.

4. 3 ready to use lecithin-based chromatographic systems (LMEEKC, LLEKC, and LMELC) have been developed and characterized through the solvation parameter model. These systems have shown similar properties regarding their interaction with neutral compounds. The hydrophobicity and the hydrogen-bond acidity are the main driven forces in the partition, and the hydrogen-bond basicity and polarizability are the main differences between the lecithin-based systems.

5. Lecithin-based chromatographic systems show a high similarity with the skin partition of neutral compounds. The best correlation has been obtained for the LMEEKC system, and hence it is the best alternative to model this biological property.

6. Similar to SDSME, good correlations have been obtained between the log $P_{o/w}$ of neutral compounds and the corresponding log k determined in the TTABME system. Therefore, the ME formed by TTAB can be an alternative to the one constituted by SDS. It has been checked that the choice of the surfactant does not affect the selectivity of the system.

7. k value of ionized compounds determined in EKC systems can be altered if the viscosities of the solutions used in its measurement are very different. This fact is specifically relevant in MEEKC since the ME components (mainly 1-butanol) enhance the viscosity of the media. In order to obtain accurate k values, a viscosity correction factor has been introduced in the calculation formulae. This factor is the mobility ratio between MEEKC and CZE modes of a compound that does not interact with the ME.

8. MEEKC systems showing different charges to the analytes cannot be used to correlate with the log $P_{o/w}$ because k is affected by the ion-pair interaction.

9. The log $D_{o/w}$ of partially ionized acid-base compounds (up to a 99% of ionization) has been estimated from only the determination of k at a given pH value. k was determined in the MEEKC system at the pH of interest, and log $D_{o/w}$ was obtained using the correlation between log k and log $P_{o/w}$ established for neutral compounds. The error obtained in these estimations has been similar to the one obtained for neutral compounds.

10. log $P_{o/w}$ of fully ionized solutes is generally overestimated compared to data from the literature. The difference can be due to the strong dependence of the log $P_{o/w}$ value on the conditions employed to do the measurements (counter-ion and its concentration). Moreover, the

bigger relative error associated to *k* determination for ionized solutes and the bigger surface area of the ME with respect to the octanol-water partition could also have an influence.

11. To obtain a new chromatographic system with a different selectivity, an optimized polymeric styrene-co-divinylbenzene monolithic column has been synthetized in a 200 µm internal diameter capillary. For the separation of a group of proteins, with molecular weights in the 6-30 kDa interval, a peak capacity of approximately 250 has been obtained at a gradient time of 120 min and applying a flow rate of 1,0 $\mu L \cdot min^{-1}$.

12. When the selected proteins were separated by ion pair chromatography, a better peak-symmetry, narrower peaks, and a better loadability have been obtained when using TFA as ion-pairing agent instead of FA. Moreover, the highest peak capacities have been observed at flow rates with a factor 10-20 higher than the optimum one determined in isocratic conditions. So, the optimum flow rate is a compromise between the magnitude of the C-term contribution (decreasing the peak capacity with flow rate) and the increase in peak capacity induced by the more favorable gradient-volume ratio.

REFERÈNCIES

[1] M.H. Abraham, H.S. Chadha, R.C. Mitchell, The factors that influence skin penetration of solutes, J. Pharm. Pharmacol. 47 (1995) 8–16.

[2] M.H. Abraham, Y.H. Zhao, J. Le, A. Hersey, C.N. Luscombe, D.P. Reynolds, G. Beck, B. Sherborne, I. Cooper, On the mechanism of human intestinal absorption, Eur. J. Med. Chem. 37 (2002) 595–605.

[3] J.A. Gratton, M.H. Abraham, M.W. Bradbury, H.S. Chadha, Molecular factors influencing drug transfer across the blood-brain barrier, J. Pharm. Pharmacol. 49 (1997) 1211–1216.

[4] C.T. Chiou, T.D. Shoup, P.E. Porter, Mechanistic roles of soil humus and minerals in the sorption of nonionic organic compounds from aqueous and organic solutions, Org. Geochem. 8 (1985) 9–14.

[5] R.L. Wershaw, A new model for humic materials and their interactions with hydrophobic organic chemicals in soil-water or sediment-water systems, J. Contam. Hydrol. 1 (1986) 29–45.

[6] K.R. Hoover, W.E. Acree, M.H. Abraham, Chemical toxicity correlations for several fish species based on the abraham solvation parameter model, Chem. Res. Toxicol. 18 (2005) 1497–1505.

[7] L.L. Dobbins, S. Usenko, R.A. Brain, B.W. Brooks, Probabilistic ecological hazard assessment of parabens using *Daphnia magna* and *Pimephales promelas*, Environ. Toxicol. Chem. 28 (2009) 2744–2753.

[8] I. Juhnke, D. Lüdemann, Results of the examination of the effects of 200 chemical compounds on fish toxicity using the Golden Orfe test, Zeitschrift Für Wasser Und Abwasser Forsch. 11 (1978) 161–164.

[9] E. Overton, Studien über die narkose, zugleich ein beitrag zur allgemeinen pharmakologie, Jena: Gustav Fischer, Zürich, Switzerland, 1901.

[10] E. Overton, Studies on Narcosis, Chapman and Hall, London, UK, 1991.

[11] H. Huang, X. Wang, W. Ou, J. Zhao, Y. Shao, L. Wang, Acute toxicity of benzene derivatives to the tadpoles (*Rana japonica*) and QSAR analyses, Chemosphere. 53 (2003) 963–970.

[12] X. Wang, Y. Dong, S. Xu, L. Wang, S. Han, Quantitative structure-activity relationships for the toxicity to the tadpole *Rana japonica* of selected phenols, Bull. Environ. Contam. Toxicol. 64 (2000) 859–865.

[13] K.H. Meyer, H. Hemmi, Beitrage zur theorie der narkose, Biochem. Zschr. 277 (1935) 39–71.

[14] Y. Kita, L.J. Bennett, K.W. Miller, The partial molar volumes of anesthetics in lipid bilayers, Biochim. Biophys. Acta - Biomembr. 647 (1981) 130–139.

[15] K.R. Bowen, K.B. Flanagan, W.E. Acree, M.H. Abraham, Correlating toxicities of organic compounds to select protozoa using the Abraham model, Sci. Total Environ. 369 (2006) 109–118.

[16] K.R. Hoover, K.B. Flanagan, W.E. Acree, M.H. Abraham, Chemical toxicity correlations for several protozoas, bacteria, and water fleas based on the Abraham solvation parameter model, J. Environ. Eng. Sci. 6 (2007) 165–174.

[17] G.. Suter, M. Lewis, eds., Aquatic toxicology and environmental fate,

ASTM, Philadelphia, USA, 2007.

[18] C. Mintz, W.E. Acree, M.H. Abraham, Correlation of minimum inhibitory concentrations toward oral bacterial growth based on the Abraham model, QSAR Comb. Sci. 25 (2006) 912–920.

[19] G. Bringmann, R. Kühn, Comparison of the toxicity thresholds of water pollutants to bacteria, algae, and protozoa in the cell multiplication inhibition test, Water Res. 14 (1980) 231–241.

[20] J.E. Rice, Partition Coefficients, in: Org. Chem. Concepts Appl. Med. Chem., Academic Press, Cambridge, USA, 2014: pp. 85–92.

[21] C. Giaginis, A. Tsantili-Kakoulidou, Alternative measures of lipophilicity: from octanol-water partitioning to IAM retention, J. Pharm. Sci. 97 (2008) 2984–3004.

[22] S. Amézqueta, X. Subirats, E. Fuguet, M. Rosés, C. Ràfols, Octanol-water partition constant, in: C.F. Poole (Ed.), Liq. Extr., Elsevier, Amsterdam, The Netherlands, 2020: pp. 183–208.

[23] A.D. McNaught, A. Wilkinson, Compendium of chemical terminology, Second edi, Blackwell science, Oxford, 1997.

[24] J. Comer, K. Tam, Lipophilicity profiles: theory and measurement, in: B. Testa, H. van de Waterbeemd, G. Folkers, R. Guy (Eds.), Pharmacokinet. Optim. Drug Res., Verlag Helvetica Chimica Acta, Zürich, Switzerland, 2007: pp. 275–304.

[25] N. Gulyaeva, A. Zaslavsky, P. Lechner, A. Chait, B. Zaslavsky, p*H* dependence of the relative hydrophobicity and lipophilicity of amino acids and peptides measured by aqueous two-phase and octanol-buffer partitioning, J. Pept. Res. 61 (2003) 71–79.

[26] OECD, Test No. 107: partition coefficient (n-octanol/water): shake flask method, OECD Guidel. Test. Chem. Sect. 1. 107 (1995).

[27] OECD, OECD draft guideline for the testing of chemicals 122: partition coefficient (n-octanol/water): p*H*-metric method for ionisable substances, (2000).

[28] OECD, Test No. 117: partitioning coefficient (n-octanol/water) HPLC method, OECD Guidel. Test. Chem. (2004).

[29] K.D. Altria, Fundamentals of capillary electrophoresis theory, in: K.D. Altria (Ed.), Capill. Electrophor. Guideb. Princ. Oper. Appl., Humana Press, Totowa, New Jersey, 1996: pp. 3–13.

[30] T.G. Morzunova, Capillary electrophoresis in pharmaceutical analysis (a review), Pharm. Chem. J. 40 (2006) 158–170.

[31] M.A. García, M.L. Marina, A. Ríos, M. Valcárcel, Separation modes in capillary electrophoresis, Compr. Anal. Chem. 45 (2005) 31–134.

[32] E. Fuguet, C. Ràfols, E. Bosch, M. Rosés, Solute-solvent interactions in micellar electrokinetic chromatography: IV. Characterization of electroosmotic flow and micellar markers, Electrophoresis. 23 (2002) 56–66.

[33] D.R. Baker, Capillary electrophoresis, Wiley, New York, USA, 1995.

[34] S. Terabe, Electrokinetic chromatography: an interface between electrophoresis and chromatography, Trends Anal. Chem. 8 (1989) 129–134.

[35] S. Terabe, K. Otsuka, K. Ichikawa, A. Tsuchiya, T. Ando, Electrokinetic separations with micellar solutions and open-tubular capillaries, Anal. Chem. 56 (1984) 111–113.

[36] M.G. Khaledi, S.C. Smith, J.K. Strasters, Micellar electrokinetic capillary chromatography of acidic solutes: migration behavior and optimization strategies, Anal. Chem. 63 (1991) 1820–1830.

[37] J.K. Strasters, M.G. Khaledi, Migration behavior of cationic solutes in micellar electrokinetic capillary chromatography, Anal. Chem. 63 (1991) 2503–2508.

[38] A. Téllez, E. Fuguet, M. Rosés, Comparison of migration models for acidic solutes in micellar electrokinetic chromatography, J. Chromatogr. A. 1139 (2007) 143–151.

[39] S. Terabe, K. Otsuka, T. Ando, Electrokinetic chromatography with micellar solution and open-tubular capillary, Anal. Chem. 57 (1985) 834–841.

[40] H. Watarai, Microemulsion capillary electrophoresis, Chem. Lett. 20 (1991) 391–394.

[41] H. Nakamura, I. Sugiyama, A. Sano, Liposome electrokinetic chromatography as a novel tool for the separation of hydrophobic compounds, Anal. Sci. 12 (1996) 973–975.

[42] C.P. Palmer, Micelle polymers, polymer surfactants and dendrimers as pseudo-stationary phases in micellar electrokinetic chromatography, J. Chromatogr. A. 780 (1997) 75–92.

[43] M. Hong, B.S. Weekley, S.J. Grieb, J.P. Foley, Electrokinetic chromatography using thermodynamically stable vesicles and mixed micelles formed from oppositely charged surfactants, Anal. Chem. 70 (1998) 1394–1403.

[44] G. Hancu, B. Simon, A. Rusu, E. Mircia, Á. Gyéresi, Principles of micellar electrokinetic capillary chromatography applied in pharmaceutical analysis, Adv. Pharm. Bull. 3 (2013) 1–8.

[45] R. Ryan, K. Altria, E. McEvoy, S. Donegan, J. Power, A review of developments in the methodology and application of microemulsion electrokinetic chromatography, Electrophoresis. 34 (2013) 159–177.

[46] A. Akbarzadeh, R. Rezaei-Sadabady, S. Davaran, S.W. Joo, N. Zarghami, Y. Hanifehpour, M. Samiei, M. Kouhi, K. Nejati-Koshki, Liposome: classification, preparation, and applications, Nanoscale Res. Lett. 8 (2013).

[47] S.S. Chrai, R. Murari, I. Ahmad, Liposomes (a review) - Part one: manufacturing issues, BioPharm. 14 (2001) 10–14.

[48] X. Li, Y. Du, Z. Feng, X. Sun, Z. Huang, A novel enantioseparation approach based on liposome electrokinetic capillary chromatography, J. Pharm. Biomed. Anal. 145 (2017) 186–194.

[49] C.W. Chang, Y.C. Chen, C.Y. Liu, Separation and on-line preconcentration of nonsteroidal anti-inflammatory drugs by microemulsion electrokinetic chromatography, Electrophoresis. 36 (2015) 2745–2753.

[50] K. Purgat, K. Borowczyk, R. Zakrzewski, R. Głowacki, P. Kubalczyk, Determination of nikethamide by micellar electrokinetic chromatography, Biomed. Chromatogr. 33 (2019).

[51] Y. Wang, J. Sun, H. Liu, J. Liu, L. Zhang, K. Liu, Z. He, Predicting skin permeability using liposome electrokinetic chromatography, Analyst. 134 (2009) 267–72.

[52] A. Fernández-Pumarega, S. Amézqueta, E. Fuguet, M. Rosés, Tadpole toxicity prediction using chromatographic systems, J. Chromatogr. A. 1418 (2015) 167–176.

[53] M. Hidalgo-Rodríguez, E. Fuguet, C. Ràfols, M. Rosés, Modeling nonspecific toxicity of organic compounds to the fathead minnow fish by means of chromatographic systems, Anal. Chem. 84 (2012) 3446–3452.

[54] M.H. Abraham, C. Treiner, M. Roses, C. Ràfols, Y. Ishihama, Linear free energy relationship analysis of microemulsion electrokinetic chromatographic determination of lipophilicity, J. Chromatogr. A. 752 (1996) 243–249.

[55] X. Subirats, H.P. Yuan, V. Chaves, N. Marzal, M. Rosés, Microemulsion electrokinetic chromatography as a suitable tool for lipophilicity determination of acidic, neutral, and basic compounds, Electrophoresis. 37 (2016) 2010–2016.

[56] S.K. Poole, D. Durham, C. Kibbey, Rapid method for estimating the octanol–water partition coefficient (log P_{ow}) by microemulsion electrokinetic chromatography, J. Chromatogr. B. 745 (2000) 117–126.

[57] S.K. Poole, S. Patel, K. Dehring, H. Workman, J. Dong, Estimation of octanol-water partition coefficients for neutral and weakly acidic compounds by microemulsion electrokinetic chromatography using dynamically coated capillary columns, J. Chromatogr. B. 793 (2003) 265–274.

[58] J. Øtergaard, S.H. Hansen, C. Larsen, C. Schou, N.H.H. Heegaard, Determination of octanol-water partition coefficients for carbonate esters and other small organic molecules by microemulsion electrokinetic chromatography, Electrophoresis. 24 (2003) 1038–1046.

[59] D.W. Armstrong, S.J. Henry, Use of an aqueous micellar mobile phase for separation of phenols and polynuclear aromatic hydrocarbons via HPLC, J. Liq. Chromatogr. 3 (1980) 657–662.

[60] A. Berthod, M.C. García-Alvarez-Coque, Micellar liquid chromatography, J. Cazes, Marcel Dekker, New York, USA, 2000.

[61] A. Marsh, B.J. Clark, K.D. Altria, A review of the background, operating parameters and applications of microemulsion liquid chromatography (MELC), J. Sep. Sci. 28 (2005) 2023–2032.

[62] T.G. Gini, G.J. Jothi, Column chromatography and HPLC analysis of phenolic compounds in the fractions of *Salvinia molesta* mitchell, Egypt. J. Basic Appl. Sci. 5 (2018) 197–203.

[63] G. Nannetti, S. Pagni, G. Palù, A. Loregian, A sensitive and validated HPLC-UV method for the quantitative determination of the new antifungal drug isavuconazole in human plasma, Biomed. Chromatogr. 32 (2018).

[64] G. Russo, L. Grumetto, R. Szucs, F. Barbato, F. Lynen, Screening therapeutics according to their uptake across the blood-brain barrier: A high throughput method based on immobilized artificial membrane liquid chromatography-diode-array-detection coupled to electrospray-time-of-flight mass spectrometry, Eur. J. Pharm. Biopharm. 127 (2018) 72–84.

[65] X. Liu, H. Hefesha, H. Tanaka, G. Scriba, A. Fahr, Lipophilicity measurement of drugs by reversed phase HPLC over wide pH range using an alkaline-resistant silica-based stationary phase, XBridge™ shield RP18, Chem. Pharm. Bull. 56 (2008) 1417–1422.

[66] M. Hidalgo-Rodríguez, S. Soriano-Meseguer, E. Fuguet, C. Ràfols, M. Rosés, Evaluation of the suitability of chromatographic systems to predict human skin permeation of neutral compounds, Eur. J. Pharm. Sci. 50 (2013) 557–568.

[67] S. Soriano-Meseguer, E. Fuguet, A. Port, M. Rosés, Estimation of skin permeation by liquid chromatography, ADMET DMPK. 6 (2018) 140–152.

[68] T. Godard, E. Grushka, The use of phospholipid modified column for the determination of lipophilic properties in high performance liquid chromatography, J. Chromatogr. A. 1218 (2011) 1211–1218.

[69] M.H. Abraham, Application of solvation equations to chemical and biochemical processes, Pure Appl. Chem. 65 (1993) 2503–2512.

[70] M. Vitha, P.W. Carr, The chemical interpretation and practice of linear solvation energy relationships in chromatography, J. Chromatogr. A. 1126 (2006) 143–194.

[71] M.H. Abraham, H.S. Chadha, F. Martins, R.C. Mitchell, M.W. Bradbury, J.A. Gratton, Hydrogen bonding part 46: a review of the correlation and prediction of transport properties by an lfer method: physicochemical properties, brain penetration and skin permeability, Pestic. Sci. 55 (1999) 78–88.

[72] M.H. Abraham, G.S. Whiting, R.M. Doherty, W.J. Shuely, Hydrogen bonding: XVI. A new solute salvation parameter, π_2^H, from gas chromatographic data, J. Chromatogr. A. 587 (1991) 213–228.

[73] M.H. Abraham, Hydrogen bonding. 31. Construction of a scale of solute effective or summation hydrogen-bond basicity, J. Phys. Org. Chem. 6 (1993) 660–684.

[74] M.H. Abraham, Scales of solute hydrogen-bonding: their construction and application to physicochemical and biochemical processes, Chem. Soc. Rev. 22 (1993) 73–83.

[75] M.H. Abraham, J.C. McGowan, The use of characteristic volumes to measure cavity terms in reversed phase liquid chromatography, Chromatographia. 23 (1987) 243–246.

[76] M.H. Abraham;, H.S. Chadha, Applications of a solvation equation to drug transport properties, in: V. Pliška, B. Testa, H. Van De Waterbeemd (Eds.), Lipophilicity Drug Action Toxicol., Wiley-VCH, Weinheim, Germany, 1996:

pp. 311–337.

[77] J.D. Walker, L. Carlsen, E. Hulzebos, B. Simon-Hettich, Global government applications of analogues, SARs and QSARs to predict aquatic toxicity, chemical or physical properties, environmental fate parameters and health effects of organic chemicals, SAR QSAR Environ. Res. 13 (2002) 607–616.

[78] E. Fuguet, C. Ràfols, E. Bosch, M.H. Abraham, M. Rosés, Solute-solvent interactions in micellar electrokinetic chromatography: III. Characterization of the selectivity of micellar electrokinetic chromatography systems, J. Chromatogr. A. 942 (2002) 237–248.

[79] E. Fuguet, C. Rafols, E. Bosch, M.H. Abraham, M. Roses, Erratum to "solute-solvent interactions in micellar electrokinetic chromatography. III. Characterization of the selectivity of micellar electrokinetic systems", J. Chromatogr. A. 942 (2002) 327–248.

[80] E. Lázaro, C. Ràfols, M.H. Abraham, M. Rosés, Chromatographic estimation of drug disposition properties by means of immobilized artificial membranes (IAM) and C18 columns, J. Med. Chem. 49 (2006) 4861–4870.

[81] M.D. Trone, M.G. Khaledi, Influence of ester and amide-containing surfactant headgroups on selectivity in micellar electrokinetic chromatography, Electrophoresis. 21 (2000) 2390–2396.

[82] M. Rosés, C. Ràfols, E. Bosch, A.M. Martínez, M.H. Abraham, Solute–solvent interactions in micellar electrokinetic chromatography: characterization of sodium dodecyl sulfate–Brij 35 micellar systems for quantitative structure–activity relationship modelling, J. Chromatogr. A. 845 (1999) 217–226.

[83] J. Liu, J. Sun, Y. Wang, X. Liu, Y. Sun, H. Xu, Z. He, Characterization of microemulsion liquid chromatography systems by solvation parameter model and comparison with other physicochemical and biological processes, J. Chromatogr. A. 1164 (2007) 129–138.

[84] S.T. Burns, A.A. Agbodjan, M.G. Khaledi, Characterization of solvation properties of lipid bilayer membranes in liposome electrokinetic chromatography, J. Chromatogr. A. 973 (2002) 167–176.

[85] C. Fujimoto, Application of linear solvation energy relationships to polymeric pseudostationary phases in micellar electrokinetic chromatography, Electrophoresis. 22 (2001) 1322–1329.

[86] A.A. Agbodjan, H. Bui, M.G. Khaledi, Study of solute partitioning in biomembrane-mimetic pseudophases by electrokinetic chromatography: dihexadecyl phosphate small unilamellar vesicles, Langmuir. 17 (2001) 2893–2899.

[87] R.J. Pascoe, J.P. Foley, Characterization of surfactant and phospholipid vesicles for use as pseudostationary phases in electrokinetic chromatography, Electrophoresis. 24 (2003) 4227–4240.

[88] S. Schulte, C.P. Palmer, Alkyl-modified siloxanes as pseudostationary phases for electrokinetic chromatography, Electrophoresis. 24 (2003) 978–983.

[89] J.A. Platts, M.H. Abraham, Y.H. Zhao, A. Hersey, L. Ijaz, D. Butina, Correlation and prediction of a large blood-brain distribution data set - an LFER study, Eur. J. Med. Chem. 36 (2001) 719–730.

[90] M.H. Abraham, The factors that influence permeation across the blood-brain barrier, Eur. J. Med. Chem. 39 (2004) 235–240.

[91] M.H. Abraham, F. Martins, Human skin permeation and partition: general linear free-enegy relationship analyses, J. Pharm. Sci. 93 (2004) 1508–1523.

[92] M.H. Abraham, C. Ràfols, Factors that influence tadpole narcosis. An LFER analysis, J. Chem. Soc. Perkin Trans. 2. (1995) 1843–1851.

[93] J.A. Platts, M.H. Abraham, A. Hersey, D. Butina, Estimation of molecular linear free energy relationship descriptors. 4. Correlation and prediction of cell permeation, Pharm. Res. 17 (2000) 1013–1018.

[94] S.K. Poole, C.F. Poole, Chromatographic models for the sorption of neutral organic compounds by soil from water and air, J. Chromatogr. A. 845 (1999) 381–400.

[95] M.H. Abraham, H.S. Chadha, G.S. Whiting, R.C. Mitchell, Hydrogen bonding. 32. An analysis of water-octanol and water-alkane partitioning and the Δlog *P* parameter of seiler, J. Pharm. Sci. 83 (1994) 1085–1100.

[96] Mathworks, Dendrogram. https://www.mathworks.com/help/stats/dendrogram.html#btk0xou-2 (5 de Gener, 2020).

[97] ArcGis Resources, Cómo funciona Dendrograma. http://resources.arcgis.com/es/help/main/10.1/index.html#//009z000000q6000000 (5 de Gener, 2020).

[98] Octave, Function reference linkage. https://octave.sourceforge.io/statistics/function/linkage.html (5 de Gener, 2020).

[99] I.T. Jolliffe, Principal component analysis, second edition, Springer, Berlín, Germany, 2002.

[100] M. Hidalgo-Rodríguez, E. Fuguet, C. Ràfols, M. Rosés, Estimation of biological properties by means of chromatographic systems: evaluation of the factors that contribute to the variance of biological-chromatographic correlations, Anal. Chem. 82 (2010) 10236–10245.

[101] M.H. Abraham, H.S. Chadha, J.P. Dixon, C. Rafols, C. Treiner, Hydrogen bonding. Part 40. Factors that influence the distribution of solutes between water and sodium dodecylsulfate micelles, J. Chem. Soc. Perkin Trans. 2. (1995) 887–894.

[102] K.R. Bowen, K.B. Flanagan, W.E. Acree, M.H. Abraham, C. Rafols, Correlation of the toxicity of organic compounds to tadpoles using the Abraham model, Sci. Total Environ. 371 (2006) 99–109.

[103] K. Roy, On some aspects of validation of predictive quantitative structure-activity relationship models, Expert Opin. Drug Discov. 2 (2007) 1567–1577.

[104] A. Tropsha, P. Gramatica, V.K. Gombar, The importance of being earnest:

validation is the absolute essential for successful application and interpretation of QSPR models, QSAR Comb. Sci. 22 (2003) 69–77.

[105] R. Veerasamy, H. Rajak, A. Jain, S. Sivadasan, C.P. Varghese, R.K. Agrawal, Validation of QSAR models - strategies and importance, Int. J. Drug Des. Discov. 2 (2011) 511–519.

[106] E.G. Hammond, L.A. Johnson, C. Su, T. Wang, P.J. White, Part 2 edible oil and fat products: edible oils. Soybean oil, in: Fereidoon Shahidi (Ed.), Bailey's Ind. Oil Fat Prod., John Wiley & Sons, Hoboken, USA, 2005.

[107] G.M. Gray, H.J. Yardley, Lipid compositions of cells isolated from pig, human, and rat epidermis, J. Lipid Res. 16 (1975) 434–440.

[108] X.Y. Liu, C. Nakamura, Q. Yang, N. Kamo, J. Miyake, Immobilized liposome chromatography to study drug-membrane interactions. Correlation with drug absorption in humans, J. Chromatogr. A. 961 (2002) 113–118.

[109] J.S. Dua, A.C. Rana, A.K. Bhandari, Liposomes: methods of preparation and applications, Int. J. Pharm. Stud. Res. 3 (2012) 14–20.

[110] F. Svec, Monolithic columns: a historical overview, Electrophoresis. 38 (2017) 2810–2820.

[111] I. Mikšík, P. Sedláková, Capillary electrochromatography of proteins and peptides, J. Sep. Sci. 30 (2007) 1686–1703.

[112] R. Bakry, C.W. Huck, G.K. Bonn, Recent applications of organic monoliths in capillary liquid chromatographic separation of biomolecules, J. Chromatogr. Sci. 47 (2009) 418–431.

[113] J. Courtois, M. Szumski, E. Byström, A. Iwasiewicz, A. Shchukarev, K. Irgum, A study of surface modification and anchoring techniques used in the preparation of monolithic microcolumns in fused silica capillaries, J. Sep. Sci. 29 (2006) 14–24.

[114] F. Svec, J.M.J. Fréchet, Molded rigid monolithic porous polymers: an inexpensive, efficient, and versatile alternative to beads for the design of materials for numerous applications, Ind. Eng. Chem. Res. 38 (1999) 34–48.

[115] H.G. Elias, Free radical polymerization, in: Macromolecules, Springer, Boston. USA, 1984: pp. 681–736.

[116] J.L. Dores-Sousa, A. Fernández-Pumarega, J. De Vos, M. Lämmerhofer, G. Desmet, S. Eeltink, Guidelines for tuning the macropore structure of monolithic columns for high-performance liquid chromatography, J. Sep. Sci. 42 (2019) 522–533.

[117] A. Vaast, H. Terryn, F. Svec, S. Eeltink, Nanostructured porous polymer monolithic columns for capillary liquid chromatography of peptides, J. Chromatogr. A. 1374 (2014) 171–179.

[118] U.D. Neue, HPLC columns: theory, technology, and practice, Wiley VCH, New York, USA, 1997.

[119] J.C. Giddings, Sample dimensionality: a predictor of order-disorder in component peak distribution in multidimensional separation, J. Chromatogr. A. 703 (1995) 3–15.

[120] M. Gilar, U.D. Neue, Peak capacity in gradient reversed-phase liquid chromatography of biopolymers. Theoretical and practical implications for the separation of oligonucleotides, J. Chromatogr. A. 1169 (2007) 139–150.

[121] L.R. Snyder, J.W. Dolan, High-performance gradient elution: the practical application of the linear-solvent-strength model, Wiley, Hoboken, USA, 1998.

[122] X. Subirats, L. Muñoz-Pascual, M.H. Abraham, M. Rosés, Revisiting blood-brain barrier: a chromatographic approach, J. Pharm. Biomed. Anal. 145 (2017) 98–109.

[123] M. Hidalgo-Rodríguez, E. Fuguet, C. Ràfols, M. Rosés, Performance of chromatographic systems to model soil-water sorption, J. Chromatogr. A. 1252 (2012) 136–145.

[124] ECHA, European Chemicals Agency, REACH. https://echa.europa.eu/es/regulations/reach/understanding-reach (5 de Gener, 2020).

[125] Y. Ishihama, Y. Oda, N. Asakawa, Hydrophobicity of cationic solutes measured by electrokinetic chromatography with cationic microemulsions, Anal. Chem. 68 (1996) 4281–4284. doi:10.1021/ac960447j.

[126] L. Wang, L. Chen, G. Lian, L. Han, Determination of partition and binding properties of solutes to stratum corneum, Int. J. Pharm. 398 (2010) 114–122.

[127] S. Winiwarter, N.M. Bonham, F. Ax, A. Hallberg, H. Lennernäs, A. Karlén, Correlation of human jejunal permeability (*in vivo*) of drugs with experimentally and theoretically derived parameters. A multivariate data analysis approach, J. Med. Chem. 41 (1998) 4939–4949.

[128] M. Kansy, H. Fischer, K. Kratzat, F. Senner, B. Wagner, I. Parrilla, High-throughput artificial membrane permeability studies in early lead discovery and development, in: B. Testa, H. van de Waterbeemd, G. Folkers, R. Guy (Eds.), Pharmacokinet. Optim. Drug Res. Biol. Physicochem. Comput. Strateg. Dev., Verlag Helvetica Chimica Acta, Zürich, Switzerland, 2001: pp. 447–464.

[129] G. Camenisch, G. Folkers, H. Van De Waterbeemd, Comparison of passive drug transport through Caco-2 cells and artificial membranes, Int. J. Pharm. 147 (1997) 61–70.

[130] F. Lombardo, M.Y. Shalaeva, K.A. Tupper, F. Gao, M.H. Abraham, Elog *P(oct)*: A tool for lipophilicity determination in drug discovery, J. Med. Chem. 43 (2000) 2922–2928.

[131] C. Zhu, L. Jiang, T.M. Chen, K.K. Hwang, A comparative study of artificial membrane permeability assay for high throughput profiling of drug absorption potential, Eur. J. Med. Chem. 37 (2002) 399–407.

[132] E.O. Dillingham, R.W. Mast, G.E. Bass, J. Autian, Toxicity of methyl- and halogen-substituted alcohols in tissue culture relative to structure—activity models and acute toxicity in mice, J. Pharm. Sci. 62 (1973) 22–30.

[133] S. Banerjee, S.H. Yalkowsky, C. Valvani, Water solubility and octanol/water partition coefficients of organics. Limitations of the solubility-

partition coefficient correlation, Environ. Sci. Technol. 14 (1980) 1227–1229.

[134] J. Li, E.M. Perdue, S.G. Pavlostathis, R. Araujo, Physicochemical properties of selected monoterpenes, Environ. Int. 24 (1998) 353–358.

[135] P.R. Rich, R. Harper, Partition coefficients of quinones and hydroquinones and their relation to biochemical reactivity, FEBS Lett. 269 (1990) 139–144.

[136] D.E. Leszczynski, R.M. Schafer, Nonspecific and metabolic interactions between steroid hormones and human plasma lipoproteins, Lipids. 25 (1990) 711–718.

[137] D.M. Miller, Evidence that interfacial transport is rate-limiting during passive cell membrane permeation, BBA - Biomembr. 1065 (1991) 75–81.

[138] T. Fujita, J. Iwasa, C. Hansch, A new substituent constant, π, derived from partition coefficients, J. Am. Chem. Soc. 86 (1964) 5175–5180.

[139] J. Iwasa, T. Fujita, C. Hansch, Substituent constants for aliphatic functions obtained from partition coefficients, J. Med. Chem. 8 (1965) 150–153.

[140] A. Avdeef, Octanol–water partitioning, in: Absorpt. Drug Dev. Solubility, Permeability, Charg. State, 2nd editio, Wiley, Hoboken, USA, 2012: pp. 174–219.

[141] L. Hitzel, A.P. Watt, K.L. Locker, An increased throughput method for the determination of partition coefficients, Pharm. Res. 17 (2000) 1389–1395.

[142] C. Hansch, S.M. Anderson, The effect of intramolecular hydrophobic bonding on partition coefficients, J. Org. Chem. 32 (1967) 2583–2586.

[143] Bio−Loom, BioByte Corp. (Claremont, CA, USA), http://www.biobyte.com, Version 1.7.

[144] T. Sotomatsu, M. Shigemura, Y. Murata, T. Fujita, Octanol/water partition coefficient of ortho-substituted aromatic solutes, J. Pharm. Sci. 82 (1993) 776–781.

[145] J. De Bruijn, F. Busser, W. Seinen, J. Hermens, Determination of octanol/water partition coefficients for hydrophobic organic chemicals with the “slow-stirring” method, Environ. Toxicol. Chem. 8 (1989) 499–512.

[146] A. Andrés, M. Rosés, C. Ràfols, E. Bosch, S. Espinosa, V. Segarra, J.M. Huerta, Setup and validation of shake-flask procedures for the determination of partition coefficients (log *D*) from low drug amounts, Eur. J. Pharm. Sci. 76 (2015) 181–191.

[147] A. Fini, I. Orienti, V. Zecchi, Analysis of a two- and three-phase dissolution process of ketoprofen, Acta Pharm. Technol. 34 (1988) 160–163.

[148] J. Rautio, H. Taipale, J. Gynther, J. Vepsäläinen, T. Nevalainen, T. Jarvinen, *In vitro* evaluation of acyloxyalkyl esters as dermal prodrugs of ketoprofen and naproxen, J. Pharm. Sci. 87 (1998) 1622–1628.

[149] F. Barbato, G. Caliendo, M.I. La Rotonda, C. Silipo, G. Toraldo, A. Vittoria, Distribution coefficients by curve fitting: application to ionogenic nonsteroidal antiinflammatory drugs, Quant. Struct. Relationships. 5 (1986) 88–95.

[150] H.C. Atkinson, E.J. Begg, Relationship between human milk lipid–ultrafiltrate and octanol-water partition coefficients, J. Pharm. Sci. 77 (1988) 796–798.

[151] J. Rautio, T. Nevalainen, H. Taipale, J. Vepsäläinen, J. Gynther, K. Laine, T. Järvinen, Synthesis and in vitro evaluation of novel morpholinyl- and methylpiperazinylacyloxyalkyl prodrugs of 2-(6-methoxy-2-naphthyl)propionic acid (naproxen) for topical drug delivery, J. Med. Chem. 43 (2000) 1489–1494.

[152] A. Chiarini, A. Tartarini, A. Fini, p*H*-solubility relationship and partition coefficients for some anti-inflammatory arylaliphatic acids, 317 (1984) 268–273.

[153] G. Orzalesi, F. Mari, E. Bertol, R. Selleri, G. Pisaturo, Anti-inflammatory agents: determination of ibuproxam and its metabolite humans. Correlation between bioavailability, tolerance and chemico-physical characteristics, Arzneimittelforschung. 30 (1980) 1607–1609.

[154] N. Gulyaeva, A. Zaslavsky, P. Lechner, M. Chlenov, O. McConnell, A. Chait, V. Kipnis, B. Zaslavsky, Relative hydrophobicity and lipophilicity of drugs measured by aqueous two-phase partitioning, octanol-buffer partitioning and HPLC. A simple model for predicting blood-brain distribution, Eur. J. Med. Chem. 38 (2003) 391–396.

[155] Y.W. Alelyunas, L. Pelosi-Kilby, P. Turcotte, M.B. Kary, R.C. Spreen, A high throughput dried DMSO Log *D* lipophilicity measurement based on 96-well shake-flask and atmospheric pressure photoionization mass spectrometry detection, J. Chromatogr. A. 1217 (2010) 1950–1955.

[156] K. Balon, B.U. Riebesehl, B.W. Müller, Drug liposome partitioning as a tool for the prediction of human passive intestinal absorption, Pharm. Res. 16 (1999) 882–888.

[157] A. Avdeef, K.J. Box, J.E.A. Comer, C. Hibbert, K.Y. Tam, p*H*-Metric log*P* 10. Determination of liposomal membrane-water partition coefficients of ionizable drugs, Pharm. Res. 15 (1998) 209–215.

[158] F. Barbato, G. Caliendo, M.I. La Rotonda, P. Morrica, C. Silipo, A. Vittoria, Relationships between octanol-water partition data, chromatographic indices and their dependence on p*H* in a set of β-adrenoceptor blocking agents, Farmaco. 45 (1990) 647–663.

[159] M. Recanatini, Partition and distribution coefficients of aryloxypropanolamine β-adrenoceptor antagonists, J. Pharm. Pharmacol. 44 (1992) 68–70.

[160] H.S. Huang, R.D. Schoenwald, J.L. Lach, Corneal penetration behavior of β-blocking agents II: assessment of barrier contributions, J. Pharm. Sci. 72 (1983) 1272–1279.

[161] D. Hellenbrecht, B. Lemmer, G. Wiethold, H. Grobecker, Measurement of hydrophobicity, surface activity, local anaesthesia, and myocardial conduction velocity as quantitative parameters of the non-specific membrane affinity of nine β-adrenergic blocking agents, Naunyn. Schmiedebergs. Arch. Pharmacol. 277 (1973) 211–226.

[162] F.H. Clarke, N.M. Cahoon, Partition coefficients by curve fitting: the use of

two different octanol volumes in a dual-phase potentiometric titration, J. Pharm. Sci. 85 (1996) 178–183.

[163] J.A. Cordero, L. Alarcon, E. Escribano, R. Obach, J. Domenech, A comparative study of the transdermal penetration of a series of nonsteroidal antiinflammatory drugs, J. Pharm. Sci. 86 (1997) 503–508.

[164] H. Bundgaard, N.M. Nielsen, Glycolamide esters as a novel biolabile prodrug type for non-steroidal anti-inflammatory carboxylic acid drugs, Int. J. Pharm. 43 (1988) 101–110.

[165] V. Sarveiya, J.F. Templeton, H.A. Benson, Ion-pairs of ibuprofen: increased membrane diffusion, J. Pharm. Pharmacol. 56 (2004) 717–724.

[166] K. Schellenberg, C. Leuenberger, R.P. Schwarzenbach, Sorption of chlorinated phenols by natural sediments and aquifer materials, Environ. Sci. Technol. 18 (1984) 652–657.

[167] N. Gulyaeva, A. Zaslavsky, P. Lechner, M. Chlenov, A. Chait, B. Zaslavsky, Relative hydrophobicity and lipophilicity of β-blockers and related compounds as measured by aqueous two-phase partitioning , octanol–buffer partitioning, and HPLC, Eur. J. Pharm. Sci. 17 (2002) 81–93.

[168] Y.Z. Da, K. Ito, H. Fujiwara, Energy aspects of oil/water partition leading to the novel hydrophobic parameters for the analysis of quantitative structure-activity relationships, J. Med. Chem. 35 (1992) 3382–3387.

[169] B.E. Nowosielski, J.B. Fein, Experimental study of octanol-water partition coefficients for 2,4,6-trichlorophenol and pentachlorophenol: derivation of an empirical model of chlorophenol partitioning behaviour, Appl. Geochemistry. 13 (1998) 893–904.

[170] K. Nishimura, Y. Nozaki, A. Yoshimi, S. Nakamura, M. Kitagawa, N. Kakeya, K. Kitao, Studies on the promoting effects of carboxylic acid derivatives on the rectal absorption of β-lactam antibiotics in rats, Chem. Pharm. Bull. 33 (1985) 282–291.

[171] R.P. Austin, P. Barton, S.L. Cockroft, M.C. Wenlock, R.J. Riley, The influence of nonspecific microsomal binding on apparent intrinsic clearance, and its prediction from physicochemical properties, Drug Metab. Dispos. 30 (2002) 1497–1503.

[172] M. Sugawara, Y. Takekuma, M. Kobayashi, K. Iseki, K. Miyazaki, Predicting the intestinal absorption of anionic drugs from their physicochemical properties, Pharm. Pharmacol. Commun. 1 (1995) 491–493.

[173] M.I. La Rotonda, G. Amato, F. Barbato, C. Silipo, A. Vittotia, Relationships between octanol-water partition data, chromatographic indices and their dependence on p*H* in a set of nonsteroidal anti-inflammatory drugs, Quant. Struct. Relationships. 2 (1983) 168–173.

[174] M.V. Ionin, T. V. Sherstneva, G.N. Koleboshin, Phase equilibria in the system butanol-1-water-dioxane, Zh. Obs. Khim. 39 (1969) 23–25.

[175] J. Gregorowicz, A. Bald, A. Szejgis, A. Chmielewska, Gibbs energy of transfer and conductivity properties of NaI solutions in mixtures of water with butan-1-ol at 298.15 K, and some physicochemical properties of

mixed solvent, J. Mol. Liq. 84 (2000) 149–160.

[176] C.M. Romero, E. Moreno, J.L. Rojas, Apparent molal volumes and viscosities of DL-α-alanine in water-alcohol mixtures, Thermochim. Acta. 328 (1999) 33–38.

[177] L.M. Kushner, B.C. Duncan, J.I. Hoffman, A viscometric study of the micelles of sodium dodecyl sulfate in dilute solutions, J. Res. Natl. Bur. Stand. (1934). 49 (1952) 85–90.

[178] C. Magallanes, A. Catenaccio, H. Mechetti, Relaxation time and viscosity of several n-alcohol/heptane systems, J. Mol. Liq. 40 (1989) 53–63.

[179] B. Slater, A. McCormack, A. Avdeef, J.E.A. Comer, p*H*-metric log *P*. 4. Comparison of partition coefficients determined by HPLC and potentiometric methods to literature values, J. Pharm. Sci. 83 (1994) 1280–1283.

[180] J.F.J. Dippy, R.H. Lewis, Chemical constitution and the dissociation constants of mono- carboxylic acids. Part V. Further substituted benzoic and phenylacetic acids, J. Chem. Soc. (1936) 644–649.

[181] T. Degim, V. Zaimoglu, C. Akay, Z. Degim, p*H*-Metric log *K* calculations of famotidine, naproxen, nizatidine, ranitidine and salicylic acid, Farmaco. 56 (2001) 659–663.

[182] Y. Ishihama, M. Nakamura, T. Miwa, T. Kajima, N. Asakawa, A rapid method for pK_a determination of drugs using pressure-assited capillary electrophoresis with photodiode array detection in drug discovery, J. Pharm. Sci. 91 (2002) 933–942.

[183] M. Shalaeva, J. Kenseth, F. Lombardo, A. Bastin, Measurement of dissociation constants (pK_a values) of organic compounds by multiplexed capillary electrophoresis using aqueous and cosolvent buffers, J. Pharm. Sci. 97 (2008) 2581–2606.

[184] M. Meloun, S. Bordovská, L. Galla, The thermodynamic dissociation constants of four non-steroidal anti-inflammatory drugs by the least-squares nonlinear regression of multiwavelength spectrophotometric p*H*-titration data, J. Pharm. Biomed. Anal. 45 (2007) 552–564.

[185] K. Takács-Novák, K.J. Box, A. Avdeef, Potentiometric p$K_{(a)}$ determination of water-insoluble compounds: validation study in methanol/water mixtures, Int. J. Pharm. 151 (1997) 235–248.

[186] G. Caron, G. Steyaert, A. Pagliara, F. Reymond, P. Crivori, P. Gaillard, P.A. Carrupt, A. Avdeef, J. Comer, K.J. Box, H.H. Girault, B. Testa, Structure-lipophilicity relationships of neutral and protonated b-blockers, part I, intra- and intermolecular effects in isotropic solvent systems, Helv. Chim. Acta. 82 (1999) 1211–1222.

[187] A. Avdeef, C.M. Berger, p*H*-metric solubility. 3. Dissolution titration template method for solubility determination, Eur. J. Pharm. Sci. 14 (2001) 281–291.

[188] E. Grunwald, A differential potentiometric method of measuring acid and base dissociation constants, J. Am. Chem. Soc. 73 (1951) 4934–4938.

[189] B. Saxton, H.F. Meier, The ionization constants of benzoic acid and of the

three monochlorobenzoic acids, at 25°, from conductance measurements, J. Am. Chem. Soc. 56 (1934) 1918–1921.

[190] J.A. Cleveland Jr, M.H. Benko, S.J. Gluck, Y.M. Walbroehl, Automated pK_a determination at low solute concentratrions by capillary electrophoresis, J. Chromatogr. A. 652 (1993) 301–308.

[191] F.G. Brockman, M. Kilpatrick, The thermodynamic dissociation constant of benzoic acid from conductance measurements, J. Am. Chem. Soc. 56 (1934) 1483–1486.

[192] F.H. Clarke, N.M. Cahoon, Ionization constants by curve fitting: determination of partition and distribution coefficients of acids and bases and their ions, J. Pharm. Sci. 76 (1987) 611–620.

[193] S.F. Donovan, M.C. Pescatore, Method for measuring the logarithm of the octanol-water partition coefficient by using short octadecyl-poly(vinylalcohol) high-performance liquid chromatography columns, J. Chromatogr. A. 952 (2002) 47–61.

[194] Q.C. Wang, F. Svec, J.M.J. Fréchet, Macroporous polymeric stationary-phase rod as continuous separation medium for reversed-phase chromatography, Anal. Chem. 65 (1993) 2243–2248.

[195] C. Viklund, F. Svec, J.M.J. Fréchet, K. Irgum, Monolithic, “molded”, porous materials with high flow characteristics for separations, catalysis, or solid-phase chemistry: control of porous properties during polymerization, Chem. Mater. 8 (1996) 744–750.

[196] F. Svec, J.M.J. Fréchet, Kinetic control of pore formation in macroporous polymers. Formation of “molded” porous materials with high flow characteristics for separations or catalysis, Chem. Mater. 7 (1995) 707–715.

[197] F. Svec, J.M.J. Fréchet, Continuous rods of macroporous polymer as high-performance liquid chromatography separation media, Anal. Chem. 64 (1992) 820–822.

[198] R.R. Walters, J.F. Graham, R.M. Moore, D.J. Anderson, Protein diffusion coefficient measurements by laminar flow analysis: method and applications, Anal. Biochem. 140 (1984) 190–195.

[199] T.M. Annesley, Ion suppression in mass spectrometry, Clin. Chem. 49 (2003) 1041–1044.

[200] S. Eeltink, J.M. Herrero-Martinez, G.P. Rozing, P.J. Schoenmakers, W.T. Kok, Tailoring the morphology of methacrylate ester-based monoliths for optimum efficiency in liquid chromatography, Anal. Chem. 77 (2005) 7342–7347.

[201] F. Detobel, K. Broeckhoven, J. Wellens, B. Wouters, R. Swart, M. Ursem, G. Desmet, S. Eeltink, Parameters affecting the separation of intact proteins in gradient-elution reversed-phase chromatography using poly(styrene-co-divinylbenzene) monolithic capillary columns, J. Chromatogr. A. 1217 (2010) 3085–3090.